University of Bath

PHD

Stabilisation, Modification, Delivery and Treatment of Phospholipid Based Vesicles for Applications in Advanced Wound Management

Marshall, Serena

Award date:
2014

Awarding institution:
University of Bath

Link to publication

General rights
Copyright and moral rights for the publications made accessible in the public portal are retained by the authors and/or other copyright owners and it is a condition of accessing publications that users recognise and abide by the legal requirements associated with these rights.

- Users may download and print one copy of any publication from the public portal for the purpose of private study or research.
- You may not further distribute the material or use it for any profit-making activity or commercial gain
- You may freely distribute the URL identifying the publication in the public portal ?

Take down policy
If you believe that this document breaches copyright please contact us providing details, and we will remove access to the work immediately and investigate your claim.

Download date: 22. May. 2019

STABILISATION, MODIFICATION, DELIVERY AND TREATMENT OF PHOSPHOLIPID BASED VESICLES FOR APPLICATIONS IN ADVANCED WOUND MANAGEMENT

Volume 1 of 6

Serena Marshall

The University of Bath

Centre for Sustainable Chemical Technologies

Department of Chemistry

December 2013

Attention is drawn to the fact that the copyright of this thesis rests with the author. A copy of this thesis has been supplied on the condition that anyone who consults it is understood to recognise that its copyright rests with the author and that they must not copy it or use material from it except as permitted by law or with consent of the author.

This thesis may be made available for consultation within the University Library and may be photocopied or lent to other libraries for the purposes of consultation.

Serena Marshall

Table of contents

List of figures 1
List of tables 4
Acknowledgements 5
Abbreviations 6
Abstract 13
Chapter 1 Introduction 15
1.1 Microbiology and microorganisms 16
1.1.1 Bacteria 17
1.1.2 Bacterial identification in a clinical setting 18
1.1.3 Bacterial pathogenesis 18
1.1.4 Biofilms 18
1.1.5 Quorum sensing 19
1.2 Innate host defences 20
1.2.1 Bacteria defences 20
1.3 Wounds 21
1.3.1 Burn wounds 21
1.3.2 Wound healing 22
1.3.3 Burn wound healing 23
1.3.4 Paediatric burns – relevant clinical examples 23
1.3.5 Burn wound treatment protocol 24
1.3.6 Recent research in burn injury 25
1.3.7 Clinical requirement 26
1.4 Current clinical detection of wound infection 27
1.4.1 Paediatric burn patient focus 27
1.4.2 An infection detection wound dressing 28
1.5 Aim of this work 29
1.6 References 30

Chapter 2 Experimental and instrumentation 33
2.1 Materials 33
2.2 Vesicle formulation process.....33
2.2.1 Solvent free vesicles 34
2.2.2 Aqueous buffer preparation 34
2.2.3 Cross linking of vesicles 35
2.3 Microbiological assays.....35
2.3.1 Bacterial growth agar.....35
2.3.2 Bacterial growth media 36
2.3.3 Bacteria preparation 36
2.3.4 Bacteria supernatant preparation.....37
2.4 Dressing prototypes 38
2.4.1 Hydrogels.....38
2.5 Vesicle sterilisation.....38
2.5.1 Gamma radiation sterilisation 39
2.5.2 Heat sterilisation 39
2.5.3 Filter sterilisation 39
2.6 Vesicle modification 39
2.6.1 Hyaluronic acid coupling.....39
2.7 Treatment of vesicles with plasma.....40
2.7.1 Microplasma jet 40
2.7.2 Synthetic sensor 40
2.8 Methods of characterisation.....41
2.8.1 FLUOstar Omega plate reader 41
2.8.2 Brightfield and fluorescence microscopy 42
2.8.3 Confocal microscopy 43
2.8.4 Nanoparticle tracking analysis 44

2.8.5 Dynamic light scattering 45
2.8.6 Osmolality 45
2.8.7 Differential scanning calorimetry 46
2.8.8 Nuclear magnetic resonance 46
2.9 Statistical analysis 46
2.10 References 47
Chapter 3 Vesicle development - stability 48
3.1 Vesicle applications 48
3.1.1 Medical applications 48
3.1.2 Intelligent vesicles 49
3.1.3 Membrane lipids 50
3.1.4 Phospholipid packing formation 52
3.1.5 Phase formation 54
3.1.6 Bilayer fluidity 55
3.1.7 Lipid diffusion in the bilayer 56
3.1.8 Unilamellar vesicles 56
3.1.9 Biological membranes and vesicles 57
3.1.10 Vesicle development – stability and sensitivity 58
3.2 Vesicles – encapsulation of a signalling agent 59
3.2.1 Fluorescence 59
3.2.2 Quenching of fluorescence 62
3.2.3 5(6)-carboxyfluorescein 64
3.3 Vesicle formulation process 65
3.3.1 Vesicle and dye concentration calculations 65
3.3.2 General vesicle composition 67
3.3.3 Less common lipids 68
3.3.4 Vesicle nomenclature 69

3.3.5 Vesicle membrane solubilisation – a positive lytic control 69
3.4 Vesicle development – measuring stability 71
3.4.1 Stability response parameter 72
3.4.2 Stabilising agents 72
3.4.3 Lipid chain length 72
3.4.4 Polydiacetylene polymers 73
3.4.5 Cholesterol concentrations 74
3.4.6 Hybrid vesicles 76
3.4.7 Anionic lipids 77
3.4.8 Cationic lipids 77
3.4.9 Stealth vesicles 78
3.4.10 Phase separating lipids 79
3.4.11 Stable vesicle candidates 80
3.4.12 Stability versus sensitivity 80
3.5 Environmental stimulus 81
3.5.1 Effects of pH and temperature 81
3.6 Vesicle stability – conclusions 89
3.7 References 90
Chapter 4 Vesicle development - sensitivity 95
4.1 Research using microorganisms 95
4.2 Bacteria 96
4.2.1 *Staphylococcus* 96
4.2.2 *Pseudomonas aeruginosa* 99
4.2.3 *Escherichia coli* 100
4.3 Bacterial toxin interactions with membranes 101
4.3.1 Relevant toxins 102
4.4 Vesicle response to bacteria 104

4.4.1 Selective sensitivity of stabilised vesicles 106
4.4.2 Observable response versus bacteria present 108
4.5 Accessory gene regulator 108
4.6 Vesicles in wound exudate 111
4.7 Vesicle sensitivity - conclusions 115
4.7.1 Further work - encapsulation of antibacterial agents 116
4.8 References 122
Chapter 5 Dressing prototypes 124
5.1 Active agent delivery using vesicles 124
5.2 Burn dressings 125
5.3 Open topical wound dressings 126
5.4 Delivery medium 126
5.4.1 Hydrogels 127
5.4.2 Prototype hydrogels 127
5.5 Osmosis 130
5.5.1 Osmolality 130
5.5.2 Osmolality and vesicles 131
5.6 Vesicles in hydrogels 132
5.7 Fluorescence response versus bacteria count 137
5.8 Dressing prototypes – conclusion 137
5.9 References 138
Chapter 6 Vesicle sterilisation 142
6.1 Medical product sterilisation 142
6.2 Physical antimicrobial control methods 143
6.3 Radiation Sterilisation 143
6.3.1 Electromagnetic radiation 143
6.3.2 Effect of radiation on biological material 144
6.3.3 Radiation resistance 145

6.3.4 Measurement of absorbed dose 146
6.3.5 Gamma radiation 147
6.3.6 Gamma radiation of vesicles 147
6.3.7 Vesicle stability – radiation sterilisation 149
6.4 Heat sterilisation 150
6.4.1 Thermal resistance 150
6.4.2 Moist (steam) sterilisation 150
6.4.4 Vesicle stability – thermal sterilisation 152
6.5 Filter sterilisation 153
6.5.1 Filtration process 153
6.5.2 Filter contamination 154
6.5.3 Filter sterilisation of vesicles 154
6.5.4 Vesicle stability – filter sterilisation 156
6.6 Vesicle sterilisation - conclusions 156
6.6.1 Alternative sterilisation technologies 157
6.6.2 Alternative solution - solvent free vesicles 158
6.7 References 159
Chapter 7 Vesicle modification 161
7.1 Vesicle modifications 161
7.1.1 Hyaluronic acid 162
7.1.2 Hyaluronidase 163
7.1.3 Hyaluronic acid coated vesicles 164
7.1.4 Incorporation of stearylamine into vesicles 165
7.1.5 Hyaluronic acid – vesicle coupling 165
7.1.6 Proof of principle 167
7.1.7 HA-coated vesicles with bacterial supernatant 168
7.2 Vesicle modifications – conclusions 170

7.3 References 170
Chapter 8 Microplasma jet treatment of vesicles 172
8.1 Plasma healthcare applications 172
8.1.1 Plasma – a brief history 172
8.1.2 The 4th state of matter 173
8.1.3 Plasma medicine 174
8.1.4 Atmospheric plasma 175
8.1.5 Microplasma jet 176
8.2 Proposal: a synthetic biological sensor 177
8.3 Plasma jet treatment of the synthetic sensor 177
8.3.1 Plasma jet parameters 177
8.3.2 Sensitivity of the biological synthetic sensor 178
8.3.3 Treatment and analysis of the synthetic biological sensor 180
8.3.4 Parallel plasma jet treatment 186
8.3.5 Plasma jet treatment through a vesicle suspension 187
8.4 Microplasma jet treatment of vesicles - conclusions 188
8.4.1 Soft tissue plasma treatment 190
8.5 References 191
Chapter 9 Conclusions 196
9.1 References 199
Appendix 1 – Supporting information 200
Appendix 2 – Original publications 211

List of figures

Figure 1-1. Bacterial mechanisms for antibiotic resistance 15
Figure 1-2. Formation of a biofilm 19
Figure 1-3. An example paediatric burn patient 23
Figure 1-4. The lytic response of vesicles in the presence of pathogenic bacterial toxins 29
Figure 2-1. Vesicle formulation process 34
Figure 2-2. Preparation of an individual bacterial strain prior to addition to a sample 37
Figure 2-3. Bacteria growth curve 37
Figure 2-4. The micro plasma reactor and jet 40
Figure 2-5. Schematic of an epi-fluorescent spectrometer 42
Figure 2-6. Confocal microscope schematic 43
Figure 2-7. Schematic diagram of a Nanoparticle tracking analysis instrument 44
Figure 3-1. The structure of phospholipids 51
Figure 3-2. The effect of phospholipid structure on packing formation. 52
Figure 3-3. The interaction of an aqueous phase with a planar and capped bilayer. 53
Figure 3-4. The three most common polymorphic phase states observed in membrane phospholipids 54
Figure 3-5. The diffusion of lipids within a bilayer 56
Figure 3-6. The ideal vesicle profile 58
Figure 3-7. Jabłoński diagram 59
Figure 3-8. The absorption / emission spectra for the fluorophore 5(6)-carboxyfluorescein 61
Figure 3-9. A graph to show fluorescence versus 5(6)-CF concentration 64
Figure 3-10. The structure of phosphatidylethanolamine (DPPE) and phosphatidylcholine (DPPC) 68
Figure 3-11. The stages of membrane solubilization following the addition of increasing concentrations of detergent to a membrane. 70
Figure 3-12. The structure and lytic effect of triton 71
Figure 3-13. The monomer and polymer structure of 10,12-tricosadiynoic acid (TCDA) and colour profile at different concentrations following UV treatment 74
Figure 3-14 The structure of cholesterol. 75
Figure 3-15. The chemical structures of fluorescein and pKa values as pH changes. 82
Figure 3-16. The effect of pH on three different concentrations of 5(6)-CF dye 83

Figure 3-17. The effect of incubation at 37 °C for 18 hours on 1 mM 5(6)-CF at pH 5, 6, 7 and 8. 84
Figure 3-18. The stability of DPPG-DP vesicles at 5 °C, -20 °C, -80 °C or following flash freezing. 86
Figure 3-19. Measuring the effect of increasing temperature from 20 °C to 40 °C at 2 °C intervals on the stability of TCDA-DS vesicles, ... 87
Figure 3-20. Vesicle concentration count using NTA 88
Figure 4-1. The hydrolysis sites of action of a range of phospholipase enzymes. 101
Figure 4-2. The different surface and secretion proteins of *S.aureus* bacteria and their bacterial growth phases related activity and production. 102
Figure 4-3. The general structure of a mono-rhamnolipid (Rha-C_{10}). 102
Figure 4-4. The expected vesicle lysis response following inoculation with bacteria in broth 104
Figure 4-5. Stabilised vesicle candidate sensitivity response to bacteria 107
Figure 4-6. Schematic representation of the two component AGR system. 109
Figure 4-7. The fluorescence intensity of three primary vesicle candidates after 24 hours with bacteria and 24 hours with bacteria and triton 110
Figure 4-8. The effect of wound exudate at different concentrations 112
Figure 4-9. The stability of the standard three vesicle types with wound exudate, SimF and a control 113
Figure 4-10. Hypothesised growth curve of bacteria in the presence of vesicles containing an antibacterial agent 116
Figure 4-11. The growth of gram positive *S.aureus* MSSA 476 when incubated with different concentrations of doxorubicin hydrochloride 118
Figure 4-12. The growth of bacteria when incubated with DSPG-DP vesicles containing Dox HCl (0.5 mg/ml) 121
Figure 5-1. The effect of a lytic agent on vesicles dispersed within a hydrogel 133
Figure 5-2. The effect of hydrogel matrices with each of the three vesicle candidates. After 14 days at 37 °C, *S.aureus* RN4282 supernatant was added to measure $F_{100\ \%}$, or HEPES as a negative control. 134
Figure 5-3. The change in fluorescence of three stable vesicle candidates in agarose gel 136
Figure 5-4. Representative image of hydrogel dressing embedded with vesicles 138
Figure 6-1. Ionising radiation survival curves representative of different bacteria, following treatment with ^{60}Co and bacteria recovery 145

Figure 6-2. The absorbed dose required for sterilisation and other applications.....146
Figure 6-3. The radiation decay of ^{137}Cs 147
Figure 6-4. The observable effect of gamma sterilisation on vesicles containing self-quenched 5(6)-CF.....148
Figure 6-5. The effect of gamma radiation on DSPG-DP vesicles.....149
Figure 6-6. Heat sterilisation of three vesicle types.....152
Figure 6-7. Filtration of three vesicle types 155
Figure 6-8. The response of solvent-free vesicles to *S.aureus* MSSA 476, *P.aeruginosa* PAO1 and *E.coli* DH5α bacteria.....158
Figure 7-1. A schematic demonstrating the desired effect of vesicles coated with hyaluronic acid (HA) in the presence of hyaluronidase (HLase) producing bacteria.....162
Figure 7-2. The copolymers of hyaluronic acid in their β-bond cross-linked form.....163
Figure 7-3. Potential sites of action of hyaluronidase on hyaluronic acid.....164
Figure 7-4. The proposed alignment of SA alongside phospholipids in a membrane.....165
Figure 7-5. Formation of the HA-SA(-vesicle) conjugate 166
Figure 7-6. DLS of HA coated vesicles compared to uncoated vesicles 167
Figure 7-7. The effect of δ-toxin with or without HLase on HA coated vesicles.....168
Figure 7-8. The addition of HLase positive (H560) and HLase negative (ST239µ2) bacterial SN to HA-coated vesicles 169
Figure 8-1. The fourth state of matter: Plasma. 174
Figure 8-2. Plasma jet contact with vesicles on a silica backed sample 178
Figure 8-3. The comparative fluorescence of the sensor 179
Figure 8-4. Perpendicular treatment of synthetic sensor with the plasma jet 181
Figure 8-5. Perpendicular treatment of synthetic sensor with the neutral gas flow only.....182
Figure 8-6. Perpendicular plasma jet treatment of the gelatin matrix prepared with 5(6)-CF 183
Figure 8-7. Analysis of 5(6)-CF fluorescence intensity profiles of the synthetic tissue.....184
Figure 8-8. Confocal microscopy images of the synthetic tissue 186
Figure 8-9. Parallel treatment of the synthetic sensor with the plasma jet 187
Figure 8-10. Plasma jet treatment of a suspension of vesicles. 188

List of tables

Table 2-1. The composition of the HEPES storage buffer and 5(6)-CF dye. 35
Table 3-1. Less typically recognised lipids 68
Table 3-2. The relation of vesicle nomenclature to primary lipid / stabilising agent composition. 69
Table 3-3. Gel-to-liquid crystal transition temperatures of the PC lipids 73
Table 3-4. Example *hybrid* vesicle lipid compositions using DPPC and DSPC 76
Table 3-5. Stable vesicle candidates and their stability response parameter (S) values. 80
Table 3-6. The stability response parameter of stable vesicle candidates after incubation at 37 °C for 14 days at pH 5, 6, 7 and 8, followed by lysis with triton. 85
Table 4-1. Toxins and pathogenicity factors produced by *S.aureus* 98
Table 4-2. The site of action of different antimicrobial agents 117
Table 4-3. The structure and activity of different antibacterial agents, and the MIC100 against gram+ *S.aureus* MSSA 476 and gram- *P.aeruginosa* PAO1 (mol L^{-1}) 120
Table 5-1. The different hydrogel mediums investigated as potential vesicle delivery systems 129
Table 5-2. The osmotic pressure of the vesicles, HEPES buffer, different hydrogels, growth mediums and SimF (mOsm/kg H_2O). 132
Table 5-3. The osmolality ratio values of the vesicles in each of the hydrogels, growth media and SimF 132
Table 5-4. The stability response parameter, S, for each of the vesicle-in-gel systems 135
Table 6-1. Radiation measurement units and conversions 146

Acknowledgements

This PhD project was carried out with funding from the Doctoral Training Centre for Sustainable Chemical Technologies (CSCT), University of Bath. Being part of this innovative centre has opened avenues to interesting projects, new friends and future collaborations. The opportunities that have come as part of being a member of the pioneering cohort, either through funding for conferences and a secondment abroad, additional relevant taught modules and public engagement activities, such as Cheltenham Science Festival, has given me experiences that have given me a well-rounded and successful PhD. I am very grateful to the CSCT for the support I have received throughout my studies.

Special thanks must go to Dr. Toby Jenkins, chief supervisor and gin drinker, for his guidance and encouragement throughout my PhD. I would also like to thank Dr. Endre Szili and Dr. Sameer Al-Bataineh, from the Mawson Institute at UniSA, who helped me achieve my first paper. I would also like to thank Will Reynolds, a fellow member of the CSCT, for his organic chemistry expertise. In addition to this, I am very grateful to the friends I have made, past and present, who have worked in the Jenkins group, and have made me feel part of a family, namely Sunny, Dave, Maisem, Jess, Thet, Diana, Oscar, June and Charby. The working we have completed together over the last three and a half years has been coupled with a lot of fun times. As part of this I would also like to thank Bacterio Safe, and all the past and present members, who have worked collaboratively towards a common goal.

I would like to thank my friends and family for all of the love they have shown me during my studies, and in fact at all stages of my life. A special thanks to Laura Garman, Caroline Hughes, Rebecca Thorne and Jess Bean for their editing skill, to Kenneth Schneider, for keeping me sane and entertained, and an additional (second) thanks to David Jamieson for everything he has done for me.

My parents, Cheralyn and Dennis are the best anyone could hope for, and this and all my other achievements could not have been managed without them. A final note of thanks goes to the person I spent eight wonderful years with - Tim Newton.

Abbreviations

$S_{0,1}^{x,y}$	Singlet energy level
T_1^x	Triplet energy level
$\bar{x}$	The most probable number of surving organisms per unit tested
°C	Degrees centigrade
µm	Micrometre
^{137}Cs	Radioactive isotope of caesium
5(6)-CF	5(6)-carboxyfluorescein
^{60}Co	Radioactive isotope of Cobalt
a	Cross sectional area
A	Absorbance
Å	Angstrom
A*	Fluorophore in its excited state
AA	Arachidonic acid
AGR	Accessory gene regulator
AHL	Acylated homoserine lactone
APL	Avanti Polar Lipids
ATP	Adenosine triphosphate
au	Arbitrary units
B	Bacteria
bp	Base pairs
c	Concentration
C_{10}	Hydroxydecanoate
C981	Carbopol 981P NF
CCD	Charge coupled device
$CDCl_3$	Deuterated chloroform
Chol	Cholesterol
cm	Centimetre
CMC	Carboxymethylcellulose
CMC	Critical micelle concentration
CMT	Critical micelle temperature
CSCT	Centre for Sustainable Chemical Technologies
d	Distance
d	Diameter

D_{10}	A decrease in the initial population of an organism by 1 log
Da	Daltons
DAP	Dimethylammonium propane
DDS	Drug delivery system
DH	Diheptadecanoyl
DH5α	An attenuated strain of non-pathogenic *E.coli*
DLS	Dynamic light scattering
DM	Dimyristoyl
dm	Decimetre
DMSO	Dimethylsulfoxide
DNA	Deoxyribonucleic acid
DO	Dioleoyl
Dox HCl	Doxorubicin hydrochloride
DP	dipalmitoyl
DS	distearoyl
DSC	Differential scanning calorimetry
D_t	Particle diffusion coefficient
Ɛ	Molar absorptivity
E.coli	*Escherichia coli*
EDC	Ethyl(dimethylaminopropyl) carbodiimide
EDTA	Ethylenediaminetetraacetic acid
EEDFs	Electron energy distribution functions
eq	Equivalent
EU	European
ExoA	Exotoxin A
F	Final value
f	Equivalent packing factor
F	Fluorophore
$F_{100\,\%}$	Maximum fluorescence
F_E	Final error value
F_f	Final vesicle fluorescence value after addition of a lytic agent
FGF2	Fibroblast growth factor-2
F_i	Initial vesicle fluorescence value
F_o	Unquenched fluorophore
FRET	Förster resonance energy transfer

g	Gram
GMT	Good microbiological techniques
GUV	Giant unilamellar vesicles
Gy	Gray
h	Hours
h	Average thickness of a bilayer
H560	Community acquired HLase positive strain of *S.aureus*
HA	Hyaluronic acid
HCl	Hydrochloric acid
HEPA	High efficiency particulate air (filter)
HEPES	4-(2-hydroxyethyl)-1-piperazineethanesulfonic acid
HEPG2	Human hepatocyte cells
HLase	Hyaluronidase
HM	Hydroxypropylmethylcellulose
HPLC	High performance liquid chromatography
hv	Photon energy
Hz	Hertz
I	Integer value
I_E	Initial error value
I_f	Intensity of fluorescence
J	Joules
k	Death rate constant
K	Kelvin
k	Kilo
k_F	Rate of fluorescence
kg	Kilogram
k_{IC}	Rate of internal conversion
k_{NR}	Rate of non-radiative decay
k_Q	Rate of quenching
K_{sv}	Stern-Volmer quenching constant
l	Maximum achievable length of the acyl chain
L	Litre
l	Path length
LA	Luria agar
LB	Luria broth
LTE	Local thermal equilibrium

LUV	Large unilamellar vesicles
L_α	Liquid crystalline phase
L_β	Liquid gel phase
m	Metre
m/z	Mass to charge ratio
mg	Milligram
MIC	Minimum inhibitory concentration
MIC100	The amount of antimicrobial required to inhibit 100 % of the bacteria growth
MIC50	The amount of antimicrobial required to inhibit 50 % of the bacteria growth
min	Minute
ml	Millilitre
mm	Millimetre
mM	Millimolar
mOsm	Milliosmoles
MW	Molar mass
MRI	Magnetic resonance imaging
MRSA	Methicillin resistant *staphylococcus aureus*
MSSA	Methicillin susceptible *staphylococcus aureus*
MSSA 476	A community acquired strain of *S.aureus*
N	New value
η	Solvent viscosity
NaCl	Sodium chloride
NaOH	Sodium hydroxide
NHS	*N*-hydroxysuccinimide
nm	Nanometre
N_{mol}	Number of moles
NMR	Nuclear magnetic resonance
N_o	Starting number of a population
N_t	Number of population surviving at a given time
NTA	Nanoparticle tracking analysis
OD	Optical density
o/n	Overnight
P	Average packing factor
P.aeruginosa	*Pseudomonas aeruginosa*
P2 and P3	Operons involved in AGR system

PA	Phosphatidic acid
PAO1	A common lab strain of *P.aeruginosa*
PC	Phosphatidylcholine
PDA	Polydiacetylene
PE	Phosphatidylethanolamine
P_E	Propagative error
PEG	Polyethylene glycol
PG	Phosphatidylglycerol
Pg	Petagram
Phos A2	Phospholipase A2
PI	Phosphatidylinositol
PL	Phospholipase
PLLA	poly(L-lactic acid)
PPE	Personal protective equipment
PS	Phosphatidylserine
psi	Pounds per square inch
PSM	Phenol soluble modulin
PSM	Plasma surface modification
PVDA	Polyvinylidene fluoride
q	The number of units succesfully sterilised
Q	Quantum yield
QS	Quorum sensing
R	Donor-acceptor distance
R_e	Molar ratio
Rha	Rhamnopyranosyl
RN4282	Naturally occurring strain of *S.aureus*
RNA	Ribonucleic acid
RONS	Reactive oxygen and nitrogen species
ROS	Reactive oxygen species
rpm	Rotations per minute
rRNA	Ribosomal RNA
S	Stability response parameter
s	Seconds
S.aureus	*Staphylococcus aureus*
S.epidermis	*Staphylococcus epidermis*
S.saprophyticus	*Staphylococcus saprophyticus*

SA	Stearylamine
S_E	Statistical error
SimF	Simulated wound fluid
SN	Supernatant
SSD	Silver sulfadiazine
ST239µ2	Attenuated HLase negative strain of *S.aureus* with the same DNA sequence as TW20
SUV	Small unilamellar vesicles
Sv	Sievert
t	Time
T	Temperature
τ	Fluorescence lifetime
TBSA	Total body surface area
T_c	Phase transition temperature
TCDA	10,12-tricosadiyanoic acid
TEM	Transmission electron microscopy
TLC	Thin layer chromatography
TOF	Time of flight
triton	Triton X-100™
TSA	Tryptic soy agar
TSB	Tryptic soy broth
TSS	Toxic shock syndrome
TSST	Toxic shock syndrome toxin
TW20	Highly resistant and transmissible strain of *S.aureus* with the same DNA sequence as ST239µ2
UniSA	University of South Australia
UV	Ultraviolet
UVR	Ultra violet radiation
UV-Vis	Ultraviolet-visible
V	Volts
v	Volume
v/v	Volume to volume ratio
V_c	Sum of the count of the values
vH_2O_2	Vaporised hydrogen peroxide
V_T	Cumulative sum of values
W	Watts
W	Water

w/v	Weight to volume ratio
WE	Wound exudate
wt	Weight
yr	Year
α	Alpha
β	Beta
γ	Gamma
δ	Delta
λ_{em}	Wavelength of emission
λ_{ext}	Wavelength of excitation
σ	Standard deviation
τ_o	Unquenched fluorophore lifetime
υ	Ionisation of a solution
ξ	Osmolality

Abstract

Despite a general increased awareness of infection control measures, the continual emergence of drug resistant bacterial isolates that are able to colonise a host with negative severe consequences is proving problematic. These bacterial strains tend to be particularly opportunistic; targeting the vulnerable and immuno-compromised host. Of particular interest to this project is paediatric burns and scalds, where an open wound potentially provides an ideal environment for bacterial colonisation. Within this vulnerable patient group the temptation remains to healthcare professionals to indiscriminately subscribe antibiotics unnecessarily. However, creation of a detection system that can be applied to a wound which can rapidly diagnose the presence of bacteria could help to alleviate the oversubscription of drugs, helping to prevent resistance.

This project focuses on the stabilisation, modification, delivery and treatment of phospholipid based vesicles for applications in advanced wound care, with a focus on paediatric burns. Vesicles, commonly referred to as liposomes or nanocapsules, are attractive drug delivery composites, due to their biocompatible properties. They have the ability to entrap active compounds within their core, which can be released at the point of use, (*in vivo* or *ex vivo)* either through passive diffusion, or in response to local environmental stimulus.

The different stabilisation, modification, delivery and treatment of vesicles within this project are depicted in the following figure.

Chapter 3 - Vesicle development - stability	Chapter 4 - Vesicle development - sensitivity
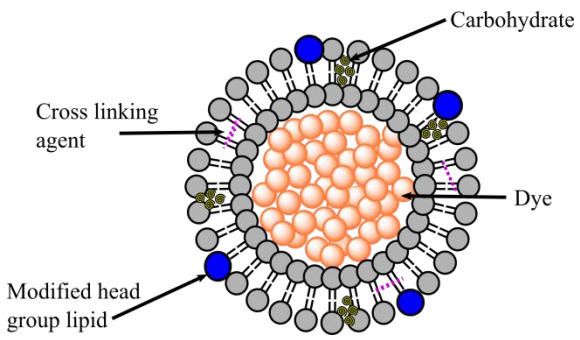	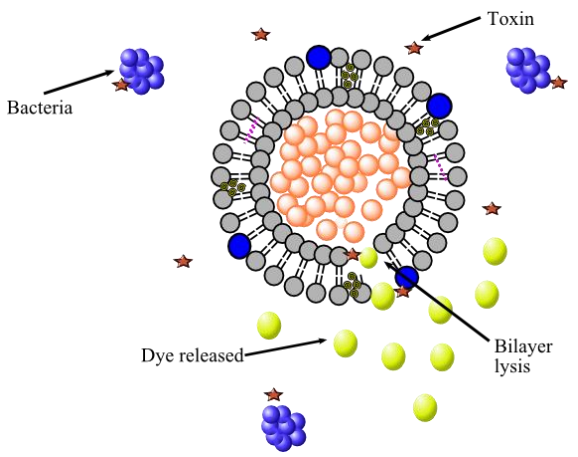

Chapter 5 - Dressing prototypes	Chapter 6 - Vesicle sterilisation
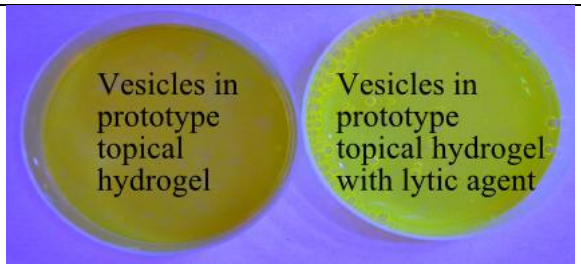	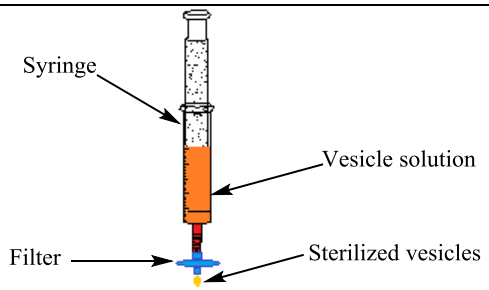
Chapter 7 - Vesicle modification	Chapter 8 - Microplasma jet treatment of vesicles
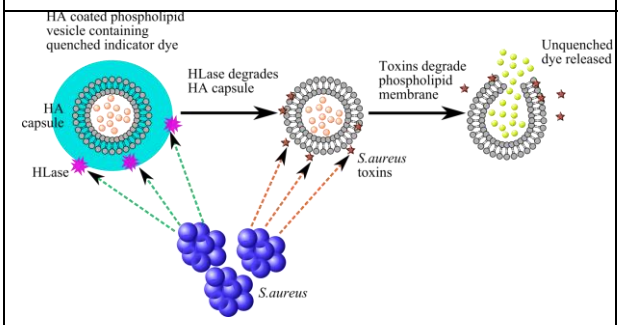	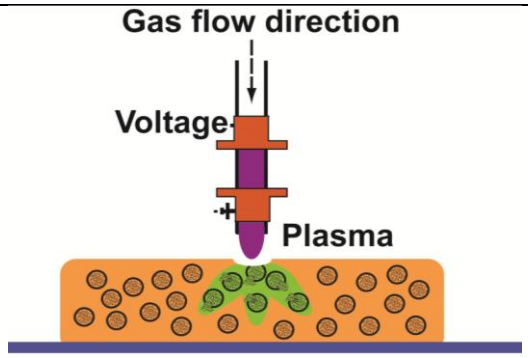

Abstract 1. The utilisation of phospholipid based vesicles.

Within this work; Chapter 3 presents work on the modifications of vesicle composition to attain stability at 37 °C for 14 days. Chapter 4 presents work on the selective sensitivity of successfully stabilised vesicles to pathogenic bacteria. Chapter 5 presents work on the development of a prototype dressing incorporating stable, sensitive vesicles. Chapter 6 presents an introductory investigation into potential vesicles sterilisation techniques. Chapter 7 presents work based on the modification of vesicle properties through alterations of phospholipid structure, and conjugation of protective agents. The final research chapter, 8, presents an investigation into the interaction of a micro plasma jet with a synthetic biological sensor composed of phospholipid vesicles in a matrix.

Chapter 1 Introduction

The need to manage wounds and treat illnesses has been a requirement since the evolution of complex species. Evidence of mankinds' struggle with this can be traced to fragmentary records dating back 5000 years. Though treatment strategies were probably attempted prior to this, evidence has not survived to the present day. It is likely that ancient treatment strategies were based on concoctions that showed some positive therapeutic effect, or on religious or superstitious beliefs that were not wholly advantageous.

The evolution of wound management has progressed from the (relatively simplistic) requirement to achieve healing and closure, to a need for treatment and prevention of infection, and this has continually pushed the boundaries of scientific discoveries. Prior to the revolutionisation of infection and wound treatment with antiseptics and antibiotics, the leading cause of death following survival of an initial wound was infection.[1]

As a result of this, antibiotics are one of the most important medical discoveries, and their introduction coupled with modernisation of the healthcare system has saved countless lives.[2] However, the oversubscribing and misuse of antibiotics has led to resistance in many strains of bacteria. Figure 1-1 simplistically depicts potential methods of bacterial resistance to antibiotics.

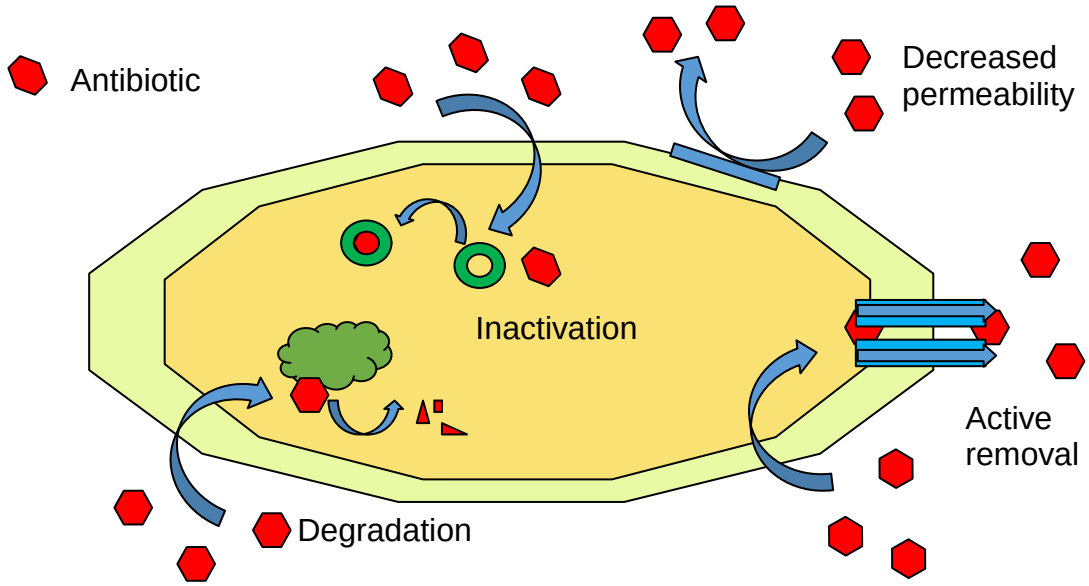

Figure 1-1. Bacterial mechanisms for antibiotic resistance, primarily achieved through enzymatic modification or degradation to inactivate or remove the active site, physical removal from within the bacterial cell, or prevention of permeability into the bacterial cell.[3]

The emergence of antibiotic resistance is complicated by the fast travelling and evolution of resistance genes of bacteria. This resistance has become a major clinical problem and is emerging as one of the world's greatest health challenges; the search for new antibiotics is pursued in direct competition with the evolution of bacteria.[4]

To intensify the challenge of multi-drug resistant bacteria, the development of new antibiotics has slowed, due to the associated costs of unsuccessful potential drugs coupled with the inherent ability of bacteria to develop resistance. Despite a 60 % decrease in new candidates and approvals in the last decade, a report published by Research and Markets titled the "Antibiotic Resistance 2013: The Antibiotics Development Pipeline and Strategies to Combat Antibiotic Resistance" states that there are more than 100 antibiotic candidates in the pipeline, with nine candidates in phase three trials, and a promising further 31 at phase two.

As an alternative, or in combination with antibiotics, the discovery and subsequent use of antimicrobials has shown promise in wound management as a result of their effectiveness, safety and diversity.[5] Antimicrobials differ from antibiotics in that they are substances with inherent inhibitory properties, with minimal effects on mammalian cells; compared to a substance produced by a microorganism that can inhibit growth (bacteriostatic) or kill (bactericidal) other microorganisms.[6] Prior to antibiotic resistance, investigations into potential antimicrobial agents were neglected. However following an increase in knowledge, research into promising and new candidates has resumed.[1] In 2000 the World Health Organisation (WHO) presented a global strategy to prevent and contain antimicrobial resistance, based on an orchestrated multidisciplinary approach. However this approach was under funded with insufficient human resources to implement the strategy, and so despite further review in 2005, little progress has been made.[4]

1.1 Microbiology and microorganisms

Microorganisms are defined as organisms that cannot be viewed without the aid of a microscope. Microbiology is the study of these organisms, their structure, physiology, molecular biology and functional ecology.[7] Microorganisms are widely acknowledged as the first form of life to develop on Earth; their numbers, adaptability and distribution in even hostile environments has helped to ensure their survival.[8]

1.1.1 Bacteria

The founding of bacteriology is accredited to Ferdinand Julius Cohn in the 19th century, however the discovery of bacteria dates back to Antoni van Leeuwenhoek in 1684. Bacteria are prokaryotic single celled organisms approximately between 0.1-10 µm in size. Prokaryotes can be initially classified according to their shape; spherical (cocci), curves, spirals and rods (bacilli). Further classification into broad groups can be achieved based on the presence of one or two cell membranes depending on whether they are gram negative (two) or gram positive (one).

All bacterial cells contain a cytoplasmic membrane composed of proteins, phospholipids and cholesterol; forming a bilayer. The membrane is involved with the synthesis and export of membrane components, respiration, secretion of enzymes and toxins and actively up-taking nutrients into the cell. The shape of the bacteria cell is maintained by the presence of the cell wall, but the structure of this varies between gram negative and gram positive organisms. Gram positive bacteria contain a relatively thick peptidoglycan based wall, composed primarily of repeating sugar subunits cross linked with peptide side chains. Gram negative bacteria have a thinner peptidoglycan layer, and an additional outer membrane composed of lipopolysaccharides, and occasionally lipoproteins and porins that aid transport of substances across the cell envelope.

The cell wall plays an important protective role for bacterial organisms and hence is often the target of β-lactams antibiotics; damage to the wall often leads to cell apoptosis. The cell wall is also a barrier against osmotic pressure variations. In addition to the cell wall, some bacteria are surrounded by a capsule composed of large polysaccharides. The capsule can aid attachment of the bacteria to host cells and shield the organism from host defences.

The structure of prokaryotic cells differs significantly from eukaryotic cells. In addition to their size, shape and external membranes, they do not contain a membrane-bound nucleus, a complex endomembrane system or cytoskeleton. Prokaryotic cells also lack two cytological features found in prokaryotes, namely; a lack of energy producing organelle (their metabolism is not compartmentalised) and an inability to carry out endocytosis.[9]

In prokaryotic cells, most of the DNA is contained within the bacterial chromosome, which aggregates to form the nucleoid, however some is extra-chromosomal arranged in circular plasmids. Plasmids contain genes that code for special properties as opposed to basic survival genes. Prokaryotes are essential to the earth's biota. They play an integral role in catalysing

unique reactions, account for a large percentage of biodiversity and produce components of the earth's atmosphere necessary for life. The number of prokaryotes is estimated to be between 4-6 x 10^{30} cells, with a weight of 350-550 Pg of C, where 1 Pg = 10^{15}g.[10]

1.1.2 Bacterial identification in a clinical setting

Within a clinical environment, the identification of bacteria requires a more pragmatic approach; guidance on the likely cause of an infection is required in a more timely and inexpensive manner. Presumptive identification can be achieved using a few simple procedures, including microscopy – staining (rapid) and culturing of pure stocks – colony growth on agar (<24 hours), however faster methods are always being sought, leading to the development and establishment of antigen and genetic detection methods.[11]

1.1.3 Bacterial pathogenesis

The interaction between a microorganism, 'parasite', and a human 'host' determines whether a tolerable (commensal or even symbiotic) relationship develops or an infection occurs. Pathogenicity is the ability of a microorganism to produce an infection, and this varied ability relates to the virulence factors that they produce.[6] In addition to this, the virulence factors released by bacterial organisms are dependent on whether they are gram negative or gram positive. This will be discussed in more detail in 4.2 Bacteria with regard to the specific bacteria utilised as part of this investigation.

1.1.4 Biofilms

For over a century a generalised belief amongst microbiologists maintained that bacteria existed as single entities of non-cooperative unicellular bacteria species. Recently, a paradigm shift in understanding has led to knowledge of networks of coordinating cells, commonly known as a biofilm.[12] The term biofilm describes association of a microbial organism with a favourable micro-environment. In natural environments, the biofilm is habitually a multi-species microbial community that is able to share genetic material at high rates and stay or leave the community with purpose; making it complex and highly differentiated.[13] Formation of single species biofilms is developmental; establishing in

multiple steps,[14] requiring intercellular signalling[15] and demonstrating a gene transcription profile that is distinct from planktonic cells.[16] Figure 1-2 depicts the biofilm formation process.

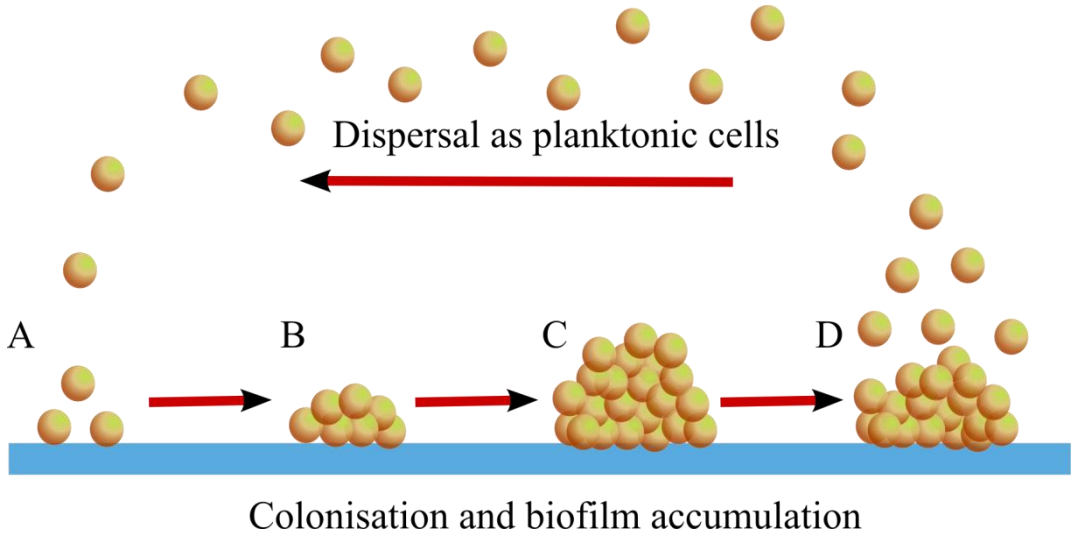

Figure 1-2. Formation of a biofilm from individual planktonic cells through A) initial attachment, B) cell aggregation, C) biofilm accumulation and finally D) dispersion of biofilm and detachment of cells.[17]

The formation of a biofilm following colonisation of a human 'host' by a microorganism 'parasite' can be tolerable / manageable; for example, in oral hygiene and the formation of dental plaque.[18] Pathogenic biofilm is however more widely recognised within the medical health profession, with formation commonly occurring on wounds and medical devices such as implants and catheters.[17, 19]

1.1.5 Quorum sensing

Within a biofilm micro environment, bacteria are able to communicate cell-to-cell, allowing for regulation of colonisation and virulence factors. This phenomenon is known as quorum sensing (QS). Simplistically, QS ensures regulation of gene expression as a function of cell population density within a network, primarily through the release of small diffusible signal molecules, commonly known as pheromones or autoinducers. As the density of bacterial cells increases, the concentration of signal molecules also increases until a threshold concentration is reached whereby activation of a signal transduction cascade occurs, providing an auto-regulatory system for sensing.[12] This communication network makes it difficult for host

defences and external defence agents to form any resistance or barricade to both the cells present and their released virulence factors following colonisation.

1.2 Innate host defences

Arguably, the best mode of defence against a bacterial infection is the prevention of a pathogen invading the host body in the first place. This method is known as germ theory and was developed by Koch and Pasteur. It resulted in a medical revolution; the knowledge that tiny bacteria could sicken and kill people led to the creation of public health agencies, particularly related to water management, and prevented epidemics.[20]

The best physical barrier that animals have to bacterial colonisation is the skin. The skin is composed of several layers, notably the epidermis (outer) and dermis (inner). Colonisation is prevented or discouraged at unbroken skin through a combination of innate techniques. Some of these include: the constant shedding of dead surface skin cells removing any bacteria that is able to successfully bind, a high concentration of the protein keratin, produced by keratinocytes, not readily degraded by microorganisms; a relatively dry localised environment, and low acidic pH (approximately pH 5) and surface temperature (34-35 °C). Despite this, some colonisation and breaching of the skin barrier is achieved at hair follicles and sweat glands, however a further barrier of toxic lipids and lysozyme, capable of degrading bacterial cell wall peptidoglycan, can be found here.[20]

1.2.1 Bacteria defences

Just as host-bodies have developed defences against bacterial penetration and pathogenicity, bacteria have evolved successful strategies for countering these effects. The pathogenicity of a bacteria depends upon its transmission pathway; either person-to-person contact, environmental exposure to a contaminant or through a vector, such as an insect. If successful colonisation and hence infection is to occur, an encounter must lead to entry, spreading, multiplication and damage.[7]

Controlling and limiting the growth of microorganisms can be achieved by restriction of access to vital nutrients, manipulation of the physical environment towards pessimal conditions of growth, addition of metabolic pathway inhibitors, and application of chemotherapeutic agents that can selectively discriminate between host and microbial cells.

The impact of this inhibition is dependent upon whether the effect is transient or permanent. Within a wound environment these control mechanisms may become compromised, leading to conditions that are favourable for bacterial growth, resulting in infection.

1.3 Wounds

In general, a non-medical based definition of a wound is a break in the continuity of any bodily tissue as a result of an external violence, such as surgery. This definition neglects wounds caused by internal gradual tissue disturbances, such as ulcers, hence a more generalised definition and classification is required.

Within the healthcare community, wounds are commonly classified as being either chronic or acute. A chronic wound is defined as one that has "failed to proceed through an orderly and timely process to produce anatomic and functional integrity or proceed through the repair process without establishing a sustained and functional result".[21] In practice this term is often used to refer to a wound that takes longer than three weeks to heal. In contrast, an acute wound is defined as one that is obtained directly from a trauma or an operative procedure, following which the healing pathway precedes in a timely manner with at least external observable manifestations of healing apparent in the post-operative period without complications.[21]

1.3.1 Burn wounds

Within this investigation a tentative focus towards burn wounds has been made. Burn trauma can be caused not only by exposure to heat, but through freezing, electricity, chemicals, radiation and friction. The severity of burn is dependent on the depth of tissue affected, and can lead to complications involving shock, infection, electrolyte imbalance and respiratory failure. In addition to these problems, if the patient survives, patients can suffer serious emotional and psychological distress due to long-term hospitalisation, scarring and deformity.[22] The classification of burn depth is according to degree I-III, and this relates to increasing skin penetration depth.

1.3.2 Wound healing

Healing can be defined broadly as a dynamic process of recovering from a trauma or illness by working toward realistic goals, restoring function, and regaining a personal sense of balance.[23] Within wounds, healing can be defined as the act of restoring the integrity of the damaged tissue with replacement of lost tissue and the repair of damaged tissue, through either the natural biological body response, or intervention of a third party to accelerate or modify the damaged tissue.[24]

The wound healing process within a simplified skin injury model, without any aid from external agents such as sutures or supports, can be thought to progress through four phases:

- Initial and temporary repair – damage limitation in the form of haemorrhage into the wound with associated clotting, to prevent further blood loss.
- Inflammatory response – inflammatory cells, leukocytes, and increased blood flow into the wound act to remove irreparably damaged tissue, aid salvageable tissue and protect against microorganism colonisation.[25]
- Stimulation of epithelial cells – an in-growth of blood vessels with fibroblasts provide granulation tissue for the growth of epithelial cells from the edges of the wound to ensure wound closure, aided by underlying contractile tissue which shrinks to bring the wound margins together.
- Remodelling – the wound may look visibly healed at this stage, however the earlier laid fibrous tissue is modified to give the final outcome: a scar. There are three possible forms a scar can take:
    1. Atrophic – indistinguishable from surrounding, unaffected skin
    2. Hypertrophic – elevated above the surrounding skin, but confined within the size of the original wound (frequently seen in burns)
    3. Keloid – elevated above and out-growing the original wound[24]

In principle, all wounds must undergo similar steps to ensure sufficient wound healing. The presence and activity of reactive oxygen species (ROS), proteases, and other soluble mediators and cells are crucial for ensuring necrosis; debris and microbial habitation are managed within a healing wound.

1.3.3 Burn wound healing

The process of healing within a burn wound is likely to follow a similar pathway to a standard wound.[26] However the degree of a burn significantly affects the biological response. For example, in a deep dermal burn the damaged skin heals very slowly, if at all, and depends heavily on surrounding keratinocytes; the predominant cells in the epidermis. A major burn is accompanied by a large inflammatory response, ensuring an acute influx of inflammatory mediators and growth factors. This inflammatory response is linked to the eventual long term scarring effects, and so there is potential for applications and strategies that reduce the response without this affecting wound repair.[27] This technology would prove beneficial for all patients, especially paediatric patients.

1.3.4 Paediatric burns – relevant clinical examples

Burn injuries to children account for the greatest length of stay of all hospital admissions, of which the majority (80 %) are scalds from hot liquids. An examples of a paediatric patient who spent time at the South West UK Children's Burn Centre and his injuries are described, from information supplied by Dr Amber Young; paediatric burn specialist at the South West UK Paediatric Burn Centre.

- Patient A – 13 months old suffering from 32 % TBSA face and body burns from a hot drink scald. Treated using a biosynthetic skin dressing Biobrane™ with full skin healing.

a) b)

Figure 1-3. An example paediatric burn patient. Patient A suffering from 32 % burns a) with Biobrane™ dressing and b) after 12 months fully healed. Information obtained from University of Bath Press Release – 06/07/2010 titled 'Revolutionary medical dressing uses nanotechnology to fight infection'.

1.3.5 Burn wound treatment protocol

Globally, there is not one definitive treatment for burn treatment. Different burn treatment centres around the world use varied dressings and techniques in the treatment of burns and this can be dependent on the thickness of the wound and the treatment centres preferences. There is insufficient data, limited in both quantity and methodological quantity, to support recommendation of a specific dressing as a treatment for all burns, and so many different types exist. The burn dressing strategies can be divided into two categories: open methods, consisting of topical antimicrobials, and closed methods, which use occlusive dressings.[28]

The use of traditional dressings-for example, silver sulfadiazine (SSD) cream, used since 1968 to minimize infection-and a combination paraffin/cotton wool layer dressing, have been reported to have problems adhering to the wound,[29] and require frequent changes resulting in trauma to growing epithelialised cells and delayed healing. Additionally, the use of SSD cream is discouraged due to its reported toxic effect on regenerating keratinocytes, increasing the scarring that results.[30]

The effectiveness of occlusive dressings for superficial and partial thickness burns have been analysed by the Cochrane Review.[31] The dressings reviewed included:

- Hydrocolloid dressings – composed of gelatin, pectin and sodium carboxymethylcellulose (CMC) in an adhesive polymer matrix, forming a gel in contact with wound exudates, aiding auto-lytic debridement of the wound.
- Polyurethane film dressings – permeable to water vapour, oxygen and carbon dioxide, impermeable to liquid water or bacteria. The amount of time this dressing can be left in place is dependent on the amount of wound exudate.
- Hydrogel dressings – high water content gels containing insoluble polymers. The ability of the dressing to absorb or donate fluid aids wound debridement and maintains a moist wound environment.
- Silicon coated nylon dressings – composed of a flexible polyamide net coated with soft silicone containing no biological compounds, allowing dual action of direct wound contact and absorption of exudates.
- Biosynthetic skin substitute dressing – mimics the skin epidermis and/or dermis allowing reepithelialisation while permitting gas and fluid exchange.
- Antimicrobial (silver and iodine containing) dressings – act to reduce the risk of invasive infection by minimising the bacterial colonisation.

- Fibre dressings – for example, calcium alginate, which is bio-derived, biodegradable, absorbent and can be removed painlessly with saline irrigation.
- Wound dressing pads – simple non-adherent dressings, knitted viscose dressings, and tulle and gauze dressings. These may contain antimicrobials or be non-medicated.

The Cochrane Review attempts to address which of these dressings is the most effective in promoting healing and minimising discomfort and infection. Evidence from different studies supports the use of hydrogel, antimicrobial, biosynthetic and silicon coated dressings due to advantageous wound healing time, decreased number of dressing changes and associated patient pain compared to other commercially available dressings.

There are important considerations for the development and measured effectiveness of a burn dressing or gel, and these include:

1. The time required for the burn to heal. Measurement of this can be carried out by tracking the wound surface area over time.
2. The number of dressing changes or reapplications required.
3. The cost of the dressing.
4. The level of pain associated with the application and removal of the wound dressing, based on physician and patient perception.
5. The required length of stay in hospital.
6. The incidence of infection.

These considerations are often balanced, with priority given to a dressing which is effective at scar reduction, especially in paediatric burn-affected patients. An emphasis on scar reduction is preferable in young patients to minimise the lifetime trauma damage, as well as associated costs incurred through psychological and scar tissue management later in life.

1.3.6 Recent research in burn injury

Examples of other recent publications relating to burn wound care techniques include those reported by Saitoh *et al.*, Kuroyanagi *et al.* and Sastry *et al.* In 2012, Saitoh *et al.* reported the development of a biocompatible, flexible, transparent and adhesive nanosheet dressing consisting of poly(L-lactic acid) (PLLA) with marked protection against wound infection and hence improved wound healing, measured through re-epithelialisation in mice models with partial thickness burns.[33] Also in 2012, Kuroyanagi *et al.* reported the development of a hyaluronic acid and cross-linked collagen sponge containing epidermal growth factor capable

of promoting re-epithelialisation and a decrease in wound size in Sprague Dawley (albino) rat models with partial thickness burns.[34] In 2013, Sastry *et al.* reported the synthesis of a biocompatible fish scale collagen / physiologically clotted fibrin biosheet dressing, incorporated with *Macrotyloma uniflorum* plant extract for enhanced antimicrobial properties, with the potential to act as a burn / wound dressing material.[35]

Within this field there is scope for continual development and improvement to current treatments and dressings used. An updated desirable properties specification of an 'ideal' burn wound dressing (for burns smaller than 20 % total body surface area (TBSA)) has been summarised and reported by Kamolz *et al* in 2012, and will be discussed below.[36]

1.3.7 Clinical requirement

An online survey into the properties of an 'ideal' burn wound dressing suitable for small burns (<20 % TBSA), involving 121 participants from 39 countries, has indicated a wish list of characteristics from a clinical perspective.[36] Essential or desirable characteristics included: a lack of adhesion to the wound bed, pain free application and removal, absorbency, antimicrobial activity, a range of sizes and, in paediatric patients, thinner dressing options. From this list of characteristics most respondents agreed that the 'ideal' dressing is not currently available.[36] Alongside these desirable attributes are those summarised in 1.3.5 Burn wound treatment protocol: minimised healing time, decreased frequency of dressing change, reduced cost (relating to dressing and hospital stay time) and scar reduction.

Additionally, an emphasis can be made on reduced microbial loading within a healing wound. An increased amount of bacterial burden (bioburden) in a healing wound increases the quantity of harmful cytokines, elevates the metabolic requirements of the local tissues, stimulates a pro-inflammatory environment and up-regulates the in-migration of monocytes, macrophages and leucocytes; negatively impacting the wound healing process.[37] As a result, decreasing / effectively eliminating the bioburden could ensure faster healing times, decreased scarring and reduced dressing changes. The presence of biocides applied directly to wounds, in gel form, or embedded within dressings, such as silver based agents, plays an important role in wound bioburden management. However, these biocide agents are applied indiscriminately; no knowledge of bacterial presence is known, and importantly, the potential bacterial strains present may even have resistance, or be capable of adapting to develop resistance, to the biocide agent used.[38]

Detection and identification of bioburden present prior to application of biocide agents could ensure a directed treatment approach, however problems arise from the time required for identification of bacteria and associated dressing removal problems. The incorporation of a detection system within a dressing, which selectively indicates the presence of pathogenic bacteria colonising a wound, could provide a promising alternative therapy treatment.[39]

1.4 Current clinical detection of wound infection

Within a clinical environment, detection of the presence of bacteria in a wound is primarily based on subjective identification of physical and clinical characteristics and symptoms. These identification symptoms can include 'classic' indicators such as pain, erythema (skin redness), oedema (swelling due to fluid), body temperature changes and purulence (pus discharge). Secondary indicators such as excessive exudate, delayed healing, foul odour and wound breakdown may give a better, if slightly belated, indication of infection. However the relationship between presence / amount of bioburden in a wound and the extent to which these signs and symptoms manifest is not definitively clear.[40]

Following symptom-based suspicion of infection within a wound, confirmation and identification within a clinical environment can be achieved using a swab or fluid taken from the wound or dressing. Traditional identification methods involve culturing the swab onto a growth plate, isolation of individual strains, followed by gram staining, monitoring growth characteristics and antibiogram testing (susceptibility to antibiotics). Highly related species of bacteria cannot be phenotypically differentiated and accurate identification cannot always be achieved.

Despite the range of microbial identification methods available, no optimal technique has yet been agreed upon. The length of time, cost, availability of equipment, level of complexity and reliability of results often determine which method should be used.

1.4.1 Paediatric burn patient focus

The classic and secondary indicators of infection, listed in 1.4 Current clinical detection of wound infection, are similar to the symptoms and side effects that accompany a burn. These indicators are magnified in a paediatric patient, where the innate immune system is less

developed, and TBSA of a burn is often larger. As a result of this, these indicators cannot be used to determine the colonisation of bacteria and presence of infection within a burn wound.

If infection is suspected, the wound dressing must be removed and the bioburden must be eliminated through extensive debridement of the wound prior to re-dressing. If the bioburden is not removed, the infection can develop, leading to manifestation of toxic shock syndrome and potentially, death. However, this process is painful for the patient, expensive, can delay or prevent wound healing; which may result in avoidable scarring, and could even lead to further infection colonisation following re-dressing of the wound. It is important to note that this process may even turn out to be completely unnecessary, as the wound may not have even been colonised.

Removal of the wound dressing could be avoided, and further scarring and pain could be reduced, with a wound dressing that signals definitively the presence of bacteria within a wound. Further development of this dressing detection system could include the incorporation of bacterial destroying agents that help manage and decrease the bioburden levels within a wound.

1.4.2 An infection detection wound dressing

The development of a wound dressing with the ability to detect and indicate the presence of pathogenic bacteria in a wound, within an appropriate time frame, could have many wound management applications. A dressing of this type could potentially ensure that painful removal of the dressing and debridement of the wound is avoided unless necessary.

The success of this dressing relies on the incorporation of a sophisticated system of internal agents, capable of indication and /or antibacterial treatment, which are only released in the presence of pathogenic bacteria. Within this project phospholipid-based vesicles are utilised and specifically engineered to develop this sophisticated system, with an emphasis on stability, selective sensitivity, and ability to be delivered to a wound, Figure 1-4.

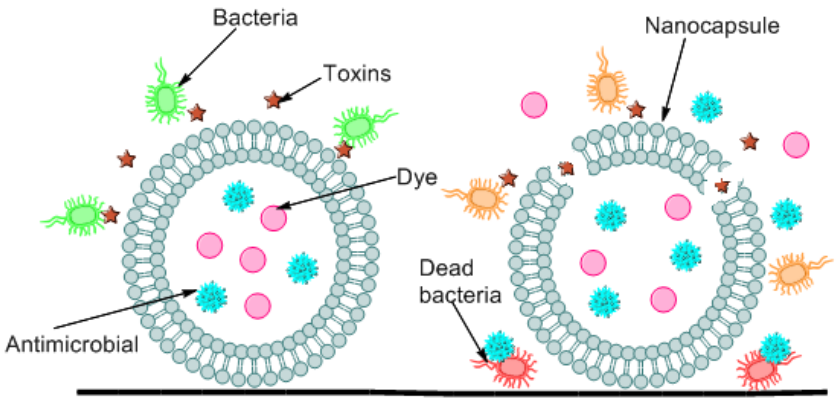

Figure 1-4. The lytic response of vesicles in the presence of pathogenic bacterial toxins

1.5 Aim of this work

This investigative work is a continuation of the EU FP7 project Bacterio Safe, which aims to develop 'a wound dressing which involves the sophisticated design of nanocapsules that release signalling molecules and antibiotic / antimicrobials in the presence of pathogenic bacteria'. This aim has been integrated, adapted and developed within this project to advance progress and address other applications of vesicles for advanced wound management and alternative therapies.

This work is divided into 7 chapters and brief summaries into the aims of each of these are given here. Chapter 2 provides an overview of the experimental procedures and analytical instrumentation, including introductive descriptions of principals, utilised as part of this investigation. More information about techniques may be found at relevant points within each succeeding chapter. Chapter 3 concentrates on the development of vesicle structural composition, containing a signalling dye that is stable to certain environmental stimulus, such as increased temperature and changes in pH. Chapter 4 concentrates on investigating the sensitivity of successfully stabilised vesicle compositions, from chapter 3, to pathogenic bacterial toxins, whilst remaining unaffected by the presence of non-pathogenic bacteria. This system will ensure that harmful bacteria can be exclusively detected. Chapter 5 concentrates on the successful incorporation of these stable and sensitive vesicle compositions into matrices that can be utilised for topical application onto a wound. Chapter 6 aims to determine a sterilising method suitable for treatment of the vesicles to ensure that they can be incorporated into dressings suitable for wound applications. An emphasis is placed on the maintenance of vesicle structure following treatment. Chapter 7 concentrates on

incorporating additional functional and protective agents to provide vesicle systems with enhanced selective activities.

Chapter 8 concentrates on investigating the depth of penetration and potential damaging effects of microplasma jet treatment using a synthetic biological sensor containing vesicles.

1.6 References

1. Percival, S. L.; Cutting, K. F. Microbiology of wounds. *Microbiology of wounds* **2010**.
2. Spellberg, B.; Bartlett, J. G.; Gilbert, D. N. The Future of Antibiotics and Resistance. *New England Journal of Medicine* **2013,** 368, 4, 299-302.
3. Engler, A. C.; Wiradharma, N.; Ong, Z. Y.; Coady, D. J.; Hedrick, J. L.; Yang, Y.-Y. Emerging trends in macromolecular antimicrobials to fight multi-drug-resistant infections. *Nano Today* **2012,** 7, 3, 201-222.
4. Cars, O.; Hedin, A.; Heddini, A. The global need for effective antibiotics-Moving towards concerted action. *Drug Resistance Updates* **2011,** 14, 2, 68-69.
5. Parisien, A.; Allain, B.; Zhang, J.; Mandeville, R.; Lan, C. Q. Novel alternatives to antibiotics: bacteriophages, bacterial cell wall hydrolases, and antimicrobial peptides. *Journal of Applied Microbiology* **2008,** 104, 1, 1-13.
6. Elliott, T.; Worthington, T.; Osman, H.; Gill, M. *Medical Microbiology and Infection*. 4th ed.; Blackwell Publishing: **2007**.
7. Baker, S.; Nicklin, J.; Khan, N.; Killington, R. *Microbiology*. Taylor & Francis: BIOS Instant Notes, **2007**.
8. Barer, M. R. Morphology and nature of micro-organisms. In *Medical Microbiology*, 16th ed.; David Greenwood, R. C. B. S., John F Peutherer, Ed. Churchill Livingstone: Elsevier science, **2002**; 9-24.
9. Vellai, T.; Vida, G. The origin of eukaryotes: the difference between prokaryotic and eukaryotic cells. *Proceedings of the Royal Society of London. Series B: Biological Sciences* **1999,** 266, 1428, 1571-1577.
10. Whitman, W. B.; Coleman, D. C.; Wiebe, W. J. Prokaryotes: The unseen majority. *Proc. Natl. Acad. Sci*. USA, **1998**; *95*, 6578-6583.
11. Pitt, T. L.; Barer, M. R. *Medical microbiology : a guide to microbial infections ; pathogenesis, immunity, laboratory diagnosis and control*. 18 ed.; Elselvier: Churchill Livingstone, **2012**.
12. Williams, P. Quorum sensing, communication and cross-kingdom signalling in the bacterial world. *Microbiology* **2007,** 153, 12, 3923-3938.
13. Watnick, P.; Kolter, R. Biofilm, City of Microbes. *Journal of Bacteriology* **2000,** 182, 10, 2675-2679.
14. Watnick, P. I.; Kolter, R. Steps in the development of a Vibrio cholerae El Tor biofilm. *Molecular Microbiology* **1999,** 34, 3, 586-595.
15. Davies, D. G.; Parsek, M. R.; Pearson, J. P.; Iglewski, B. H.; Costerton, J. W.; Greenberg, E. P. The Involvement of Cell-to-Cell Signals in the Development of a Bacterial Biofilm. *Science* **1998,** 280, 5361, 295-298.
16. Prigent-Combaret, C.; Vidal, O.; Dorel, C.; Lejeune, P. Abiotic Surface Sensing and Biofilm-Dependent Regulation of Gene Expression in Escherichia coli. *Journal of Bacteriology* **1999,** 181, 19, 5993-6002.

17. Arciola, C. R.; Campoccia, D.; Speziale, P.; Montanaro, L.; Costerton, J. W. Biofilm formation in Staphylococcus implant infections. A review of molecular mechanisms and implications for biofilm-resistant materials. *Biomaterials* **2012,** *33*, 26, 5967-5982.
18. Hooper, L. V.; Gordon, J. I. Commensal Host-Bacterial Relationships in the Gut. *Science* **2001,** 292, 5519, 1115-1118.
19. Mack, D.; Rohde, H.; Harris, L. G.; Davies, A. P.; Horstkotte, M. A.; Knobloch, J. K. Biofilm formation in medical device-related infection. *Int J Artif Organs* **2006,** 29, 4, 343-59.
20. Salyers, A. A.; Whitt, D. D. *Bacterial Pathogenesis A Molecular Approach*. 2 ed.; ASM Press: **2002**; 560.
21. Lazarus Gs, C. D. M. K. D. R.; et al. Definitions and guidelines for assessment of wounds and evaluation of healing. *Archives of Dermatology* **1994,** 130, 4, 489-493.
22. Feck, G. A.; Baptiste, M. S.; Tate, C. L. Burn injuries: epidemiology and prevention. Accident Analysis Prevention, **1979**; 11, 129-136.
23. Hsu, C.; Phillips, W. R.; Sherman, K. J.; Hawkes, R.; Cherki, D. C. Healing in Primary Care: A Vision Shared by Patients, Physicians, Nurses, and Clinical Staff. *Ann. Fam. Med*., **2008**; 6, 307-314.
24. Shakepeare, P. Burn wound healing and skin substitutes. *Burns*, **2001**; 27, 517-522.
25. Martin, P. Wound Healing-Aiming for perfect skin regeneration. *Science*, **1997**; 276, 75-81.
26. Thomas, S. Wound Healing. London: The Pharmaceutical Press, 1990; p Chapter I.
27. Evers, L. H.; Bhavsar, D.; Mailander, P. The biology of burn injury. *Experimental Dermatology* **2010,** 19, 9, 777-783.
28. Oostema, J. A.; Ray, D. J. Evidence-based emergency medicine - No clear winner among dressings for partial thickness burns. Annals of emergency medicine, **2010**; 56, 98-299.
29. Thomas, S. S.; Lawrence, J. C.; Thomas, A. Evaluation of hydrocolloids and topical medication in minor burns. *Journal of Wound care*, **1995**; 4, 218-220.
30. Wasiak, J.; Cleland, H. Minor thermal burns. BMJ Publishing Group: Clinical Evidence, **2005**.
31. Wasiak, J.; Cleland, H.; Campbell, F. Dressings for superficial and partial thickness burns. John Wiley & Sons, Ltd: The Cochrane Collaboration, **2010**; 10.
32. Griffiths, H. R.; Thornton, K. L.; Clements, C. M.; Burge, T. S.; Kay, A. R.; Young, A. E. R. The cost of a hot drink scald. *Burns*, **2006**; 32, 372-374.
33. Miyazaki, H.; Kinoshita, M.; Saito, A.; Fujie, T.; Kabata, K.; Hara, E.; Ono, S.; Takeoka, S.; Saitoh, D. An ultrathin poly(l-lactic acid) nanosheet as a burn wound dressing for protection against bacterial infection. *Wound Repair and Regeneration* **2012,** 20, 4, 573-579.
34. Kondo, S.; Kuroyanagi, Y. Development of a Wound Dressing Composed of Hyaluronic Acid and Collagen Sponge with Epidermal Growth Factor. *Journal of Biomaterials Science, Polymer Edition* **2012,** 23, 5, 629-643.
35. Muthukumar, T.; Senthil, R.; Sastry, T. P. Synthesis and characterization of biosheet impregnated with Macrotyloma uniflorum extract for burn/wound dressings. *Colloids and Surfaces B: Biointerfaces* **2013,** 102, 0, 694-699.
36. Selig, H. F.; Lumenta, D. B.; Giretzlehner, M.; Jeschke, M. G.; Upton, D.; Kamolz, L. P. The properties of an "ideal" burn wound dressing--what do we need in daily clinical practice? Results of a worldwide online survey among burn care specialists. *Burns* **2012,** 38, 7, 960-6.
37. Gabriel, A.; Heinrich, C.; Shores, J. T.; Baqai, W. K.; Rogers, F. R.; Gupta, S. Reducing Bacterial Bioburden in Infected wounds with vacuum assisted closure and a new silver dressing -- A Pilot study. *Wounds* **2006,** 245-255.

38. Silver, S.; Phung, L.; Silver, G. Silver as biocides in burn and wound dressings and bacterial resistance to silver compounds. *Journal of Industrial Microbiology and Biotechnology* **2006,** 33, 7, 627-634.
39. Zhou, J.; Loftus, A. L.; Mulley, G.; Jenkins, A. T. A. A Thin Film Detection/Response System for Pathogenic Bacteria. *Journal of the American Chemical Society* **2010,** 132, 18, 6566-6570.
40. Gardner, S. E.; Frantz, R. A.; Doebbeling, B. N. The validity of the clinical signs and symptoms used to identify localized chronic wound infection. *Wound Repair and Regeneration* **2001,** 9, 3, 178-186.

Chapter 2 Experimental and instrumentation

This chapter provides an introduction to the formulation and treatment of vesicles within this project, and the range of analytical techniques used to characterise the results obtained.

2.1 Materials

Chemicals and solvents, of HPLC grade, were sourced primarily through Sigma Aldrich, with the following exceptions. The majority of the lipid derivatives were obtained from Avanti Polar Lipids (APL) (except from DSPC and DSPE which were obtained from Sigma Aldrich). Sephadex NAP-25 columns were obtained from GE healthcare. 6-, 12- and 96- well costar plates were obtained from Fisher Scientific. Carbopol 981 P NF was obtained from Surfachem.

2.2 Vesicle formulation process

Vesicles were composed primarily of phosphatidylcholine (PC) lipids, phosphatidylethanolamine (PE) lipids, and cholesterol. The vesicle components were stored at -20 °C, and dissolved individually in chloroform at a concentration of 0.1 $moldm^{-3}$, followed by combination together to enable synthesis of different vesicle compositions.

The vesicles were synthesised in a similar procedure to that carried out by Nayar, Hope and Cullis reported in 1993.[1] 100 µl total of different stock solutions was added to 200 µl of chloroform, followed by drying with nitrogen gas to form a thin film. 5 ml of 50 mM [5,6]-carboxyfluorescein was added, heated to 75 °C, cooled, and freeze-thawed three times before pressurised using Nitrogen (10-15 bar) five times through two 100 nm polycarbonate membranes in the LiposoFast LF 50 extruder, at approximately 60 °C. Purification from unencapsulated dye was achieved using a Sephadex NAP 25 column and HEPES buffer. The vesicles were then stored overnight at 4 °C prior to use. The process is depicted visually in Figure 2-1.

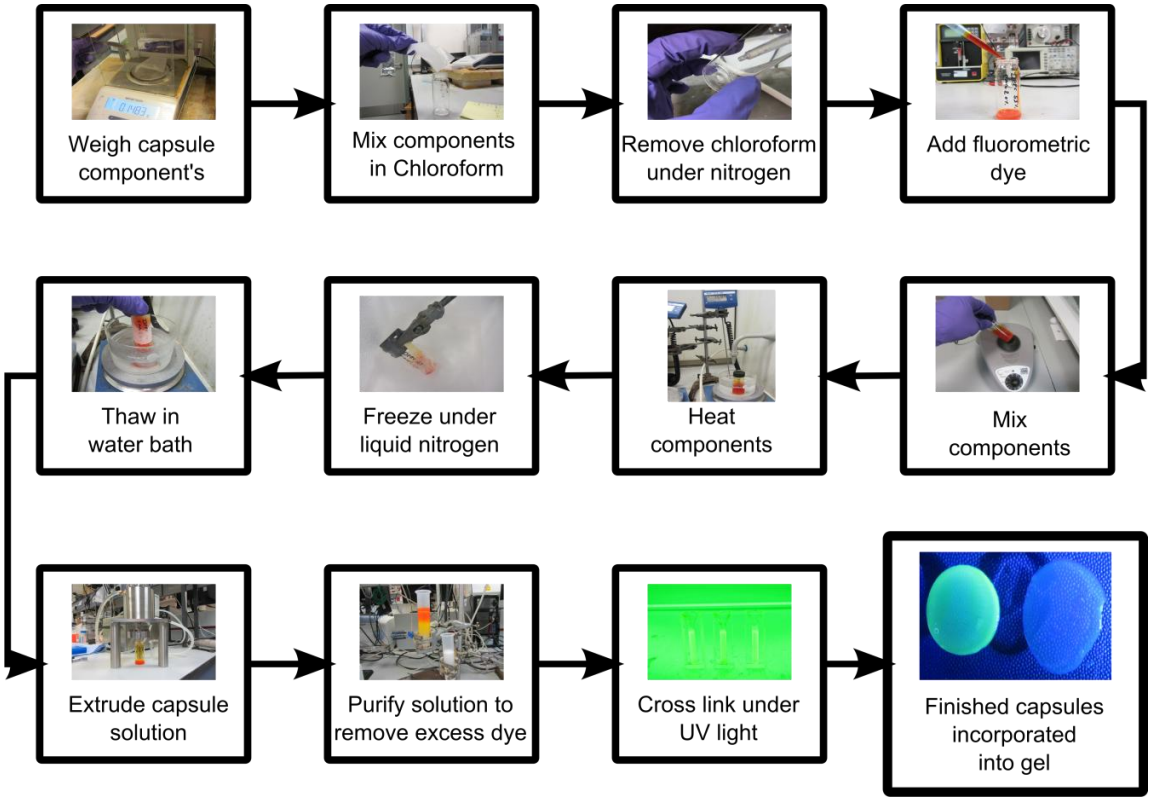

Figure 2-1. Vesicle formulation process. Image acknowledgements to W. D. Jamieson

2.2.1 Solvent free vesicles

Preparation of vesicles involved hydrating lipid components, (DSPC, DPPC and DSPE), in 2 ml 50 mM 5(6)-CF buffer under a nitrogen atmosphere at room temperature for one hour. After this time, cholesterol was heated to 120 °C following addition of 3 % (v/v) glycerol for 20 minutes, until dissolution occurred. The temperature was lowered to 75 °C and the lipid components were added, followed by stirring for 30 minutes. To encourage formation of vesicles, and in parallel to the standard method used, this solution underwent three freeze-thaw cycles, followed by extrusion in a LF-50 extruder through a 100 nm membrane, and purification through a NAP-25 column.

2.2.2 Aqueous buffer preparation

The aqueous buffer solutions were made according to the compositions given below. The chemicals were weighed using a HR120 A&D analytical balance able to resolve to 0.1mg and

dissolved in ultra-pure deionised water obtained from Thermo scientific Barnstead easy pure II purification system, sonicated as required, and stored at 4 °C.

Chemical	HEPES buffer – pH 7.4	5(6)-CF dye
Deionised water	750 ml	100 ml
NaCl	4.680 g	0.0585 g
NaOH	0.168 g	0.5405 g
HEPES	1.7895 g	0.2387 g
EDTA	0.219 g	0.0285 g
5(6)-CF	-	1.8789 g

Table 2-1. The composition of the HEPES storage buffer and 5(6)-CF dye.

2.2.3 Cross linking of vesicles

Vesicles formed with TCDA were irradiated with UV light, following purification and storage for a minimum of 5 hours at 5 °C; at 254 nm for 12 seconds using a commercial flood exposure UV source from Hamamatsu™, for cross linking of polymerisable components.

2.3 Microbiological assays

All microbiology assays were carried out in a class II safety cabinet where aseptic techniques were utilised. Sterilisation of surfaces and gloved-hands was achieved using 70 % v/v ethanol. All equipment used for contact with microbes (e.g. pipette tips and tubes) were decontaminated through autoclaving; the heating of a sample to a minimum of 121 °C, 15 psi for 15 minutes. A ScanLaf class II Microbiological safety cabinet was utilised for all microbiological based work.

2.3.1 Bacterial growth agar

The agar, Luria (LA) and Tryptic soy (TSA), used for gram negative and gram positive bacterial growth respectively, were made from their dehydrated forms, according to the compositions given on the containers. The chemicals were dissolved in ultra-pure deionised

water obtained from Thermo scientific Barnstead easy pure II purification system, autoclaved, and whilst a liquid, poured into petri dishes. Formation of colonies on the agar prior to inoculation with a bacterial strain indicated contamination.

2.3.2 Bacterial growth media

Bacteria growth in media solution was carried out in the aqueous broth, Luria (LB) and Tryptic soy (TSB), used for gram negative and gram positive bacterial growth respectively. These were made from their dehydrated forms, according to the compositions given on the containers. The chemicals were weighed using a HR120 A&D analytical balance able to resolve to 0.1 mg and dissolved in ultra-pure deionised water obtained from Thermo scientific Barnstead easy pure II purification system, autoclaved, and stored. Cloudiness in solution following storage indicated contamination.

2.3.3 Bacteria preparation

Bacteria were obtained from glycerol stock cultures stored at -80 °C and streaked onto Luria Broth (LB) agar plates in the case of gram negative organisms, and Tryptic Soy Broth (TSB) agar plates in the case of gram positive organisms. These agar plates were place into an incubator at 37 °C for 16 hours. Following growth of individual colonies, and utilising aseptic techniques, a single colony was transferred from the plates into 10 ml of LB or TSB and incubated with agitation for 16 hours at 37 °C, shown in Figure 2-2.

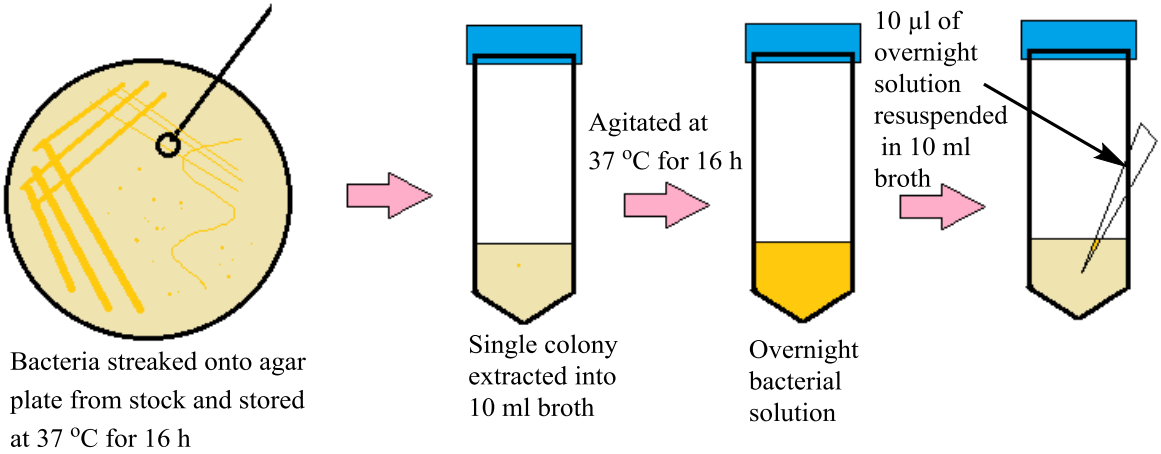

Figure 2-2. Preparation of an individual bacterial strain prior to addition to a sample

Following overnight growth in broth, the cultures have reached the stationary phase of their growth cycle, Figure 2-3, however log phase growth is required prior to addition to samples and so 10 µl of this culture is re-suspended in 10 ml of LB or TSB.

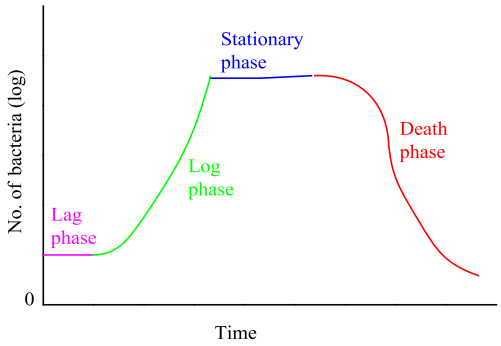

Figure 2-3**.** Bacteria growth curve. The log and stationary phase is desired for the bacteria to be producing and releasing toxins that have a potential effect of the stability of the vesicles

Following re-suspension, the log-phase bacteria was applied to test samples in a 2:1 ratio, under constant agitation, at 37 °C for a minimum of 16 hours.

2.3.4 Bacteria supernatant preparation

Within this investigation the term ‘supernatant’ refers to the separable solution obtained from a bacteria culture following centrifugation and discarding of the pellet (whole bacterial cells). Bacteria were prepared as described above; however following overnight growth in broth the bacteria / growth medium solution was centrifuged for 20 minutes to form a pellet, followed by pressurisation of the solution through a 0.22 µm filter. The solution obtained could be

used instantly or frozen into aliquots. Supernatant was applied to test samples in a 1:1 ratio primarily for time periods of less than two hours.

2.4 Dressing prototypes

The delivery medium of vesicles was based on hydrogel formulations suitable for topical applications. These formulations were required to provide stability to the vesicles, and a diffusible network through which bacterial toxins and internal vesicle active agents can diffuse.

2.4.1 Hydrogels

The hydrogels used in this project to create a prototype wound dressing were synthesised at different concentrations and compositions using HEPES buffer as the aqueous phase and were pH adjusted as required. These different hydrogel agents were formulated to ensure provision of a stabilised environment for incorporation of the vesicles, whilst maintaining a structure appropriate for potential application to skin. Primary hydrogel candidates included Carbopol 981P NF, gelatin, hypromellose and agarose. Individual gels were composed of the following: 5 wt % gelatin, 1.5 wt % carbopol, 1 wt % agarose and 2 wt % hypromellose, with HEPES buffer and 30 % v/v of the stabilised and sensitive vesicle solutions.

2.5 Vesicle sterilisation

The decontamination, disinfection and sterilisation of vesicles was investigated using a variety of physical methods. These methods include sterilisation by applying radiation (electromagnetic or particle), increasing the temperature (heat) and filtration (micro-porous membranes). Within these techniques an emphasis was placed on vesicle stability following sterilisation. Vesicle stability comparisons were obtained using the fluorescence response after addition of a lytic agent or HEPES buffer to sterilised vesicles. Non-sterilised vesicles were utilised as a control.

2.5.1 Gamma radiation sterilisation

The gamma sterilisation of different vesicle compositions was carried out using a Gammacell GC1000 with a Caesium 137 (^{137}Cs) radioisotope source. The ^{137}Cs source was used at a calibration of 7.713 Gy, for 58 hours to give a sterilising gamma radiation dose of 25 kGy (carried out by the Blonde McIndoe Research Centre, UK). This sterilising dose is sufficient to ensure absolute sterilisation of vesicles.

2.5.2 Heat sterilisation

The sterilisation of vesicles to thermal moist sterilisation treatment was carried out by heating samples to 80 °C for 10 minutes, 30 minutes and 60 minutes, and using a standard autoclave machine, with a treatment time of 60 minutes at 120 °C.

2.5.3 Filter sterilisation

The filter sterilisation of vesicle samples was carried out following pressurisation of the vesicles through 0.1, 0.22 and 0.45 µm filter membranes. The 0.22 and 0.45 µm filter membranes, manufactured by Merck Millipore, were composed of mixed cellulose esters, and the 0.1 µm filter was composed of polyvinylidene fluoride (PVDF), both with a process volume capability of 100 ml.

2.6 Vesicle modification

Vesicle modification was investigated on the formed vesicles to improve both the specificity and stability of vesicles.

2.6.1 Hyaluronic acid coupling

The hyaluronic acid was prepared by dissolving in HEPES buffer (10 mg ml^{-1}), followed by stirring for 4 hours; and activation with ethyl(dimethylaminopropyl) carbodiimide (EDC) (1 eq) and *N*-hydroxysuccinimide (NHS) (1 eq). This was added in a 2:1 ratio to standard TCDA-DS vesicles (200 nm) containing the self-quenched dye 5(6)-CF, or modified TCDA-DS vesicles containing 6 mol % stearylamine in the bilayer (added at the same point of

formulation as the other membrane components, followed by the formation of the dehydrated thin film).

2.7 Treatment of vesicles with plasma

Plasma was utilised to treat vesicles dispersed in a gelatin matrix as a synthetic biological sensor to monitor the effects of microplasma jet treatment on biomimetic vesicles.

2.7.1 Microplasma jet

The plasma jet assembly consisted of a glass capillary tube with an inner diameter of 0.8 mm that was surrounded by two external hollow electrodes separated 4 mm apart, as shown in B in Figure 2-4. The plasma was operated with 100 ml min^{-1} of helium at an applied voltage potential of 5.5 $kV_{peak\text{-}peak}$ and a frequency of 10 kHz. These operational conditions produced a plasma plume of approximately 10 mm in length. The plasma jet was housed inside a custom-built reactor (Cantech Pty Ltd, Adelaide, Australia) equipped with a 3-axis sample positioning stage, mass flow controllers and a power supply, [294] depicted in A in Figure 2-4.

A B

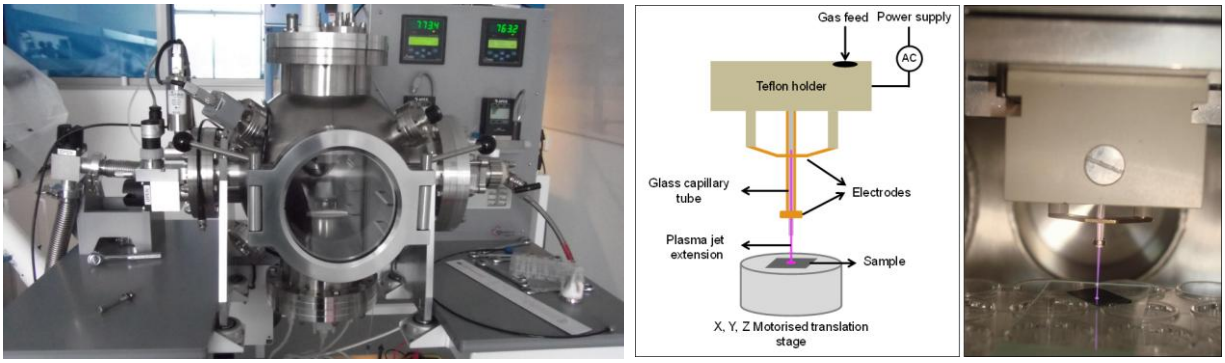

Figure 2-4. The micro plasma reactor and jet**,** where (A) is a photograph of the custom built micro-plasma reactor system and (B) is a schematic and photograph of the microplasma jet.

2.7.2 Synthetic sensor

The synthetic sensor was created utilising DSPG-DP vesicles (for composition see Table 3-5) containing 50 mM 5(6)-CF. These were added (30 % v/v) to 5 % gelatin in HEPES and placed onto sample petri dishes at a depth of 2 mm. A control gelatin matrix was also

prepared with non-encapsulated (5(6)-CF (30 % v/v)). Treatment of the synthetic tissue was performed at 2 and 3 mm separation distances (*d*) between the end of the glass capillary tube and the surface of the gelatin matrix and for treatment times of 15, 60 and 300 s. Treatment was performed at two different angles: either perpendicular or in parallel to the sample surface (comparison carried out by S. Hong). To analyse treatment from the neutral helium gas (no plasma) the treatment was carried out using the same flow rate of helium but with no applied voltage. As a control experiment treatment of 5(6)-CF-gelatin was also carried out.

2.8 Methods of characterisation

The following techniques were used to measure, characterise or observe the vesicles and their response to various agents, in addition to other related chemicals, at different stages of the investigation.

2.8.1 FLUOstar Omega plate reader

A FLUOstar Omega plate reader is a modular multi-mode microplate reader platform that allows flexible measurement of UV-Vis absorption and fluorescence intensity at a wide range of wavelengths. Fluorescence band pass excitation and emission filters of 485 ± 12 nm and 520 nm were used, with a gain of 650. Optical density, utilised for monitoring bacterial growth, was measured at 600 nm (OD_{600}).

The general schematic of a spectrometer is given in Figure 2-5. Application of a light source with a high intensity, broad wavelength output is focussed onto and through an excitation monochromator. The monochromator ensures selection of the desired wavelength, which can then be focussed onto the fluorophore containing sample. A proportion of the incident light is absorbed of by the fluorophore, and consequentially emitted. Isolation of the emitted light from contamination is achieved by passing the emission through a second monochromator, which can then be photomultiplied and detected.

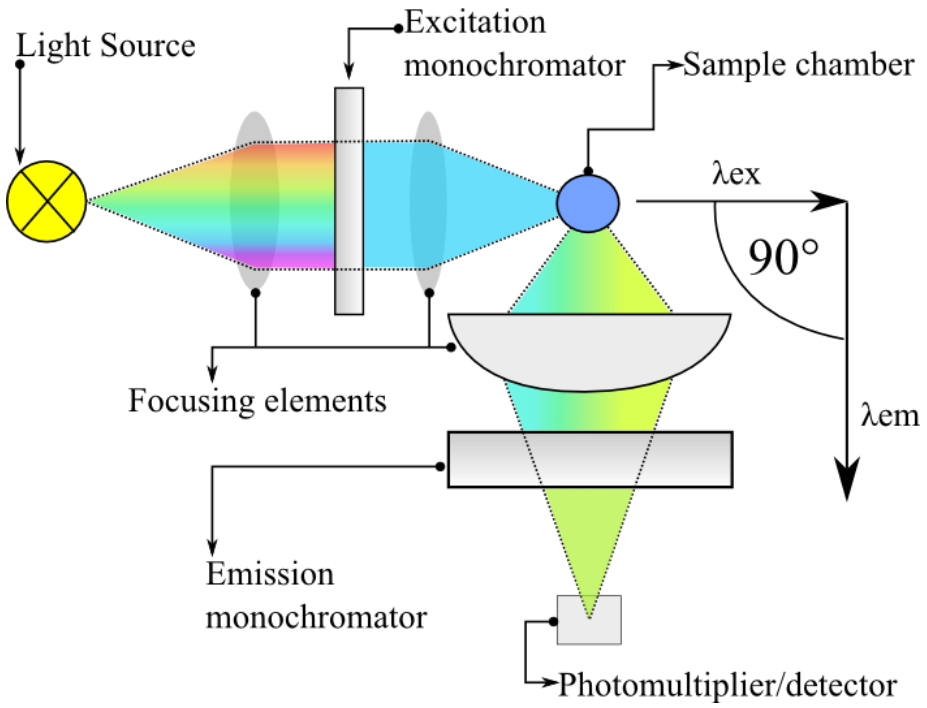

Figure 2-5. Schematic of an epi-fluorescent spectrometer. Acknowledgements to W. D. Jamieson, PhD thesis 2013.

Fluorescence intensity is defined in terms of arbitrary units (au). In addition to this the introduction of the stability response parameter (Equation 3-29) allows comparisons between different experiments to be made.

Experiments were carried out using nunc 6 or 12 or costar 96 well plates, and endpoint or continual readings were obtained. The use of micro titre plates for fluorescence and absorption readings ensured that focussing and detection of emitted light from the fluorophore was required at an angle of 45° as opposed to the conventional 90° detection angle (relative to the path of the incidence excitation light). All measurements were completed in triplicate.

2.8.2 Brightfield and fluorescence microscopy

Brightfield microscopy allows for simple optical microscopy illumination following transmission of white light through a sample. Fluorescence microscopy utilises the emitted fluorescence following excitation to visualise a sample (discussed in more detail in chapter 3 (3.2.1 Fluorescence)).

Brightfield and fluorescence microscopy was carried out using a Nikon Inverted Microscope TE-2000. Fluorescence images were captured through a Nikon filter with 455-485 nm excitation and 500-545 nm emission using a 4x objective. Images were recorded with a Nikon DXM1200C digital camera and processed using NIS-Elements Basic Research v2.2 software. Fluorescence intensity profiles were recorded using the same exposure time of 48 ms for all of the samples. Fluorescence intensity values for each treatment were produced from 60 data points by measuring 20 different positions at a distance of 45 µm across the centre of each treatment area. Experiments were performed in triplicate.

2.8.3 Confocal microscopy

Confocal microscopy is utilised in this project to visualise vesicles and assess the impact of micro plasma jet treatment containing a fluorescent dye (5(6)-CF) or a fluorescently tagged lipid (Texas red DPPE). As shown in Figure 2-6, an incident light is passed through an objective lens and directed onto a sample; emitted light then passes to the detector. A 3D image of the sample can be generated following detection of scans in the x, y and z directions.

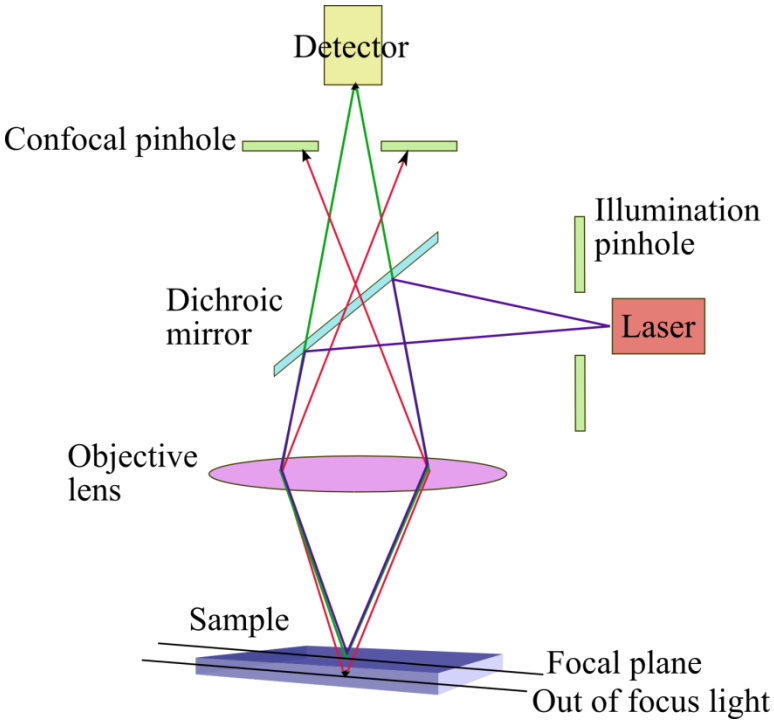

Figure 2-6**.** Confocal microscope schematic

Two different confocal microscopes were used for the purpose of analysis of these results. For analysis of vesicle containing samples the confocal microscopy images were obtained using a laser scanning Zeiss LSM510, equipped with a 488 nm laser. For analysis of plasma treated samples the confocal microscopy images were obtained using a Nikon A1-R Microscope, equipped with a 488 nm DAPI laser and a 10x CFI Plan Fluor DL objective. Z-stack images through the sample were obtained with 5 µm incremental adjustments of the sample height. NIS-Elements Advanced Research software was used for image processing and analysis.

2.8.4 Nanoparticle tracking analysis

Nanoparticle tracking analysis (NTA) is a technique utilised to measure size and visualise vesicles on a particle-by-particle basis, in polydispersed liquids at real time with minimal sample preparation. A laser light source illuminates nanoscale particles from approximately 10 nm to 1000 nm, Figure 2-7.

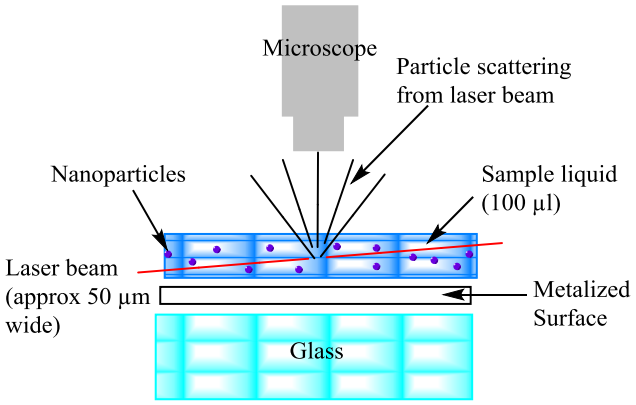

Figure 2-7**.** Schematic diagram of a Nanoparticle tracking analysis instrument

A finely focused 635 nm laser beam is passed through a prism-edged optical flat, of which the refractive index is such that the beam refracts at the interface between the optical flat and the liquid sample layer placed above it. Due to the refraction, the beam compresses to a low profile, intense illumination region in which nanoparticles present in the liquid film can be easily visualised via a long-working distance, x20 magnification microscope objective fitted to an otherwise conventional microscope. The metalized surface reduces the amount of light scattering, which decreases the background noise, hence it is at the beam point of contact here that videos are obtained. A charge coupled device (CCD) camera, operating at 30 frames per second, is used to capture a video with a field of view approximately 100 µm x 80 µm.

Particle concentration and size measurements were obtained using a Nanosight Nanoparticle Tracking Analysis NS500. Sizes between 50-2000 nm could be detected, following 50 - 100x dilution.

2.8.5 Dynamic light scattering

Dynamic light scattering (DLS) allows accurate measurement of the size of particles in a solution through the scattering of a monochromatic light source by a particle. Vesicle diameter was obtained using a Zetasizer Nanoscale Dynamic Light Scatterer, manufactured by Malvern instruments, Malvern UK. Measurements were taken of multiple samples each with multiple readings and through the average of these values. 5-10 µl of sample was dispersed into 1 ml of buffer solution prior to measurement.

2.8.6 Osmolality

Osmolality measures the number of milliosmoles/kg (mOsm/kg) of solvent present within an aqueous solution. The osmolality ξ of a sample is defined in Equation 2-1 as

$$\xi = \upsilon \text{ x } N_{mol} \qquad \text{Equation 2-1}$$

Where υ is a measure of ionisation of a solution (υ = 1 if the solution is undissociated), and N_{mol} is the number of moles of undissociated substance within a solution.

Osmolality can be found from measuring the freezing point depression of a sample, and incorporating the values into a rearranged form of Equation 2-2;

$$\xi = \frac{\Delta T\ (°C) \text{ x } 1000\ (mOsm)}{1.858\ (°C)} \qquad \text{Equation 2-2}$$

The freezing point depression of a sample can be compared against pure water to give the osmotic concentration. Pure water freezes at 0 °C; an aqueous undissociated ideal solution with an osmolarity of 1 osmol / kg H_2O freezes at -1.858 °C.

Osmometer measurements on vesicles and hydrogel preparations were carried out using a Löser Micro-Osmometer Type 15 to give an indication of compatibility between vesicles and hydrogel matrices. Calibration was carried out using distilled water. 50 µl of sample was cooled using a Peltier-element; a semiconductor which uses the Peltier effect to create a heat flux within the sample. A thermistor measures the temperature of the sample; at a specific

super cooling temperature a needle containing ice crystals is added to initiate the freezing process, followed by a rise in temperature due to latent heat of crystallisation. The linear correlation between osmolality and the freezing point allows osmolality to be determined; units are mOsm /kg H_2O.

2.8.7 Differential scanning calorimetry

Differential scanning calorimetry (DSC) is a thermoanalytical technique that measures the temperatures and heat flows associated with a phase transition of a material as a function of time and temperature applied, versus a reference sample. The thermal transitions were measured using a TA Instruments DSC Q20. Temperature ranges were obtained 10-15 °C above or below predicted transition temperature. Aluminium hermetic T_{zero} pans with lids filled with a sample volume of 10 µl, able to withstand temperatures between -180 to 600 °C, were used. Reference pans containing the relevant buffer solution, omitting the lipid, were utilised as a control. Data obtained was analysed using TA Universal Analysis software.

2.8.8 Nuclear magnetic resonance

^{1}H and ^{13}C NMR samples were analysed using a Bruker AV300 MHz spectrometer. Sample preparation involved dissolving approximately 5 mg of substance in an appropriate solvent, commonly deuterated chloroform ($CDCl_3$), DMSO or methanol depending on solubility, and transferring to a clean sealable NMR tube.

2.9 Statistical analysis

The data was processed using Microsoft Excel and OriginPro8. Statistical analysis was performed using a Student t-Test by comparing the means of each independent group (sample type) assuming that the variances of each group are equal. A *p* value of less than 0.05 (65 % confidence limit) was considered to be of significant difference, Equation 2-3;

$$S_E = \frac{\sigma\,(V_T)}{\sqrt{(V_c)}} \qquad \text{Equation 2-3}$$

Where S_E is the statistical error, σ is the standard deviation, V_T is the cumulative sum of the values, and V_c is the sum of the count of the values. The propagation of combined errors was achieved using Equation 2-4;

$$P_E = (\sqrt{(\left(\frac{F_E}{F}\right)^2)} + \sqrt{(\left(\frac{I_E}{I}\right)^2)}\, N) \qquad \text{Equation 2-4}$$

Where P_E is the propagative error, F_E is the final error value, F is the final value, I_E is the initial value error, I is the initial value and N is the new value calculated.

2.10 References

1. Weinstein, J.; Ralston, N. E.; Leserman, L. D.; Klausner, R. D.; Dragsten, P.; Henkart, P.; Blumenthal, R. *Liposome Technology*. Gregoriadis G ed ed.; CRC Press: **1984**.

Chapter 3 Vesicle development - stability

The quantity of books, research papers, and patents published on the use of vesicles to deliver encapsulated aqueous active agents, either *in vivo* or *ex vivo* to a potential patient has increased steadily since the 1980s, although they were initially discovered in 1964.

Vesicles, also commonly referred to as liposomes or nanocapsules, are attractive drug delivery vehicles due to their biocompatible and bioavailable properties. Vesicles have the ability to entrap aqueous solutions of different lipophilicities within their core, surrounding them by inert naturally derived or synthetic phospholipids; as such they have been extensively studied and applications include cosmetics, the food industry, diagnostics and medical drugs delivery.[1, 2]

3.1 Vesicle applications

The ability of vesicles to act as protective carriers for expensive, reactive or readily degraded active ingredients has ensured their popularity for a variety of applications. Delivery of an active agent to a target site, either *in vivo* or *ex vivo* can be problematic. This can either be due to penetration difficulties, e.g. through the stratum corneum,[3] or as a result of active agent hydrolysis prior to arrival at intended site, e.g. enzyme mediated degradation.[4] As a result of this, the majority of research into the utilisation of vesicles for active agent delivery has focused on modifying the vesicles' lipid composition, which affects the physical characteristics, and vesicle size, to increase penetration of vesicle to target site and decrease the passive leakage of agents prior to arrival.

Despite the range of industries that have adopted the use of vesicles to deliver active agents, it comes as no surprise that the most widely investigated area of their practical application is within medical applications; for drug delivery.

3.1.1 Medical applications

Vesicles provide an ideal model, reagent and tool in many areas of scientific research, including maths and theoretical physics, biophysics, chemistry, colloid science, biochemistry and biology.[5] Uses within these fields include investigations into cell membrane and channel

properties, catalysis, energy conversion, stability and thermodynamics of finite systems and excretion, cell function, trafficking and signalling.[1]

The popularity and interest surrounding the utilisation of vesicles for drug delivery has increased significantly in the last ten years. The concept of vesicles as drug delivery vehicles was introduced in the 1970's, following initial investigations and publications into vesicles in the 1960's. Initial results proved disappointing, due to colloidal and biological instability effects, and an inability to efficiently encapsulate drug molecules. However, following further fundamental research into understanding interaction characteristics and inherent stability, improvements ensured that some commercial ventures were launched.[6]

The stability of vesicles and their internal components can be sub-divided into physical, chemical and biological stability categories. These divisions relate to storage conditions, shelf life time and interaction of host agents following application or *in-vivo* administration. A major breakthrough towards obtaining a desired stability was achieved through the use of inert hydrophilic polymer coatings, to create sterically stabilised vesicles. These are also commonly referred to as *stealth* liposomes, due to their inherent ability to evade host immune defences, prior to ultimate low rate removal by macrophages.[1]

Current applications involving vesicle administration that are in the product or pre-clinical stage include anticancer therapy, where the adverse toxicity effects of the drug can be shielded from the host prior to extravasation at the tumour site[7] using doxorubicin (Doxil),[8] and daunorubicin (DaunoXome);[9] systemic fungal treatments using amphotericin B formulations (AmBisome[10] and Amphotec[11]); vaccines against hepatitis A, influenza, hepatitis B, diphtheria and tetanus, where the purified virus is incorporated into the bilayer envelope (Swiss Serum Institute);[12] and gene therapy using lipids to deliver nucleic acids into cell DNA.[13]

Importantly, the efficiency of vesicles as drug delivery vehicles depends on their composition, size, loading efficiency, stability, and their biological interaction with cells.

3.1.2 Intelligent vesicles

Vesicles which are engineered to respond to specific environmental triggers such as pH, temperature and ultrasound, or within a predictive time frame, are commonly referred to as *intelligent* vesicles.[14] Responses can include leakage rate amplification, fusogenic activity or

interaction with specific cells. These engineered changes generally relate to the various phase transitions and fluidic properties of the bilayer, discussed further in 3.1.6 Bilayer fluidity. Briefly, phospholipid bilayers can exist in a low-temperature solid-ordered phase or a fluid-disordered phase; and the temperature at which this transition occurs is known as the phase transition temperature T_c. These phase effects can be tailored depending on the phospholipid selected. Passive leakage of active agents from a vesicle is at its greatest at temperatures around the T_c due to the coexistence of two phases and the resulting defects between the boundaries.[15] As a result of this, delivery of the active agent can be controlled by applying a temperature increase at the target location. An example of this, published in 2010 by Smet *et* al, investigates the delivery of the cytostatic agent doxorubicin encapsulated within temperature sensitive liposomes to cancerous cells in chemotherapy treatment. The process was monitored using magnetic resonance imaging (MRI) contrast agent tracers.[16]

The transition between phases can also be achieved by increasing the total or average area of phospholipid polar head on the outer monolayer of a bilayer, through protonation of lipids containing weak basic groups or hydrolysis, triggering a configuration transition from lamellar to micellar. Alternatively, decreasing the total or average area of phospholipid polar head in the monolayer can induce membrane fusion and the release of active agents.[1] A popular method for achieving this is the incorporation of stabilising PEG, to form PEGylated liposomes, commonly known as stealth vesicles. This protective PEG-coating ensures a long-circulating profile *in-vivo,* enhances permeability and aids host retention.[17] The PEG-coating can be readily detached under localised pathological conditions, such as acidic pH in tumours, ensuring delivery of active agents from the unprotected liposomes.[18]

Intelligent vesicles play an important role in controlled agent activity; tailoring of this inherent intelligence depends on the phospholipids and other constituents incorporated into the bilayer membrane.

3.1.3 Membrane lipids

A typical biological membrane is composed of hundreds of lipid species, varying in acyl chain length, degree of saturation and level of complexity.[19] One of the major structural lipid classes in eukaryotic membranes is the Glycerophospholipids; composed of a hydrophobic diacylglycerol portion which becomes chiral when derivatized to glycerol-3-phosphate, and contains saturated or cis-unsaturated fatty acyl chains of varying length. The phospholipid

membrane backbone is the L isomer, dictating stereochemistry: *sn*-glycerol-3-phosphate. An ester linkage between carbon chains gives phosphatidic acid (PA). Esterification of PA with another alcohol creates Phosphatidylcholine (PC) which accounts for >50 % of the phospholipids found in membranes, phosphatidylethanolamine (PE), phosphatidylserine (PS), phosphatidylglycerol (PG) and phosphatidylinositol (PI). The combination of the phosphate group and the head group yields the polar portion; with the acyl chains forming the non-polar components of the amphiphilic molecules. Glycerophospholipids spontaneously self-organise into a planar bilayer, with the lipids forming a nearly cylindrical molecular geometry.[20]

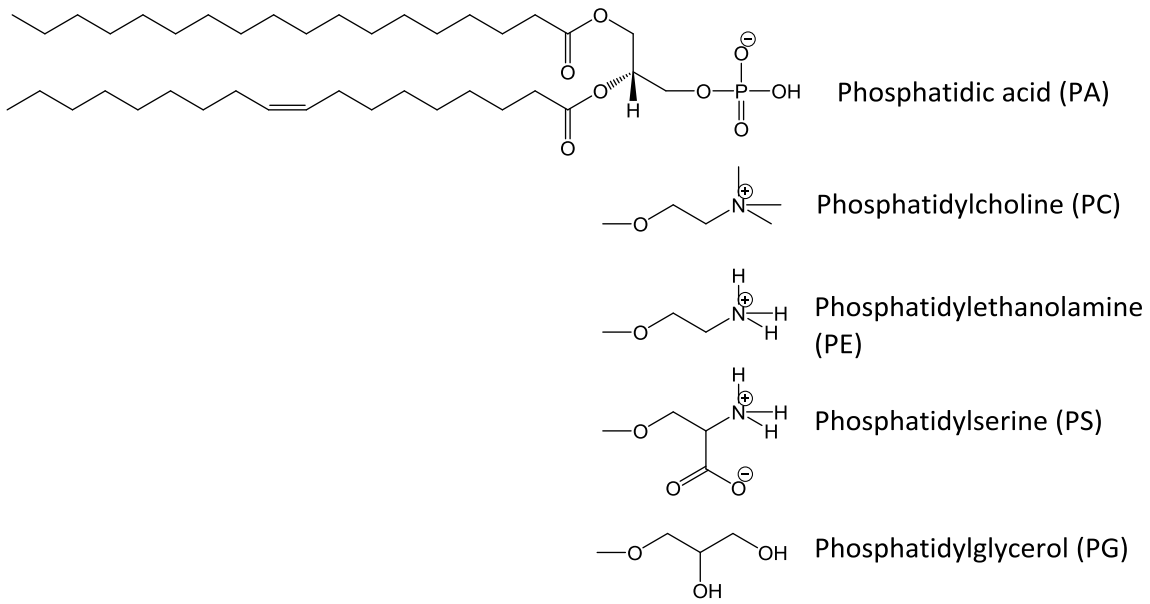

Figure 3-1. The structure of phospholipids; the acyl chain is the non-polar component and can be saturated or *cis* unsaturated, and the phosphate and other head group components form the polar portion of the amphiphilic molecule.

Two other types of lipids found in membranes are sphingolipids; which are based on a long chain amino acid to which a fatty acid acyl chain is attached by amide linkage; and sterol and linear isoprenoids; which are compounds derived from five-carbon isoprene units and cyclised polyisoprene precursors. The variation in head groups and aliphatic chains found in nature ensures that biomembranes are typically composed of over a thousand different lipid types.[21] A common feature of phospholipids in vesicles is their cylindrical shape and the general presence of more than 11 carbons in their acyl chains.[19]

3.1.4 Phospholipid packing formation

The dual (amphiphilic) nature of phospholipids, to be both polar and non-polar, is integral to membrane structures. Variations between different phospholipid compositions ensure different phases are formed. The preferred phase formed is dependent on the different individual steric and ionic interactions that result from variations in sizes and polarity of phospholipid head group and acyl chain. The packing of phospholipids can be defined using the equivalent packing factor (f), Equation 3-1, assuming an environment where water is the aqueous phase, the solution is at a neutral pH and room temperature.[22]

$$f = \frac{v}{al} \qquad \text{Equation 3-1}$$

Where v is the volume of the acyl chain, l the maximum achievable length of the acyl chain (hydrophobic portion), and a is the cross sectional area of the polar head group. The area a can be determined using the van der Waals volume and hydration shell of the polar headgroup.[23] The equivalent packing factor can be used to determine the organisation of individual lipids within different structures, shown in Figure 3-2.

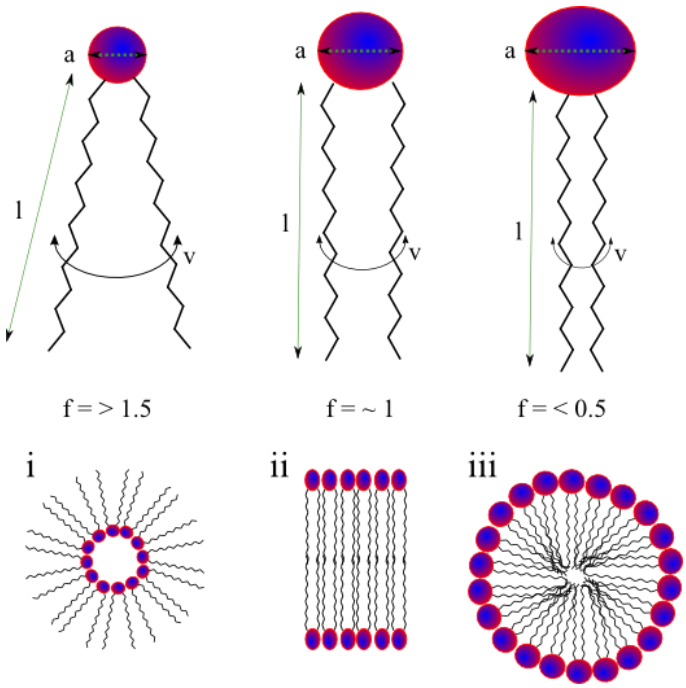

Figure 3-2. The effect of phospholipid structure on packing formation. The three lipids depicted have the same acyl chain length (l) but vary in head group area (a) and acyl chain volume (v). Lipids with a small head group area and large acyl volume favor formation of inverted micelles (i), lipids with similar head group area and acyl chain volume (relative to each other), resulting in cylindrical-like structures, favor formation of lamellar bilayers (ii),

and lipids with a large head group area and small acyl chain volume favors formation of micelles (iii).[24]

Of course, the packing factor (f) defined in Equation 3-1 is only applicable to packing formations of single-phospholipid structures. For mixtures of lipids this equation requires expansion; the average packing factor (P) can be determined using Equation 3-2.

$$\mathrm{P} = \frac{N_x v_x + N_y v_y}{(N_x a_x + N_y a_y)h} = \frac{v_x + R_e v_y}{(a_x + R_e a_y)h} \qquad \text{Equation 3-2}$$

Where v_x and v_y is the volume of the two lipids, a_x and a_y their corresponding polar head group area, h is the average thickness of the mixed layer and R_e is the molar ratio (N_y/N_x). A packing factor of one indicates that the cross sectional area of the polar head group and spatial volume of the acyl chain are equal, indicating that the lipids are essentially cylindrical; a planar bilayer would form.

The transformation of planar bilayer structures into closed bilayer structures, such as vesicles, depends upon an energy barrier trade-off. The interaction of an aqueous solution with an 'open' planar bilayer will be energetically unfavourable, especially compared to the same aqueous interaction with a 'capped' bilayer. However, the spacing between individual molecules within an open bilayer will be energetically favourable compared to the energy involved in forming and maintaining a capped bilayer, where the intermolecular spacing between bilayer components is decreased. This is depicted in Figure 3-3.

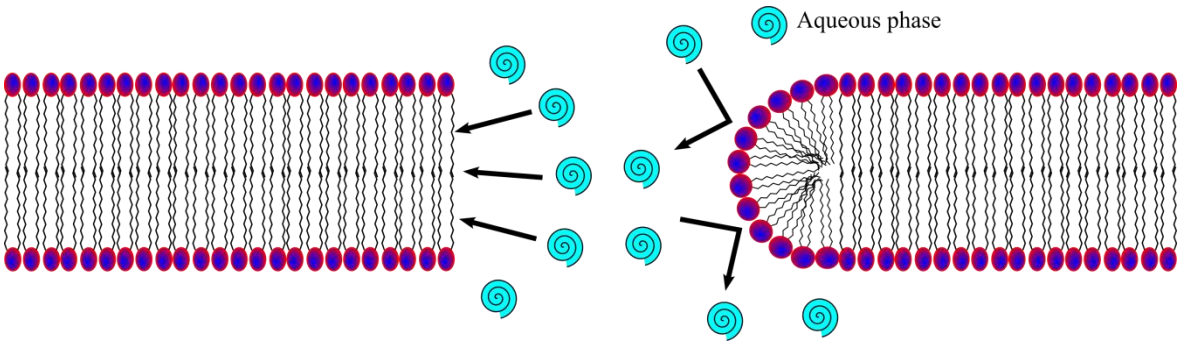

Figure 3-3. The interaction of an aqueous phase with a planar and capped bilayer.

Within most systems, a tendency exists towards the lowest energy state. In this case, formation of capped systems, such as vesicles, provides the lowest energy system.[25] Synthetically, the formation of vesicles can be achieved using a variety of methods, although a common feature is the hydration of lipids with an aqueous solution. The bilayer edges seal to prevent acyl chain contact with the aqueous medium. Although this process is energetically favourable (it is often erroneously reported to be spontaneous), within a synthetic

environment some energy (for example, sonication or extrusion) must be dissipated into the system.[1]

3.1.5 Phase formation

The commonly recognised lamellar phase bilayer is only one possible spontaneous lipid aggregate that can form when amphiphilic lipids are mixed with an aqueous solution. The formation and characteristics of phospholipid behaviour in membranes depend on the lipid-lipid interactions and lipid-protein interactions. Three different polymorphic phase states can be observed depending on the lipids present in a localised membrane; cubic, hexagonal and lamellar, Figure 3-4.

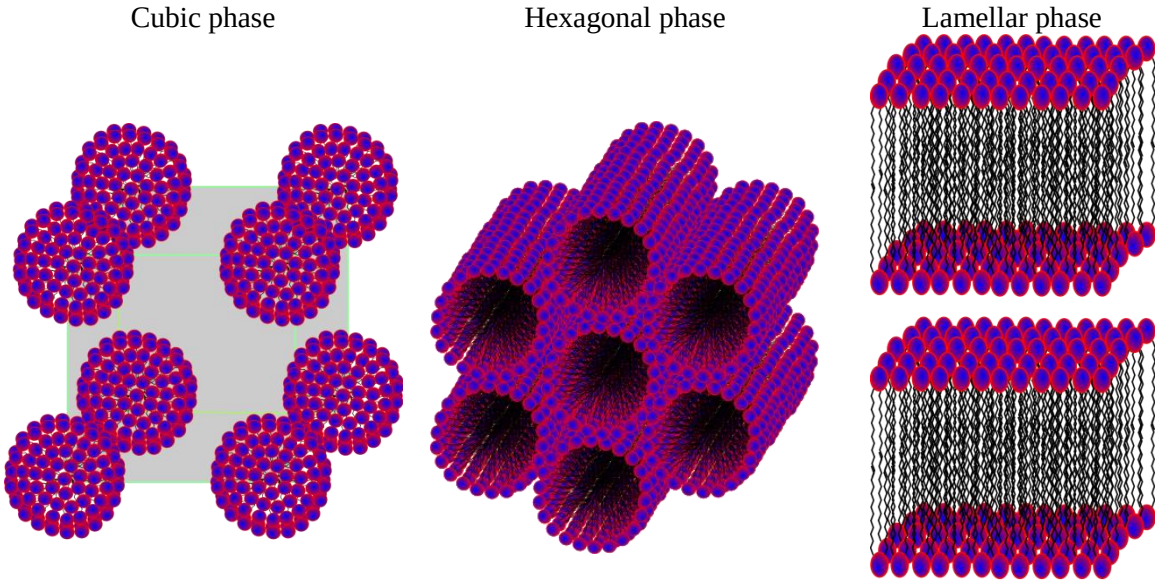

Figure 3-4**.** The three most common polymorphic phase states observed in membrane phospholipids; cubic, hexagonal and lamellar. It should be noted that the phospholipids in the hexagonal phase could be inverted.[26]

These three membrane phase states are all relevant to biomembranes. The non-bilayer lipid hexagonal or cubic phases often relate to transient biomembrane shifts such as fusion, fission and pore formation.[20] Within this project an emphasis has been placed upon capped lamellar phase bilayers (in the form of vesicles).

3.1.6 Bilayer fluidity

As previously discussed, the molecular structures of each phospholipid within a bilayer (in addition to other bilayer components) affect the properties of a bilayer. The bilayer fluidity is dependent on both these internal interactions and the temperature of the system. The level of bilayer fluidity affects the ease with which rupture of the vesicle membrane can be achieved. Within a lipid-pure bilayer there are primarily two common phases, which relate to the phase transition temperature (T_c) introduced briefly in 3.1.2 Intelligent vesicles. These phases are known as the liquid crystalline phase (L_α or solid lipid) and the liquid gel phase (L_β or fluid lipid).[27]

The liquid crystalline phase, at lower temperatures, is characterised by higher viscosities, fatty acid lipid tails are fully extended, packing of the overall system is relatively ordered, and van der Waals interactions between adjacent chains are maximal. Comparatively, at increased temperatures, the liquid gel phase is characterised by a lower viscosity and higher diffusion coefficient, resulting from partial melting of the acyl chains, yielding an increasingly disordered system in constant motion.[28] As a result of this disorder, the fluid phase has a 'self-healing' ability – allowing rearrangement of the bilayer when necessary.

The transition between the liquid crystalline phase and liquid gel phases is the T_c, and the temperature at which it is achieved varies depending on phospholipid composition – with an emphasis on acyl chain length and hence system disorder. The T_c of phospholipids can be measured using differential scanning calorimetry (DSC). The peaks correspond to the enthalpic 'melting' event indicating the transition from crystalline to gel phase, which occurs at higher temperatures as the acyl chain length increases.[29] The difference in T_c for different isomers reflects the small variations in the packing of the membrane. This packing variation could potentially lead to different interactions between other components in the membrane, affecting the stability of the membrane to external stimulus.[19]

In addition to acyl chain length, the presence of double or triple bonds in the lipid can lower the T_c of a membrane. The liquid gel phase to liquid crystalline transition temperature of four different relevant phosphatidylcholine (PC) molecules with acyl chains of 14 carbons (dimyristoyl PC), 16 carbons (dipalmitoyl DP), 17 carbons (diheptadecanoyl DH) and 18 carbons (distearoyl PC) were measured by DSC and T_c values are given in Table 3-3.

3.1.7 Lipid diffusion in the bilayer

Lipids can diffuse within a bilayer by three different mechanisms; lateral diffusion, rotation and bilayer translocation, shown in Figure 3-5.

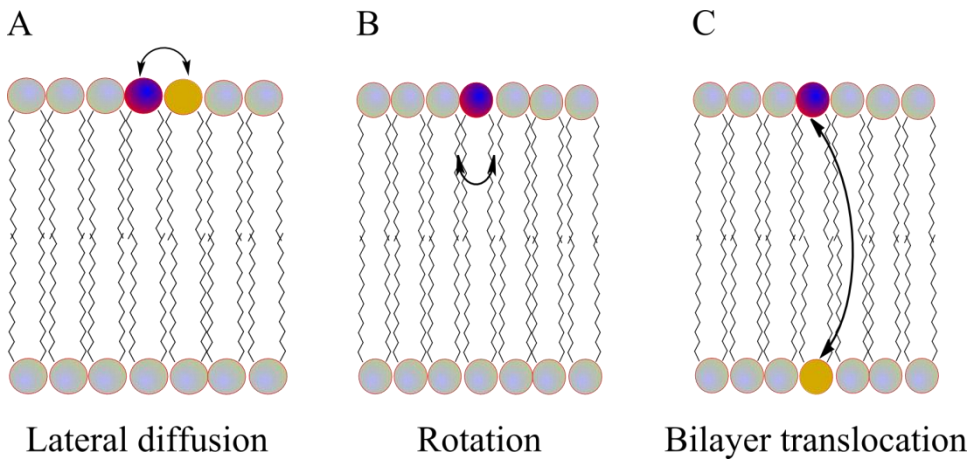

Figure 3-5. The diffusion of lipids within a bilayer where A) depicts lateral diffusion between neighbouring lipids, B) indicates lipid rotation within the same position and C) depicts translocation of a lipid through a bilayer.

Lateral diffusion occurs when neighbouring molecules can exchange places via Brownian motion, enabling lipids to travel within a monolayer. The diffusional rates for freely diffusing lipid molecules in model membranes have typically been observed to be between 10^{-7} to 10^{-8} cm^2/s, fast enough for a single lipid molecule to diffuse around the erythrocyte plasma membrane in seconds. However, this lateral diffusion rate of phospholipids varies depending upon the various cell types and can be retarded (by factors up to 100). Bilayer translocation - more commonly known as “flip-flop” - involves the exchange of lipid molecules between leaflets through the movement of the polar head groups passing the non-polar centre of the bilayer. This process is energetically unfavourable, often occurring as an induced response through transient pores generated from ion concentration discrepancies across a membrane.[30] Rotation involves the spinning of a lipid around its axis, without any altering of its position.

3.1.8 Unilamellar vesicles

The formation of capped bilayers into vesicles is a requirement of this project. Vesicles can be divided into three classes based on their size; small, large and giant. Small unilamellar vesicles (SUVs) form from extensive sonication to give diameters between 20 – 50 nm. The extreme curvature of the bilayer can make encapsulation of large agents problematic, and

fusion between SUVs can occur as a result of an increased free energy per unit area relative to LUVs and GUVs.[31] Large unilamellar vesicles (LUVs) can be made by the fusion of SUVs, or extrusion through polycarbonate membranes, to give diameters between 50 – 1000 nm. In comparison to SUVs, LUVs can encapsulate a larger volume within their internal cavity, although their disadvantages include a fragility of structure and heterogeneous size distributions. Giant unilamellar vesicles (GUVs) have diameters between 5 – 300 μm akin to the sizes of eukaryotic cells. GUVs make ideal membrane mimics, however their large internal volumes can make them unstable due to variations in osmotic potential.[19] The thickness of the membrane is independent of this size distinction, with a diameter of approximately 4 nm for SUVs, LUVs and GUVs.

The size range of homogenous unilamellar vesicles commonly utilised in drug delivery applications is between 50-150 nm. This is a compromise between loading efficiency of vesicles (increases with increasing size as a result of a greater internal cavity volume) and liposome stability (decreases with increasing size, no longer optimal i.e. lysis, fusion or bursting occurs > 200 nm as a result of osmotic pressure considerations).[1]

3.1.9 Biological membranes and vesicles

Biological membranes are fundamental for cell compartmentalisation, they are multi-functional, with the potential to provide cell energy in the form of ATP from charge (proton) and chemical gradients, regulate and organise enzyme activity, aid information transfer, and provide components for signalling and biosynthesis.

Conventional unilamellar vesicles are considered useful in the modelling of eukaryotic cell membranes. Their structures are similar to prokaryotic cells, where shared characteristics, aside from composition, include a single compartment delimited by a single bilayer. This bilayer forms a space-defining, protective barrier that is fundamental for cell and organism survival.

Prokaryotic and eukaryotic biomembranes consist of lipids, proteins and carbohydrates. Basic vesicle biomembranes form a bilayer based on amphiphilic phospholipids and sphingolipids arranged in two layers along an interface, with the polar head groups extending out and the non-polar acyl chains filling in the expanse in between. Within eukaryotic and prokaryotic cells, different unique compositions of varying phase-forming lipids and proteins can give multiple functionalities that allow the formation of embedded channels for the transport and

regulation of components into and out of a cell, ensuring the maintenance of charge and concentration gradients.[32] Other bilayer functions can include the provision of cell energy from charge and chemical gradients, regulation and organised enzyme activity, information transfer, and provision of components for signalling and biosynthesis. Within research, modification of vesicle structure can be carried out to mimic, optimise and understand some of these functions.[33]

3.1.10 Vesicle development – stability and sensitivity

The potential opportunities involving the use of intelligent vesicles in both the cosmetic and medical fields indicate a wide scope of promising applications. Continually increasing knowledge about the stabilising profile of different lipid and chemical components, protective activity of possible coatings and phase transition temperatures of mixtures can be utilised to aid the discovery of vesicle compositions with a suitable profile for use within a paediatric burn wound dressing. The desired profile is depicted in Figure 3-6.

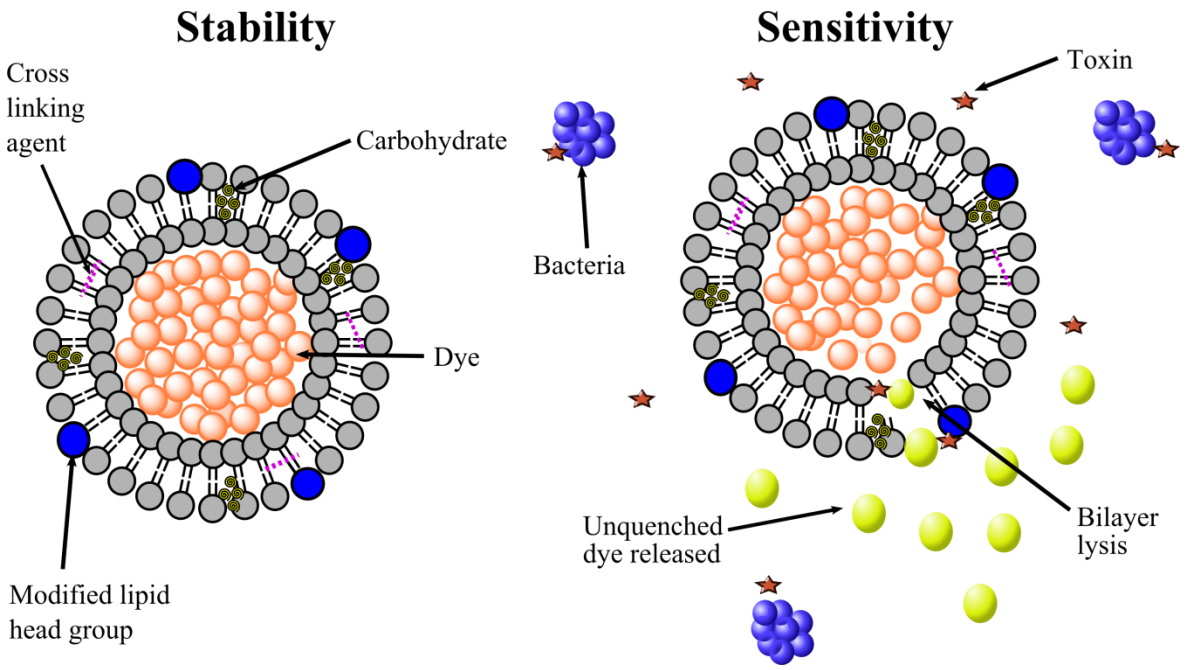

Figure 3-6. The ideal vesicle profile for an application within a pathogenic-bacteria-signaling paediatric burn wound dressing, with an emphasis on stability during storage and application, and selective sensitivity to pathogenic bacterial toxins.

3.2 Vesicles – encapsulation of a signalling agent

Figure 3-6 indicates the stability and sensitivity profile required for the use of vesicles within a pathogenic bacteria signalling paediatric wound dressing. An important aspect of this is the detection / signalling agent that can be successfully encapsulated into the vesicles. An ideal candidate for this is a dye with a fluorescence profile.

3.2.1 Fluorescence

Photoluminescence is defined as the spontaneous emission of radiation from an electronically excited species or from a vibrationally excited species not in thermal equilibrium with its environment[34] and can be classified as either fluorescence or phosphorescence. The difference between fluorescence and phosphorescence is depicted in the Jabłoński diagram in Figure 3-7.

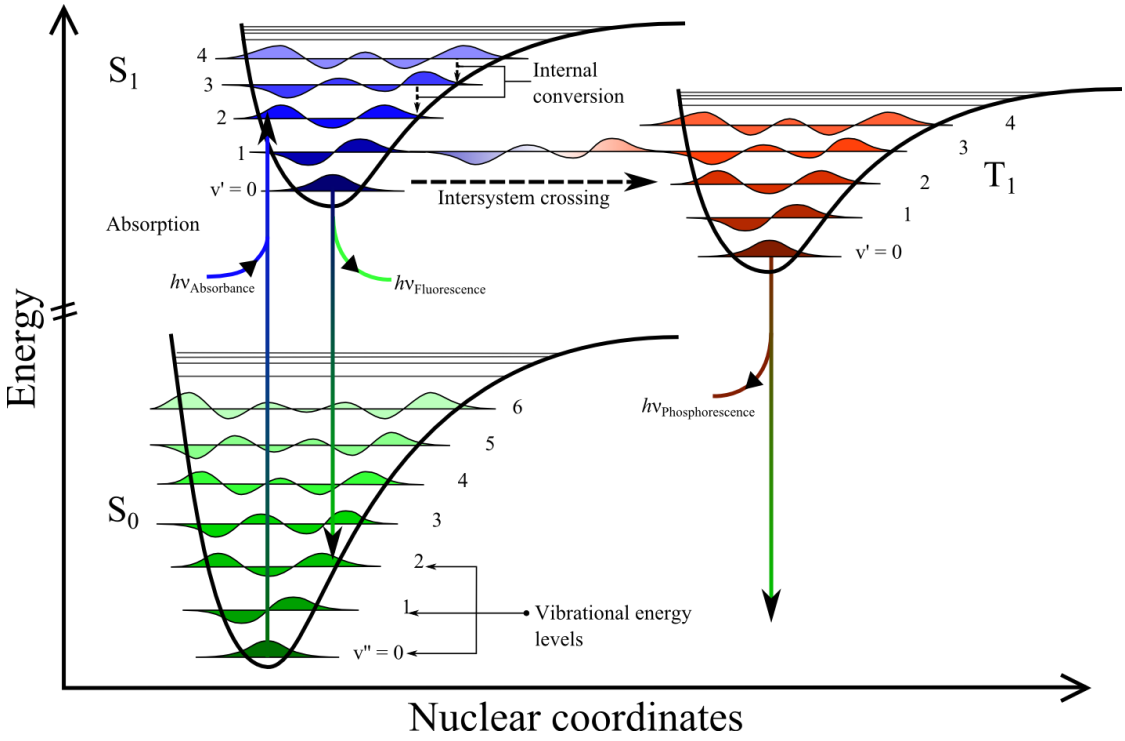

Figure 3-7. Jabłoński diagram, representing the electronic states in a molecule, and the transitions between them; which form the basis of luminescence. This was developed by Aleksander Jabłoński in 1935. Acknowledgement to W. D. Jamieson, PhD thesis 2013.

Electronic states can be classified as singlet and triplet, in the case of Figure 3-7, S_0 and S_1, and T_1 respectively. A singlet state is one in which all of the electrons in the molecule have

their spins paired. Triplet states are those in which electron spin sets have become unpaired. A triplet state will always lie lower in energy than its corresponding singlet state. All molecules are assumed to be in the lowest vibrational level of the ground state at room temperature.

Once the molecule is excited to the higher energy state $S_{1,2}^{x,y}$, by absorption of electromagnetic radiation, several processes can occur to cause the molecule to lose its excess energy, a process known as decay. The two most important are fluorescence emission and vibrational relaxation. Fluorescence involves transitions from the low lying energy state $S_{1,2}^{x,y}$ to vibrational levels of the ground state S_0. Vibrational relaxation involves the decay of the electron to the ground state of an energy level from a higher vibrational level within the same singlet or triplet state, through a process known as internal conversion. Internal conversions and vibrational relaxation processes are very rapid relative to fluorescence, with timescales of approximately 10^{12} s^{-1}.[35] Decay through phosphorescence results from intersystem crossing ($T_1 \rightarrow S_0$).

The Franck-Condon principle, proposed by J. Franck in the early 1920's, can be used to determine which vibrational energy levels in the S_1 electronic state transitions are made into, following a consideration of nuclear motions. Nuclear motions are relatively very slow; hence electronic transitions are favoured between vibrational levels that are in the same phase shift as each other, ensuring that minimal disruption will be caused. As a result of this, transitions between vibrational levels, for example from S_0 to S_1, will be favoured between vibrational energies in the same phase. Consequently, the excitation transition from $S_0^1 \rightarrow S_1^1$ may not be the most energetically favourable. In 1950 M. Kasha proposed Kasha's rule to state the favourability of low energetic burden transitions over higher electronic energy level transitions (i.e. excited state molecules quickly relax to the lowest level of that excited energy level -internal conversion is preferred). As a result of this, fluorescence and phosphorescence occur in appreciable yield only from the lowest excited state of a given energy level (S_x^0).[36]

The Frank-Condon principle and Kasha's rule dictate that a) phase matching between absorbed and emitted wavelengths causes a mirror effect (observable in spectra with multiple peaks), b) photons produced through electronic relaxation have a lower energy and wavelength than absorbed photons, and c) emitted photons will have the same wavelength regardless of the energy of the photon absorbed.

The molecular fluorescence of a sample is measured through excitation at the absorption wavelength, known as the excitation wavelength, and measuring the emission at a longer fluorescence wavelength. The difference in energy between the excitation and emission is known as the 'stokes shift' after Sir G. G. Stokes who described the phenomenon in 1852, shown in Figure 3-8. This arises from the photon energy in the emitted being less than the incident, accounted for by the vibrational relaxation and internal conversion pathways which require energy but do not yield emission spectra.

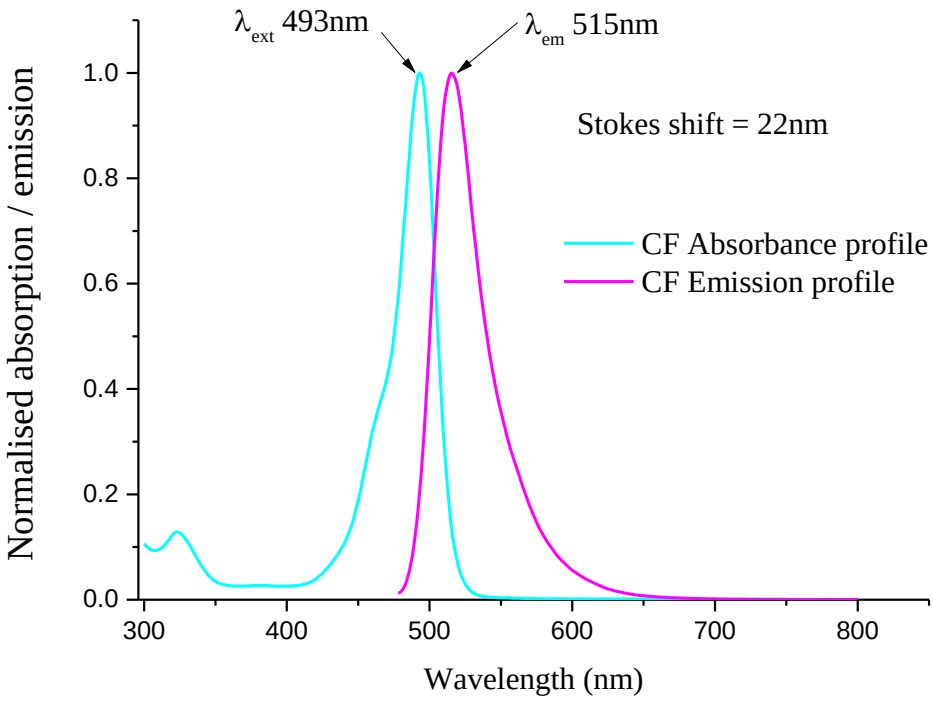

Figure 3-8. The absorption / emission spectra for the fluorophore 5(6)-carboxyfluorescein. The maximum excitation (λ_{ext}) and maximum emission (λ_{em}) peaks occur at 493 nm and 515 nm. These occur as a result of $S_0^x \leftrightarrow S_1^y$ transition energies, and the difference between these, as indicated, is the Stokes shift (22 nm).

The absorption spectra for most common fluorophores are generally the mirror image of the emission spectra. This is a result of the phase matching within the vibrational energy levels within the ground and excited state ($S_0^x \leftrightarrow S_1^x$).

There are two physiochemical characteristics of a fluorophore; the quantum yield (Q), which is the ratio of emitted photons to the absorbed photon, and the fluorescence lifetime (Ʈ).

The quantum yield can be depicted in Equation 3-3, using the rate of fluorescence (k_F) and the rate of non-radiative decay (k_{NR}), and gives a measure of the emission efficiency of a fluorophore:

$$Q = \frac{k_F}{k_F + k_{NR}} \qquad \text{Equation 3-3}$$

As a result of the Stokes shift, and collision and conversion related energy loss, the quantum yield is never equal to one. The lifetime of fluorescence (τ) is defined as the average time a molecule spends in the excited state before returning to the ground state, and a typical time span for this is 10 ns. The lifetime of fluorescence can be found using in Equation 3-4;

$$\tau = \frac{1}{k_F + k_{NR}} \qquad \text{Equation 3-4}$$

The fluorescence intensity and emission spectrum may be affected by the fluorophores dipole, and hence by charge transfer, ionisation, and hydrogen bonding. The local environment, such as solvent type, presence of heavy metals and pH value can also have an effect, and these can be manipulated in chemical and biological systems.

3.2.2 Quenching of fluorescence

There are some distinct mechanistic techniques towards fluorescence quenching that result in a dissipation of energy without fluorescence occurring, including:

- Förster resonance energy transfer (FRET) quenching – a dynamic method over long distances 40-100Å, involving energy transfer from the excited state donor to the acceptor. It is based on dipole-dipole interactions and is reliant on the donor-acceptor distance (R) at a rate of $1/R^6$. The dye-quencher complex has the same absorption and fluorescence spectra as the individual molecules.
- Heavy metal quenching – halogenated compounds can act as collisional quenchers, through intersystem crossing to an excited triplet state, or electron donation from the fluorophore to the quencher.
- Dexter / collisional quenching – diffusive collision encounters between the fluorophore and quencher during the lifetime of the excited state without fluorescence emission.
- Static quenching – a ground state complex forming mechanism from hydrophobic and electrostatic interactions within short distances (<15 Å). It occurs through Dexter mechanism, and is dependent on e^{-R} and temperature. The dye-quencher complex has a different absorption and fluorescence spectra than the individual molecules.[37]

An important mechanism of quenching worth noting in more detail is collision quenching, during which an excited state molecule collides with another molecule, deactivating the fluorophore. This is a dynamic process in which the quencher and fluorophore are not altered, and can be measured using the Stern-Volmer equation, Equation 3-5;

$$\frac{F_o}{F} = 1 + K_{sv}\,[Q] = 1 + K_Q \tau_o\,[Q] \qquad \text{Equation 3-5}$$

Where F_o is the unquenched fluorophore, F is the fluorophore, K_{sv} is the Stern-Volmer quenching constant, K_Q is the bimolecular quenching rate coefficient, τ_o is the unquenched lifetime, and [Q] is the concentration of the quencher. A large value of K_{sv} indicates an easily quenched species.

Static quenching can also be achieved if the quencher forms a non-fluorescent complex with the fluorophore, where K_s is the constant derived from the association of the quencher-fluorophore complex, given in Equation 3-5.

The rate equations relating to fluorescence quenching are given below, where A represents the fluorophore, A^* represents the fluorophore in its excited state and k_Q is the quenching rate constant.

$$A + h\upsilon \rightarrow A^* \qquad \text{Rate} = k_a\,[A] \qquad \text{Equation 3-6}$$

$$A^* \rightarrow A + h\upsilon \qquad \text{Rate} = k_f\,[A^*] \qquad \text{Equation 3-7}$$

$$A^* + Q \rightarrow A + Q^* \qquad \text{Rate} = k_Q\,[A^*]\,[Q] \qquad \text{Equation 3-8}$$

Under steady state:

$$[A^*] = \frac{k_a\,[A]}{K_f + k_q\,[Q]} \qquad \text{Equation 3-9}$$

The intensity of fluorescence in the absence of the quencher is given by Equation 3-10;

$$I_f\,(0) = k_a\,[A] \qquad \text{Equation 3-10}$$

The intensity of fluorescence in the presence of the quencher is given by Equation 3-11;

$$I_f\,(Q) = k_f\,[A^*] \qquad \text{Equation 3-11}$$

Therefore, the following fluorescence ratio is given by Equation 3-12;

$$\frac{I_f\,(0)}{I_f\,(Q)} = 1 + \frac{k_Q}{k_f}\,[Q] \qquad \text{Equation 3-12}$$

Plotting of I_f (0) / I_f (Q) versus [Q] gives a linear relationship, where the gradient is equal to Stern-Volmer constant K_{sv}, hence;

$$K_{sv} = \frac{k_Q}{k_f} \qquad \text{Equation 3-13}$$

The quenching and fluorescence phenomenon will be utilised within this project as a signalling system to indicate degree of vesicle stability and sensitivity, and will be measured through vesicle lysis and resulting fluorescence intensity.

3.2.3 5(6)-carboxyfluorescein

An appropriate detection dye, with an extensive history as a marker for measuring the mechanical stability of vesicle membranes,[38] was utilised for encapsulation within the vesicle formulations; 5(6)-carboxyfluorescein (5(6)-CF). This dye was first investigated by Weinstein *et al.* in 1977[39] to track liposome endocytosis. 5(6)-CF is an organic fluorophore that is quenched and non-fluorescent at high concentrations (< 10 mM), but un-quenched and fluorescent at low concentrations (> 10 mM), shown in Figure 3-9.

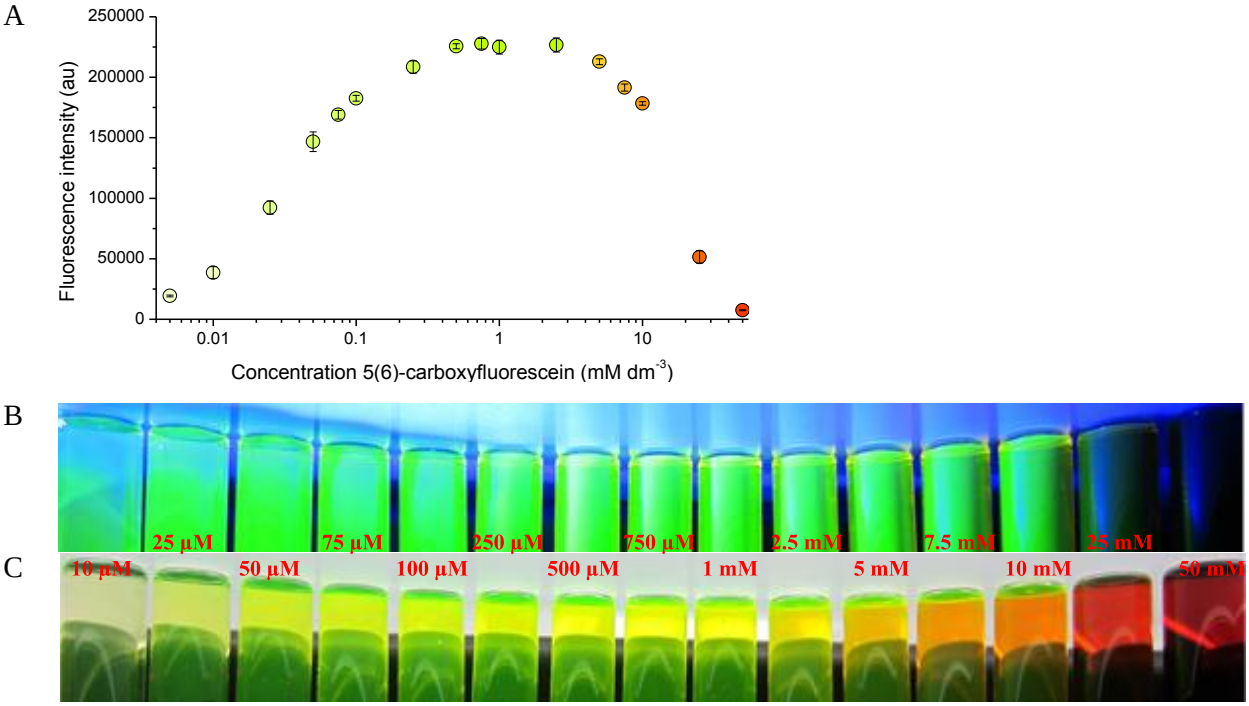

Figure 3-9. A graph to show fluorescence versus 5(6)-CF concentration (A), and two photographs showing dye concentration versus fluorescence, where (B) is taken using UV light and (C) is taken using white light. Acknowledgement to W. D. Jamieson, PhD thesis 2013.

Non-fluorescent quenching of 5(6)-CF has been primarily proven to be a result of dimerisation of the dye and energy transfer to non-fluorescent dimers, although collisional

quenching between dye monomers could play a role. These quenching processes do not give 100 % quenching, and this is due to the interaction of the dye with the lipids in the vesicle.[40]

5(6)-CF has two wavelengths of maximum absorbance, 465 and 490 nm, and an emission wavelength of 515 nm. Its structural polarity helps prevent passive leakage from vesicles, and it is known to have a pH dependence, with fluorescence increasing as the pH increases.[41] The implications of this with regard to its proposed use as a pathogenic bacterial indicator in a wound dressing will be further investigated, and discussed in 3.5.1.1 Effects of pH and temperature on 5(6)-carboxyfluorescein.

Importantly, 5(6)-CF can be incorporated into vesicles alongside other water-soluble active agents, for example drugs, and utilised to measure passive diffusion / delivery of agent over time or following an environmental stimulus change. The lack of toxicity of the dye has been investigated and confirmed by Lutty.[42] As a result of this it has been used to fluorescently label proteins, nucleotides, nucleic acids and peptides, following interactions of the carboxylic acid with amines, and as a starting material in the synthesis of other fluorescein-derived reagents.[43]

3.3 Vesicle formulation process

Vesicles were composed primarily of different concentration compositions of PC and PE lipids, and cholesterol, and synthesised as directed in 2.2 Vesicle formulation process, with the encapsulation of the fluorescently active dye 5(6)-CF.

3.3.1 Vesicle and dye concentration calculations

The following calculations can be used to calculate the theoretical quantity of lipids per 100 nm vesicle, total number of vesicles per synthesis, and the total volume of aqueous solution encapsulated. The quantity of lipids can be calculated based on an average 4 nm bilayer diameter;

Area of outer sphere $= \frac{4}{3}\pi r^2 = \frac{4}{3}\pi(100 \times 10^{-9})^2 = 1.3 \times 10^{-13}\ \mathrm{m}^2$ Equation 3-14

Area of inner sphere $= \frac{4}{3}\pi r^2 = \frac{4}{3}\pi(96 \times 10^{-9})^2 = 1.2 \times 10^{-13}\ \mathrm{m}^2$ Equation 3-15

Average area of a PC lipid polar head[44]	$= 66\ \text{Å}^2 = 6.6 \times 10^{-19}\ \text{m}^2$	
Number of lipids in outer bilayer	$= \frac{1.3 \times 10^{-13}\ \text{m}^2}{6.6 \times 10^{-19}\ \text{m}^2} = 190399.6$	Equation 3-16
Number of lipids in inner bilayer	$= \frac{1.2 \times 10^{-13}\ \text{m}^2}{6.6 \times 10^{-19}\ \text{m}^2} = 175472.2$	Equation 3-17
Total number of lipids per vesicle	$= 190399.6 + 175472.2 = 365871.7$ $= 3.6 \times 10^5$	Equation 3-18

Using the value calculated for the theoretical total number of lipids per vesicle (3.6 x 10^5); the theoretical total number of vesicles per formulation process can be calculated. This calculation is based on 100 mM vesicles, composed of 78 mol % of the common phosphatidylcholine DPPC (with the remaining composition comprising of cholesterol and phosphatidylethanolamine DPPE). General vesicle compositions and the general structures of PC and PE (Figure 3-10) are discussed in the following sections. The amount of DPPC starting material will be 5.72 × 10^{-3} g and the vesicles formulated within a sample can be found;

Moles of lipid (DPPC)	$= \frac{\text{mass}}{\text{MW}} = \frac{5.7 \times 10^{-3}\ \text{g}}{734.4\ \text{g mol}^{-1}} = 7.8 \times 10^{-6}\ \text{mol}$	Equation 3-19
Number of lipid molecules	$= 7.8 \times 10^{-6}\ \text{mol} \times 6.022 \times 10^{23}\ \text{mol}^{-1}$ $= 4.69 \times 10^{18}$ lipids	Equation 3-20
Total number of vesicles per formulation process	$= \frac{4.69 \times 10^{18}}{3.6 \times 10^5} = 1.3 \times 10^{13}$ vesicles	Equation 3-21

The total theoretical encapsulated volume of aqueous agent inside the vesicles can then be calculated using;

Internal volume of vesicle	$= \left(\frac{4}{3}\right)\pi r^3 = \left(\frac{4}{3}\right)\pi\ 4.8 \times 10^{-8}\ \text{m}$ $= 4.4 \times 10^{-22}\ \text{m}^3$ $= 4.4 \times 10^{-19}\ \text{dm}^3$	Equation 3-22
Encapsulation volume per 5 ml synthesis	$= 4.4 \times 10^{-19}\ \text{dm}^3 \times 1.3 \times 10^{13}$ $= 5.6 \times 10^{-6}\ \text{dm}^3$	Equation 3-23
Encapsulation volume	$= 5.6 \times 10^{-6}\ \text{dm}^3 \times 200 = 1.1 \times 10^{-3}\ \text{dm}^3$	Equation 3-24

per dm^3

The 5(6)-CF dye will be encapsulated at a self-quenched concentration of 50 mM;

Moles of 5(6)-CF	$= \frac{\text{mass}}{\text{mr}} = \frac{1879 \times 10^{-3}\text{g}}{376.32\ \text{g mol}^{-1}} = 0.00499$	Equation 3-25
Concentration of 5(6)-CF	$= \frac{\text{moles}}{\text{volume}} = \frac{0.00499\ \text{mol}}{100 \times 10^{-3}\ \text{dm}}$ $= 5.0 \times 10^{-2}\ \text{mol dm}^{-3}$	Equation 3-26

From this, and Equation 3-23 the theoretical amount of 5(6)-CF released following total lysis of vesicles within a sample of 5 ml can be calculated;

Moles of 5(6)-CF in vesicles	$= 5.0 \times 10^{-2}\ \text{mol dm}^{-3} \times 5.6 \times 10^{-6}\ \text{dm}^3$ $= 2.8 \times 10^{-7}\ \text{mol}$	Equation 3-27
Amount of 5(6)-CF encapsulated and released following total lysis	$= 2.8 \times 10^{-7}\ \text{mol} \times 376.32\ \text{g mol}^{-1}$ $= 1.1 \times 10^{-4}\ \text{g} = 0.02\ \text{g dm}^3$ $= 0.02\ \text{mg ml}^{-1}$	Equation 3-28

From these calculations the theoretical number of vesicles synthesised in a 5 ml, 100 mM sample, composed of 78 % DPPC is 1.3 x 10^{13}, and the encapsulated and released amount of carboxyfluorescein following total lysis is 0.02 mg ml^{-1}. These values will change depending on the lipids used to compose the bilayer, and the surface area of their individual polar head groups.

3.3.2 General vesicle composition

The vesicles developed in this project were composed primarily of saturated (n:0) or unsaturated (0 = 1,2,3...) phospholipids with differing carbon lipid chain lengths; dimyristoyl (DM, 14:0), dipalmitoyl (DP, 16:0), diheptadecanoyl (DH, 17:0), dioleoyl (DO, 18:1) and distearoyl (DS, 18:0). These are primarily phosphatidylcholines (PC), and the corresponding phosphatidylethanolamines (PE), Figure 3-10, both of which are common major structural constituents of eukaryotic membranes.[32]

Phosphatidylethanolamine - DPPE

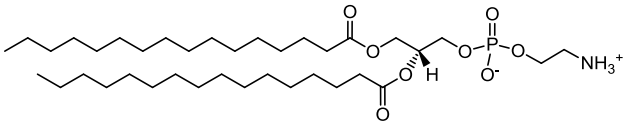

Phosphatidylcholine - DPPC

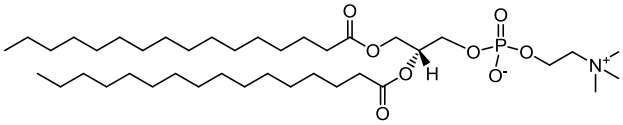

Figure 3-10. The structure of phosphatidylethanolamine (DPPE) and phosphatidylcholine (DPPC), both of which are common major structural constituents of eukaryotic membranes

3.3.3 Less common lipids

To increase the stability of the vesicles synthesised, other components were incorporated into these formulations such as different lipids, of which some of the less typical ones are given in Table 3-1. The properties of these vesicles, which make them suitable for incorporation into vesicle membranes, are discussed in the following sections.

Lipid component	Structure	Lipid component	Structure
1,2-(dipalmitoyl / distearoyl) - *sn*-glycero-3-phospho-(1'-*rac*-glycerol) (sodium salt)	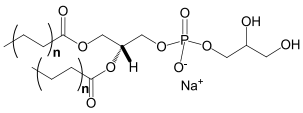 n = 6 = palmitoyl (16:0, DPPG), 7 = stearoyl (18:0, DSPG) See: 3.4.7 Anionic lipids	1,2-dimyristoyl-*sn*-glycero-3-phosphoethanol amine-methoxy(poly-ethylene glycol (ammonium salt) 14:0 $PEG_{(n)}$ PE	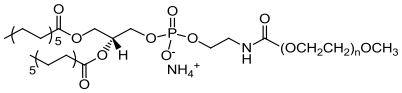 n = 12 (550), 22 (1000) or 45 (2000) See: 3.4.9 Stealth vesicles
1,2-dimyrisitoyl-3-dimethyl-ammonium-propane 14:0 DMDAP	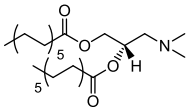 See: 3.4.8 Cationic lipids	1,2-dioleoyl-*sn*-glycero-3-phosphocholine 18:1 PC (DOPC)	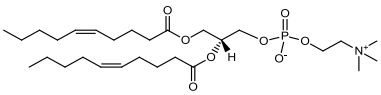 See: 3.4.10 Phase separating lipids

Table 3-1. Less typically recognised lipids incorporated for their stabilisation potential, in varying mol % ratios.

Commonly recognised lipids, less common lipids, and other chemicals, have all been combined together to synthesise vesicles of varying compositions, en-route to an ideal vesicle composition, which is both stable, and sensitive to specific environmental stimulus, in the form of pathogenic bacterial toxins.

3.3.4 Vesicle nomenclature

Nomenclature of the vesicles synthesised and used within this project follows the naming pattern previously developed in the group,[45] and is based on an easily identifiable acronym for the primary stabilising agent, followed by its primary lipid component. Examples of this are given in Table 3-2.

Vesicle Name	Main lipid constituent	Secondary component	Stabilising agent
DMPC/DMPE	DMPC (14:0) 78 %	Cholesterol 20 % DMPE 2 %	None
DSPG-DP	DPPC (16:0) 53 %	Cholesterol 20 % DSPC 15 % DPPE 2 %	DSPG 10 %
TCDA-DS	DSPC (18:0) 63 %	Cholesterol 20 % DSPE 2 %	TCDA 15 %

Table 3-2**.** The relation of vesicle nomenclature to primary lipid / stabilising agent composition.

A comprehensive library of over 70 different vesicle compositions can be found in the supporting information (SI-Table 1), along with an indication of their stability over 14 days at 37 °C, in relation to the stability response parameter, given in Equation 3-29.

3.3.5 Vesicle membrane solubilisation – a positive lytic control

Detergents are defined as water-soluble surfactants that are effective at solubilising membrane components. The mechanism of action involves micelle formation, directly resulting from the amphiphilicity of the surfactant. Self-association of detergents into micelles occurs at a defined critical micelle concentration (CMC). At concentrations below the CMC, the amphipath is found in its' monomer form; above the CMC, the monomer concentration is unchanged whilst the concentration of micelles increases. The critical

micelle temperature (CMT) also plays a role in micelle formation, and is defined as the temperature above which micelles form.

The solubilisation of a bilayer into its constituent membrane lipids and other components can be achieved through addition of these water soluble detergents. At different detergent concentrations, the detergent molecules can intercalate into the membrane, and form detergent-lipid complexes, shown in Figure 3-11. Addition of the detergent above its CMC value ensures the formation of mixed micelles of varying structure and size.

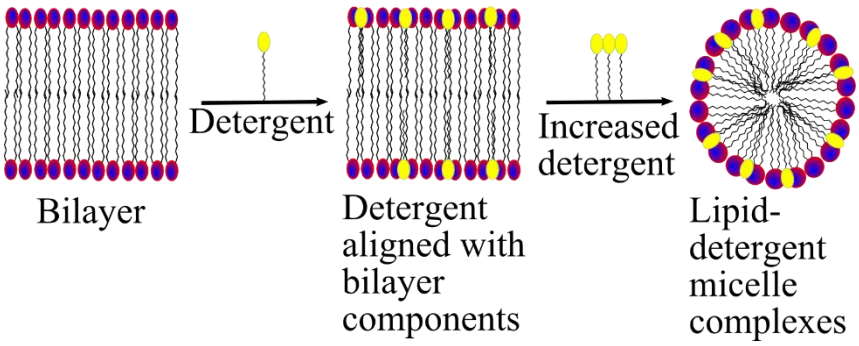

Figure 3-11**.** The stages of membrane solubilization following the addition of increasing concentrations of detergent to a membrane. At low concentrations, the detergent can penetrate without damaging the bilayer; at increasing concentrations disruption occurs to form detergent-lipid complexes.[19]

Triton X-100™, henceforth referred to as triton, but less commonly known as polyethylene glycol p-(1,1,3,3-tetramethylbutyl)-phenyl ether, is a widely-used non-ionic surfactant for the solubilisation of membranes and the recovery of membrane components under mild non-denaturing conditions.[46] The addition of triton results in vesicle solubilisation and the formation of mixed micelles within the bilayer, subsequently followed by the formation of surfactant stabilised holes on the vesicle surface, leading to complete solubilisation.[47]

Triton was utilised at a concentration of 0.01 % v/v[38] to breakdown vesicles in a positive control experiment. 0.01 % v/v triton was deemed to be effective on three trial vesicle formulations utilised in this study, as was 1 and 0.1 % v/v. This was determined following a small study into vesicle lysis, measured by fluorescent dye release, upon addition of different concentrations of triton. This, and the structure, is shown in Figure 3-12.

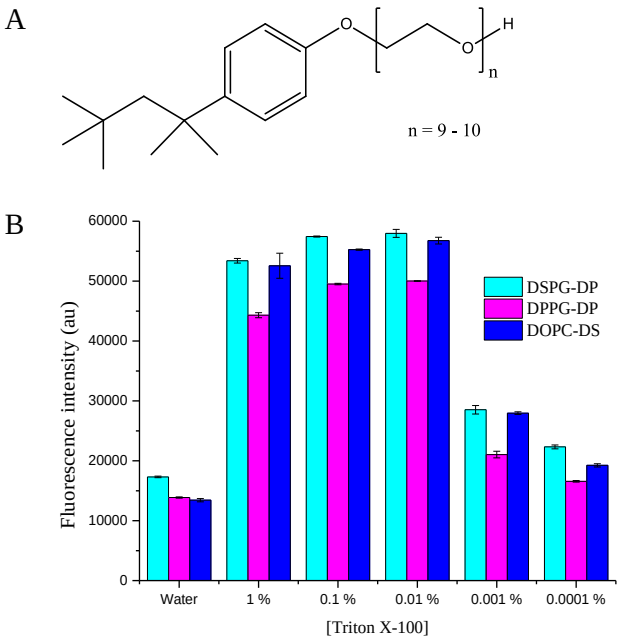

Figure 3-12**.** The structure and lytic effect of triton, where A) gives the chemical structure of triton X-100^{TM} and B) the lytic effect on three different vesicle formulations, each encapsulating 5(6)-CF, of different concentrations of triton (v/v) measured utilising fluorescent intensity measurements.

From Figure 3-12, an acceptable lysis of vesicles can be achieved with 1, 0.1 and 0.01 % v/v triton. As a result of this any of these concentrations are acceptable as a positive lytic control, within these experiments 0.01 % v/v triton was utilised.

3.4 Vesicle development – measuring stability

Within this initial investigation, the vesicle stability required will focus on point-of-use parameters. Specified guidelines, obtained from collaboration with the paediatric burn centre at Frenchay Hospital, UK, suggested a requirement for a product that can be placed upon a wound for more than 10 days, at an elevated skin surface temperature of 34 - 35 °C.[48] This can be compared to undamaged skin temperature, which can be between 16 - 32 °C depending on localised conditions.[49] In addition to this, the majority of pharmaceutical products, including wound dressings, are created to be stable at room temperature, which can be between 2-30 °C, and for extended periods of time (often in excess of 6 months). Stability considerations are often dependent on distribution and long term storage conditions, as well as point-of-use requirements.

Based on and expanding from this, the vesicles synthesised will be investigated for stability at pH 7, at a temperature of 37 °C and for a period of 14 days. The stability between vesicle compositions can be compared using the stability response parameter.

3.4.1 Stability response parameter

The long-term stability response parameter equation was created as a way of allowing easily understandable comparisons between the stability of different vesicle compositions. This was calculated using Equation 3-29:

$$\text{Stability response parameter}, S = \frac{F_f}{F_i} \qquad \text{Equation 3-29}$$

Where F_i is the initial vesicle fluorescence intensity value and F_f is the final vesicle fluorescence intensity value after addition of a lytic agent following a time study. For stability assays, F_i is the fluorescence value obtained following incubation for 14 days at 37 °C. The addition of the surfactant triton was considered to deliver the maximum fluorescence obtainable following total vesicle disruption for most vesicle systems,[38] however *Staphylococcus aureus* RN4282 supernatant (discussed in 4.2.1.2 The relevance of MSSA RN4282) was also utilised. A higher S value was deemed desirable for long-term stability - indicating a large fluorescence intensity increase on addition of the lytic agent. In initial stability studies an S value higher than two was required from a vesicle composition; if this was achieved further environmental stimulus testing could be carried out.

3.4.2 Stabilising agents

The incorporation of different lipids and other chemicals into a vesicle bilayer membrane is a common method towards achieving stabilised vesicles. The different agents incorporated into the vesicles, in varying mol %, and their overall stabilising outcome will be discussed and summarised in the following sections. Stability response parameter indications upon changing each of these variables can be found in the supporting information, SI-Table 1.

3.4.3 Lipid chain length

Four saturated PC lipids, varying only with regard to the number of carbons in their lipid chain lengths, were investigated. These PC lipids included DM (14), DP (16), DH (17), and

DS (18); the number parameter in brackets indicates the number of carbon atoms in the lipid chain. In each case the corresponding PE lipid was incorporated at a concentration of 2 mol %. This was due to their known prevalence in biological membranes[50] and potential to act as a target / binding site for external lipid bilayer-targeting agents.[51]

The lipid chain length relates to the gel-to-liquid crystal transition temperature, T_c, discussed in 3.1.6 Bilayer fluidity. Values for the T_c of each of these lipids were obtained using a TA Instruments DSC Q20. This thermo-analytical technique measured the temperatures and heat flows associated with a phase transition within the lipid as a function of time and temperature applied, versus a reference sample, with results given in Table 3-3.

PC Lipid	Transition temperature
DMPC	23.3 °C
DPPC	38.2 °C
DHPC	48.8 °C
DSPC	54.6 °C

Table 3-3. Gel-to-liquid crystal transition temperatures of the PC lipids. Data acquired with S. Hong and W. D. Jamieson.

As previously discussed, passive leakage of active agents from a vesicle is at its greatest at temperatures around and above the T_c, due to the coexistence of two phases and the resulting defects between the boundaries.[15] This means that vesicles composed primarily of DMPC will be affected by passive leakage and hence will be inherently unstable. The T_c of DPPC is very close to the temperatures investigated (37 °C), and so an increased level of passive leakage may be measured, although incorporation of other agents may be effective in increasing DPPC stability. DHPC and DSPC have relatively high T_c values, which should ensure good stability. However, this stability may have a negative effect on their susceptibility to other external environmental stimulus.

3.4.4 Polydiacetylene polymers

The use of polydiacetylene (PDA) polymers for the investigation of peptide-membrane interactions is well known. A colour transition (blue-to-red) can be used to indicate peptide conformation and lipid association.[52] The structure of the relevant diacetylene monomer,

10,12-tricosadiynoic acid (TCDA), its polymer structure, and its colour profile at different concentrations following UV treatment is given in Figure 3-13.

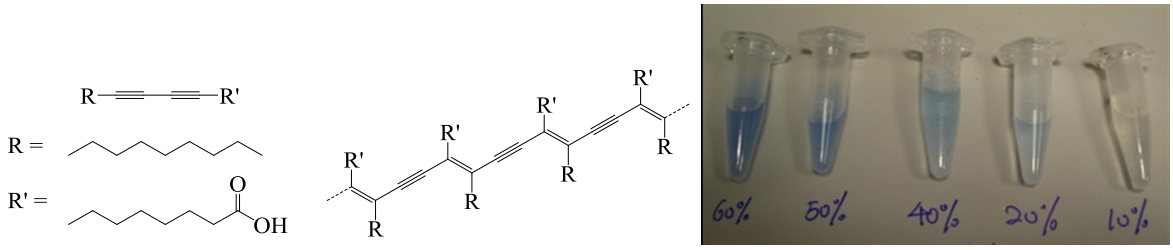

Figure 3-13. The monomer and polymer structure of 10,12-tricosadiynoic acid (TCDA) and colour profile at different concentrations following UV treatment. Photo Acknowledgement to J. Zhou, PhD thesis 2010.

The colour transition of TCDA from blue to red can occur following the association with lipids, and / or on an application of external stimulus, including heat, organic solvents, mechanical stress, molecular recognition and UV light.[53] However, the colour change can be quite diffuse, and the presence of the 5(6)-CF dye within the vesicles can mask any observable colour change. TCDA, when in a highly ordered state (i.e. closely packed) can undergo polymerisation, following initiation with 254 nm UV irradiation. The polymerisation of TCDA occurs through a radical initiated chain reaction within the membrane of vesicle, forming cross-links with itself, and potentially other unsaturated bilayer components.

The *pseudo*-amphiphilic chemical structure of TCDA allows for easy incorporation into a phospholipid bilayer; the polar carboxylic acid can align with the hydrophilic head group of a phospholipid, and the acyl chain can align with the hydrophobic acyl chain of a phospholipid. Incorporation of TCDA into vesicle membranes was first reported by Kolusheva *et al.* in 2000,[52] and initial research into this concept within the Jenkins group was reported by Zhou *et al.* in 2011.[54]

3.4.5 Cholesterol concentrations

Cholesterol is an essential component in biological membranes, where it is required for viability and cell proliferation. The structure of cholesterol includes a tetracyclic fused ring skeleton, with a single hydroxyl group and a flexible iso-octyl hydrocarbon side chain, Figure 3-14.[55]

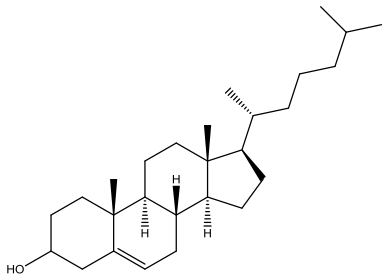

Figure 3-14 The structure of cholesterol.

The presence of a hydroxyl group is very important; it gives this otherwise hydrophobic compound its amphiphilic character, allowing the formation of hydrogen bonds with water and other components of cell membranes and allows the molecule to orientate in membranes.[56] Within a bilayer, the polar hydroxyl group is orientated towards the aqueous phase, with the hydrophobic steroid ring structure aligned and embedded within the chains of the phospholipid hydrocarbons.

Cholesterol has been found to interact with phospholipids and influence their behaviour. Increasing cholesterol concentration broadens and can eliminate the gel-to-liquid crystal transition temperature, T_c, of the related lipids.[57] It induces an *intermediate state* to the lipids it interacts with, playing an important role in inducing fluidity, both above and below corresponding lipids T_c.[58] Cholesterol reduces the rate of motion of the phospholipid hydrocarbon chain and increases the order in the membrane, leading to a laterally more condensed membrane with a higher density of packing.[59] As a result of this, cholesterol can increase the mechanical strength and decrease the permeability of the membrane.[60] In addition to this, cholesterol may play a role in the susceptibility of cell membranes to interaction with bacterial toxins.[61]

The maximum solubility of cholesterol within bilayers is reported to be below 50-66 mol %,[62] depending on the lipid; above this value lamellar structures are unable to form. Different mol % of cholesterol, between 20 – 40 %, was investigated within a variety of vesicle compositions, all of which showed good thermal stability for over 24 hours at 37 °C. However, an optimum concentration of cholesterol was found to be 20 %; these were found to have the potential to form vesicles with the desired stability, and so the majority of vesicles synthesised had this mol % of cholesterol.

3.4.6 Hybrid vesicles

Hybrid vesicles is a term used within this investigation to describe vesicles with varying mol % compositions of lipids with different structures and acyl chain lengths, in an attempt to attain the stability parameters desired. Clustering, segregation and domain formation of lipids with different polar head groups and hydrophobic chain lengths have the potential to alter the phase transition temperature T_c of lipids within a bilayer.[63] This change could result in an increased or decreased T_c of the clustered lipids. Increasing the T_c of certain lipids, for example DPPC which has a T_c of 38.24 °C, could decrease passive diffusion of active agent delivery at 37 °C, making it a better candidate for use within stable vesicle bilayers. Equally, decreasing the T_c of certain lipids, for example DSPC which has a T_c of 54.55 °C, could ensure that the lipid-vesicle system is susceptible to certain environmental stimuli, as discussed in further detail in 3.1.2 Intelligent vesicles. This project investigated mixing DP, DH and DS PC lipids together in different mol % ratios to attain the desired stability parameters. Some examples are given in Table 3-4.

Vesicle Name	Primary PC	Secondary PC	Other components	Stability
DSPC-DP1	DPPC 73 %	DSPC 5 %	DPPE 2 % Cholesterol 20 %	Good
DSPC-DP2	DPPC 63 %	DSPC 15 %	DPPE 2 % Cholesterol 20 %	Good
DSPC-DP3	DPPC 53 %	DSPC 25 %	DPPE 2 % Cholesterol 20 %	Good

Table 3-4. Example *hybrid* vesicle lipid compositions using DPPC and DSPC. *Good* indicates that the vesicles were stable for 1<14 days at 37 °C. A full list can be found in the SI (SI-Table 1).

The formation of *hybrid* vesicles with mixed PC compositions indicated potentially favourable stability. In addition, a beneficial increase in sensitivity to pathogenic bacterial toxin stimulus was demonstrated when lipids with a higher T_c were mixed with lipids with a lower T_c. The potential for favourable stability and enhanced sensitivity was therefore exploited, and following the addition of 10 mol % of glycerol containing lipids, stability reached the desired parameters. The use of glycerol containing lipids is discussed in 3.4.7 Anionic lipids.

3.4.7 Anionic lipids

Phosphatidylglycerol (PG) is a ubiquitous anionic lipid that is present in low concentrations in animal and plant membranes (1-2 %) and higher concentrations in bacterial membranes (up to 20 %).[64] PG is utilised within a cell as the biosynthetic precursor of cardiolipin; subsequently used to generate an electrochemical potential for substrate transport and ATP synthesis,[65] lysobisphosphatidic acid and many other glycophospholipids.[66] PG also has an increased presence in cellular membranes of organisms that carry out aerobic photosynthesis, where it is thought to play a role in photosynthetic electron transfer, cell fission and division.[67]

Within this investigation, 1,2-dipalmitoyl-sn-glycero-3-phospho-(1'-rac-glycerol) (sodium salt) (DPPG) and 1,2-distearoyl-sn-glycero-3-phospho-(1'-rac-glycerol) (sodium salt) (DSPG) were investigated in a variety of vesicle compositions at a concentration of 10 mol %. The negative charge on the phosphate group ensures the lipid is anionic at neutral pH values. The presence of both of these glycerol lipids in *hybrid* vesicles demonstrated an enhanced stability when compared to glycerol lipids incorporated into standard vesicles composed of one phosphatidylcholine lipid only; in the former case, a promising stability response parameter (at 37 °C for 14 days). Both of these glycerol lipids have phase transition temperatures that are very similar to their counter phosphatidylcholine lipids (41 °C DPPG, 38 °C DPPC, 55 °C DSPG, 54 °C DSPC). Hence it can be hypothesised that the similar T_c's may enable the formation of mixed phases with reduced boundaries between the different lipids, ensuring that vesicles are more inherently stable. In addition to this, the accumulation of glycerol in biological environments under stress has been reported to increase vesicle stability in lyophilized environments.[68]

3.4.8 Cationic lipids

Cationic lipids have been investigated extensively following the discovery that they can be used to form cationic liposomes capable of complexing and condensing DNA,[69] giving them the potential to act as a delivery vessel for intracellular DNA.[70] The success of this alternative transfection system was attributed to the electrostatic reaction between a cationic vesicle and anionic DNA, where the resultant vesicle net positive charge association with negatively charged cell surfaces and the fusion / destabilisation of cationic vesicles with plasma membranes, aids the intracellular release of DNA.[71] The low toxicity, safety and versatility of

cationic lipids make this therapeutic route to gene transfer a promising alternative to viral vectors.

The properties of cationic lipids and hence cationic vesicles make them an interesting potential candidate for applications within this investigation. The use of 1,2-dimyristoyl-3-dimethylammonium-propane (14:0 DMDAP), a cationic lipid with a small-polar head group, was therefore hypothesised to provide a stabilising effect to vesicle compositions in anionic environments, whilst safely delivering an active agent. Following the incorporation of DMDAP into various membrane compositions (primarily DMPC based) at 5 and 10 mol %, no increased stability was observed. This effect is thought to be due to a low T_c and an increased sensitivity to external stimulus; resulting from the pH sensitive nature of cationic lipids and the potential ability of the cationic vesicles to fuse prematurely with anionic surfaces.

3.4.9 Stealth vesicles

Incorporation of PEG-phospholipids is a popular method of providing a protective vesicle shell, ensuring a long-circulation *in-vivo*, enhanced permeability and host retention.[17] PEGylated lipids have been thoroughly investigated by fundamental research into the modelling of the conformation of grafted polymer chains, steric stabilisation, bio-nonfouling, membrane self-assembly, and biomolecular interactions.[9] These studies have enabled the successful emergence of *stealth* vesicles, with applications in both therapeutic and diagnostic healthcare.[72-74]

The predictable and controllable nature of phase behaviour of PEGylated bilayer membranes is important in ensuring that the retention and release profile required for active agent delivery is maintained.[75] Below the phase transition temperature in the gel phase, the presence of PEGylated lipids in the bilayer is believed to increase active agent retention,[9, 76] and a transition to the disordered liquid phase is thought to trigger release,[77] as discussed in 3.1.2 Intelligent vesicles. Within PEGylated bilayers, the concurrent formation of immiscible and homogenous phases depends upon corresponding aliphatic chain length, PEG content and temperature,[74] and these factors must be considered for the design of vesicles with suitable stability response parameters.

There is an extensive selection of PEGylated lipids available, with PEG_n molecular weights commonly ranging from 350 to 5000. Within this investigation 1,2-dimyristoyl-sn-glycero-3-

phosphoethanolamine-N-[methoxy(polyethylene glycol)-*n*] (ammonium salt) was utilised, with n equalling 550, 1000 or 2000. These were incorporated into various membrane compositions, which were primarily DMPC based, at 5 and 10 mol %. These formulations proved unsuccessful at attaining the stability profile required for this investigation, and this is thought to result from phase immiscibility and excessive passive diffusion at temperatures above the lipids T_c. It should be noted however, that formulations of PEGylated lipids with higher T_c lipids could potentially provide the stability required.

3.4.10 Phase separating lipids

Phase separating lipids enable the formation and stabilisation of rafts of similar lipids and other agents within a bilayer. These rafts can coexist in gel and liquid form.[78] The phase separating lipid 1,2-dioleoyl-*sn*-glycero-3-phosphocholine (DOPC) was investigated for its stabilising potential. DOPC is a doubly unsaturated lipid able to form stable, well characterised bilayer structures, and is commonly used in membrane models.[79] The presence of unsaturation in both of the hydrophobic lipid chains can be hypothesised as a key explanation for the formation of the separated liquid-gel phases, and is a direct cause of its low T_c; -17 °C. In addition to lipid phases, DOPC enhances the formation of cholesterol-rich raft domains.

The incorporation of 1,2-dioleoyl-*sn*-glycero-3-phosphocholine (DOPC) at concentrations of 2, 4 or 8 mol % was investigated in vesicles with the aim to enhance phase separation and the formation of gel-liquid boundaries between vesicle components. The primary lipid component within these vesicles was DSPC, which was utilised due to its inherent stability relating to its high T_c (54.55 °C). The addition of DOPC, a lipid with a low T_c (-17 °C), was speculated to form phase boundaries that would be more susceptible to selected environmental stimulus. This low T_c is a result of unsaturation in the hydrophobic chain

Vesicles comprising 2 mol % DOPC showed an increased stability at 37 °C for 14 days, although increasing the DOPC composition further to 4 or 8 mol % showed a decreased stability hypothesised to be as a result of an increased sensitivity to environmental stimulus. Results by Mady, who utilised phosphorus-31 NMR, show that increased DOPC concentrations can promote a pH dependent phase transition of a bilayer from lamellar (pH 4) to hexagonal (pH 8),[80] see Figure 3-4. This transition is essentially an inversion of the vesicular bilayer structure, causing total release of the internal agent.

3.4.11 Stable vesicle candidates

Following investigation into different stabilising agents and the synthesis of more than 70 vesicle compositions; a select few were deemed suitable for further investigations as shown in Table 3-5. A stability response parameter, S, value greater than two was desirable.

Vesicle Name	Main lipid constituent	Secondary component	Stabilising agent	Stability response parameter, S pH 7 / 37 °C / 14 days
DSPC/DSPE	DSPC 78 %	Cholesterol 20 % DSPE 2 %	None	1.7
DOPC-DS	DSPC 76 %	Cholesterol 20 % DSPE 2 %	DOPC 2 %	2.3
TCDA-DS	DSPC 63 %	Cholesterol 20 % DSPE 2 %	TCDA 15 %	3.7
DPPG-DP	DPPC 53 %	Cholesterol 20 % DSPC 15 % DPPE 2 %	DPPG 10 %	3.8
DSPG-DP	DPPC 53 %	Cholesterol 20 % DSPC 15 % DPPE 2 %	DSPG 10 %	5.1

Table 3-5. Stable vesicle candidates and their stability response parameter (S) values. A high value for S indicates that after 14 days at 37 °C a high level of fluorescence can be measured following addition of a lytic agent (triton).

The vesicle named DSPC/DSPE has been included here as a comparison; it is a vesicle which is inherently stable, with a promisingly low fluorescent value after 14 days at 37 °C. However upon addition of triton there was no increase in fluorescence, indicating the vesicle would not have the desired sensitivity to bacterial toxins.

3.4.12 Stability versus sensitivity

The stability of vesicles is very important in ensuring that the encapsulated active agent, in this case 5(6)-CF, does not passively diffuse out. However, that is not the only requirement of vesicles within this investigation. The vesicles, in addition to stability at pH 7 and at 37 °C, must be able to release the encapsulated agent in response to pathogenic bacterial species.

Prior to this, the stability of the most stable vesicle candidates, determined above, was tested in varying environmental conditions (pH and temperature) to ensure that the ideal vesicle composition could be found prior to inoculation with bacteria.

3.5 Environmental stimulus

As discussed in 3.1.2 Intelligent vesicles, vesicles can be tuned to be responsive to localised environmental changes in pH and temperature.[73, 81] Although this responsive nature is beneficial within many applications,[16, 73, 81] the sensitivity does not fit with the parameters required for this application. Consequently the stability of vesicles at a range of pH and temperature values is required.

3.5.1 Effects of pH and temperature

The vesicles utilised within this investigation must maintain their stability regardless of pH and temperature changes within the localised environment. This is because within a wound the pH and temperature cannot necessarily be controlled and localised changes could result from contact with the wound surface, exudate produced or during the growth cycle of any colonising bacteria.

Within this investigation, the pH range used for investigation of 5(6)-CF dye and vesicle stability was between pH 5 to pH 8. An acidic pH, such as that found on normal skin, is believed to be favourable for wound healing.[82] As the wound healing progresses the pH of a wound has been proven to change from alkaline to neutral to acidic.[83] Hence it is now believed that different pH ranges are required for different distinct phases of the wound healing process.

A report in 2013 by Sharp *et al.* investigated the potential correlation between wound surface pH, burn depth and healing time from 30 adult burn patients. The pH of the burn surface (0.4-4 % TBSA and ranging from superficial to full thickness) was measured following admission and at each dressing change. Interestingly, the pH in healing and non-healing wounds was found to decrease with each dressing change. A correlation between pH value, depth (superficial – acidic, 6,1 full thickness – alkaline, 8.0) and rate of wound healing (healing – neutral 7.3, non-healing – neutral 7.7) was also found.[84] Consequently from this, the vesicle stability was investigated at varying relevant pH values (5, 6, 7 and 8)

3.5.1.1 Effects of pH and temperature on 5(6)-carboxyfluorescein

Different fluorophores are known to have varying sensitivities to changes in localised pH conditions. These variations result from changes in ionisation of the molecule; 5(6)-CF is susceptible to protonation at low pH values and deprotonation at high pH values at both the phenol and carboxyl groups, shown in Figure 3-15.[85]

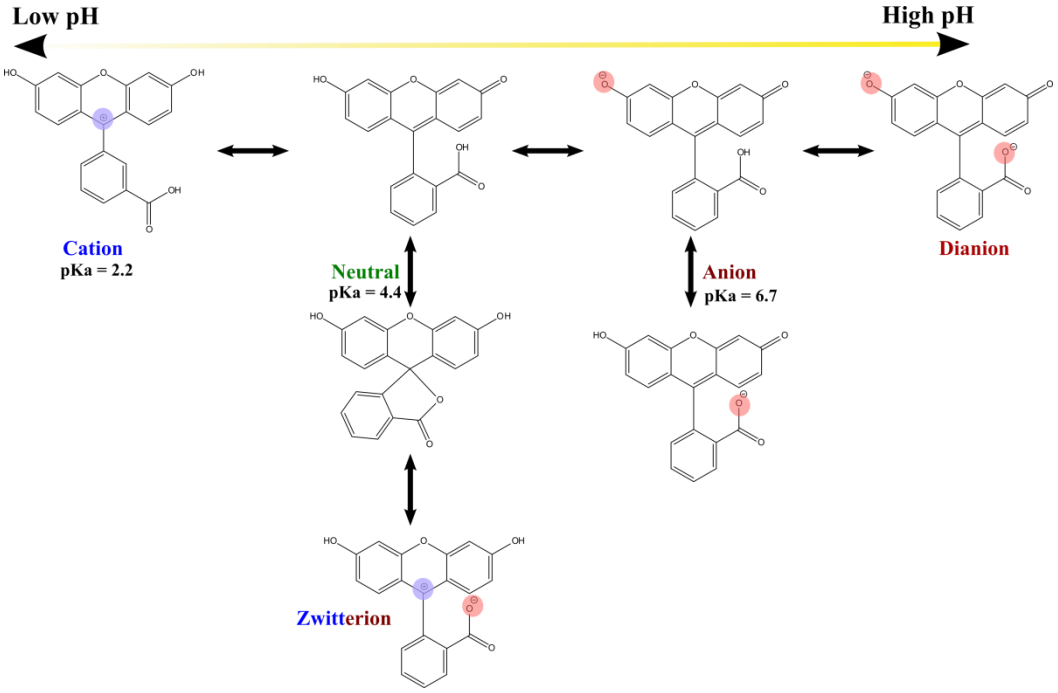

Figure 3-15. The chemical structures of fluorescein and pKa values as pH changes.

Initially, the 5(6)-carboxyfluorescein dye fluorescence was measured at different pH values (pH 5 - 8, adjusted with 1 M NaOH / HCl) at three different concentrations; the concentration that is loaded into the vesicles during synthesis (50 mM), an intermediate quenched concentration (25 mM) and a concentration representative of the unquenched fluorescence measurable following release of the encapsulated dye from the vesicles (1 mM), shown in Figure 3-16.

A

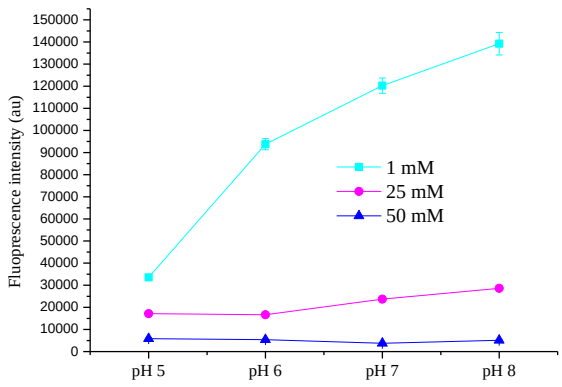

B

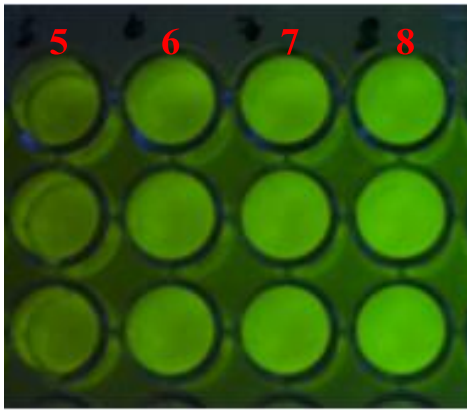

Figure 3-16. The effect of pH on three different concentrations of 5(6)-CF dye. 50 mM is the quenched concentration loaded into the vesicles during synthesis and 1 mM represents an unquenched dye concentration following release from the vesicles. B) is a photograph of the unquenched 1 mM dye at pH 5 to pH 8 under UV light.

Based on Figure 3-16, a relationship between unquenched dye fluorescence and pH can be measured and observed. The fluorescence intensity increased as the pH changes, with a maximum intensity measured at pH 8. This pH-signal dependent relationship could be problematic at a wound interface, where localised acidic conditions could decrease the signal observed. To overcome this, the vesicles could be protected from the variable nature of the wound environment, i.e. localised changes in pH, through careful control of the pH of the medium in which vesicles are stored and delivered. Potential prototypes of delivery and protection are discussed further in chapter 5.

In addition to pH, the effect of temperature on the 5(6)-CF dye was also investigated at 5 °C and 37 °C for 18 hours at the pH values measured above (5, 6, 7 and 8). At 37 °C the fluorescence of the quenched dye (50 mM and 25 mM) was unaffected, although the unquenched dye (1 mM) had a slightly increased fluorescence after 18 hours, Figure 3-17.

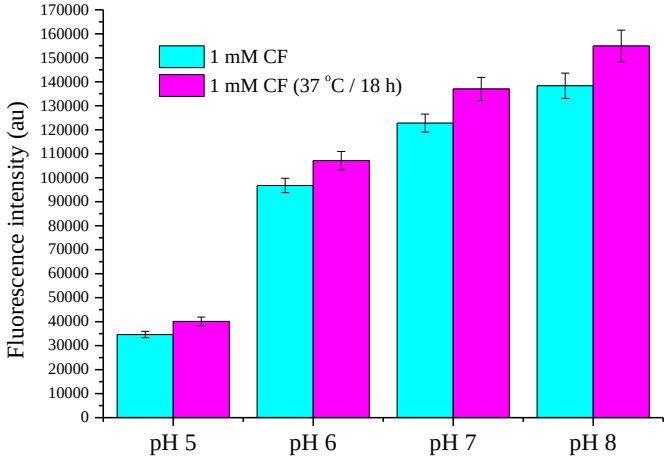

Figure 3-17**.** The effect of incubation at 37 °C for 18 hours on 1 mM 5(6)-CF at pH 5, 6, 7 and 8. A slight amplification in intensity could be measured following storage.

This slight amplification could prove beneficial at a wound interface, where increased temperatures are likely and fluorescence signals will be visually observed. At 5 °C the fluorescence of the quenched and unquenched dye was unaffected (data not shown).

3.5.1.2 Effects of pH and temperature on vesicles

A decrease in pH is known to potentially decreasing electrostatic head group repulsion, increasing the likelihood of hydrolysis of bilayer components and cause the protonation of basic head group moieties and fatty acid chains. This can potentially destabilise the vesicles. In addition to this, it has been reported that vesicle compositions containing substantial amounts of PE lipids are able to undergo a phase transition from bilayer lamellar structures to inverted micelle structures at an acidic pH.[86] PE has been reported to be essential in bilayer membranes for protein and bacterial attachment and targeting,[87] hence it has been incorporated into vesicles within this investigation at 2 mol %. At this low concentration the unfavourable destabilising transition should be avoided.

The effects from changing pH and temperature values were investigated using the vesicle candidates that indicated favourable stability in initial investigations from Table 3-5. The stability of vesicles at pH 5, 6, 7 and 8 was measured using fluorescence intensity measurements at day 14, following storage at 37 °C. After this time the surfactant triton was added, and the results were analysed according to the stability response parameter, Equation 3-29, and given in Table 3-6. Using this parameter ensured that relative fluorescence increase

values are obtained, even at acidic (pH 5) conditions where the 5(6)-CF dye fluorescence response is decreased.

Vesicles	pH stability at 37 °C (Stability Response Parameter, S)			
	5	**6**	**7**	**8**
DSPC/DSPE	2.9 (±0.1)	2.6 (±0.1)	1.7 (±0.1)	2.1 (±0.2)
DOPC-DS	4.9 (±0.2)	6.4 (±0.4)	2.3 (±0.3)	1.2 (±0.1)
TCDA-DS	3.2 (±0.2)	3.6 (±0.1)	3.7 (±0.2)	1.1 (±0.2)
DPPG DP	5.1 (±0.4)	4.5 (±0.5)	3.8 (±0.4)	1.9 (±0.6)
DSPG-DP	8.5 (±0.7)	4.7 (±0.6)	5.1 (±0.4)	1.4 (±0.9)

Table 3-6. The stability response parameter of stable vesicle candidates after incubation at 37 °C for 14 days at pH 5, 6, 7 and 8, followed by lysis with triton. A high S value was desirable at all pH values; indicative of good stability for 14 days, followed by successful lysis of vesicles on addition of triton.

From the stability response values given in Table 3-6, where a high value is favourable and indicative of good stability followed by successful lysis, it is possible to argue that each of these vesicle compositions would be suitably stable in an acidic to neutral pH range. However an increased level of passive diffusion was shown to occur at pH 8, indicating instability in alkaline conditions. The vesicle DSPC/DSPE may have an increased sensitivity to lytic agents at acidic or alkaline pH values, demonstrated by its increased response after 14 days to triton, and hence its increased S value at pH 5, 6 and 8 compared to the S value obtained at pH 7.

The effect of temperature on vesicle stability was initially investigated at 37 °C for 14 days. Further stability investigations were carried out with storage of the vesicles at 5 °C, -20 °C and -80 °C for 14 days (pH 7). The effect of flash freezing (submerging in liquid nitrogen) followed by storage at -20 °C for 14 days was also investigated. These temperature conditions were chosen as they were determined to be potentially relevant as vesicle storage and transport temperatures prior to product application. Each of the vesicles showed a similar level of stability, and so data for one stable vesicle candidate, namely DPPG-DP, along with a table of stability response parameter values, is shown in Figure 3-18.

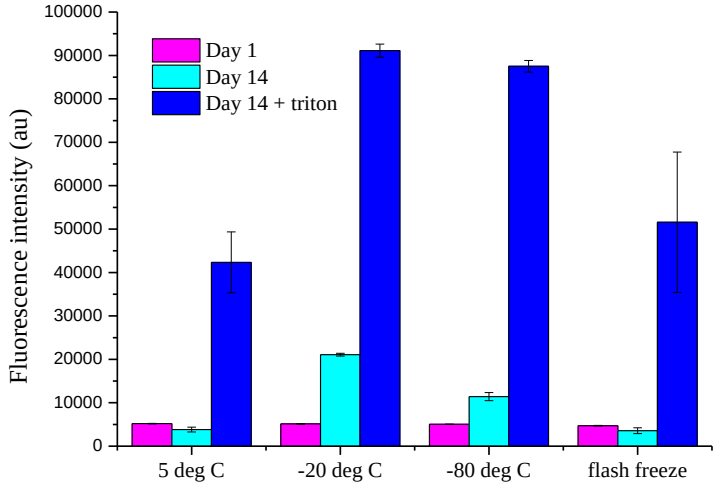

Temperature	Stability Response Parameter, S
5 °C	11.1 (±1.7)
-20 °C	4.3 (±0.1)
-80 °C	7.7 (±0.6)
Flash freeze at -80 °C	14.5 (±3.0)

Figure 3-18. The stability of DPPG-DP vesicles at 5 °C, -20 °C, -80 °C or following flash freezing. The vesicles were stored for 14 days followed by addition of triton; the original data for day 1, day 14 and day 14 plus triton is shown, as well as the stability response parameter values calculated.

The vesicles were determined to be sufficiently stable at these temperatures, indicating that a decrease in temperature does not promote passive leakage, hence it was possible to conclude that storage of vesicles at 5 °C prior to use is optimum. The stability and count of vesicles at higher temperatures – between 20 °C and 40 °C, assumed to be representative of both room temperatures and elevated body temperatures - was investigated using Nanoparticle Tracking Analysis.

3.5.1.3 Temperature stability of vesicles - Nanoparticle Tracking Analysis

Nanoparticle Tracking Analysis (NTA), manufactured by Nanosight, is a relatively new technique developed in 2006 to measure nanoparticles. This technique allows size measurements and visualisation of vesicles on a particle-by-particle basis, in solutions in real time with minimal sample preparation. NTA visualisation provides size, count and concentration measurements.

NTA, similarly to dynamic light scattering, utilises Brownian motion to make measurements and visualise rapidly moving nanoparticles individually. A variation of the Stokes-Einstein equation can be used to calculate the particle diffusion coefficient D_t, from the average trajectory (distance moved) of particles in x and y, the temperature T and solvent viscosity η,

Equation 3-30, and from this the particle hydrodynamic diameter can be identified, Equation 3-31.

$$D_t = \frac{(x,y)^2}{4} \qquad \text{Equation 3-30}$$

$$D_t = \frac{TK_B}{3\pi\eta d} \qquad \text{Equation 3-31}$$

NTA was used to investigate the effect of temperature on the size, count and concentration of vesicles. An example (TCDA-DS vesicles) is given in Figure 3-19. The experimental protocol involved making automated measurements, of 60 second videos, at a starting temperature of 20 °C which increased slowly to 40 °C at 2 °C intervals, over a period of approximately 30 minute. The videos could then be analysed using the associated software to form relevant graphs and obtain the number of particles count data.

A

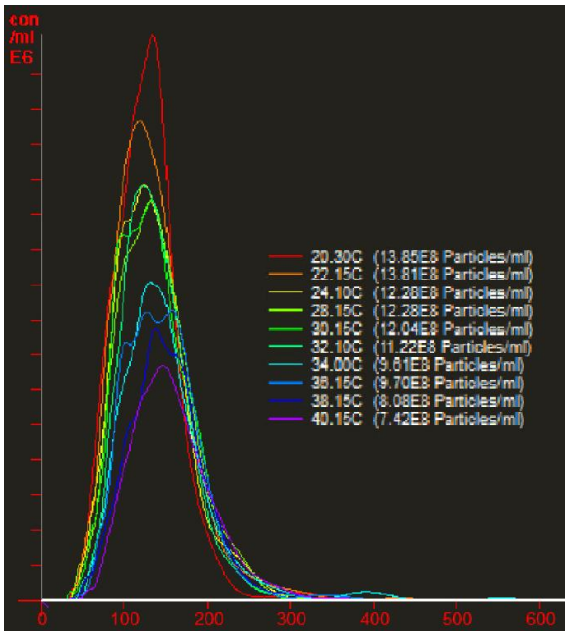

B

Temp (°C)	No. of particles / mL	Percentage of total (%)
20	13.9 x10^8	100
22	13.8 x10^8	99.7
24	12.3 x10^8	88.7
28	12.3 x10^8	88.7
30	12.0 x10^8	87
32	11.2 x10^8	81
34	9.6 x10^8	69.4
36	9.7 x10^8	70
38	8.1 x10^8	58.3
40	7.4 x10^8	53.6

Figure 3-19. Measuring the effect of increasing temperature from 20 °C to 40 °C at 2 °C intervals on the stability of TCDA-DS vesicles, using NTA, where A) is the actual graph obtained with all of the data displayed (diameter in nm on the x-axis) and B) indicates the reduction of vesicles present in the sample after each incremental increase (based on 20 °C arbitrarily being assigned as 100 % of the total possible vesicles present)

The results displayed in Figure 3-19 suggests a large dependency of stability on the temperature of the local environment, with a reduction of 30-50 % of total vesicles at 36-40 °C, taken as a conservative guide of the average skin surface temperature in paediatric burn patients.[88] Three of the stable vesicle candidates, see Table 3-5, were then compared to the less stable vesicle DMPC/DMPE, and concentration count measurements were made at +2 °C intervals between 20 °C and 40 °C. The difference between the concentration count minimum and maximum is given in Figure 3-20, and a smaller difference indicated increased vesicle stability at increased temperatures.

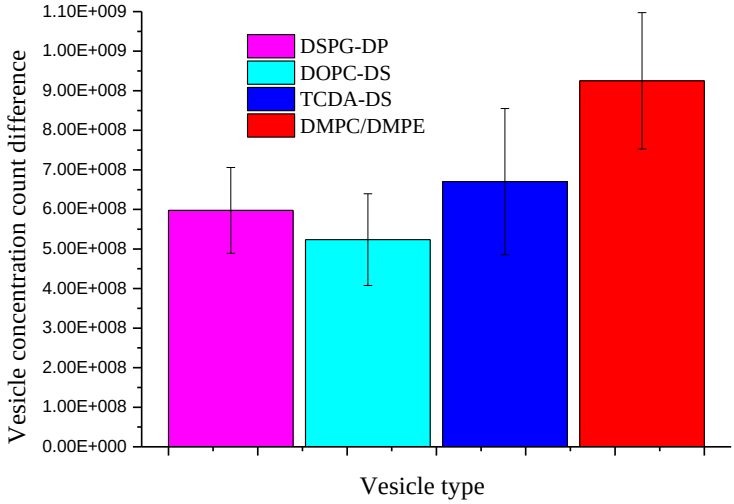

Figure 3-20**.** Vesicle concentration count using NTA carried out on three stable vesicle candidates, see Table 3-2, and a comparable vesicle which showed thermal instability, DMPC/DMPE. A concentration count was obtained at +2 °C temperature increments from 20 °C to 40 °C, and the calculated difference is plotted. A smaller value was indicative of similar concentration counts between 20 °C and 40 °C and hence was desirable.

Despite the difference in concentration count, the actual number of vesicles still in solution at 40 °C was still found to be between the orders of $x10^8$ to $x10^9$ for each of the three stable vesicle candidates, recognised as a significantly large number of vesicles. However, the large error values obtained potentially indicate that more readings are required for accurate conclusions to be made. The results from Figure 3-20 indicate that the three stable vesicle candidates are more temperature stable compared to the less stable DMPC/DMPE.

3.6 Vesicle stability – conclusions

The stability of a large range of vesicles of varying compositions have been investigated for their potential to act as a vehicle system. The encapsulation of a fluorescent dye (5(6)-CF) ensured that lysis of bilayer membranes and passive leakage of internal components could be tracked and measured. Vesicle formulations were required to demonstrate stability at pH 7, at 37 °C for a period of 14 days, and the stability response parameter was developed to allow comparisons between compositions to be made.

From this comprehensive investigation into a range of vesicle compositions and their stability five stable vesicle candidates, given in Table 3-5, were identified. These vesicles have indicated an increased stability against passive diffusion, according to the stability response parameter, S, defined in Equation 3-29. Further investigations into the stability of these vesicles with regard to a range of pH values (5, 6, 7 and 8) and temperature ranges (5 °C, -20 °C, -80 °C and flash freezing) for 14 days have indicated that these compositions show good potential for continued investigation.

Further work could be carried out into the development of other vesicle compositions utilising the wide variety of phospholipids currently commercially available. This would increase the library developed as part of this investigation, (SI-Table 1), and offer alternative vesicles that have the potential to attain the desired characteristics for incorporation into a wound dressing. In addition to this, the developed vesicles could be investigated at a wider range of pH values, for longer periods of time, and at a more comprehensive range of temperatures.

It should be noted that a significant decrease in vesicle concentration count was measured above 36 °C, using Nanosight NTA. This is a result of the transition temperature of the phospholipids incorporated within the bilayer being similar to the given temperatures, and hence an increased likelihood of passive diffusion and lysis occurring. Despite this, the actual number of vesicles still in solution above this temperature was still found to be between the orders of $x10^8$ to $x10^9$ for each of the stable vesicle candidates measured; a large number of vesicles which would arguably still be sufficient for observing a response following lysis.

The sensitivity of these five stable vesicles candidates, with regard to selective susceptibility to pathogenic bacterial toxins, can now be investigated, to determine if they would be appropriate for placement within an infection-signalling / treating burn wound dressing.

3.7 References

1. Lasic, D. D. Novel applications of liposomes. *Trends Biotechnol* **1998,** 16, 7, 307-21.
2. Weiss, J.; Decker, E.; McClements, D. J.; Kristbergsson, K.; Helgason, T.; Awad, T. Solid Lipid Nanoparticles as Delivery Systems for Bioactive Food Components. *Food Biophysics* **2008,** 3, 2, 146-154.
3. Foldvari, M. Non-invasive administration of drugs through the skin: challenges in delivery system design. *Pharmaceutical Science & Technology Today* **2000,** 3, 12, 417-425.
4. Malmsten, M. Soft drug delivery systems. *Soft Matter* **2006,** 2, 9, 760-769.
5. Lasic, D. D. Liposomes: From Physics to Applications. Elsevier: **1993**; p 575.
6. Lasic, D. D.; Papahadjopoulos, D. Liposomes revisited. *Science* **1995,** 267, 5202, 1275.
7. Jain, R. K. Delivery of molecular and cellular medicine to solid tumors. *Advanced Drug Delivery Reviews* **2012,** 64, Supplement, 353-365.
8. Lasic, D. D. Doxorubicin in sterically stabilized liposomes. *Nature* **1996,** 380, 6574, 561-562.
9. Lasic, D. D.; Needham, D. The "Stealth" Liposome: A Prototypical Biomaterial. *Chemical Reviews* **1995,** 95, 8, 2601-2628.
10. Adler-Moore, J. P.; Proffirr, R. T. Development, Characterization, Efficacy and Mode of Action of Ambisome, A Unilamellar Liposomal Formulation of Amphotericin B. *Journal of Liposome Research* **1993,** 3, 3, 429-450.
11. Lasic, D. D. Mixed micelles in drug delivery. *Nature* **1992,** 355, 6357, 279-280.
12. Gluck, R.; Mischler, R.; Finkel, B.; Que, J. U.; Scarpa, B.; Cryz, S. J., Jr. Immunogenicity of new virosome influenza vaccine in elderly people. *Lancet* **1994,** 344, 8916, 160-3.
13. Felgner, P. L.; Tsai, Y. J.; Sukhu, L.; Wheeler, C. J.; Manthorpe, M.; Marshall, J.; Cheng, S. H. Improved Cationic Lipid Formulations for In Vivo Gene Therapy. *Annals of the New York Academy of Sciences* **1995,** 772, 1, 126-139.
14. Voinea, M.; Simionescu, M. Designing of 'intelligent' liposomes for efficient delivery of drugs. *J Cell Mol Med* **2002,** 6, 4, 465-74.
15. Papahadjopoulos, D.; Nir, S.; Ohki, S. Permeability properties of phospholipid membranes: Effect of cholesterol and temperature. *Biochimica et Biophysica Acta (BBA) - Biomembranes* **1972,** 266, 3, 561-583.
16. de Smet, M.; Langereis, S.; den Bosch, S. v.; Grüll, H. Temperature-sensitive liposomes for doxorubicin delivery under MRI guidance. *Journal of Controlled Release* **2010,** 143, 1, 120-127.
17. Maeda, H.; Sawa, T.; Konno, T. Mechanism of tumor-targeted delivery of macromolecular drugs, including the EPR effect in solid tumor and clinical overview of the prototype polymeric drug SMANCS. *J Control Release* **2001,** 74, 1-3, 47-61.
18. Karanth, H.; Murthy, R. S. pH-sensitive liposomes--principle and application in cancer therapy. *J Pharm Pharmacol* **2007,** 59, 4, 469-83.
19. Luckey, M. Membrane structural Biology: With Biochemical and Biophysical Foundations. 1st edition ed.; Cambridge University Press: **2008**.
20. Meer, G. v.; Voelker, D. R.; Feigenson, G. W. Membrane lipids:where they are and how they behave. Nature Publishing Group: Nat Rev Mol Cell Biol, **2008**; 9, 112-124.
21. Sud, M.; Fahy, E.; Cotter, D.; Brown, A.; Dennis, E. A.; Glass, C. K.; Merrill, A. H., Jr.; Murphy, R. C.; Raetz, C. R.; Russell, D. W.; Subramaniam, S. LMSD: LIPID MAPS structure database. In *Nucleic Acids Res*, England, **2007**; 35, D527-32.
22. Goltsov, A. N.; Barsukov, L. I. Synergetics of the Membrane Self-Assembly: A Micelle-to-Vesicle Transition. *J Biol Phys* **2000,** 26, 1, 27-41.

23. Sen, A.; Hui, S. W. Direct measurement of headgroup hydration of polar lipids in inverted micelles. *Chem Phys Lipids* **1988,** 49, 3, 179-84.
24. Hui, S. W.; Sen, A. Effects of lipid packing on polymorphic phase behavior and membrane properties. *Proc Natl Acad Sci U S A* **1989,** 86, 15, 5825-9.
25. Sackmann, E. Membrane bending energy concept of vesicle- and cell-shapes and shape-transitions. *FEBS Letters* **1994,** 346, 1, 3-16.
26. Blunk, D.; Bierganns, P.; Bongartz, N.; Tessendorf, R.; Stubenrauch, C. New speciality surfactants with natural structural motifs. *New Journal of Chemistry* **2006,** 30, 12, 1705-1717.
27. Feigenson, G. W. Phase boundaries and biological membranes. *Annu Rev Biophys Biomol Struct* **2007,** 36, 63-77.
28. Koyama, T. M.; Stevens, C. R.; Borda, E. J.; Grobe, K. J.; Cleary, D. A. Characterizing the Gel to Liquid Crystal Transition in Lipid-Bilayer Model Systems. *The Chemical Educator* **1999,** 4, 1, 12-15.
29. Lewis, R. N.; Mak, N.; McElhaney, R. N. A differential scanning calorimetric study of the thermotropic phase behavior of model membranes composed of phosphatidylcholines containing linear saturated fatty acyl chains. *Biochemistry* **1987,** 26, 19, 6118-26.
30. Gurtovenko, A. A.; Vattulainen, I. Molecular Mechanism for Lipid Flip-Flops. *The Journal of Physical Chemistry B* **2007,** 111, 48, 13554-13559.
31. Lee, J. Y.; Schick, M. Calculation of Free Energy Barriers to the Fusion of Small Vesicles. *Biophysical journal* **2008,** 94, 5, 1699-1706.
32. van Meer, G.; Voelker, D. R.; Feigenson, G. W. Membrane lipids: where they are and how they behave. *Nat Rev Mol Cell Biol* **2008,** 9, 2, 112-24.
33. Boyer, C.; Zasadzinski, J. A. Multiple Lipid Compartments Slow Vesicle Contents Release in Lipases and Serum. *ACS Nano* **2007,** 1, 3, 176-182.
34. Braslavsky, S. E. Glassary of terms used in photochemistry, 3rd Edition (IUPAC Recommendations 2006). 3rd ed.; Pure Appl. Chem., **2007**; 79, 293-465.
35. Skoog, D. A.; West, D. M.; Holler, F. J.; Crouch, S. R. *Analytical Chemistry An Introduction*. 7th ed.; Brooks/Cole: **1999**.
36. Kasha, M. Characterization of electronic transitions in complex molecules. *Discussions of the Faraday Society* **1950,** 9, 14-19.
37. Lakowicz, J. R. *Principles of fluorescence spectroscopy, Volume 1*. Third edition ed.; Springer, **2006**.
38. Sila, M.; Au, S.; Weiner, N. Effects of Triton X-100 concentration and incubation temperature on carboxyfluorescein release from multilamellar liposomes. *Biochimica et Biophysica Acta (BBA) - Biomembranes* **1986,** 859, 2, 165-170.
39. Weinstein, J.; Yoshikami, S.; Henkart, P.; Blumenthal, R.; Hagins, W. Liposome-cell interaction: transfer and intracellular release of a trapped fluorescent marker. *Science* **1977,** 195, 4277, 489-492.
40. Chen, R. F.; Knutson, J. R. Mechanism of fluorescence concentration quenching of carboxyfluorescein in liposomes: Energy transfer to nonfluorescent dimers. *Analytical Biochemistry* **1988,** 172, 1, 61-77.
41. Mordon, S.; Maunoury, V.; Devoisselle, J. M.; Abbas, Y.; Coustaud, D. Characterization of tumorous and normal tissue using a pH-sensitive fluorescence indicator (5,6-carboxyfluorescein) in vivo. *Journal of Photochemistry and Photobiology B: Biology* **1992,** 13, 3–4, 307-314.
42. Lutty, G. A. The acute intravenous toxicity of biological stains, dyes, and other fluorescent substances. *Toxicology and Applied Pharmacology* **1978,** 44, 2, 225-249.
43. Fischer, R.; Mader, O.; Jung, G.; Brock, R. Extending the Applicability of Carboxyfluorescein in Solid-Phase Synthesis. *Bioconjugate Chemistry* **2003,** 14, 3, 653-660;

Fischer, R.; Köhler, K.; Fotin-Mleczek, M.; Brock, R. A Stepwise Dissection of the Intracellular Fate of Cationic Cell-penetrating Peptides. *Journal of Biological Chemistry* **2004,** 279, 13, 12625-12635.
44. Lewis, B. A.; Engelman, D. M. Lipid bilayer thickness varies linearly with acyl chain length in fluid phosphatidylcholine vesicles. *Journal of Molecular Biology* **1983,** 166, 2, 211-217.
45. Marshall, S. E.; Hong, S.-H.; Thet, N. T.; Jenkins, A. T. A. Effect of Lipid and Fatty Acid Composition of Phospholipid Vesicles on Long-Term Stability and Their Response to Staphylococcus aureus and Pseudomonas aeruginosa Supernatants. *Langmuir* **2013,** 29, 23, 6989-6995.
46. Razin, S. Reconstitution of biological membranes. *Biochimica et Biophysica Acta (BBA) - Reviews on Biomembranes* **1972,** 265, 2, 241-296.
47. López, O.; de la Maza, A.; Coderch, L.; López-Iglesias, C.; Wehrli, E.; Parra, J. L. Direct formation of mixed micelles in the solubilization of phospholipid liposomes by Triton X-100. *FEBS Letters* **1998,** 426, 3, 314-318.
48. Salyers, A. A.; Whitt, D. D. *Bacterial Pathogenesis A Molecular Approach*. 2 ed.; ASM Press: **2002**; 560.
49. Lenhardt, R.; Sessler, D. I. Estimation of mean body temperature from mean skin and core temperature. *Anesthesiology* **2006,** 105, 6, 1117-21.
50. Murzyn, K.; Róg, T.; Pasenkiewicz-Gierula, M. Phosphatidylethanolamine-Phosphatidylglycerol Bilayer as a Model of the Inner Bacterial Membrane. *Biophysical Journal* **2005,** 88, 2, 1091-1103.
51. Henriques, S. T.; Huang, Y. H.; Castanho, M. A.; Bagatolli, L. A.; Sonza, S.; Tachedjian, G.; Daly, N. L.; Craik, D. J. Phosphatidylethanolamine binding is a conserved feature of cyclotide-membrane interactions. *J Biol Chem* **2012,** 287, 40, 33629-43.
52. Kolusheva, S.; Shahal, T.; Jelinek, R. Peptide-membrane interactions studied by a new phospholipid/polydiacetylene colorimetric vesicle assay. *Biochemistry* **2000,** 39, 51, 15851-9.
53. Okada, S.; Peng, S.; Spevak, W.; Charych, D. Color and Chromism of Polydiacetylene Vesicles. *Accounts of Chemical Research* **1998,** 31, 5, 229-239.
54. Zhou, J.; Tun, T. N.; Hong, S.-h.; Mercer-Chalmers, J. D.; Laabei, M.; Young, A. E. R.; Jenkins, A. T. A. Development of a prototype wound dressing technology which can detect and report colonization by pathogenic bacteria. *Biosensors and Bioelectronics* **2011,** 30, 1, 67-72.
55. Vance, J. E.; Vance, D. E. *Biochemistry of lipids, lipoproteins and membranes*. Access Online via Elsevier: **2008**.
56. Tanford, C. *The Hydrophobic Effect: Formation of Micelles and Biological Membranes 2d Ed*. J. Wiley.: **1980**.
57. Maulik, P. R.; Shipley, G. G. Interactions of N-stearoyl sphingomyelin with cholesterol and dipalmitoylphosphatidylcholine in bilayer membranes. *Biophysical Journal* **1996,** 70, 5, 2256-2265.
58. Demel, R. A.; De Kruyff, B. The function of sterols in membranes. *Biochimica et Biophysica Acta* **1976,** 457, 2, 109-132.
59. Smaby, J. M.; Brockman, H. L.; Brown, R. E. Cholesterol's interfacial interactions with sphingomyelins and phosphatidylcholines: Hydrocarbon chain structure determines the magnitude of condensation. *Biochemistry* **1994,** 33, 31, 9135-9142.
60. Yeagle, P. L. Cholesterol and the cell membrane. *Biochimica et Biophysica Acta - Reviews on Biomembranes* **1985,** 822, 3-4, 267-287.
61. Palmer, M. Cholesterol and the activity of bacterial toxins. *FEMS Microbiology Letters* **2004,** 238, 2, 281-289.

62. Huang, J.; Buboltz, J. T.; Feigenson, G. W. Maximum solubility of cholesterol in phosphatidylcholine and phosphatidylethanolamine bilayers. *Biochimica et Biophysica Acta - Biomembranes* **1999,** 1417, 1, 89-100.
63. Wadhwani, P.; Epand, R. F.; Heidenreich, N.; Bürck, J.; Ulrich, A. S.; Epand, R. M. Membrane-Active Peptides and the Clustering of Anionic Lipids. *Biophysical Journal* **2012,** 103, 2, 265-274.
64. van Klompenburg, W.; de Kruijff, B. The Role of Anionic Lipids in Protein Insertion and Translocation in Bacterial Membranes. *The Journal of Membrane Biology* **1998,** 162, 1, 1-7.
65. Claypool, S. M.; Koehler, C. M. The complexity of cardiolipin in health and disease. *Trends in Biochemical Sciences* **2012,** 37, 1, 32-41.
66. Agassandian, M.; Mallampalli, R. K. Surfactant phospholipid metabolism. *Biochimica et Biophysica Acta (BBA) - Molecular and Cell Biology of Lipids* **2013,** 1831, 3, 612-625.
67. Domonkos, I.; Laczkó-Dobos, H.; Gombos, Z. Lipid-assisted protein–protein interactions that support photosynthetic and other cellular activities. *Progress in Lipid Research* **2008,** 47, 6, 422-435.
68. Alonso-Romanowski, S.; Biondi, A. C.; Disalvo, E. A. Effect of carbohydrates and glycerol on the stability and surface properties of lyophilized liposomes. *Journal of Membrane Biology* **1989,** 108, 1, 1-11.
69. Behr, J. P. DNA strongly binds to micelles and vesicles containing lipopolyamines or lipointercalants. *Tetrahedron Letters* **1986,** 27, 48, 5861-5864.
70. Felgner, P. L.; Gadek, T. R.; Holm, M.; Roman, R.; Chan, H. W.; Wenz, M.; Northrop, J. P.; Ringold, G. M.; Danielsen, M. Lipofection: a highly efficient, lipid-mediated DNA-transfection procedure. *Proceedings of the National Academy of Sciences of the United States of America* **1987,** 84, 21, 7413-7417.
71. Pedroso de Lima, M. C.; Simões, S.; Pires, P.; Faneca, H.; Düzgüneş, N. Cationic lipid–DNA complexes in gene delivery: from biophysics to biological applications. *Advanced Drug Delivery Reviews* **2001,** 47, 2–3, 277-294.
72. Blume, G.; Cevc, G. Liposomes for the sustained drug release in vivo. *Biochimica et Biophysica Acta (BBA) - Biomembranes* **1990,** 1029, 1, 91-97.
73. Karve, S.; Bandekar, A.; Ali, M. R.; Sofou, S. The pH-dependent association with cancer cells of tunable functionalized lipid vesicles with encapsulated doxorubicin for high cell-kill selectivity. *Biomaterials* **2010,** 31, 15, 4409-4416.
74. Tanwir, K.; Shahid, M. N.; Thomas, A.; Tsoukanova, V. Coexisting Phases in PEGylated Phosphocholine Membranes: A Model Study. *Langmuir* **2012,** 28, 39, 14000-14009.
75. Bedu-Addo, F. K.; Tang, P.; Xu, Y.; Huang, L. Effects of polyethyleneglycol chain length and phospholipid acyl chain composition on the interaction of polyethyleneglycol-phospholipid conjugates with phospholipid: implications in liposomal drug delivery. *Pharm Res* **1996,** 13, 5, 710-7.
76. Stepniewski, M.; Pasenkiewicz-Gierula, M.; Róg, T.; Danne, R.; Orlowski, A.; Karttunen, M.; Urtti, A.; Yliperttula, M.; Vuorimaa, E.; Bunker, A. Study of PEGylated Lipid Layers as a Model for PEGylated Liposome Surfaces: Molecular Dynamics Simulation and Langmuir Monolayer Studies. *Langmuir* **2011,** 27, 12, 7788-7798.
77. Ickenstein, L. M.; Arfvidsson, M. C.; Needham, D.; Mayer, L. D.; Edwards, K. Disc formation in cholesterol-free liposomes during phase transition. *Biochimica et Biophysica Acta (BBA) - Biomembranes* **2003,** 1614, 2, 135-138.
78. Mills, T. T.; Huang, J.; Feigenson, G. W.; Nagle, J. F. Effects of cholesterol and unsaturated DOPC lipid on chain packing of saturated gel-phase DPPC bilayers. *Gen Physiol Biophys* **2009,** 28, 2, 126-39.

79. Parker, A.; Miles, K.; Cheng, K. H.; Huang, J. Lateral Distribution of Cholesterol in Dioleoylphosphatidylcholine Lipid Bilayers: Cholesterol-Phospholipid Interactions at High Cholesterol Limit. *Biophysical Journal* **2004,** 86, 3, 1532-1544.
80. Mady, M. M. The influence of DOPC on the permeability of lipid membrane: Detergent solubilization and NMR study. *Romanian J. Biophys.* **2007,** 17, 4, 259-267.
81. Stegemann, S. Capsules as a Delivery System for Modified-Release Products Controlled Release in Oral Drug Delivery. Wilson, C. G.; Crowley, P. J., Eds. Springer US: **2011**; 277-298.
82. Gethin, G. T.; Cowman, S.; Conroy, R. M. The impact of Manuka honey dressings on the surface pH of chronic wounds. *International Wound Journal* **2008,** 5, 2, 185-194; Leveen, H. H.; Falk, G.; Borek, B.; Diaz, C.; Lynfield, Y.; Wynkoop, B. J.; Mabunda, G. A.; Rubricius, J. L.; Christoudias, G. C. Chemical acidification of wounds. An adjuvant to healing and the unfavorable action of alkalinity and ammonia. *Ann Surg* **1973,** 178, 6, 745-53.
83. Kaufman, T.; Eichenlaub, E. H.; Angel, M. F.; Levin, M.; Futrell, J. W. Topical acidification promotes healing of experimental deep partial thickness skin burns: a randomized double-blind preliminary study. *Burns Incl Therm Inj* **1985,** 12, 2, 84-90; Gethin, G. The significance of surface pH in chronic wounds. *Wounds UK* **2007,** 3, 3, 52-56.
84. Sharpe, J. R.; Booth, S.; Jubin, K.; Jordan, N. R.; Lawrence-Watt, D. J.; Dheansa, B. S. Progression of wound pH during the course of healing in burns. *J Burn Care Res* **2013,** 34, 3, e201-8.
85. Sjöback, R.; Nygren, J.; Kubista, M. Absorption and fluorescence properties of fluorescein. *Spectrochimica Acta Part A: Molecular and Biomolecular Spectroscopy* **1995,** 51, 6, L7-L21.
86. Fattal, E.; Couvreur, P.; Dubernet, C. “Smart” delivery of antisense oligonucleotides by anionic pH-sensitive liposomes. *Advanced Drug Delivery Reviews* **2004,** 56, 7, 931-946.
87. Barnett Foster, D.; Abul-Milh, M.; Huesca, M.; Lingwood, C. A. Enterohemorrhagic Escherichia coliInduces Apoptosis Which Augments Bacterial Binding and Phosphatidylethanolamine Exposure on the Plasma Membrane Outer Leaflet. *Infection and Immunity* **2000,** 68, 6, 3108-3115.
88. Childs, C. Fever in burned children. *Burns Incl Therm Inj* **1988,** 14, 1, 1-6.

Chapter 4 Vesicle development - sensitivity

The tailoring of vesicle sensitivity with regards to membrane lysis and the release of active internal agents in the presence of pathogenic bacterial toxins is a key requisite of this investigation. This response must be achieved selectively; the vesicles must remain un-lysed in the presence of non-pathogenic bacteria. The vesicles identified as showing an increased stability to environmental stimulus, such as pH or temperature changes over a defined period of time (14 days), shown in Table 3-5, can now be tested with specific relevant gram negative and gram positive bacteria strains commonly found in burn wounds.[1]

4.1 Research using microorganisms

The extent to which microorganisms can infect a host can vary, and as such they can be divided into four classes on the basis of their threat to laboratory workers and the community, should contamination occur. According to classifications made by the World Health Organisation (WHO) in 1979, class 1 encompasses microorganisms with low individual and low community risk, class 2 encompasses microorganisms with moderate individual but low community risk, class 3 encompasses microorganisms with high individual but low community risk and class 4 encompasses microorganisms with high individual and community risk. Within a laboratory environment, contamination can occur through the lungs, the mouth, and the skin or into the eyes.

The relevant strains of bacteria were prepared as described in chapter 2. Broth and agar utilised for growth of the gram positive and negative microorganisms provided the ideal enriched environment, based on salt content and provision of growth promoters and carbon metabolites. The bacteria are required at an inoculation optical density (OD) value of 0.01, measured on a Jenway 7300 Spectrophotometer. This OD was difficult to measure accurately, and so an OD of 0.1 was obtained by dilution in broth, followed by a 10 fold dilution. This can then be added directly into the vesicles.

OD is a measure of absorbance of a culture of cells and is measured according to the Beer-Lambert Law, where A = absorbance, I_o = incident light intensity, I = transmitted light intensity, ε = molar absorptivity, c = concentration and l = path length:

$$A = \log \frac{I_o}{I} = \varepsilon cl \qquad \text{Equation 4-1}$$

The absorbance of a bacterial culture was measured at 600 nm, and is a measure of the degree of light scattering caused by the cells in the culture, relative to a standard, to estimate the number of cells in a culture.

4.2 Bacteria

Investigations into the sensitivity of vesicles were carried out initially with four strains of bacteria (referred to as standard bacteria strains in other sections of this report). This was to determine the vesicle response, through release of a fluorescent dye, to the presence of lytic agents. The three organisms and four strains used within these investigations are *Staphylococcus aureus* MSSA 476, *Staphylococcus aureus* MSSA RN4282, *Pseudomonas aeruginosa* PAO1 and *Escherichia coli* DH5α. Of these; three strains *S.aureus* MSSA 476, *S.aureus* RN4282 and *P.aeruginosa* PAO1 are pathogenic, and *E.coli* DH5α is non-pathogenic. Each of these will be discussed in more detail.

4.2.1 *Staphylococcus*

The genus *Staphylococcus* contains pathogens common to both humans and animals that are responsible for infections of skin or wounds. In some cases these colonising-bacteria can cause infections that are life-threatening. *Staphylococci* are gram positive cocci of between 0.8-1.0µm in diameter; they are non-sporulating, resistant to drying and readily dispersed in dust particles through the air and on surfaces. In humans, three major species are recognised; *S.epidermis*, *S.aureus* and *S.saprophyticus.* Aside from their disease profile, these can be differentiated according to whether they are negative (*S. epidermis, S.saprophyticus*) or positive (*S.aureus*) for coagulase, a surface protein that causes blood to clump.[2] Within this investigation species of *S.aureus* were utilised for applications involving vesicles.

4.2.1.1 Staphylococcus aureus

S.aureus is a non-motile, yellow pigmented, cluster species commonly associated with skin and other infections. Examples of these include impetigo, boils and scalds, food borne diseases, wound and implant infections and toxic shock syndrome and sepsis. *S.aureus* is an

opportunistic virulent pathogen that is currently the most common cause of infections in hospitalised patients. This is due to its extensive amount of virulence factors, and its ability to evolve new virulent and drug-resistant variants. It has particular relevance to this investigation as it is the most common colonising bacteria in burn wounds. It is able to adhere to cells, spread in tissues and form abscesses, and produce extracellular enzymes or exotoxins. The common toxins and pathogenicity factors are given in Table 4-1:

Toxin produced	**Effect**
Enterotoxins	*Released following colonisation of food - food poisoning*
Exfoliative or epidermolytic	*Peeling layers of epidermis*
Hemolysins	*Lysis of erythrocytes*
Leukocidins	*Lysis of leucocytes and macrophages*
Toxic shock syndrome (TSST)	*Vascular collapse, rash with desquamation, systemic shock*
Pathogenicity factor	**Effect**
Microbial surface components recognising adhesives matrix molecules (MSCRAMMs)	*Mediate adherence to host cells*
Protein A	*Evade host defences*
Fibronectin-binding protein	*Mediates binding to fibronectin*
Fibrogen-binding protein	*Clumping factors*
Capsule	*Evade host defences*
Coagulase	*Generates protective fibrin layer around S.aureus*
Staphylokinase	*Fibrinolysis*
Proteases	*Degrade matrix and antibacterial proteins*
Lipases	*Promote interstitial spreading of organism*
Hyaluronidase	*Degrades hyaluronic acid*
α-hemolysin	*Lyses erythrocytes and damages platelets*

β-hemolysin	*Degrades sphingomyelin*
Leukocidin / leucotoxin	*Lyse Leukocytes*

Table 4-1**.** Toxins and pathogenicity factors produced by *S.aureus*.[3]

S.aureus is part of the natural flora of the nasopharynx (the upper respiratory tract) of healthy individuals known as carriers (approximately 33 % of the population), where it is thought that other microorganisms compete successfully for resources and therefore pathogen growth is limited. There are five general stages of *S.aureus* infection during which extracellular proteins are secreted to damage the host cell (pathogenesis). These are colonisation, localised infection, systemic dissemination and/or sepsis, metastatic infection and toxinosis.[4]

The resistance of *S.aureus* to the β-lactam antibiotic was first described in the 1960s, however methicillin resistant *staphylococcus aureus (*MRSA) strains spread rapidly between the 1980s to 1990s, with 40-60 % of all bacterial infections now being resistant.[5] Within this investigation Methicillin susceptible *staphylococcus aureus* (MSSA) 476 is utilised. MSSA 476 is a community acquired strain isolated in 1998 from a 9 year old patient who had no predisposing risk factors. MSSA 476 is composed of 2,799,802 bp chromosomes in size with 2,565 genes. Although it is resistant to penicillin and fusidic acid, it is susceptible to commonly used antibiotics including gentamicin, ciprofloxacin and tetracycline.[6] MSSA RN4282 is a naturally occurring strain that produces and secretes small amounts of exoproteins but elevated quantities of TSST.[7]

4.2.1.2 The relevance of MSSA RN4282

Toxic shock syndrome (TSS) is a severe systemic toxin mediated disease, produced by some strains of bacteria, but most commonly *S.aureus*. It is characterised by shock, pyrexia (fever), gastrointestinal disturbance and problems with the central nervous system. These symptoms mimic many other childhood illnesses, and so it is often misdiagnosed. It is the most common cause of unexpected mortality in children with small burns, with a mortality of ~50 % if left untreated. At particular risk to TSST colonisation are skin damaged children under four years old, who have not yet developed antibodies to the toxins produced by the bacteria. Paediatric burn patients have an increased risk of developing TSS as a result of the damage to the protective skin barrier and impaired immunity. In addition to this the damaged area provides advantageous environmental conditions for toxin production following colonisation. These

conditions include an aerobic environment, a neutral pH, elevated levels of CO_2, raised temperatures and increased quantities of host serum available for use as a food source. The true incidence of TSS is unknown due to the difficulty of accurate diagnosis.[8]

4.2.2 *Pseudomonas aeruginosa*

Pseudomonas aeruginosa (*P.aeruginosa*) is a versatile, mobile gram negative rod-shaped bacteria that grows ubiquitously on plant and animal tissue. In addition to this it can colonise soil, marshes and coastal habitats; forming biofilm structures on wet surfaces.[9] Despite the virulence characteristics more commonly recognised and associated with *P.aeruginosa*, it is worth noting that some strains play an important role in soil ecology, with the ability to degrade a variety or organic compounds, making them useful for bioremediation applications.[2]

P.aeruginosa was previously thought to be innocuous, or even beneficial, to host organisms, however its ability to take advantage of breaches in host defences ensures that it is now considered an opportunistic pathogen. Consequentially, *P.aeruginosa* targets the immuno-compromised. It is a significant source of bacteraemia in burn patients, it can colonise at surgical sites (where the skin has been breached), and be problematic for cystic fibrosis patients, resulting in pulmonary failure. These negative colonisation effects are amplified as a result of its intrinsic resistance to antibiotics and disinfectants.[10]

P.aeruginosa bacteria contain regulatory pathways that are capable of eliciting a feedback response, ensuring that the density of cells within their own population is controlled. This feedback control is known as quorum sensing, and assists in biofilm formation, discussed previously in 1.1.4 Biofilm and 1.1.5 Quorum sensing. This process involves the expression of an enzyme that synthesises acylated homoserine lactone (AHL), which is actively diffused out of the cell and therefore reaches high concentrations if there are a high number of the same cells present. As the homoserine lactones accumulate they function as chemotactic agents, recruiting nearby *P.aeruginosa* cells and developing biofilms.

The virulence and pathogenic factors of *P.aeruginosa* include adhesins, lipopolysaccharides and exotoxin A (ExoA). Adhesins can selectively attach to specific host cells, lipopolysaccharides, such as ExoS and ExoU, can be injected directly into the cytoplasm of host cells, and exotoxin A is involved in binding to host cell protein synthesis receptors; potentially causing tissue damage and decreasing host cell phagocytic response.[2]

P.aeruginosa PAO1 is the most widely used lab strain of *P.aeruginosa*. It has an intrinsic resistance to many front line antibiotics due to its low outer membrane permeability and the presence of antibiotic efflux pumps.[11] The bacterial genome sequence of PAO1 is 6.3 million base pairs, of which a large number code for control and command systems, enabling a complexity that allows evolutionary adaptations in diverse ecological niches.[10]

4.2.3 *Escherichia coli*

Escherichia coli (*E.coli*) are a versatile microorganism, with commensal strains having the ability to colonise the gastrointestinal tract within hours of birth (of a host) and coexisting in good health with mutual benefit for decades. These commensal strains rarely cause disease except in immune-compromised hosts, although adaptive *E.coli* strains are known that have acquired specific virulence attributes, allowing a broad spectrum of diseases and survival in different environments.[12]

E.coli is a gram negative rod-shaped bacterium, of which both pathogenic and non-pathogenic strains are commonly utilised for model systems of bacteria study. These strains of bacteria are commonly known as enteric, due to specific innate characteristics. For example, they can be non-sporulating, non-motile or motile by flagella, and able to produce acid from glucose. As with all gram negative bacteria, *E.coli* contains endotoxin in their cell walls. This can be liberated on cell lysis, resulting in complement activation and endotoxic shock.

E.coli is commonly resistant to the antibiotics penicillin and amphicillin; however it is susceptible to cephalosporins, trimethoporim and aminoglycosides. Strains isolated from hospitals often have an increased resistance to antibiotics, resulting in localised geographical areas with a greater susceptibility to infections that are difficult to treat.[3] *E.coli* DH5 is a non-pathogenic laboratory strain named after the biologist Doug Hanahan in 1985, originating from the K12 sequence through a sequence of useful mutations. DH5α is a cell line based on DH5 developed in 1986.[13]

4.3 Bacterial toxin interactions with membranes

The interactions of bacterial toxins with membranes can occur through several mechanisms. A relevant example of a toxin capable of interacting with membranes is phospholipases (PL). Within cells, these are membrane active enzymes essential for mediation of intracellular and intercellular transformations. They can function as hydrolysing enzymes to generate required bioactive compounds, such as diacylglycerol, phosphatidic acid, lysophosphatidic acid and arachidonic acid, from membrane phospholipids, depicted in Figure 4-1.[14]

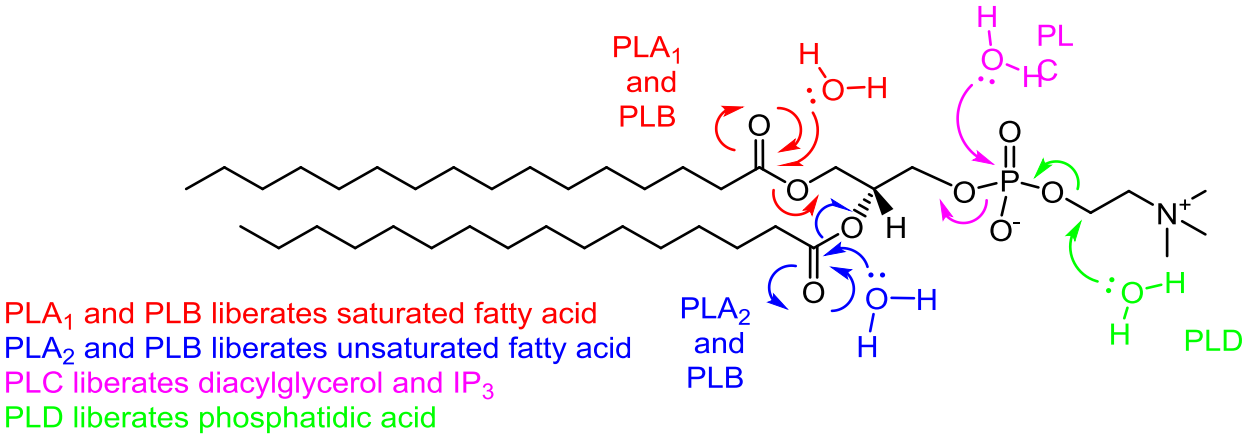

Figure 4-1. The hydrolysis sites of action of a range of phospholipase enzymes.

These PLs can be released from bacterial species as toxins able to hydrolytically degrade host membrane phospholipids, modulate host immune response and interfere with cellular signalling cascades, aiding the colonisation process.[15]

Many other bacterial toxins hydrolyse phospholipids at the sites indicated in Figure 4-1, ensuring formation of pores within host membranes, for example α-toxin secreted from *S.aureus*.[16] α-toxin, alongside other host-damaging proteins can be secreted from *S.aureus* during its' stationary phase of bacteria growth; depicted in Figure 4-2, alongside many other surface attached proteins produced during exponential cell growth.

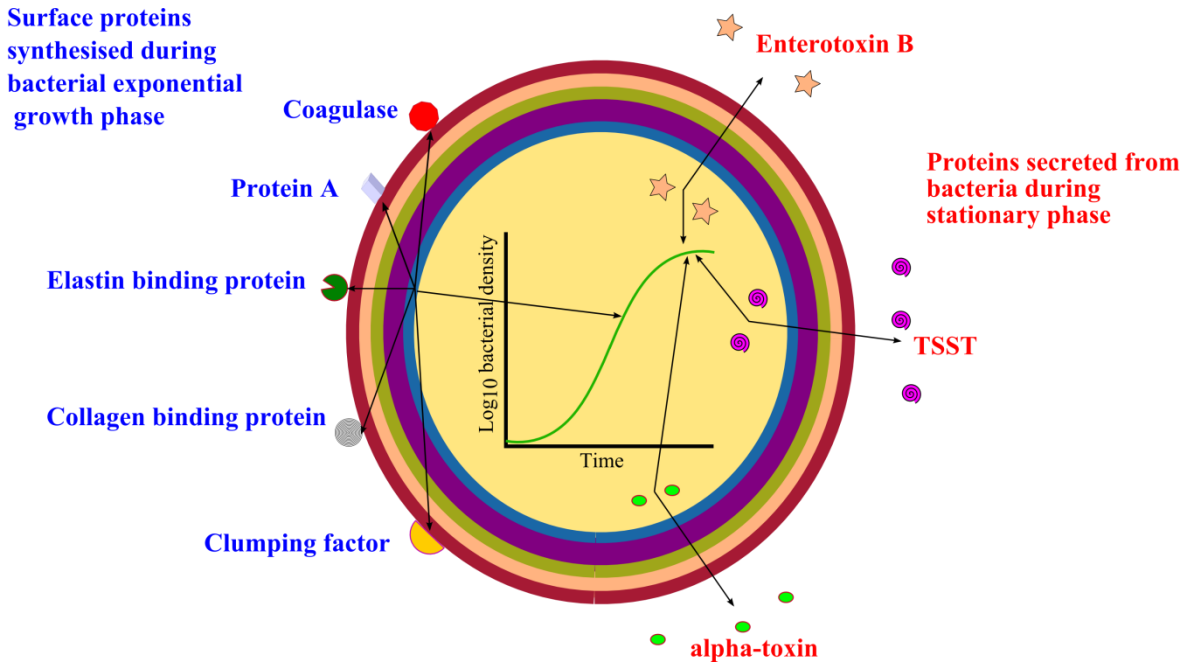

Figure 4-2. The different surface and secretion proteins of *S.aureus* bacteria and their bacterial growth phases related activity and production.[17]

4.3.1 Relevant toxins

The toxic components of bacteria which attribute directly to vesicle lysis have been investigated by other members of the group (W.D Jamieson and M. Laabei, papers with reviewers). The membrane lytic effect of *P.aeruginosa* has been found to be a result of phospholipase C, see Figure 4-1, and rhamnolipid interactions. Rhamnolipid is an opportunistic glycolipid bio-surfactant produced from *P.aeruginosa*, as well as other various bacterial species. Rhamnolipid is composed of one (mono) or two (di) rhamnose hydrophilic heads, coupled to one or two fatty acid hydrophobic tails.[18] The general structure for a mono-rhamnolipid is given in Figure 4-3.

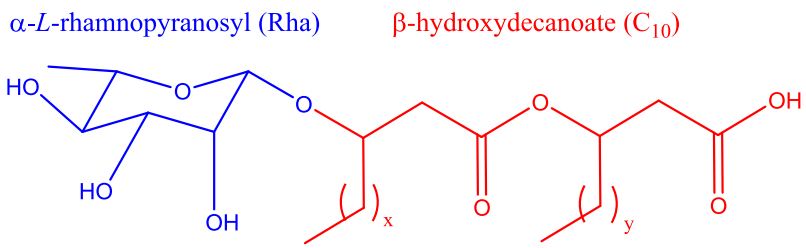

Figure 4-3. The general structure of a mono-rhamnolipid (Rha-C_{10}). There are approximately 60 homologues of four congeners; two di-rhamnolipids: Rha-Rha-C_{10}-C_{10} and Rha-Rha-C_{10}, and two mono-rhamnolipids: Rha-C_{10}-C_{10} and Rha-C_{10}.[19]

The dirhamnolipid-induced leakage of contents from vesicles is known to be affected by membrane composition; where the presence of increased levels of PE lipids and cholesterol decrease the rate and extent of internal agent leakage.[18] The mechanism of leakage is reportedly not due to membrane solubilisation, but in fact due to adsorption of the rhamnolipid onto the outer layer of the membrane, diffusion (flip-flopping) to the inner membrane, followed by intercalation to; and hence increased disorder of, the phospholipid hydrocarbon conformers. This effectively ensures a disruption to the phospholipid packing, and a lowering of the gel-to-liquid transition temperature T_c.[20]

The membrane lytic effects of *S.aureus* are a result of δ-hemolysin and phenol soluble modulin (PSM) peptides. The peptide δ-hemolysin is α-helical and composed of 26-amino acids. Its amphipathic nature allows it to form aggregates in water, bind to membranes, and be soluble in both aqueous and organic solvents. The mode of action of δ-hemolysin depends on a threshold concentration, which varies according to lipid concentration and local environment. If the concentration is below this variable threshold, the δ-hemolysin is thought to either insert in the membrane between acyl chains and polar head groups, either in a parallel manner,[21] a perpendicular manner,[22] or a disordered manner.[23] Following this the peptide can aggregate within the bilayer; resulting in the formation of pores. If the concentration is above the threshold, the δ-hemolysin is thought to act in a similar manner to the surfactant Triton X-100™, (mechanism discussed in 3.4.4 Polydiacetylene polymers). The δ-hemolysin induces a detergent-like solubilization of the membrane,[24] leading to the formation of disk shaped structures or micelles.[25]

PSM peptides can be one of four short peptides (~20 amino acids - α-type), or two longer peptides (~40 amino acids – β-type). The amino acid sequences of α-type PSMs are similar to δ-hemolysin, indicating a similar mode of action at membranes. PSMs are reported to destroy host leukocytes, and therefore play a role in evasion of innate defences. The regulation of PSM production is carried out by the accessory gene regulator (AGR) quorum sensing system,[26] discussed in detail and with respect to vesicles interactions in 4.5 Accessory gene regulator.

4.4 Vesicle response to bacteria

The effect of the bacterial toxins on the stabilised vesicles developed in chapter 3 should be akin to the pattern indicated in the graph in Figure 4-4. The release of 5(6)-CF dye from the vesicles, indicating that degradation of the membrane has occurred, only happens after growth of bacteria and consequential release of lytic toxins. The release of lytic peptides following bacterial colonisation elicits a fast vesicle-lysis response with *P.aeruginosa* PAO1 (PAO1) and a slightly slower, slightly lower intensity response with *S.aureus* MSSA 476 (MSSA 476). The response with non-pathogenic non-toxin releasing *E.coli* DH5α (DH5α) should be similar to the stability of the nanocapsules in HEPES, although there is an insignificantly slight increase in fluorescence after about 8 hours – when the bacteria is in the middle of its' exponential growth phase. These responses can be compared to the instantaneous reaction following addition of the surfactant triton.

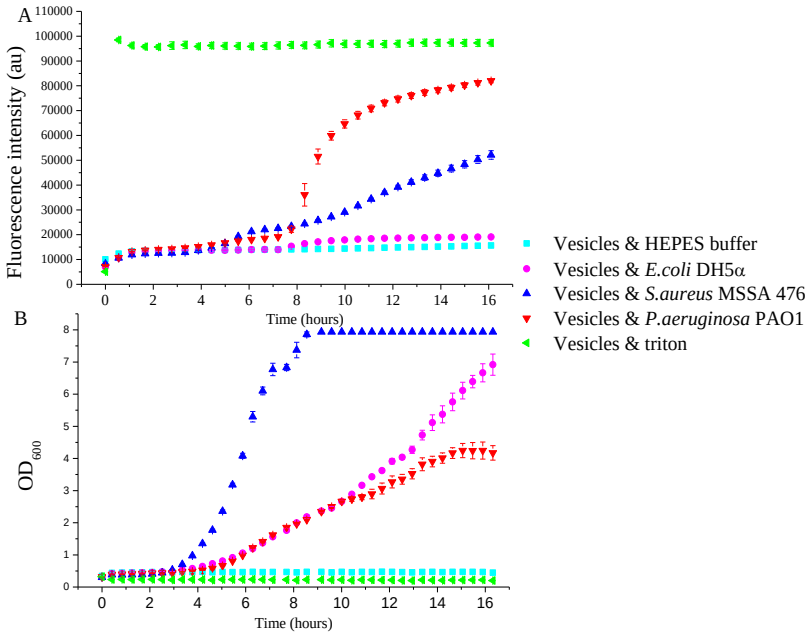

Figure 4-4. The expected vesicle lysis response following inoculation with bacteria in broth, where A) is the fluorescence response of the vesicles to the bacteria, and B) is the absorption intensity (OD_{600}) of the corresponding bacteria utilised as a measure of bacteria growth. The growth of bacteria in vesicles with HEPES buffer and triton is included to confirm that contamination of controls is not occurring.

The growth curves of the bacteria in Figure 4-4 (B) can be compared to the standard growth curve depicted in Figure 2-3**.** Bacteria growth curve, and can be related to vesicle lysis. From this an assumption can be made about when in the growth cycles of PAO1 and MSSA 476

there is sufficient numbers of bacteria cells producing sufficient quantities of lytic toxins to ensure membrane degradation. The beginning of the PAO1 toxin induced vesicle lysis response occurs after approximately 8 hours of growth, in the middle of logarithmic cell growth. A slowing of fluorescence increase and therefore vesicle lysis occurs at approximately 11 hours. Despite this still being log-phase bacteria growth, this slowing response could be due to either the majority of vesicles having already been lysed, or the rate of production and quantity of lytic toxins being decreased. It is not until approximately 15 hours that PAO1 growth reaches its' stationary phase, at this point minimal additional vesicle lysis is occurring.

MSSA 476 toxin-induced vesicle lysis response, within the time scale of this experiment, is less than the response measured from PAO1, after the same incubation time (16 hours = ~ 64 % relative to PAO1). In addition to the decreased overall response, the lysis of vesicles is much slower than for PAO1, and this could be speculated to indicate a decreased lytic ability of the toxins produced or a decreased quantity of toxin. Despite this, the MSSA 476 toxin induced vesicle lysis response slowly begins after only approximately 5 hours of growth.

It is important to note that the proportional relationship between optical density (OD_{600}) and cell density only exists at approximately OD $\leq$ 0.4. Above this OD the growth curve is distorted, hence it can only be used as an indication of bacteria growth phase. Accurate measurements regarding the number of bacteria present would require dilutions and inoculations onto plates to find colony forming units per ml (cfu ml^{-1}).

There may be slight variations in the growth of bacteria and the consequential response of vesicles between different experiments, due to the different vesicle compositions present affecting bacteria growth, and the potential, but unlikely occurrence of point mutations within the bacteria cultures utilised.

Ideally, the response of vesicles to all host-damaging lytic toxins would be equal, instantaneous, and yield a maximum indication (fluorescence) response, similar to that observed following addition of triton. However this is not the case. The growth and proliferation of bacterial cells does not occur at the same rate. This could be due to the inherent rate of multiplication of the bacterial cell and the conditions within the localised environment, such as presence of nutrients, pH fluctuations and host defences. In relation to this, the production, secretion and quantity of toxins from different bacterial species, even

within the same strain, (taking account of point mutations and location acquired: hospital and community)[26] can occur at different rates.

4.4.1 Selective sensitivity of stabilised vesicles

From chapter 3, three stabilised vesicle candidates were chosen for further testing with regard to their sensitivity to bacteria. The vesicle types chosen were DOPC-DS, TCDA-DS and DSPG-DP (compositions can be found in Table 3-5). The other two potential candidates, DPPG-DP and DSPC/DSPE, were not used for further sensitivity testing. This was due to the structural similarity of DPPG being hypothesized to give a similar sensitivity response as DSPG, and the known inherent stability of vesicles composed primarily of DSPC and therefore the postulated lack of sensitivity to external stimulus (see Table 3-5 and its stability response parameter).

The three vesicle compositions were incubated with pathogenic *S.aureus* RN4282; a relevant high TSST producing strain and *P.aeruginosa* PAO1, and non-pathogenic *E.coli* DH5α, and compared to the lytic response with the positive control: the surfactant triton, and the non-lytic negative control response with HEPES buffer. This incubation was carried out with bacterial supernatant; the separated solution obtained from a bacteria culture following centrifugation and discarding of the pellet (whole bacterial cells), and with whole bacteria cells. This is shown in Figure 4-5, where the graph indicates vesicle response to bacterial supernatant, displaying actual fluorescence intensity values obtained, and the table indicates the stability response parameter (introduced in 3.4.1 Stability response parameter) of vesicles following inoculated with whole bacterial cells for 16 hours.

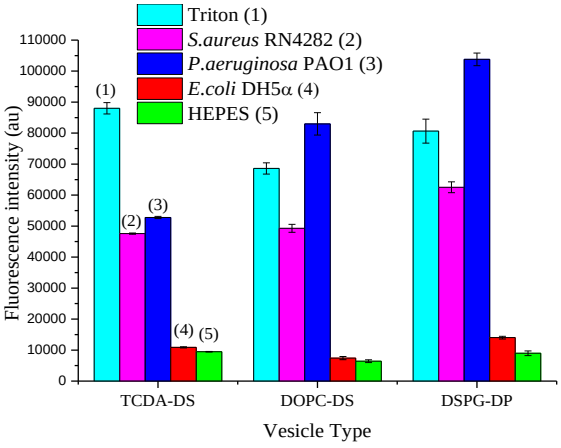

Agent added	Vesicle type		
	TCDA-DS	**DOPC-DS**	**DSPG-DP**
Triton	31.9 (±0.33)	25.1 (±0.36)	43.4 (±0.15)
RN4282	6.34 (±0.33)	6.38 (±0.06)	7.70 (±0.09)
PAO1	12.0 (±0.09)	33.2 (±2.77)	36.9 (±2.17)
DH5α	3.21 (±0.45)	1.93 (±0.05)	2.44 (±0.16)
HEPES	4.48 (±0.19)	3.06 (±0.15)	5.24 (±0.01)

Figure 4-5. Stabilised vesicle candidate sensitivity response to bacteria, where the graph gives response to supernatant of pathogenic *S.aureus* RN4282 (2), *P.aeruginosa* PAO1 (3) and non-pathogenic *E.coli* DH5α (4)**;** triton (1); and a control (HEPES buffer) (5) after 2 hours.

The table gives the stability response parameter (S) of vesicle candidates to the same pathogenic bacteria cells, triton and HEPES, after incubation for 16 hours. A large stability response parameter was desired for the vesicles treated with pathogenic bacteria and the positive control, conversely a small instability parameter was desired for vesicles treated with the negative controls.

The supernatant data plotted within the graph shows final fluorescence intensity after incubation with the supernatant and controls for 100 minutes, however the majority of vesicle lysis was achieved within 30 minutes. The vesicles containing whole bacterial cells is displayed in a table in terms of the stability response parameter, S, where a ratio of final fluorescence (after 16 hours incubation) was compared to initial fluorescence at time = 0. A high S value was indicative of a large degree of vesicle lysis which was desirable for the pathogenic bacteria (*S.aureus* RN4282 and *P.aeruginosa* PAO1) and the positive control (triton). Conversely a small S value was desired for vesicles treated with the negative controls (*E.coli* DH5α and HEPES).

From Figure 4-5, each of the three vesicle candidates can be seen to be having the desired response to pathogenic bacterial toxins, whilst remaining relatively unaffected by the non-pathogenic bacteria. The extent of the response to bacterial toxins, and even to the surfactant triton, varies according to vesicle composition. This could be postulated to be due to differences between the growth and production of bacteria, and hence toxins, within the individual wells of a 96-well plate. It could also be due to the differences between the

localised charge distributions or availability of phase boundaries within the membrane; potentially affecting the quantities and availability of toxin-vesicle sites available for interactions.

4.4.2 Observable response versus bacteria present

The actual number of pathogenic bacteria within a wound required for a signal to be observed is an important parameter within the scope of this investigation. The difficulties associated with obtaining this number will be discussed further in Fluorescence response versus bacteria count.

4.5 Accessory gene regulator

The accessory gene regulator (AGR) quorum sensing system, is involved in the regulation of toxin production primarily within *S.aureus* bacteria.[27] It is therefore important with regard to vesicle response in a burn wound environment. The complexity of the quorum sensing system and its role in down-regulation of surface proteins and up-regulation of secreted proteins during *in-vitro* growth[28] is depicted in Figure 4-6. The AGR operon consists of four genes which are encoded within a two component divergently transcribed signal systems; the P2 operon – which contains the AGR_B, AGR_D, AGR_C and AGR_A genes. The P3 operon consists of the regulatory effector molecule RNA III, which can act to repress self-repressing toxin molecules, and hence increase exo-toxin production.

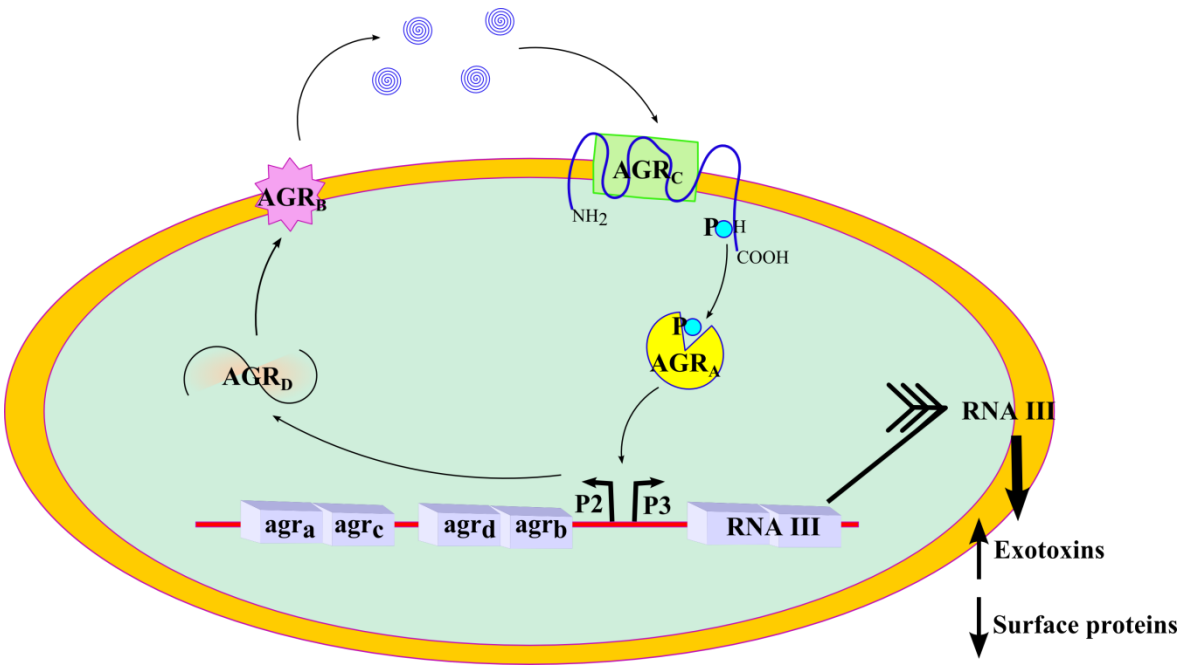

Figure 4-6. Schematic representation of the two component AGR system. Within the P2 operon, AGR_A activity results in the secretion of the auto-inducing pheromone, AGR_D. This short peptide is exported by AGR_B and consequentially binds and activates the histidine kinase receptor, AGR_C. When a sufficient concentration is achieved the response regulator AGR_A is activated, which can then act upon the P2 and P3 promoters to up-regulate AGR genes and RNA III.,[29]

The relevance and importance of this quorum sensing system is demonstrated by incubating the three stabilised vesicle candidates with *S.aureus* RN6390B, an AGR positive strain (AGR+ contains the up-regulatory system gene), and with *S.aureus* RN6911, an AGR negative strain (AGR- the gene that codes for the AGR system have been removed). The results are shown in Figure 4-7.

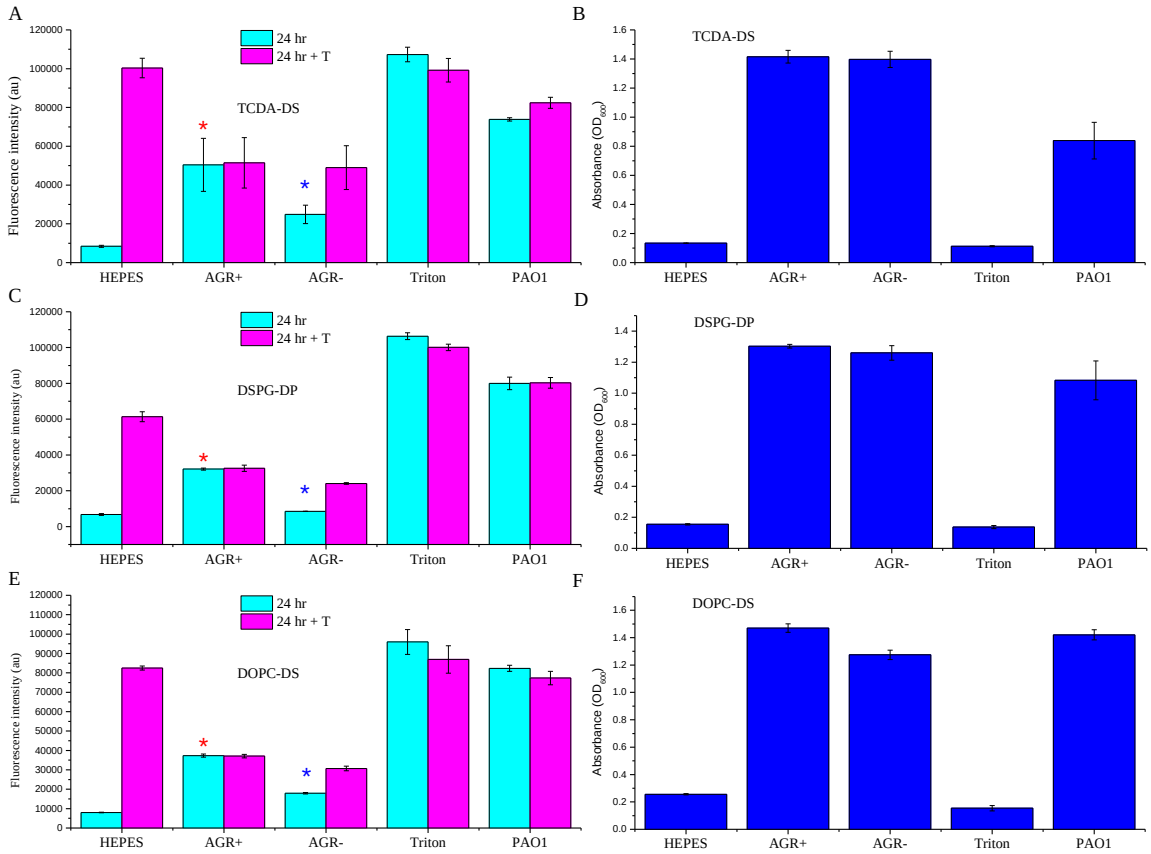

Figure 4-7. The fluorescence intensity of three primary vesicle candidates after 24 hours with bacteria and 24 hours with bacteria and triton (T), where A) is TCDA-DS vesicles, C) is DSPG-DP vesicles and E) is DOPC-DS vesicles; and B) D) and F) show corresponding bacteria growth within the same time frame in each of the vesicle types. The growth and fluorescence kinetic profiles over 18 hours for each vesicle type and bacterial species, as well as the growth of each bacteria species in a comparative, non-vesicle containing solution (HEPES) and in ideal nutrient rich conditions (broth) after 24 hours are given in the SI (SI-Figure 2 and SI-Figure 3).

The important points of interest within the graphs in Figure 4-7 are highlighted with different coloured asterisks, where the effect of the AGR+ and AGR- toxins can be measured against the three different vesicle candidates. In all three cases, the presence of AGR+ (red asterisk) increases the toxicity of the bacterial strain to the vesicles compared to AGR- (blue asterisk). Interestingly, the comparative *P.aeruginosa* PAO1, which produces rhamnolipid and PLC lytic peptides, show a larger degree of toxicity to the vesicles.

The production of different toxins within a bacterial strain is very complex, with the interaction of up-regulating and feedback systems playing a role in both expression and

quantity. Within a wound environment it is hence difficult to discern which toxins will be produced from the different bacteria present, their quantity, and the extent of their effect on the vesicles. It is possible, however to obtain wound exudate from paediatric burn patients, to attempt to imitate the conditions the vesicles would be exposed to, and measure their stability within this potentially bacteria containing medium.

4.6 Vesicles in wound exudate

The stability of the vesicles that would be placed within a dressing and applied to a wound environment is of paramount importance to this project. This project has attempted to emulate the conditions found at a wound interface, through manipulation of temperature, change in pH, dressing application (within a topical hydrogel – discussed in chapter 5), addition of bacteria, and even storage in simulated wound fluid (SimF - primarily composed of fetal calf serum). However, to increase the relevance of these studies, the vesicle stability could be tested in fluid that has been extracted from a paediatric burn wound afflicted patient. This fluid, henceforth called wound exudate (WE), can be extracted from the patient via syringe and stored on ice, if used on the day of collection, or frozen.

As part of this investigation, WE (approximately 500 µl) was extracted via syringe from a young female patient and incubated at different percentage ratios with the three primary vesicle candidates. This incubation was for a time period of 16 hours at 37 °C, results shown in Figure 4-8. The WE was also streaked onto agar nutrient plates and incubated at 37 °C overnight to check for bacteria growth; however the sample was found to be free of bacterial contamination.

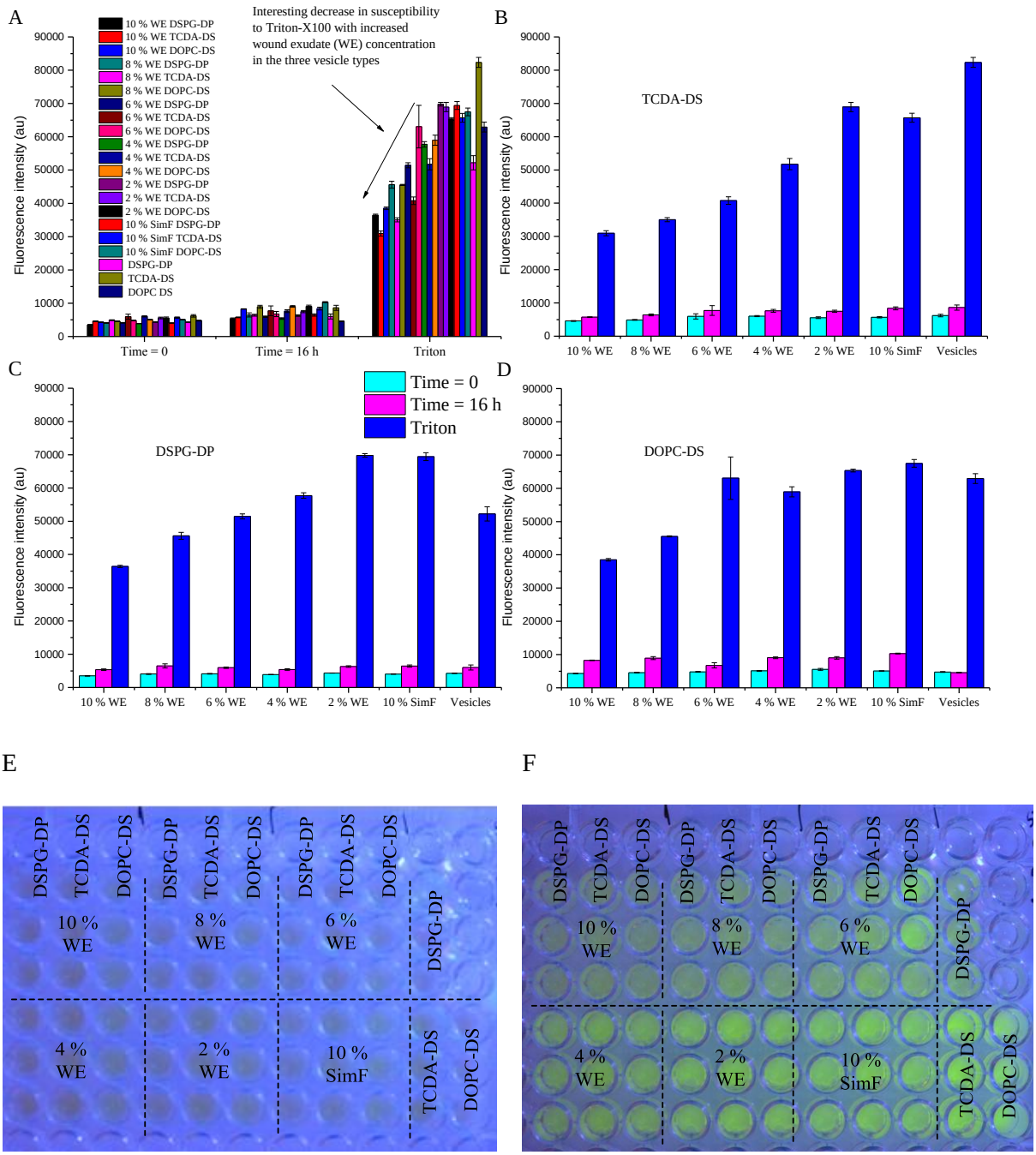

Figure 4-8. The effect of wound exudate at different concentrations, 2, 4, 6, 8, and 10 % v/v on the three primary vesicle candidates, A) shows all of the data for all three vesicle types at time = 0 hours, time = 16 hours and following addition of triton. Promising stability following multiple readings and storage for 16 hours at 37 °C can be measured; however a decreased susceptibility to triton was identified linearly with increased wound exudate concentration. B) C) and D) show the individual data for TCDA-DS, DSPG-DP and DOPC-DS vesicles respectively. The photos in E) and F) are taken under UV light, and allow for

observed differences in fluorescence to be monitored both pre (E) and post (F) Triton after 16 hours.

The results obtained in Figure 4-8 indicate favourable stability in the different concentrations of wound exudate. The decrease in fluorescence with increased wound exudate indicates an interaction is taking place between the WE and fluorophore, or WE and triton, and potential reasons for this are hypothesised following further investigation into long term stability. The stability of the vesicles in the same wound exudate, i.e. the same patient / same blister, from Figure 4-8, was carried out with 10 % v/v exudate at 5, 20 and 37 °C for 14 days, shown in Figure 4-9.

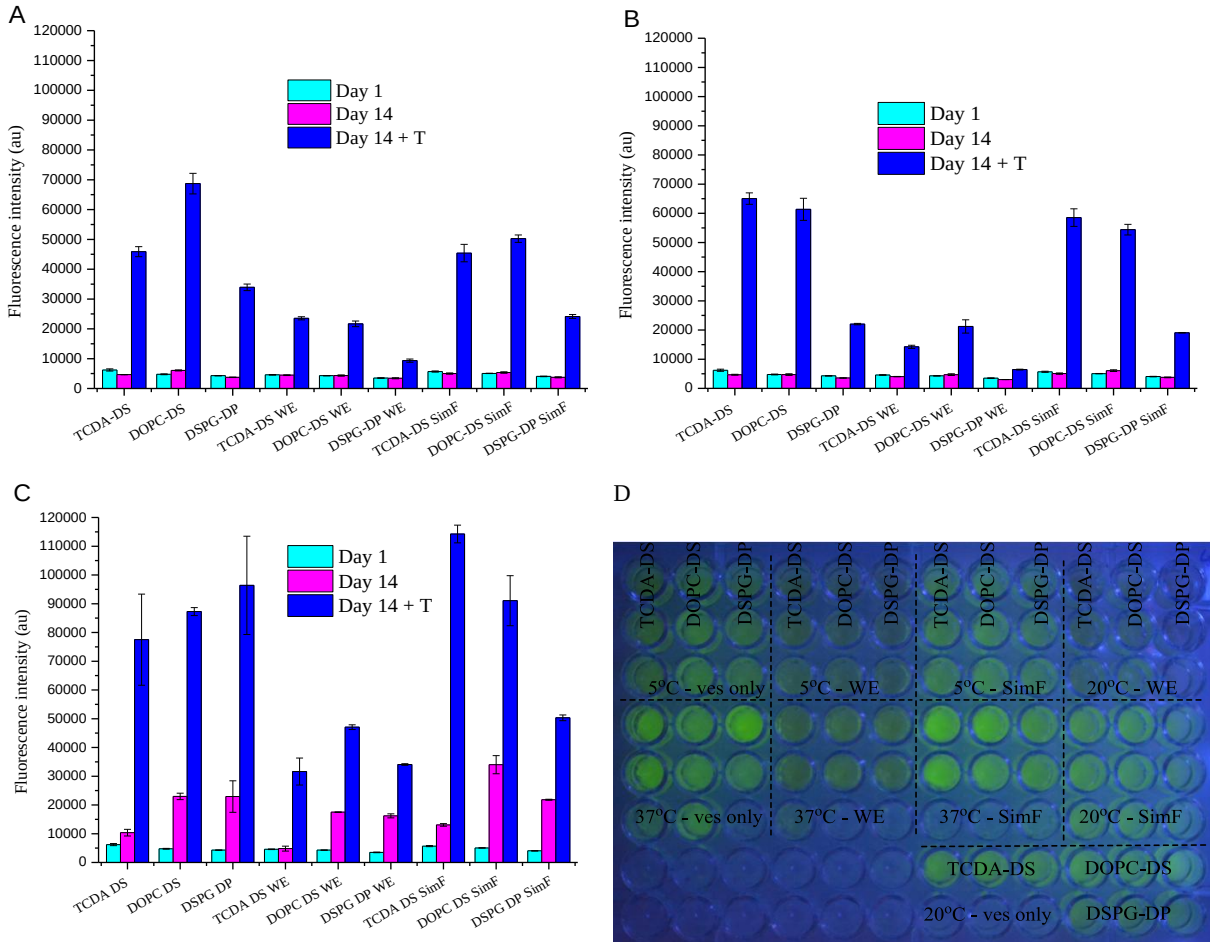

Figure 4-9. The stability of the standard three vesicle types with wound exudate, SimF and a control at day 1, after 14 days and following addition of triton at a) 5 °C, B) 20 °C and C) 37 °C. The photograph in D) shows the three vesicle types in wound exudate, SimF or in HEPES at 5, 20 and 37 °C, taken under UV light.

The vesicle solutions stored at 37 °C suffered from dehydration effects, ensuring that there was not enough vesicle volume to aliquot out three samples of each, and although this affects the validity of the results, a general trend can still be measured and observed. The vesicles

show comparative favourable stability at 5 and 20 °C. The fluorescent switch on following addition of triton to vesicles in both WE and SimF followed the expected trend for TCDA-DS and DOPC-DS vesicles at 5 and 20 °C, however for DSPG-DP vesicles the increase is much less (approximately 0.5x). These results potentially suggest that the DSPG-DP vesicles are not present in as high a concentration, indicating formation issues during extrusion or following NAP-25 column separation from the unencapsulated dye. This effect was not observed during other experiments and so this response was therefore deemed to be an anomaly rather than an actual effect of the experimental conditions.

Upon addition of triton to the vesicles incubated in WE, after the 14 day period, the expected increased fluorescence response was not observed. This potentially indicated that the WE was reacting with the triton, sequestering its ability to disrupt and dissolve membranes or preventing it accessing the vesicles. In addition to this the wound exudate could be interacting with the carboxyfluorescein and having a quenching effect. As shown in Figure 4-8, as the concentration of the wound exudate is decreased, the fluorescence response increases in a linear fashion. This effect is potentially due to the changes in pH caused by the wound exudate, as it is well known that fluorophores are affected by pH changes.[30]

The stability of vesicles in WE looks very promising, and these preliminary results indicate that the vesicles synthesised would maintain their structure successfully at a wound interface. Further experiments would be required to confirm and clarify these results. The use of pure toxins or incubation with common bacterial strains, as well as basic pH measurements, would be beneficial and provide more information about how sensitive the vesicles would be within a wound environment.

Unfortunately, the constraint on this investigation is the availability of fresh viable wound exudate. The obtaining of a sample is wholly dependent on the presence of a burn in a paediatric patient, formation of an appropriate blister from which a large enough volume of exudate can be obtained (ideally <500 µl), consent from guardians being given and successful extraction of the wound exudate through a syringe being achieved. Notice of this process is given to relevant researchers approximately two hours before a sample is ready to be collected, hence there is only a small opportunity to ensure your potential experiment is prepared correctly. Alternatively, and more practically, the sample can be frozen following arrival in the lab, to allow time for relevant vesicle formulation and growth of appropriate bacteria.

4.7 Vesicle sensitivity - conclusions

The synthesis of vesicles that not only maintain stability over time and at different temperatures and pH values, but also release their active agents, in this case the dye 5(6)-CF, in a specific sensitive manner, i.e. in the presence of pathogenic bacterial toxins has been successfully achieved within this investigation. Each of the three potential candidates investigated in chapter 3 (TCDA-DS, DSPG-DP and DOPC-DS) have indicated selective sensitivity to the different relevant strains of pathogenic bacteria. The measured differences between the degrees of response between the different vesicle candidates to the bacteria strains investigated can be postulated to be due to two primary reasons. There may be differences between the growth and production of bacteria, and hence toxins, within the individual wells of a 96-well plate. Equally, there may be variations between localised charge distributions or availability of phase boundaries within the vesicle bilayer membrane; potentially affecting the quantities and availability of favourable toxin-vesicle interaction sites.

In addition to this the importance of the AGR quorum sensing system on toxicity has been investigated with respect to the vesicle candidates. Initial results have indicated that the presence of AGR is important in ensuring vesicle lysis. The release of toxins is known to be a complex process; with large variations between expression, quantity, and even affectivity on membrane destruction varying. This was shown by the comparison of the three vesicle candidate's fluorescence response following incubation with strains of *S.aureus* AGR+, *S.aureus* AGR-, and *P.aeruginosa* PAO1.

The effect of wound exudate, obtained from a female paediatric patient with a small burn, was measured against the three vesicle candidates. The stability of vesicles in the WE looked promising, and these preliminary results indicate that the vesicles synthesised would maintain their structure successfully at a wound interface. However, following addition of triton to the vesicles incubated in WE after the 14 day period, the expected increased fluorescence response was not observed. This potentially indicated that the wound exudate is both reacting with the triton and disrupting its' ability to dissolve membranes or preventing it accessing the vesicles. Alternatively the wound exudate could be interacting with the 5(6)-CF and having a quenching effect. Further experiments would be required to confirm and clarify these results. These could involve the use of pure toxins or incubation with the standard bacterial strains,

potentially providing more information about how sensitive the vesicles would be in a wound environment.

The three selectively sensitive and stable vesicle compositions can now be used for incorporation into a wound-dressing prototype system that will allow delivery of the signalling system to a wound. The development of this is discussed further in chapter 5.

The pathogenic bacteria strains used for investigating the sensitivity of vesicles to toxins have proven effective at lysing the membranes, ensuring effective release of the 5(6)-CF. The signalling aspect of this system is of large importance, however the incorporation of antibacterial agents within the vesicles, that could destroy the bacteria cells following release would prove beneficial; therefore it requires investigation. Preliminary further work results are discussed in the following section.

4.7.1 Further work - encapsulation of antibacterial agents

The encapsulation of antimicrobial and/or antibiotic agents into the vesicles, alongside a dye, offers a promising potential to create a system that could detect and treat an infection within a wound. It is hypothesised that following successful incorporation of an antibacterial agent within the vesicle the bacteria growth (measured through absorbance OD_{600}) would follow that shown in Figure 4-10.

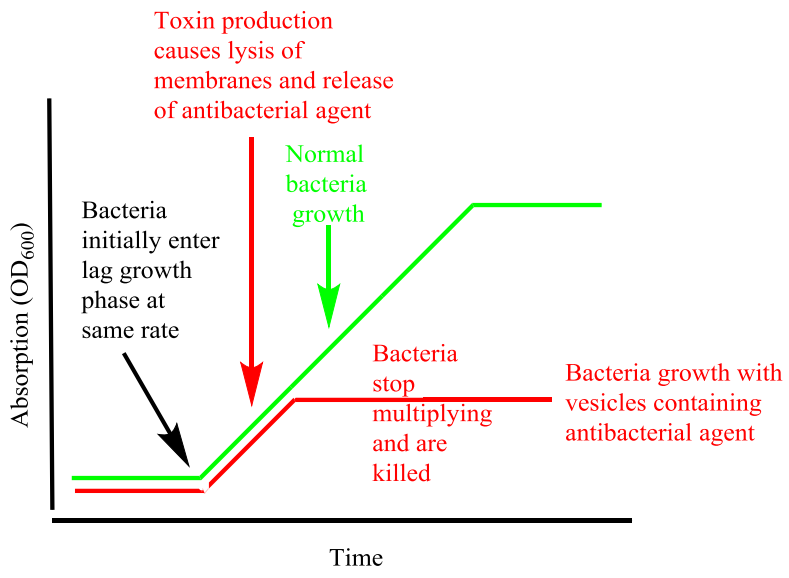

Figure 4-10. Hypothesised growth curve of bacteria in the presence of vesicles containing an antibacterial agent, compared to normal bacteria growth in favourable conditions (with regard to pH, temperature and nutrient supply)

4.7.1.1 Antimicrobial agents

An antimicrobial agent can be defined as a substance with inhibitory properties against microorganisms that has little or no effects on mammalian cells. This can include antibiotics and other synthetic compounds. An antibiotic agent is a substance produced by a microorganism that has the ability to inhibit the growth of (bacteriostatic) or kill (bactericidal, viricidal, fungicidal) other microorganisms. This term does not apply to purely synthetic agents; however chemical modification of antibiotics to improve properties such as spectrum of activity and stability can yield the more widely recognised semi-synthetic antibiotics.[3]

Different agents can be classified according to their target mode of action. This can, for example include interference with the bacterial cell wall or membrane, or provoke a preventative mechanism against protein or nucleic acid synthesis. Examples of antimicrobial agents with different sites of action are given in Table 4-2.

Site of action	**Antimicrobial agent**
Cell wall	Penicillins, cephalosporins, vancomycin
Cell membrane*	Polymyxins*
Protein synthesis	Aminoglycosides, chloramphenicol, fusidic acid, macrolides, tetracyclines
DNA synthesis	Sulphonamide, Trimethoprim, Quinolones
RNA synthesis	Rifampicin

Table 4-2. The site of action of different antimicrobial agents. *Cell membrane active agents are predicted to have a negative disruption effect on the stability of lipids prior to formation of vesicle membranes and hence will not be incorporated into formulations.*[3]

4.7.1.2 Minimum inhibitory concentration

A minimum inhibitory concentration (MIC) assay can be used to determine the lowest concentration of an antibacterial (the maximum dilution), required to restrict the growth of bacteria over a given time period. Visual measurements were firstly utilised to gauge an appropriate range, followed by appropriate narrowing of agent concentration and consecutive growth measurements (OD_{600}) for the same. The affectivity of an antibacterial agent was

tested against a gram negative and a gram positive bacterial species, in this case *P.aeruginosa* PAO1and *S.aureus* MSSA 476, both discussed in 4.2 Bacteria. From the approximate MIC concentration range identified, an accurate concentration range was investigated between the two values of growth and non-growth.

From this data the concentration of an antibacterial agent required to inhibit a certain amount of bacteria can be estimated. The two most common values are the MIC50 and MIC100; the amount of antimicrobial required to inhibit 50 % and 100 % of the bacteria growth, respectively. Complete encapsulation of an agent into vesicles during the manufacturing process does not always occur; unencapsulated agents are separated during NAP-25 column separation. As a result of this a concentration slightly above the experimentally derived necessary amount was utilised to try and ensure that an MIC100 was available following vesicle lysis.

An example of OD_{600} bacterial growth curves of *S.aureus* MSSA 476 versus different concentrations of doxorubicin HCl (see Table 4-3) is given in Figure 4-11.

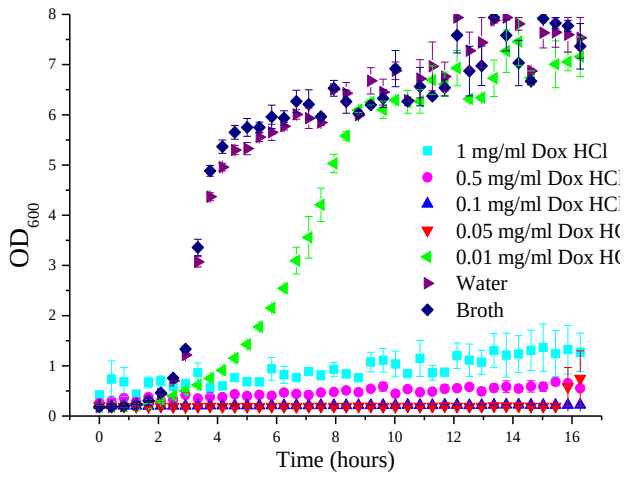

Figure 4-11. The growth of gram positive *S.aureus* MSSA 476 when incubated with different concentrations of doxorubicin hydrochloride, compared to growth in nutrient rich broth or water.

4.7.1.3 Antibacterial agents

The MIC100 of different antibacterial agents against gram+ *S.aureus* MSSA 476 and gram- *P.aeruginosa* PAO1 was determined, and this, along with their structure and activity, is given in Table 4-3.

Antimicrobial / Antibiotic	**Structure**	**Activity**	**MIC for Gram+ *S.aureus* MSSA 476 (mol L^{-1})**	**MIC for Gram- *P.aeruginosa* PAO1 (mol L^{-1})**
Tetracycline	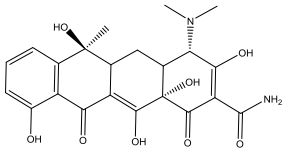	Reversible inhibition of protein synthesis[31]	No inhibition	2.3×10^{-3}
Doxorubicin hydrochloride (Dox HCl)	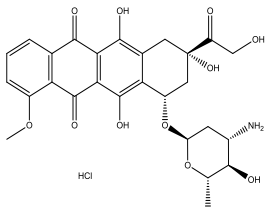	Inhibition of DNA and RNA synthesis[32]	1.7×10^{-4}	8.6×10^{-4}
Vancomycin	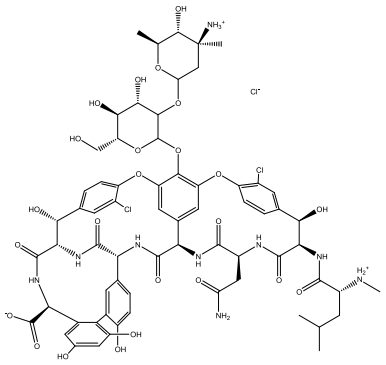	Inhibition of bacterial cell wall peptidoglycan synthesis[33]	6.9×10^{-5}	6.9×10^{-3}
Ampicillin	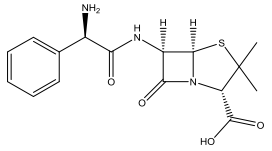	Inhibition of bacterial cell wall peptidoglycan synthesis[34]	1.4×10^{-3}	2.9×10^{-2}
Oxacillin	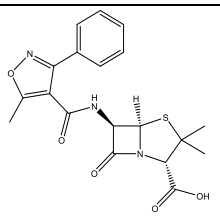	Inhibition of bacterial cell wall peptidoglycan synthesis[34]	2.5×10^{-4}	2.5×10^{-2}
Ciprofloxacin	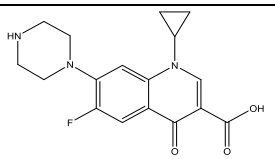	Inhibition of bacterial DNA gyrase – preventing DNA replication[35]	3.0×10^{-3}	3.0×10^{-6}

Table 4-3. The structure and activity of different antibacterial agents, and the MIC100 against gram+ *S.aureus* MSSA 476 and gram- *P.aeruginosa* PAO1 (mol L^{-1})

These antibiotic agents were investigated due to their broad spectrum of activity against gram+ and / or gram- bacteria, their mode of actions being potentially compatible with encapsulation in phospholipid vesicle membranes, and their good solubility profiles in aqueous solutions.

4.7.1.4 Incorporation of antibacterial agents into vesicles

Following MIC_{100} results, the different antibiotics were added to HEPES buffer at their required concentration, as an alternative to the 5(6)-CF dye, and this antibacterial solution was added to the vesicles following dehydration of membrane components into a thin film. Standard vesicles formulation procedures were followed from this point.

Initial experiments investigating the success of each active agent encapsulation did not prove massively successful. Absorbance (OD_{600}) measuring bacteria growth versus active-agent-encapsulated-in-vesicles results indicated that either the active agent was potentially within the solution as well as in the vesicles, as no bacteria growth was detected, or the active agent was not within the vesicles solution at all, and standard bacteria growth was observed. To try and improve the separation of unencapsulated active agent from vesicles containing the active agent, ultra-centrifugation was utilised as a secondary purification technique, with speeds up to 30,000 rpm for 1 hour.

Despite this, many of the antibacterial agents proved incompatible with encapsulation within vesicles, and promising results were not achieved. Although, the most promising results were achieved following the encapsulation of Dox HCl (0.5 mg/ml) into DSPG-DP vesicles and comparative growth curves of Dox HCl vesicles with bacteria and positive bacteria controls is given in Figure 4-12.

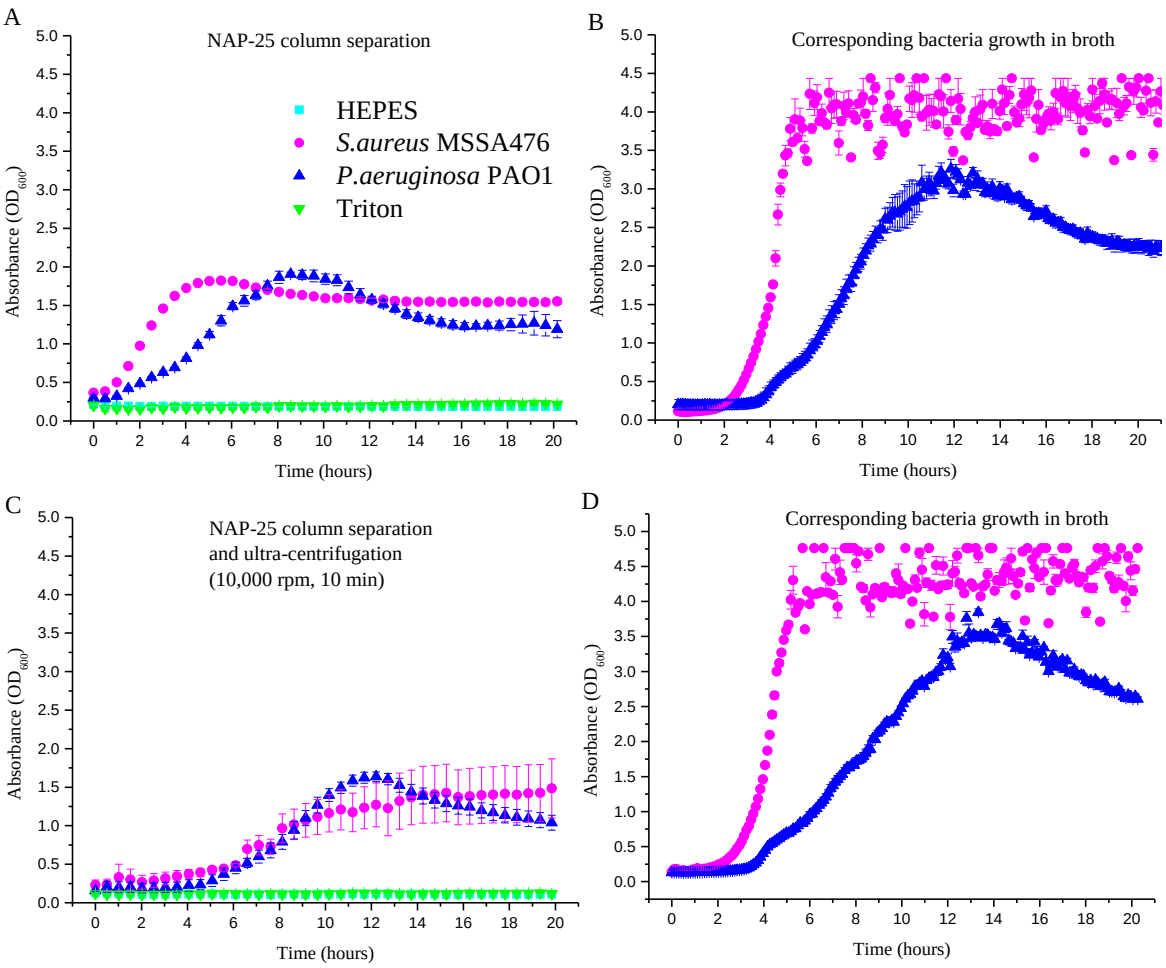

Figure 4-12. The growth of bacteria when incubated with DSPG-DP vesicles containing Dox HCl (0.5 mg/ml) where A) is the growth of bacteria with vesicles that have undergone standard separation procedures and C) is the growth of bacteria with vesicles that have undergone a secondary purification step using ultra-centrifugation (10,000 rpm, 10 min). B) and D) are the respective corresponding positive control: bacteria growth in nutrient rich broth.

From Figure 4-12, the disturbance of bacteria growth from the standard bacteria control growth can be seen to be in a manner similar to that predicted and depicted in Figure 4-10, indicating the desired response has been achieved. Further confirmation of this result would be beneficial, and could be achieved using comparative bacterial strains that are both susceptible and resistant to Dox HCl. In addition to this the incorporation of Dox HCl into the 5(6)-CF dye prior to encapsulation into vesicles would allow the progress to be monitored based on a fluorescence intensity assay. These results confirm the reported results relating to Dox HCl encapsulation in vesicles in the literature.[36] It should be noted that a variation on

this system has already been commercialised; Avanti Polar Lipids (APL) manufacture a PEGylated liposomal doxorubicin nanodrug for injection related applications (Dox-NP®).[37]

4.8 References

1. Church, D.; Elsayed, S.; Reid, O.; Winston, B.; Lindsay, R. Burn Wound Infections. *Clinical Microbiology Reviews* **2006,** *19* (2), 403-434.
2. Salyers, A. A.; Whitt, D. D. *Bacterial Pathogenesis A Molecular Approach*. 2 ed.; ASM Press: **2002**; 560.
3. Elliott, T.; Worthington, T.; Osman, H.; Gill, M. *Medical Microbiology and Infection*. 4th ed.; Blackwell Publishing: **2007**.
4. Archer, G. L. Staphylococcus aureus: A Well-Armed Pathogen. *Clinical Infectious Diseases*, **1998**; 26, 1179-1181.
5. Lindsay, J. A.; Holden, M. T. G. Understanding the rise of the superbug: investigation of the evolution and genomic variation of Staphylococcus aureus. *Funct. Integr. Genomics*, **2006**; 6, 186-201.
6. Holden, M. T. G.; Feil, E. J.; *al, e.* Complete genomes of two clinical *Staphylococcus aureus* strains: Evidence for the rapid evolution of virulence and drug resistance. *Proceedings of the National Academy of Sciences USA*, **2004**; 101, 9786-9791.
7. Vojtov, N.; Ross, H. F.; Novick, R. P. Global repression of exotoxin synthesis by staphylococcal superantigens. *Proceedings of the National Academy of Sciences* **2002,** 99, 15, 10102-10107; Subedi, A.; Ubeda, C.; Adhikari, R. P.; Penadés, J. R.; Novick, R. P. Sequence analysis reveals genetic exchanges and intraspecific spread of SaPI2, a pathogenicity island involved in menstrual toxic shock. *Microbiology* **2007,** 153, 10, 3235-3245.
8. Young, A. E.; Thornton, K. L. Toxic shock syndrome in burns: Diagnosis and management. *Arch Dis Child Educ Pract Ed*, **2007**; 92, 97-100.
9. Hardalo, C.; Edberg, S. C. *Pseudomonas aeruginosa*: assessment of risk from drinking water. *Crit. Rev. Microbiol*., **1997**; 23, 47-75.
10. Stover, C. K.; Pham, X. Q.; *al, e.* Complete genome sequence of *Pseudomonas aeruginosa* PA01, an opportunistic pathogen. *Nature*, **2000**; 406, 959-964.
11. Hancock, R. E. W. Resistance mechanisms in *Pseudomonas aeruginosa* and other nonfermentative gram-negative bacteria. *Clinical Infectious Diseases*, **1998**; 27, S93-S99.
12. Kaper, J. B.; Nataro, J. P.; Mobley, H. L. T. Pathogenic *Escherichia coli* Nature Reviews: *Microbiology*, **2004**; 2, 123-140.
13. Hanahan, D. Studies on transformation of Escherichia coli with plasmids. *Journal of molecular biology*, **1983,** 166, 4, 557-580.
14. Park, J. B.; Lee, C. S.; Jang, J. H.; Ghim, J.; Kim, Y. J.; You, S.; Hwang, D.; Suh, P. G.; Ryu, S. H. Phospholipase signalling networks in cancer. *Nat Rev Cancer*, **2012,** 12, 11, 782-92.
15. Schmiel, D. H.; Miller, V. L. Bacterial phospholipases and pathogenesis. *Microbes Infect*, **1999,** 1, 13, 1103-12.
16. Bhakdi, S.; Tranum-Jensen, J. Alpha-toxin of Staphylococcus aureus. *Microbiological Reviews*, **1991,** 55, 4, 733-751.
17. Lowy, F. D. Staphylococcus aureus infections. *New England Journal of Medicine*, **1998,** 339, 8, 520-532.
18. Sanchez, M.; Aranda, F. J.; Teruel, J. A.; Espuny, M. J.; Marques, A.; Manresa, A.; Ortiz, A. Permeabilization of biological and artificial membranes by a bacterial dirhamnolipid produced by Pseudomonas aeruginosa. *J Colloid Interface Sci*, **2010,** 341, 2, 240-7.

19. Abdel-Mawgoud, A.; Lépine, F.; Déziel, E. Rhamnolipids: diversity of structures, microbial origins and roles. *Applied Microbiology and Biotechnology,* **2010,** 86, 5, 1323-1336.
20. Ortiz, A.; Teruel, J. A.; Espuny, M. J.; Marques, A.; Manresa, A.; Aranda, F. J. Effects of dirhamnolipid on the structural properties of phosphatidylcholine membranes. *Int J Pharm,* **2006,** 325, 1-2, 99-107.
21. Silvestro, L.; Axelsen, P. H. Membrane-induced folding of cecropin A. *Biophys J,* **2000,** 79, 3, 1465-77.
22. Pokorny, A.; Almeida, P. F. Permeabilization of raft-containing lipid vesicles by delta-lysin: a mechanism for cell sensitivity to cytotoxic peptides. *Biochemistry,* **2005,** 44, 27, 9538.
23. Sengupta, D.; Leontiadou, H.; Mark, A. E.; Marrink, S. J. Toroidal pores formed by antimicrobial peptides show significant disorder. *Biochim Biophys Acta* **2008,** 1778, 10, 2308.
24. Bechinger, B.; Lohner, K. Detergent-like actions of linear amphipathic cationic antimicrobial peptides. *Biochim Biophys Acta,* **2006,** 1758, 9, 1529-39.
25. Verdon, J.; Girardin, N.; Lacombe, C.; Berjeaud, J. M.; Hechard, Y. delta-hemolysin, an update on a membrane-interacting peptide. *Peptides,* **2009,** 30, 4, 817-23.
26. Wang, R.; Braughton, K. R.; Kretschmer, D.; Bach, T. H.; Queck, S. Y.; Li, M.; Kennedy, A. D.; Dorward, D. W.; Klebanoff, S. J.; Peschel, A.; DeLeo, F. R.; Otto, M. Identification of novel cytolytic peptides as key virulence determinants for community-associated MRSA. *Nat Med* **2007,** 13, 12, 1510.
27. Bunce, C.; Wheeler, L.; Reed, G.; Musser, J.; Barg, N. Murine model of cutaneous infection with gram-positive cocci. *Infection and Immunity,* **1992,** 60, 7, 2636-2640; Cheung, A. L.; Eberhardt, K. J.; Chung, E.; Yeaman, M. R.; Sullam, P. M.; Ramos, M.; Bayer, A. S. Diminished virulence of a sar-/agr- mutant of Staphylococcus aureus in the rabbit model of endocarditis. *J Clin Invest,* **1994,** 94, 5, 1815.
28. Novick, R. P.; Ross, H.; Projan, S.; Kornblum, J.; Kreiswirth, B.; Moghazeh, S. Synthesis of staphylococcal virulence factors is controlled by a regulatory RNA molecule. *The EMBO Journal,* **1993,** 12, 10, 3967.
29. Robinson, D. A.; Monk, A. B.; Cooper, J. E.; Feil, E. J.; Enright, M. C. Evolutionary Genetics of the Accessory Gene Regulator (agr) Locus in Staphylococcus aureus. *Journal of Bacteriology,* **2005,** 187, 24, 8312-8321.
30. Sjöback, R.; Nygren, J.; Kubista, M. Absorption and fluorescence properties of fluorescein. *Spectrochimica Acta Part A: Molecular and Biomolecular Spectroscopy,* **1995,** 51, 6, L7-L21.
31. Schnappinger, D.; Hillen, W. Tetracyclines: antibiotic action, uptake, and resistance mechanisms. *Archives of Microbiology,* **1996,** 165, 6, 359-369.
32. Momparler, R. L.; Karon, M.; Siegel, S. E.; Avila, F. Effect of adriamycin on DNA, RNA, and protein synthesis in cell-free systems and intact cells. *Cancer Res,* **1976,** 36, 8, 2891.
33. Reynolds, P. E. Structure, biochemistry and mechanism of action of glycopeptide antibiotics. *European Journal of Clinical Microbiology and Infectious Diseases,* **1989,** 8, 11, 943-950.
34. Best, G. K.; Best, N. H.; Koval, A. V. Evidence for Participation of Autolysins in Bactericidal Action of Oxacillin on Staphylococcus aureus. *Antimicrobial Agents and Chemotherapy,* **1974,** 6, 825.
35. Campoli-Richards, D. M.; Monk, J. P.; Price, A.; Benfield, P.; Todd, P. A.; Ward, A. Ciprofloxacin. A review of its antibacterial activity, pharmacokinetic properties and therapeutic use. *Drugs,* **1988,** 35, 4, 373-447.

36. Gabizon, A. A. Pegylated Liposomal Doxorubicin: Metamorphosis of an Old Drug into a New Form of Chemotherapy. *Cancer Investigation,* **2001,** 19, 4, 424-436; Gabizon, A.; Shmeeda, H.; Barenholz, Y. Pharmacokinetics of Pegylated Liposomal Doxorubicin. *Clinical Pharmacokinetics,* **2003,** 42, 5, 419-436.
37. Barenholz, Y. Doxil(R)--the first FDA-approved nano-drug: lessons learned. *J Control Release* **2012,** 160, 2, 117-34; Charrois, G. J. R.; Allen, T. M. Multiple Injections of Pegylated Liposomal Doxorubicin: Pharmacokinetics and Therapeutic Activity. *Journal of Pharmacology and Experimental Therapeutics,* **2003,** 306, 3, 1058-1067.

Chapter 5 Dressing prototypes

The creation of a prototype delivery system to ensure distribution of active-agent containing vesicles to a wound interface will need to fulfil certain requirements. These requirements include; good biocompatibility with the host – especially at the site of damage, an ability to provide a stabilising environment to the vesicles, and a network that ensures the released agents can diffuse out of the vesicles following lysis. In relation to this, the network must contain channels of a sufficient size as to allow bacteria and toxins to penetrate without actively promoting bacterial colonisation. These properties are in addition to those discussed in 1.3.5 Burn wound treatment protocol, where qualities such as a lack of adhesion to the wound bed, pain free application and removal, absorbency, antimicrobial activity, availability in a range of sizes, minimised healing time, decreased frequency of dressing change, reduced cost (relating to dressing and hospital stay time) and scar reduction are all desirable.[1]

5.1 Active agent delivery using vesicles

The utilisation of vesicles for the systemic or localised administration of a drug often faces challenges relating to controlled release. Mapping of pharmacokinetics can determine the drug activity profile; however bio-distribution is more difficult to control and assess.[2] If delivery of the active agent to the required site is not achieved, there is the potential problem of toxic side effects at alternative sites, resulting in secondary complications. The use of mechanical devices can alter the pharmacokinetics, but does not influence bio-distribution to any large extent. However, the use of particulate drug carriers, such as vesicles; can have a positive effect. The use of particulate drug carriers as a drug delivery system (DDS) has been investigated successfully for a variety of drugs. These have been found to contain an enhanced ability to target and impact action sites where required, relative to conventional methods.[3]

As previously investigated and discussed in chapter 3, the morphology of vesicles; with relation to stability, reactivity, functionality and membrane permeability, is dependent on the bilayer composition and localised environmental conditions. An example of this is the use of large unilamellar vesicles (LUVs), between 50 to 200 nm, in systemic drug administration. These LUV compositions ensure an increase in the blood circulation time and volume available for bioadministration.[4]

As discussed in 3.1.2 Intelligent vesicles, the coating of a vesicle membrane surface with inert hydrophilic polymers, such as polyethylene glycol, has been shown to improve the biological stability and circulation time *in vivo*.[5] As the efficiency in drug encapsulation has improved, techniques have been developed that allow 'remote loading' of preformed vesicles with drug molecules using gradients,[6] primarily based either on pH or ammonium sulphate.[6, 7]

The formulation of deliverable vesicles can be accomplished through incorporation into a solution, dry powder, aerosol, cream or lotion. As a result of this a wide range of administration routes can be considered. The administration of potent drugs through encapsulation in vesicles, either orally or externally, has proven popular, with reported uses including the stimulation of immune response and vaccination, treatment of infectious diseases, cancer therapy, and gene therapy.[8] The topical delivery of vesicles containing active agents; incorporated within gels, creams and attached to medical dressings, has been continually developed, however if penetration of delivered active agents through the skin barrier is desired this can prove problematic.

5.2 Burn dressings

Globally, there are large variations between the specific methods of burn treatment and dressing utilisation within burn treatment centres. There is no ideal definitive dressing or treatment exists that fulfils all of the desired healing traits. There is insufficient data, limited in both quantity and methodological quantity, to support recommendation of a specific dressing as a treatment for all burns, and so many different types exist. Burn dressings can be divided into two categories: *open* methods, consisting of topically applied antimicrobials, and *closed* methods, which use occlusive dressings.[9]

The performance of occlusive dressings, with regard to promoting healing and minimising discomfort and infection, used in the treatment of superficial and partial thickness burns, were analysed by the Cochrane Review.[10] This review included hydrocolloid dressings,

polyurethane film dressings, hydrogel dressings, silicon coated nylon dressings, biosynthetic skin substitute dressings, antimicrobial (silver and iodine containing) dressings, fibre dressings and wound dressing pads.

This investigation will focus on the development of an open topical dressing treatment, utilising biocompatible hydrogels for the incorporation and delivery of vesicles containing an active agent to a wound.

5.3 Open topical wound dressings

The topical open delivery of active agents via hydrogels, ointments, emulsions and creams to a specified site is commonly utilised in the management of skin related problems such as acne, eczema and psoriasis.

Within burn injuries, traditional open topical dressings, for example silver sulfadiazine (SSD) creams have been used since the late 1960's to minimize infection. SSD can be applied to a wound in combination with a paraffin/cotton wool layer dressing; however this system has not been without its problems. Issues have arisen from dressing adherence to the wound[11] and a frequent requirement for dressing changes, both of which cause trauma to any re-epithelialisation occurring; resulting in delays to the healing process. In the case of SSD cream there have been related reported toxic effects on regenerating keratinocytes; increasing the scarring damage, ensuring that its use has been discouraged.[12]

Despite this, there is scope for development of an active agent-in-vesicle-in-topical-delivery system for applications in burn injuries. Importantly, within this investigation the passive diffusion of the 5(6)-CF (active agent) from within the vesicle can be investigated to indicate the membrane integrity during dispersion in the different potential delivery mediums.

5.4 Delivery medium

The delivery medium must be able to not only provide stability to the vesicles, but also provide a network through which the active agents can diffuse. Prior to this, adequate penetration of bacterial toxins must be possible. Hydrogel formulations may provide an ideal system towards achieving these requirements.

5.4.1 Hydrogels

Hydrogels are water-swollen, superabsorbent polymers that can form cross-linked networks of structures based on hydrophilic homopolymers. The cross-links allow formation of swollen networks, and can be formed from covalent or ionic bonds, or weaker bonds, such as van der Waals forces and hydrogen bonds. Preparation of these networks can be achieved through chemical cross-linking, photo-polymerisation or irradiative cross-linking.

The most efficient water absorbers are polymers that carry dissociated, ionic functional groups. Hydrogels absorb water through diffusion; forcing the polymer particles to move in an opposing direction to that of the water molecules. This disturbance elongates the chain and a proportional relationship exists between disturbance and water diffusion. The equilibrium reached between water concentration inside and outside the particle depends on the polymer structure and the liquid being absorbed.

Diffusion is described by Fick's law, Equation 5-1, relating the diffusional flow rate f to the concentration gradient $\Delta c/\Delta x$ of the diffusing substance in the sample, where f is the flow rate in the x direction, A is the cross-sectional area of the sample and D is the diffusion constant. It is important to recognise that temperature and pressure can also have an effect.[13]

$$\frac{f}{\mathrm{A}} = -D\frac{\Delta \mathrm{c}}{\Delta x} \qquad \text{Equation 5-1}$$

The physical behaviour of a hydrogel is dependent on its equilibrium and dynamic swelling behaviour in water; however the localised environment can also have an effect. Environmentally responsive materials show drastic changes in their swelling ratio as a consequence of pH, temperature, ionic strength, nature and composition of the swelling agent and electrical or magnetic stimuli.[14]

5.4.2 Prototype hydrogels

As part of prototype development many different hydrogel delivery matrices were investigated, and their structure, activity, and precedence for being investigated is given in Table 5-1

Delivery medium	Structure	Activity	Precedence for use
Chitosan	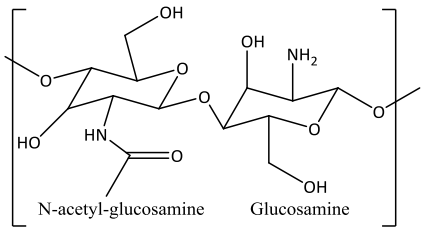	Natural polysaccharide derived from crustacean shells by deacetylation of the naturally occurring chitin. Advantages include biocompatibility, biodegradability, high abundance and low cost.[15]	Applications in controlled localised drug delivery,[16] in antimicrobial films for food preparation[17] and in silica hybrid membranes for bone regeneration.[18]
Carbopol	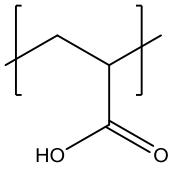	High molecular weight cross-linked polymer of acrylic acid. Swelling ability (≤1000x) through ionisation of the carboxylic groups.[19] Advantages include biocompatibility and non-sensitizing effects.[20]	Applications in the treatment of insomnia,[21] in oral care formulations for malodour control,[22] as a carrier in nasal drug delivery[23] and in colonic drug delivery.[24]
Gelatin	Complex heterogeneous product of a mixture of α-, β- and γ- peptides, from irreversibly hydrolysed collagen.	Natural fibrous protein derived from collagen, found in skin, bones and connective tissue. Advantages include biocompatibility, biodegradability, and solubility.[25]	Applications in ophthalmic use,[26] in tissue engineering[27] and for injectable drug delivery.[28]
Agarose	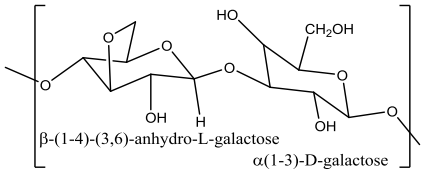	Natural linear polysaccharide from red algae. Advantages include biocompatibility, biodegradability and non-toxicity.[29]	Used primarily for electrophoresis, recent applications in injectable protein delivery systems.[30]

Carboxy-methyl-cellulose (CMC)	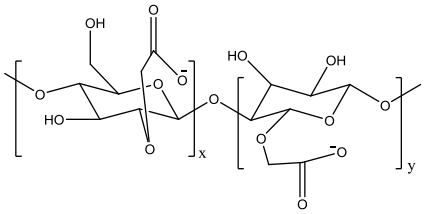	Ionic polysaccharide cellulose derivative. Ionisation of the carboxylic acid provides advantageous negative repulsion in gel formation.[31]	Applications in venous leg ulcer[32] and for surgical wound dressings.[33]
Polyethylene glycol (PEG)	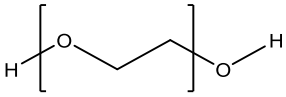	Polymer of ethylene oxide that can be synthesised to a defined chain length (molecular weight). Advantages include versatility and biocompatibility.	Applications in controlled active agent release[34], for example in insulin release dressings.[35]
Oxidised cellulose	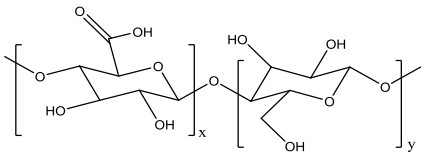	Soluble polymer formed through the oxidation of naturally occurring cellulose, obtained from cell walls of green plants.[36] Advantages include biodegradability and bioresorbability[37]	Applications in haemorrhage control as a mucoadhesive,[38] and in post-surgery adhesion prevention.
Hydroxypropyl methylcellulose (HM)	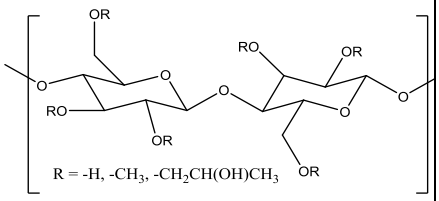	Semi-synthetic mixed alkyl hydroxyalkyl cellulose ether with varying properties depending on substituents.[39] Advantages include non-toxicity and enzyme resistance.	Applications in contact lens care[40] and in the coatings of active ingredients.[41]

Table 5-1. The different hydrogel mediums investigated as potential vesicle delivery systems

From preliminary formulations and initial vesicle stability investigations four of these different hydrogel mediums indicated the potential to act as an appropriate medium for the delivery of vesicles, whilst maintaining a structure appropriate for potential application to skin. These were gelatin, Carbopol 981P NF (C981), hyproxypropylmethylcellulose

(Hypromellose, HM) and agarose. Initially, osmotic pressure measurements were obtained and compared to the osmolality of the three stabilised and sensitive vesicles formulated in Chapter 3, to aid determination of longer term compatibility.

5.5 Osmosis

Osmosis is conventionally defined as the net movement of water across a selectively permeable membrane. This is driven by a difference in osmotic pressure across the membrane, from a region of low osmotic pressure to a region of high osmotic pressure.

The osmotic pressure of a system is determined by the total number of particles, regardless of the molecular nature, and so is dependent on the degree of dissociation. Dissociation can be incomplete; some association between particles may exist, and this deviation from 'ideal' behaviour is accounted for using the osmotic coefficient.

The importance of osmosis and osmotic pressure must be taken into account when considering the suitability of solutions for storage or delivery of vesicles. Osmometry can be used to measure the concentration of particles in a solution; the osmolar concentration,[42] and can be expressed as osmolarity or osmolality. These terms are often confused with each other, and hence require careful distinction, especially within a clinical environment.[43] Osmolarity is a measure of the mmol/L of particles in a sample solution, and osmolality is a measure of the mmol/kg of particles in a solvent solution.[44]

5.5.1 Osmolality

Dissolving a solute in a solvent will increase the osmotic pressure and boiling point, and decrease the vapour pressure and freezing point. These colligative properties can all be used individually to measure the osmolality, however the most common method is freezing point depression, and this was utilised within this project. As discussed in chapter 2, the freezing point depression of a sample can be compared against pure water to give the osmotic concentration. Pure water freezes at 0 °C; an aqueous undissociated ideal solution with an osmolarity of 1 osmol / kg H_2O freezes at -1.858 °C.

5.5.2 Osmolality and vesicles

Osmolality provides a measurement of the number of milliosmoles/kg (mOsm/kg) of solvent present, and hence gives an indication of the compatibility between the vesicle and the hydrogel system. It is integral to the stability of the vesicles that the osmolality of the vesicles within the solution they are synthesised in be similar to the storage or topical gel matrix osmolality. If a large difference exists, diffusion of water can occur either into or out of the vesicles, through the semi permeable phospholipid membrane, causing the vesicles to burst as a result of osmotic pressure.

The osmotic pressure values of the three stable vesicle candidates, discussed previously, were measured using a Löser Micro-Osmometer Type 15. These values were compared to those obtained for bacterial growth mediums (LB and TSB), SimF, and the four promising hydrogels synthesised for vesicle delivery, given in Table 5-2.

	Osmotic Pressure mOsm/kg H_2O	***Error* ±**		**Osmotic Pressure mOsm/kg H_2O**	***Error* ±**
TCDA-DS	215	0.88	**Gelatin**	224	5.24
DOPC-DS	221	0.33	**C981**	338	1.45
DSPG-DP	219	2.00	**Hypromellose**	224	0.88
HEPES	211	1.73	**Agarose**	230	1.76
LB	387	0.45	**SimF**	286	0.88
TSB	311	0.33			

Table 5-2. The osmotic pressure of the vesicles, HEPES buffer, different hydrogels, growth mediums and SimF (mOsm/kg H_2O).

The osmolality values of the vesicle and hydrogel systems give an indication of the compatibility between the systems, and from these values osmotic pressure ratios can be calculated, Table 5-3. A value close to 1 indicates a higher likelihood of compatibility between vesicle and hydrogel.

	TCDA-DS	**DOPC-DS**	**DSPG-DP**
HEPES	1.02 (± 0.004)	1.05 (± 0.002)	1.04 (± 0.010)
Gelatin	0.960 (± 0.005)	0.984 (± 0.002)	0.977 (± 0.01)
C981	0.638 (± 0.003)	0.654 (± 0.001)	0.649 (± 0.006)
Hypromellose	0.960 (± 0.004)	0.984 (± 0.002)	0.976 (± 0.009)
Agarose	0.938 (± 0.004)	0.961 (± 0.002)	0.954(± 0.009)
LB	1.80 (±3 x 10^{-5})	1.751 (±4 x 10^{-6})	1.767 (±0.002)
TSB	1.446 (±0.001)	1.474 (±0.002)	1.420 (±0.002)
SimF	1.330 (±0.004)	1.294 (±0.004)	1.355 (±0.004)

Table 5-3**.** The osmolality ratio values of the vesicles in each of the hydrogels, growth media and SimF, based on the ratio of the osmotic pressure (mOsm/kg H_2O) of each vesicle type against each solution. A value close to 1 is optimal.

From the osmotic pressure ratio values calculated in Table 5-3, the gelatin, hypromellose and agarose hydrogel systems indicate that good compatibility could be achieved for storage and delivery of the vesicles. However, osmotic pressure ratios calculated for the C981 hydrogel indicate that this system is likely to be the least compatible hydrogel for storage and delivery of vesicles.

5.6 Vesicles in hydrogels

Following on from osmolality measurements, the four hydrogels, each with known applications at biological interfaces and formation at favourable pH values, were incubated

with each of the three stabilised vesicle candidates. An example of a vesicle candidate (DSPG-DP) in one of the hydrogels (C981) with and without addition of a lytic agent is depicted in Figure 5-1.

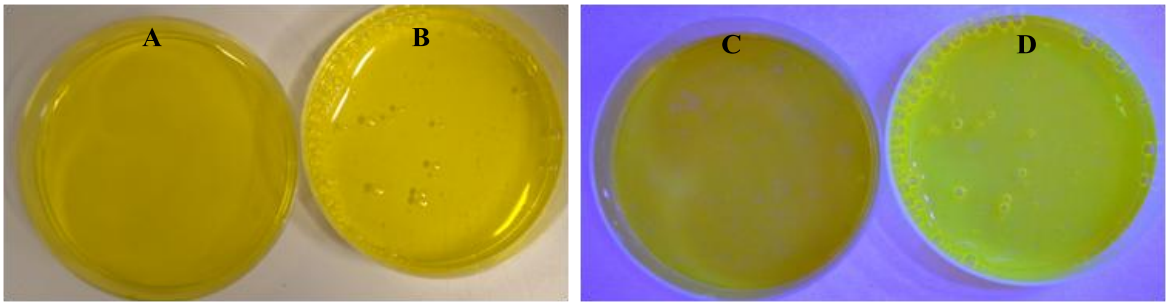

Figure 5-1. The effect of a lytic agent on vesicles dispersed within a hydrogel (B and D), compared to un-lysed vesicles (A and C). Photo taken in white light (A and B) and UV light (C and D).

The stability of the three stabilised, selectively sensitive vesicle candidates, when dispersed in different hydrogel based delivery matrixes, was investigated using the same fluorescence assay as for stability of vesicles during vesicle composition development in Chapter 3: 14 days at 37 °C. The results are shown in

Figure 5-2. Despite the incompatibility and hence predicted induced-vesicle-instability indicated by the C981 osmolality ratios, this gel was still formulated as a comparison.

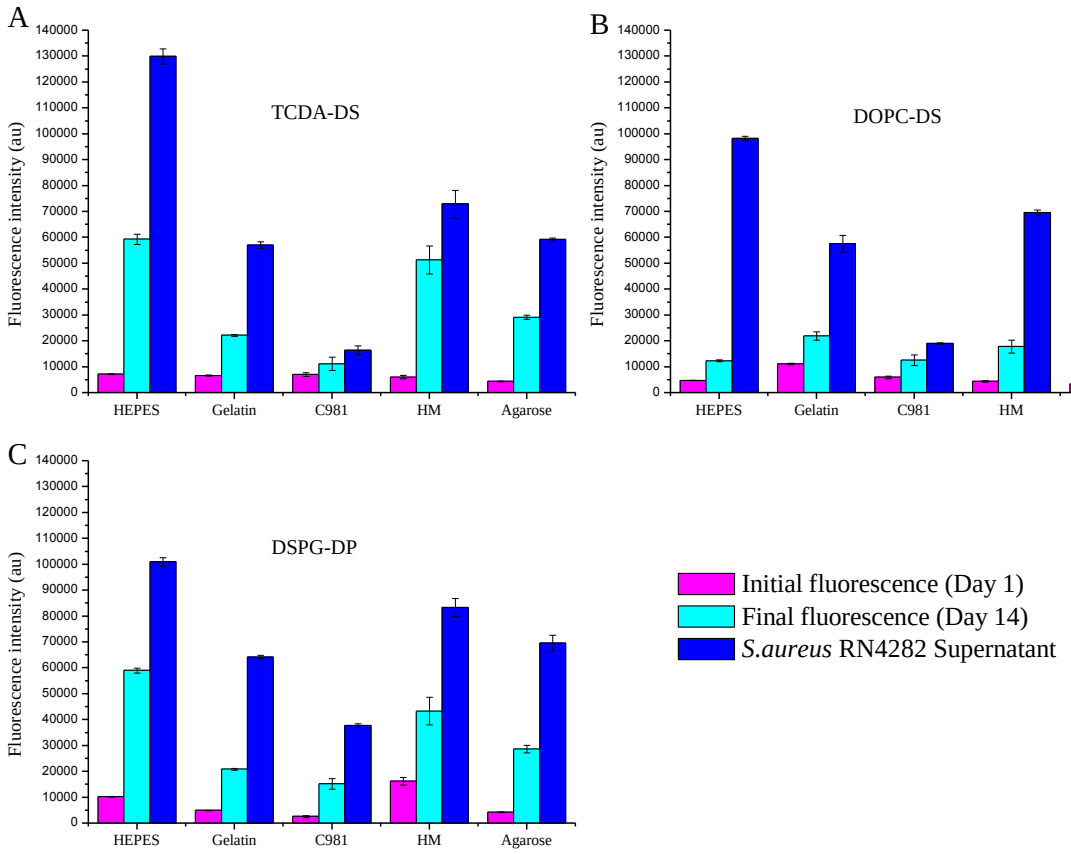

Figure 5-2. The effect of hydrogel matrices with each of the three vesicle candidates. After 14 days at 37 °C, *S.aureus* RN4282 supernatant was added to measure $F_{100\ \%}$, or HEPES as a negative control. The supernatant (SN) from *S.aureus* RN4282 was added to each of the vesicle-in-gel or vesicle-in-HEPES systems, with a large increase in fluorescence being the desired response after 14 days incubation.

S.aureus and the RN4282 strain are discussed in detail in chapter 4. Briefly, *S.aureus* RN4282 is a naturally occurring strain that produces and secretes small amounts of exoproteins but elevated quantities of TSST.[45] It is responsible for the systemic toxin mediated disease TSS, which can be especially problematic in paediatric burns, making it of particular relevance to this investigation.[46] From Figure 5-2, fluorescence results following incubation of the three vesicle candidates within the C981 gel system appear to indicate adequate stability after 14 days at 37 °C. This is despite initial predictions that it would provide a destabilising environment for the vesicles. However, following addition of SN only a small increase in sensitivity (measured through fluorescence) was observed. This could be due to the initial rapid destabilisation of vesicles with the released dye being locally quenched in the gel matrix, or the formation of a network of poly-acrylic acid cross links that is

impenetrable by the lytic toxins in the SN. These results confirm that C981 would not be an appropriate delivery matrix for the vesicles.

The stability response parameter, S (developed in 3.4.1 Stability response parameter), was used to calculate the fluorescence intensity ratio between fluorescence after 14 days at 37 °C, and the fluorescence after addition of SN (considered maximum fluorescence - $F_{100\ \%}$) for each of the vesicle-in-hydrogel systems, data displayed in Table 5-4.

	TCDA-DS	***DOPC-DS***	***DSPG-DP***
HEPES	2.19 (±0.05)	7.96 (±0.08)	1.71 (±0.03)
Gelatin	2.57 (±0.06)	2.62 (±0.16)	3.08 (±0.03)
C981	1.47 (±0.23)	1.51 (±0.06)	2.48 (±0.09)
HM	1.42 (±0.12)	3.91 (±0.13)	1.92 (±0.11)
Agarose	2.04 (±0.18)	2.05 (±0.59)	2.4 (±0.19)

Table 5-4. The stability response parameter, S, for each of the vesicle-in-gel systems, with lysis after 14 days at 37 °C following addition of supernatant from *S.aureus* RN4282 (100 minutes incubation).

The fluorescence results depicted in Figure 5-2, and the corresponding stability response parameter, S in Table 5-4, can be used to clearly indicate which vesicle and hydrogel systems are compatible. The DSPG-DP vesicle had an increased stability in each of the hydrogels, with the best stabilisation-followed-by-response profile being measured in gelatin. The DOPC-DS vesicles have demonstrated favourable stability followed by response in the gelatin and agarose hydrogel, with the best profile being measured in HM. This could be hypothesised to be due to the formation of stabilising lipid and cholesterol rafts, which allow vesicle membranes to exist concurrently in gel and liquid forms.[47] Comparatively with the other vesicle compositions, and the vesicle in HEPES buffer, the stability of TCDA-DS vesicles in each of the hydrogels was not favourable.

The rheology of the hydrogels can differ at elevated temperature, as observed by the fluid 'sticky' natures of C981 and HM at 37 °C, as opposed to agarose, which does not display 'sticky' properties. Agarose in this formulation produces a product which has a solid-like viscosity, and this is important in the engineering of prototypes, where a firmer hydrogel will be preferred for ease of fabrication. Despite the favourable stability and sensitivity of vesicles

in gelatin, it can occasionally be unfavoured in prototyping, as a result of its animal derivitisation. This can make the related regulatory landscape with regard to its use in medical devices complicated and problematic.

Following on from these results, and for further indicative information about the stability of the vesicles over the 14 day period, each of the three vesicle candidates were incubated in agarose gel at 37 °C and fluorescence intensity measurements were obtained every three days. The passive leakage assay of the vesicles is shown in Figure 5-3, where it can be seen that the dye is slowly passively released by all three vesicle candidates into the agarose gel.

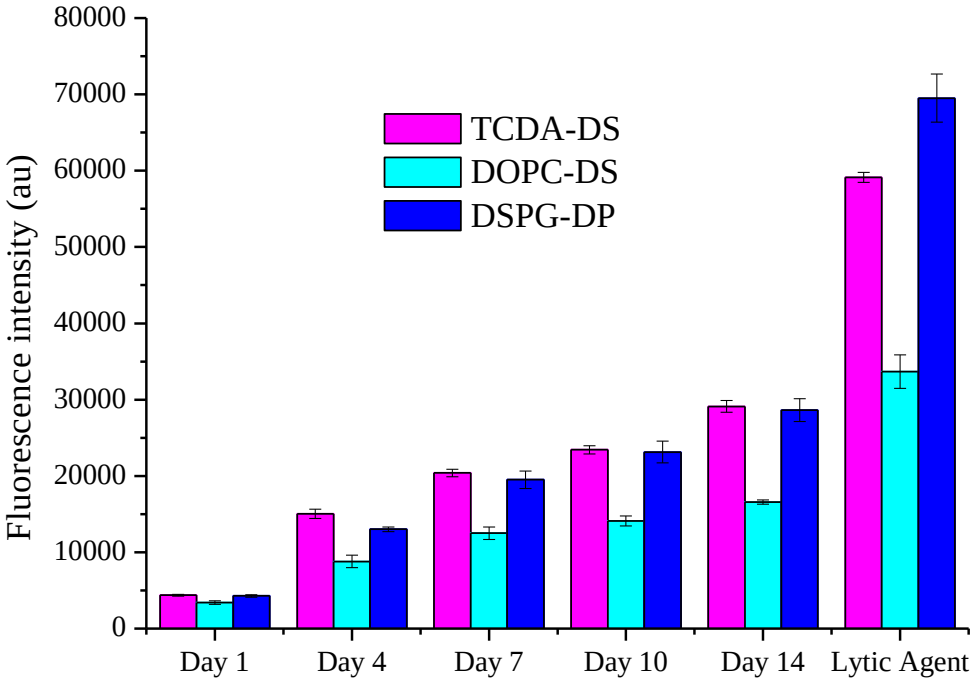

Figure 5-3. The change in fluorescence of three stable vesicle candidates in agarose gel at 37 °C over 14 days, followed by addition of *S.aureus* RN4282 supernatant.

The diffusion of the dye over time indicates that this hydrogel system would not be suitable for the delivery of vesicles to a wound. However, it should be noted that a 2 fold increase in fluorescence can still be measured following addition of the SN after 14 days; equivalent to an S value of approximately 2 for each vesicle-hydrogel system. This relative doubling in fluorescence should be observable above the pre-lysed fluorescence intensity, ensuring that pathogenic bacteria and toxin presence can be identified. Despite this the inherent instability of the vesicles in the agarose would make the use of this hydrogel impractical.

5.7 Fluorescence response versus bacteria count

On application to a wound it is important to ensure that the signalling-dressing will be able to indicate pathogenic bacteria presence at the quantity that it will be at within a wound environment. It is therefore important to know how much bacteria is required for a response to be elucidated. However, there are many difficulties associated with obtaining this value, and this is for a variety of reasons. One primary reason for this is the difference between different species and strains of bacteria, and hence the synthesis time taken, amount and virulence of the toxins that they produce. This variance is widely acknowledged.[48] Bioassays exist for measuring bacteria and enzyme toxicity, [49] and this has been the subject of intense investigations within the group (W. D. Jamieson – MRSA paper in preparation). A further reason for the variance is the imbalance of bacteria present.[50] Uncontrollable localisation of bacterial colonisation within a wound, relating to the formation of patches of high densities of bacterial cells; biofilms, and patches of low densities of bacterial cells, can exist. This will have an effect on localised toxin production, and hence the lysis of vesicles in the dressing. Work within the group has suggested that 10^5-10^6 colony forming units per ml (cfu/ml) of pathogenic bacteria (based on a small selection of strains) is required for a lytic response of the vesicles to be detected.

5.8 Dressing prototypes – conclusion

Four topical open hydrogel dressings have been investigated, with a focus on their ability to provide a stabilising environment (through the minimisation of passive leakage) for vesicles, whilst ensuring that sensitivity to pathogenic toxins is maintained. Three of the four hydrogel systems, namely gelatin, hypromellose and agarose, have indicated some compatibility with the vesicle candidates and have achieved the required sensitivity profile. However, the fourth hydrogel, C981, has proven insufficient at stabilising the vesicle candidates, and this was predicted based on osmolality data, and measured through the fluorescence intensity assay.

The creation of prototype vesicle-in-hydrogel dipped fabrics could be developed based on the successful formulations created here, shown in Figure 5-4. This could potentially allow formation of occlusive closed dressings, and consequentially an alternative delivery method of the vesicles to a burn wound.

Figure 5-4. Representative image of hydrogel dressing embedded with vesicles. The dressing on the left is a control, and the dressing on the right is a dressing treated with the supernatant of *S.aureus* RN4282.[51] Image acknowledgements to S. Hong.

In addition to the stability and sensitivity profile required for incorporation of vesicles into a topical dressing, there are other important factors that have not been actively considered. These include analysing how the vesicle-hydrogel system affects the time required for the burn to heal, the number of dressing changes or reapplications required, the level of pain associated with application, and the overall cost of the dressing. In addition to this, the incidence of infection and whether the dressing will act as a bacterial growth promoter requires further investigation. This could be carried out by comparing the growth of bacteria in standard broth solutions to bacteria grown in hydrogel solutions, and obtaining cfu/ml following plate dilutions.

5.9 References

1. Selig, H. F.; Lumenta, D. B.; Giretzlehner, M.; Jeschke, M. G.; Upton, D.; Kamolz, L. P. The properties of an "ideal" burn wound dressing--what do we need in daily clinical practice? Results of a worldwide online survey among burn care specialists. *Burns* **2012,** 38, 7, 960-6.
2. Li, S. D.; Huang, L. Pharmacokinetics and biodistribution of nanoparticles. *Molecular Pharmaceutics* **2008,** 5, 4, 496-504.
3. Kingsley, J. D.; Dou, H.; Morehead, J.; Rabinow, B.; Gendelman, H. E.; Destache, C. J. Nanotechnology: A focus on nanoparticles as a drug delivery system. *J. Neuroimmune Pharmacol.*, **2006**; 1, 340-350.
4. Mufamadi, M. S.; Pillay, V.; Choonara, Y. E.; Du Toit, L. C.; Modi, G.; Naidoo, D.; Ndesendo, V. M. K. A review on composite liposomal technologies for specialised drug delivery. *Journal of Drug Delivery*, **2011**; 1-19.
5. Immordino, M. L.; Dosio, F.; Cattel, L. Stealth liposomes: review of the basic science, rationale, and clinical applications, existing and potential. *International journal of nanomedicine*, **2006**; Vol. 1, pp 297-315.
6. Ceh, B.; Lasic, D. D. A rigorous theory of remote loading of drugs into liposomes. *Langmuir* **1995,** 11, 9, 3356-3368.

7. Hwang, S.; Maitani, Y.; Qi, X.-R.; Takayama, K.; Nagai, T. Remote loading of diclofenac, insulin and fluorescein isothiocyanate labeled insulin into liposomes by pH and acetate gradient methods. *International Journal of Pharmaceutics* **1999,** 179, 1, 85-95.
8. Lasic, D. D.; Papahadjopoulos, D. *Medical applications of liposomes*. Elselvier: **1998**.
9. Oostema, J. A.; Ray, D. J. Evidence-based emergency medicine - No clear winner among dressings for partial thickness burns. *Annals of emergency medicine*, **2010**; 56, 298-299.
10. Wasiak, J.; Cleland, H.; Campbell, F. Dressings for superficial and partial thickness burns. John Wiley & Sons, Ltd: The Cochrane Collaboration, **2010**; 10.
11. Thomas, S. S.; Lawrence, J. C.; Thomas, A. Evaluation of hydrocolloids and topical medication in minor burns. *Journal of Wound care*, **1995**; 4, 218-220.
12. Wasiak, J.; Cleland, H. Minor thermal burns. BMJ Publishing Group: Clinical Evidence, **2005**.
13. Buchholz, F. L. *Modern Superabsorbent Polymer Technology*. Wiley VCH: **1998**.
14. Peppa, N. A. *Biomaterials Science: An Introduction to Materials in Medicine*. Second edition ed.; Elsevier Academic Press: **2004**.
15. Ruel-Gariépy, E.; Chenite, A.; Chaput, C.; Guirguis, S.; Leroux, J. C. Characterization of thermosensitive chitosan gels for the sustained delivery of drugs. *International Journal of Pharmaceutics* **2000,** 203, 1-2, 89-98.
16. Bhattarai, N.; Gunn, J.; Zhang, M. Chitosan-based hydrogels for controlled, localized drug delivery. *Advanced Drug Delivery Reviews* **2010,** 62, 1, 83-99.
17. Dutta, P. K.; Tripathi, S.; Mehrotra, G. K.; Dutta, J. Perspectives for chitosan based antimicrobial films in food applications. *Food Chemistry* **2009,** 114, 4, 1173-1182.
18. Lee, E.-J.; Shin, D.-S.; Kim, H.-E.; Kim, H.-W.; Koh, Y.-H.; Jang, J.-H. Membrane of hybrid chitosan-silica xerogel for guided bone regeneration. *Biomaterials* **2009,** 30, 5, 743-750.
19. Bonacucina, G.; Martelli, S.; Palmieri, G. F. Rheological, mucoadhesive and release properties of Carbopol gels in hydrophilic cosolvents. *International Journal of Pharmaceutics* **2004,** 282, 1-2, 115-130.
20. Hosmani, A. H.; Thorat, Y.; Kasture, P. Carbopol and its pharmaceutical significance: a review. *Pharmainfo. net* **2006,** 4, 5.
21. Kulkarni, S. V.; Patel, N.; Rao B, S.; Kheni, P.; Priti, P.; Ammanage, A. Formulation and *In vitro* evaluation of sustained release matrix tablet of Zolpidem Tartrate. *International Journal of PharmTech Reserach*, **2011**; 3, 858-863.
22. Boyd, T.; Leigh, L. Oral care formulations for malodor control. WO2011094497A2, **2011**.
23. Coucke, D.; Pringels, E.; Foreman, P.; Adriaensens, P.; Carleer, R.; Remon, J. P.; Vervaet, C. Influence of heat treatment on spray-dried mixtures of Amioca starch and Carbopol 974P used as carriers for nasal drug delivery. *Int. J. Pharm.* **2009,** 378 (Copyright (C) **2011** American Chemical Society (ACS). All Rights Reserved.), 45-50.
24. Varum, F. J. O.; Veiga, F.; Sousa, J. S.; Basit, A. W. Mucoadhesive platforms for targeted delivery to the colon. *International Journal of Pharmaceutics* **2011,** 420, 1, 11-19.
25. Rokhade, A. P.; Agnihotri, S. A.; Patil, S. A.; Mallikarjuna, N. N.; Kulkarni, P. V.; Aminabhavi, T. M. Semi-interpenetrating polymer network microspheres of gelatin and sodium carboxymethyl cellulose for controlled release of ketorolac tromethamine. *Carbohydrate Polymers* **2006,** 65, 3, 243.
26. Lai, J.-Y. Biocompatibility of chemically cross-linked gelatin hydrogels for ophthalmic use. *Journal of Materials Science: Materials in Medicine* **2010,** 21, 6, 1899-1911.

27. Hu, X.; Ma, L.; Wang, C.; Gao, C. Gelatin Hydrogel Prepared by Photo-initiated Polymerization and Loaded with TGF-β1 for Cartilage Tissue Engineering. *Macromolecular Bioscience* **2009,** 9, 12, 1194-1201.
28. Sakai, S.; Hirose, K.; Taguchi, K.; Ogushi, Y.; Kawakami, K. An injectable, in situ enzymatically gellable, gelatin derivative for drug delivery and tissue engineering. *Biomaterials* **2009,** 30, 20, 3371.
29. Bao, X.; Hayashi, K.; Li, Y.; Teramoto, A.; Abe, K. Novel agarose and agar fibers: Fabrication and characterization. *Materials Letters* **2010,** 64, 22, 2435-2437.
30. Wang, N.; Wu, X. S. Preparation and Characterization of Agarose Hydrogel Nanoparticles for Protein and Peptide Drug Delivery. *Pharmaceutical Development and Technology* **1997,** 2, 2, 135.
31. Barbucci, R.; Magnani, A.; Consumi, M. Swelling Behavior of Carboxymethylcellulose Hydrogels in Relation to Cross-Linking, pH, and Charge Density. *Macromolecules* **2000,** 33, 20, 7475.
32. Guest, J. F.; Ruiz, J. F.; Mihai, A.; Lehman, A. Cost effectiveness of using carboxymethylcellulose dressing compared with gauze in the management of exuding venous leg ulcers in Germany and the USA. *Current Medical Research and Opinion* **2005,** 21, 1, 81-92.
33. Guest, J. F.; Ruiz, F. J. Modelling the cost implications of using carboxymethylcellulose dressing compared with gauze in the management of surgical wounds healing by secondary intention in the US and UK. *Current Medical Research and Opinion* **2005,** 21, 2, 281-290.
34. Lin, C.-C.; Anseth, K. PEG Hydrogels for the Controlled Release of Biomolecules in Regenerative Medicine. *Pharmaceutical Research* **2009,** 26, 3, 631-643.
35. Calceti, P.; Salmaso, S.; Walker, G.; Bernkop-Schnürch, A. Development and in vivo evaluation of an oral insulin–PEG delivery system. *European Journal of Pharmaceutical Sciences* **2004,** 22, 4, 315-323.
36. Crawford, R. J.; Scott, J. L.; Unali, G. F. Structured aqueous detergent compositions. 2010.
37. Coseri, S.; Biliuta, G.; Simionescu, B. C.; Stana-Kleinschek, K.; Ribitsch, V.; Harabagiu, V. Oxidized cellulose—Survey of the most recent achievements. *Carbohydrate Polymers* **2013,** 93, 1, 207-215.
38. Gruen, R. L.; Brohi, K.; Schreiber, M.; Balogh, Z. J.; Pitt, V.; Narayan, M.; Maier, R. V. Haemorrhage control in severely injured patients. *The Lancet*, 380, 9847, 1099-1108.
39. Williams, R. O., 3rd; Sykora, M. A.; Mahaguna, V. Method to recover a lipophilic drug from hydroxypropyl methylcellulose matrix tablets. *AAPS PharmSciTech* **2001,** 2, 2, E8.
40. Simmons, P. A.; Kelly, W.; Prather, W.; Vehige, J. Clinical benefits and physical properties of addition of hydroxypropyl methylcellulose to a multi-purpose contact lens care solution. *Adv Exp Med Biol* **2002,** 506, 981-5.
41. Bruce, H. F.; Sheskey, P. J.; Garcia-Todd, P.; Felton, L. A. Novel low-molecular-weight hypromellose polymeric films for aqueous film coating applications. *Drug Development and Industrial Pharmacy* **2011,** 37, 12, 1439-1445.
42. Bevan, D. R. Osmetry. 2. Osmoregulation. *Anaesthesia* **1978,** *33* (9), 801-808.
43. Deardorff, D. Osmotic strength, osmolality, and osmolarity. *American Journal of Health-System Pharmacy* **1980,** 37, 4, 504-509.
44. Lord, R. C. C. Osmosis, osmometry, and osmoregulation. *Postgraduate Medical Journal* **1999,** 75, 880, 67-73.
45. Vojtov, N.; Ross, H. F.; Novick, R. P. Global repression of exotoxin synthesis by staphylococcal superantigens. *Proceedings of the National Academy of Sciences* **2002,** 99, 15, 10102-10107; Subedi, A.; Ubeda, C.; Adhikari, R. P.; Penadés, J. R.; Novick, R. P. Sequence

analysis reveals genetic exchanges and intraspecific spread of SaPI2, a pathogenicity island involved in menstrual toxic shock. *Microbiology* **2007,** 153, 10, 3235-3245.
46. Young, A. E.; Thornton, K. L. Toxic shock syndrome in burns: Diagnosis and management. *Arch Dis Child Educ Pract Ed*, **2007**; 92, 97-100.
47. Mills, T. T.; Huang, J.; Feigenson, G. W.; Nagle, J. F. Effects of cholesterol and unsaturated DOPC lipid on chain packing of saturated gel-phase DPPC bilayers. *Gen Physiol Biophys* **2009,** 28, 2, 126-39.
48. Chen, L.; Yang, J.; Yu, J.; Yao, Z.; Sun, L.; Shen, Y.; Jin, Q. VFDB: a reference database for bacterial virulence factors. *Nucleic Acids Res* **2005,** 33, 325-8; Chen, L.; Xiong, Z.; Sun, L.; Yang, J.; Jin, Q. VFDB 2012 update: toward the genetic diversity and molecular evolution of bacterial virulence factors. *Nucleic Acids Res* **2012,** 40, D641-5.
49. Bitton, G.; Koopman, B. Bacterial and enzymatic bioassays for toxicity testing in the environment. *Rev Environ Contam Toxicol* **1992,** 125, 1-22; van Beelen, P. A review on the application of microbial toxicity tests for deriving sediment quality guidelines. *Chemosphere* **2003,** 53, 8, 795-808.
50. Robson, M. C. WOUND INFECTION: A Failure of Wound Healing Caused by an Imbalance of Bacteria. *Surgical Clinics of North America* **1997,** 77, 3, 637-650.
51. Marshall, S. E.; Hong, S.-H.; Thet, N. T.; Jenkins, A. T. A. Effect of Lipid and Fatty Acid Composition of Phospholipid Vesicles on Long-Term Stability and Their Response to Staphylococcus aureus and Pseudomonas aeruginosa Supernatants. *Langmuir* **2013,** 29, 23, 6989-6995.

Chapter 6 Vesicle sterilisation

The control of microbial growth in terms of reducing or eliminating bacterial loading and related effects is of huge importance. In some situations the reduction of bacteria, instead of complete elimination, is sufficient, for example in washing of fresh food or body surfaces. In these situations complete elimination, known as sterilisation, is not attainable or practical. Inhibition of microbial growth can be achieved through decontamination or disinfection processes. Decontamination involves the removal of contaminating microorganisms and their potential nutrients from a material to make it safe to handle. Disinfection involves the targeted removal of microorganisms, through the use of specialised chemicals or agents, however complete elimination may not be achieved.

The complete elimination of microorganisms is required for certain applications, for example in the sterilisation of biological media, medical equipment and wound dressings. During this process all pathogenic cells, viruses and endospores (dormant, highly resistant cellular structures utilised for genetic material preservation at times of great stress for some bacterial species[1]) are destroyed. Sterilisation *in-vivo* can be challenging. Bacteriostatic or bactericidal agents can be utilised, however these agents must be able to selectively target reduction or prevention of bacterial cell growth, whilst causing no harm to host cells. *In-vitro* sterilisation is less challenging, a physical treatment can be applied to a product or device to eliminate bacterial loading.

6.1 Medical product sterilisation

The sterilisation of pharmaceutical products, medical devices and their related packaging is very important in controlling and preventing the spread of infection. This can be considered especially integral when one considers that the primary target users of these products are often immuno-vulnerable patients.

It is important to note that if during the sterilisation process of a medical product even one in a billion organisms survives, there is the likelihood of rapid multiplication and re-colonisation. However, there are often difficulties in obtaining absolute sterilisation as a result of the variations in resistance to chemical and physical sterilisation methods of microorganisms of different species, and even of the same species. The effect of sterilisation

on the stability of vesicles was investigated using different physical decontamination methods.

6.2 Physical antimicrobial control methods

The decontamination, disinfection and sterilisation of materials can be achieved using a variety of physical methods. These include sterilisation by applying radiation (particle or electromagnetic), increasing the temperature (heat), filtration (micro-porous membranes) and treatment with low temperature plasma. The sterilisation of vesicles has been investigated using the first three of these techniques. Additionally, in chapter 8 the application of low temperature plasma onto vesicles (within a sensor) for an alternative application is investigated.

6.3 Radiation Sterilisation

The processing potential of radiation was first investigated in the 1950s using electron beam radiation. Inconsistencies produced from the equipment used meant that this method was abandoned until the advent of the use of cobalt 60 (^{60}Co) isotope in the 1960s. Following further developments and improved equipment there are now two primary means of radiation utilised, namely electron beam and gamma. The radiation effect may be classified into two groups, particle and electromagnetic. The different types of radiation in the electromagnetic spectrum can transfer the energy of a photon into characteristic ionisations in or near a biological target, resulting in bactericidal effects, discussed below. The term *cold sterilisation*, where there is no appreciable increase in temperature, has been coined as a resulted of these microorganism-elimination processes.[2]

6.3.1 Electromagnetic radiation

Radiation based sterilisation within this project was carried out using electromagnetic radiation. There are four possible types generally utilised for the sterilisation of materials; microwave, ultra violet, gamma and x-rays. The bactericidal effects are identical in their nature, but differ in origin, and are caused by absorption of high-energy radiation, resulting in ionisation, production of free radicals, and activation of molecules.

The primary bactericidal effect from the absorption of high energy electromagnetic radiation is the ionisation of the material components. This is caused by direct or indirect interactions. Direct interactions involve charged particles dislodging ions and atomic particles, whereas indirect interactions involve photon interactions with atoms, causing electrons to be ejected. This ionisation results in the transfer of an atom or molecule from its ground state to a charged or excited state, which alters the exposed materials properties following treatment. It is important to note that the treatment of a material by radiation is not uniform; not all sections of a material are equally subjected to the ionising radiation energy. Ionisation radiation is discrete, and can therefore cause localised areas of intense treatment compared to surrounding areas. This can result in the secondary production of free radicals and excited atoms, which can, if they contain sufficient energy, continue to ionise and excite adjacent atoms. The process of breaking bonds and the formation of free radicals (known as excitation changes) are the cause of material property changes and bactericidal effects in treated microorganisms.[2]

6.3.2 Effect of radiation on biological material

The effects of radiation damage on microorganisms is likely to be through a wide variety of physical and biochemical reactions, however the primary loss of viability of the cell is reportedly due to intracellular DNA degradation.[3] A correlation of radiation sensitivity to chromosome size, by Sparrow *et al.*, has concluded that the larger the chromosome volume the more sensitive the organism is to radiation damage.[4] Although, it is worth noting that the differences in apparent DNA sensitivity to radiation damage may be the result of some organisms' ability to heal its DNA, as opposed to an inherent resistance to radiation damage.[5]

The survival of a microorganism following treatment with radiation is defined by its' ability to reproduce significantly in broth, or form colonies on a suitable nutrient containing medium. This potential for survival and reproduction occurs in geometric progression, shown in Figure 6-1. This means that the same fraction of organisms is inactivated following application of successive increments of radiation.

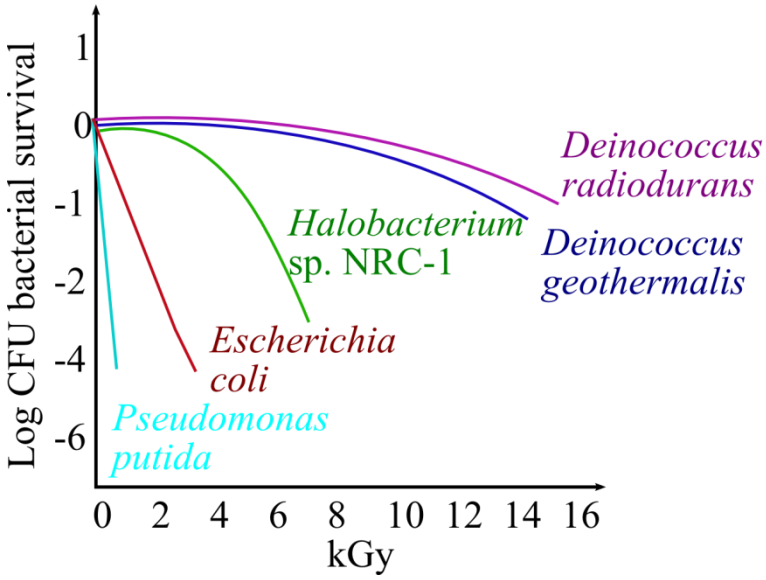

Figure 6-1. Ionising radiation survival curves representative of different bacteria, following treatment with ^{60}Co and bacteria recovery.[6]

A decrease in the initial population of an organism by 1 log is known as D_{10}. This can be calculated by the straight line section of a survival graph, assuming exponential inactivation is taking place, using Equation 6-1 and Equation 6-2:

$$\bar{x} = 2.303 \log \frac{n}{q} \qquad \text{Equation 6-1}$$

$$D_{10} = \frac{\text{dose}}{\log \text{bioburden} - \log \bar{x}} \qquad \text{Equation 6-2}$$

where $\bar{x}$ is the most probable number of surving organisms per unit tested, n is the number of organisms, and q is the number of units that were succesfully sterilised.

6.3.3 Radiation resistance

The radiation resistance of a microorganism can be increased or decreased by altering the localised environment of the species during the ionisation process. These variations can include altering the atmosphere, adding protectors or sensitizers, and changing the temperature, water content or dose rate. An example environmental alteration could be the provision of an anaerobic atmosphere; which could decrease the resistance of an organism to radiation damage.

Determination of the minimum required sterilisation dose for complete elimination of an organism from a material is not only dependent upon the organisms' inherent resistance to

radiation damage. Other factors, such as the quantity of the bioburden present in the first place and the environmental conditions surrounding it have an effect. For example, presence of a support medium, geographic location, product design and size can all influence the amount of radiation required for complete elimination.

6.3.4 Measurement of absorbed dose

The *absorbed dose* is the fundamental radiation parameter used to measure the amount of energy deposited on a material, measured in Gray (Gy), with conversions given in Table 6-1. This measurement typically relates to absorbed dose in water, based on density similarities between a sample and water. The dose equivalent, measured in sievert and rem, can be used to express the quantity of dose used during radiation protection.

Unit of measure for sterilisation or pasteurization	**Units of measure for personal safety**
1 Gray (Gy) = 1 joule/kg	1 Sievert (Sv) = 1 joule/kg
1 Gray (Gy) = 10^2 rad	1 Sievert (Sv) = 1 rem
1 kilogray (kGy) = 10^5 rad	

Table 6-1. Radiation measurement units and conversions

The general absorbed dose required for achieving sterilisation, as well as other radiation-processing applications is given in Figure 6-2:

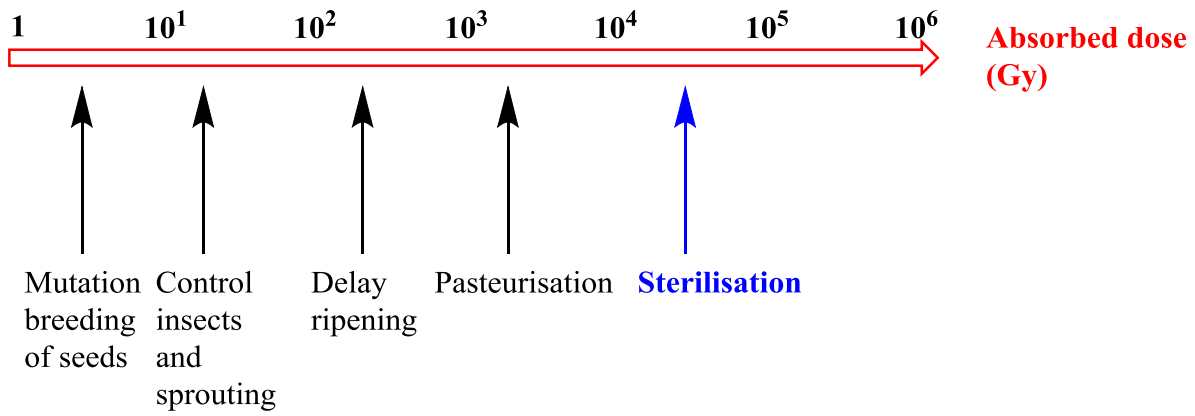

Figure 6-2. The absorbed dose required for sterilisation and other applications (measured in Gray)

6.3.5 Gamma radiation

The industrial treatment of a substance with gamma radiation requires specialised facilities. This includes a radiation shield, an isotope source, the facilities for safe storage when the isotope is not in use, and a method of transporting a sample through the radiation process. The requirement for this complex set up is as a result of the penetrating depth of gamma rays. Radiation of this type can pass through an organism, aluminium, and thin layers of lead and concrete, hence a radiation shield is commonly composed of concrete - with a thickness of nearly two metres.

6.3.6 Gamma radiation of vesicles

The use of gamma radiation on phospholipid vesicles has been a widely investigated technique for modelling the effect of irradiation on cells and food. In addition to this, there is precedence for the sterilisation of vesicle-based samples.[7, 8]

The gamma sterilisation of different vesicle compositions was carried out using a Gammacell GC1000 with a Caesium 137 (^{137}Cs) radioisotope source. ^{137}Cs is a nuclear reactor by-product that can be separated from nuclear waste, following which it can be protectively encapsulated. The radioisotope has a half-life of 30.1 years, and decay occurs to yield barium 137 (^{137}Ba) through the emission of two beta (β) particles and one low-energy gamma (γ) ray, shown in Figure 6-3.

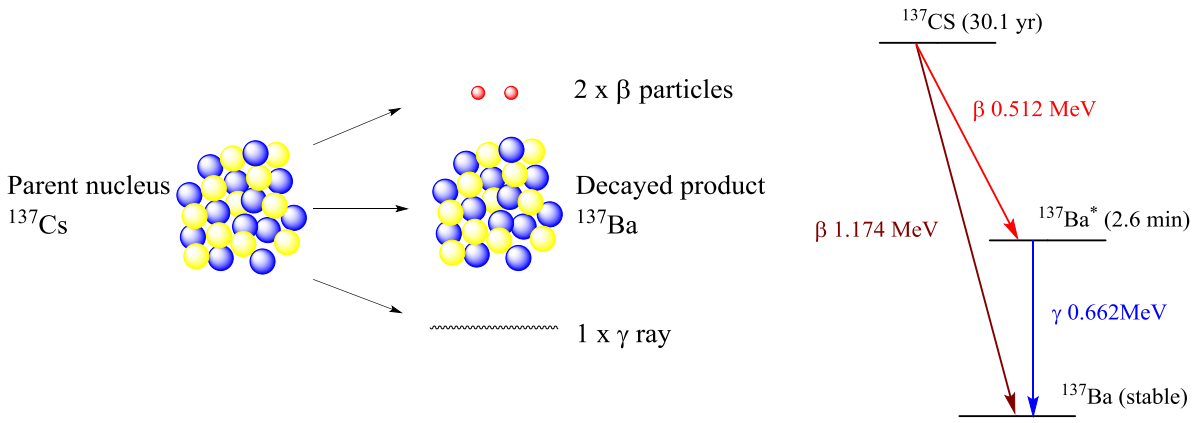

Figure 6-3. The radiation decay of ^{137}Cs to produce ^{137}Ba, through the emission of two β particles and one γ ray.

The ^{137}Cs source was used at a calibration of 7.713 Gy for 58 hours to give a sterilising gamma radiation dose of 25 kGy. This was carried out by Dr J. Sharpe at the Blonde

McIndoe Research Centre, UK. This sterilising dose should be sufficient to ensure absolute sterilisation, according to Figure 6-2, and the absorbed dose requirements.

Initial investigations involved the sending of stable vesicle compositions containing quenched 5(6)-CF, formulated as discussed in chapter 3, for gamma sterilisation treatment. On receipt of the vesicles back from the gamma treatment process it was possible to observe a colour difference between the vesicles that had been sterilised and those that had not, Figure 6-4.

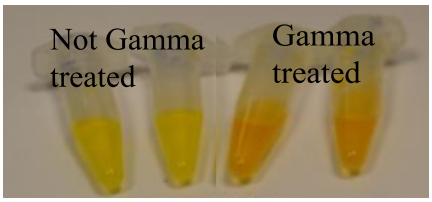

Figure 6-4. The observable effect of gamma sterilisation on vesicles containing self-quenched 5(6)-CF.

This colour change did not appear to indicate vesicle lysis. There was no significant difference in fluorescence intensity measurements between the gamma sterilised and non-sterilised vesicles. However the effect of this colour change on the vesicle stability long term and the efficiency of the dye to act as a signalling agent following treatment required further investigation.

In parallel with the radiated sample, control vesicles were sent to accompany the radiated sample to ensure exact mimicry of conditions aside from the gamma treatment. Both of these were then compared to the same vesicles that had been kept at room temperature (~20 °C) within the lab. The sensitivity and stability results for the vesicle named DSPG-DP is given in Figure 6-5, following addition of bacterial supernatant. The bacterial organisms utilised were those utilised previously within this body of work (namely *P.aeruginosa* PAO1, *S.aureus* MSSA 476 and *E.coli* DH5α) added in a 1:1 ratio.

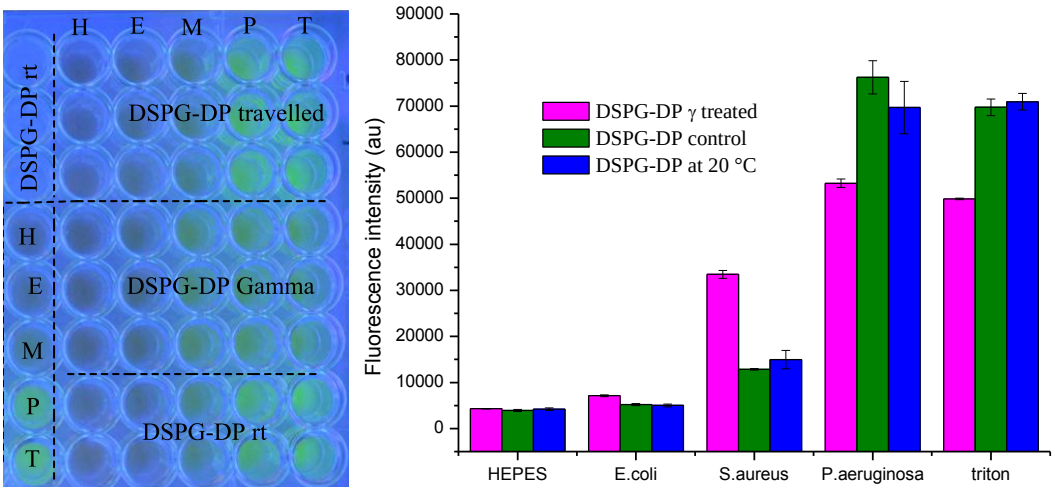

Figure 6-5. The effect of gamma radiation on DSPG-DP vesicles. The photograph and fluorescence intensity graph indicates good observable and measurable fluorescence of all vesicles treated with lytic agents (M = MSSA 476, P = PAO1, T = triton), compared to the low fluorescence of all vesicles with non-lytic agents (H = HEPES, E = DH5α).

Initial results indicated good stability of the vesicles to gamma sterilisation treatment, with maintenance of susceptibility to external pathogenic stimulus. Interestingly, the susceptibility of the treated vesicles compared to non-treated vesicles to MSSA 476 supernatant was increased. This result was also measured for DPPG-DP vesicles, shown in SI-Figure 4.

6.3.7 Vesicle stability – radiation sterilisation

Damage caused to the phospholipids and other vesicle components by the gamma radiation could be a result of the interaction and breakage of bilayer component bonds. This could have been achieved through direct or indirect rupture (secondary species activated by the gamma radiation e.g. radicals). This could lead to the reforming of the acyl chain without any physical changes and cross-linking and dimerisation between aligned structures. The irreparable breakage of bonds, such as formation of the dehydrogenation product phosphatidic acid; causing a physical change and a decrease in vesicle stability could also be occurring.

Following gamma radiation of phospholipid vesicles, Zuidam *et al.* reported a size-dependent decrease in pH and a linear decrease in vesicle concentration.[7] Hence, additional information about concentration count, pH and vesicle sizing following gamma treatment would be beneficial in aiding understanding of how the radiation affects the vesicle stability. Initial

results obtained indicate that the application of gamma radiation could provide a suitable sterilising technique for treatment of vesicles.

6.4 Heat sterilisation

The use of heat to obtain materials that are bioburden-free is perhaps the oldest and best-recognised sterilisation technique. Sterilisation using this method can be achieved with moist heat – a fast process utilising saturated steam or boiling water, or with dry heat – a slower, higher temperature process with the benefit of increased permeability. The death of bacterial cells by thermal treatment is exponential, progressing through a first-order reaction mechanism which can be defined in Equation 6-3:

$$N_t = N_o e^{-kt} \qquad \text{Equation 6-3}$$

Where N_o is the starting number of a population, N_t is the number surviving at any time, t, and k is the death rate constant. The regressing nature of the curve is indicated by the minus sign.[2]

6.4.1 Thermal resistance

The presence of heat resistant bacterial strains can cause deviations from the expected linear logarithmic nature of the survival curve. Often, an *inactivation energy* is required to initiate the destruction of microorganisms. The extent of dependency on this varies depending on the innate heat resistance of the strain, the temperature of the heat treatment applied to the sample, the local growth media conditions, such as pH and ion concentrations, and the initial incubation temperature of the sample. In addition to this the thermal resistance of a bacterial strain can vary depending on whether dry or moist heat is applied.[2]

6.4.2 Moist (steam) sterilisation

Steam sterilisation is an efficient technique for achieving bacterial spore elimination within short time frames, hence related equipment for it can commonly be found in hospitals, research environments and industrial facilities. This equipment commonly takes the form of an autoclave machine, capable of sterilising equipment through the application of high pressure saturated steam at ~120 °C for < 20 minutes. Despite its efficiency, problems can

arise from the deleterious effects relating to the rate of material degradation relative to the rate of biological inactivation. For example, proteins, and in the case of vesicles; carbohydrates and active encapsulated agents could suffer from degradation or caramelisation. It is also possible that undesired products with the potential to cause toxic side effects can form.[2]

6.4.3 Thermal treatment of vesicles

The stability of vesicles to thermal moist sterilisation treatment was carried out on three stable vesicle candidates containing 5(6)-CF, developed in chapter 3, namely DSPG-DP, DOPC-DS and TCDA-DS. This involved heating each of the vesicle samples up to 80 °C for 10 minutes, 30 minutes and 60 minutes, and comparing the fluorescence response obtained following addition of the lytic surfactant triton and the control HEPES buffer. In addition to this, a comparison could be made with vesicle samples that were sterilised using a standard autoclave machine, with a treatment time of 60 minutes at 120 °C. The results for these treatment parameters are given in Figure 6-6. Correlating photographs can be found in SI-Figure 5.

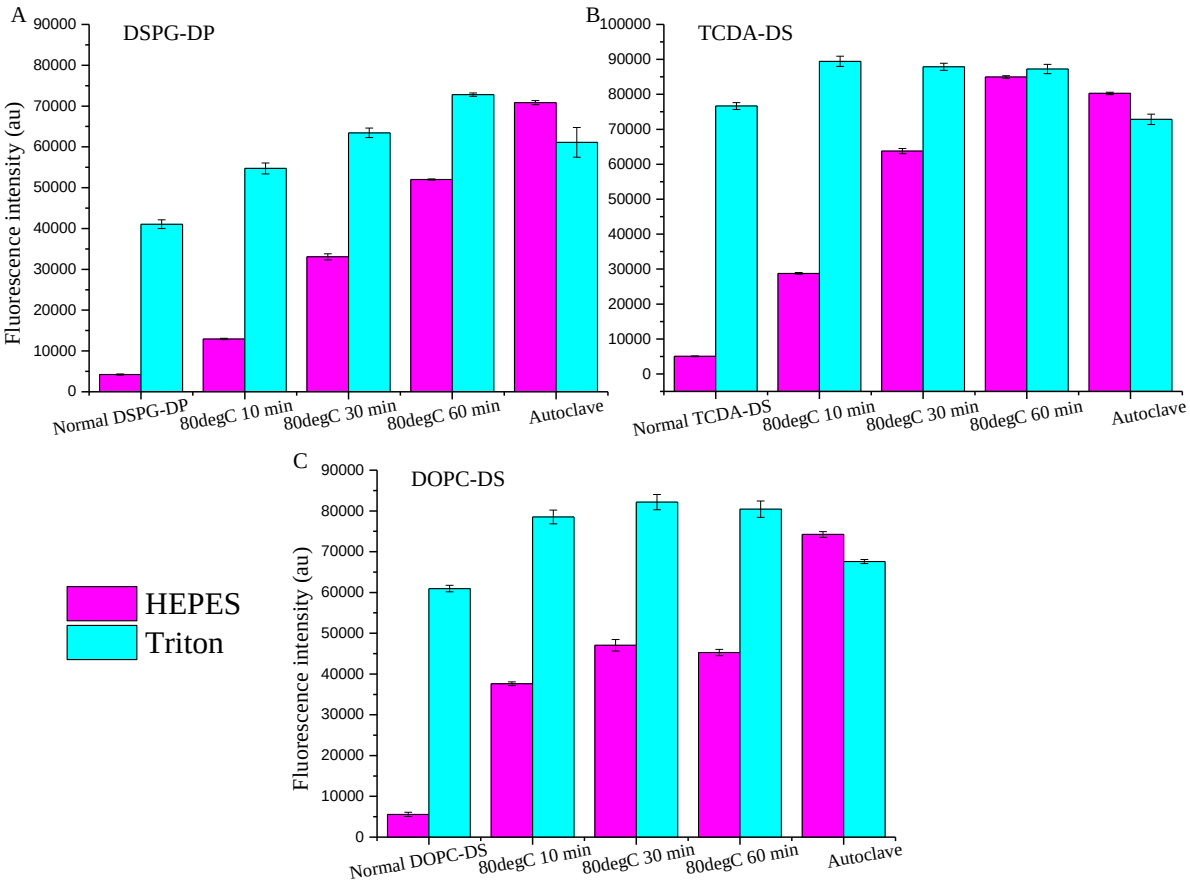

Figure 6-6. Heat sterilisation of three vesicle types; carried out at 80 °C for 10, 30 and 60 minutes, and compared to control (untreated) vesicles, and autoclaving (120 °C, 60 minutes), all with HEPES and Triton; where A), B) and C) are fluorescence intensity measurement graphs of DSPG-DP, TCDA-DS, and DOPC-DS vesicles respectively.

Total passive release of the dye or lysis of all vesicles present in each of the three samples was measured following sterilisation through autoclave treatment. Interestingly, the presence of the phospholipid 1,2-dioleoyl-*sn*-glycero-3-phosphocholine (DOPC) at 2 mol %, and even, to some extent, 1,2-distearoyl-*sn*-glycero-3-phospho-(1'-*rac* glycerol) (sodium salt) (DSPG) at 10 mol % has decreased the passive release of the dye at 80 °C, compared to the 10,12-tricosadiynoic acid (TCDA).

6.4.4 Vesicle stability – thermal sterilisation

As discussed in 3.1.6 Bilayer fluidity, phospholipids found within bilayers can exist in a low-temperature solid-ordered (crystalline) phase or a higher temperature fluid-disordered (gel) phase. The temperature at which a transition occurs from one phase to the other is known as

the phase transition temperature T_c. The T_c and hence the creation of phases can be tailored depending on the phospholipid selected. Passive leakage of internal agents from a vesicle is at its greatest at temperatures around the T_c, due to the coexistence of two phases, and the resulting defects between the boundaries.[9] From what is known and reported about phospholipid membrane bilayer susceptibility to degradation around the crystalline-to-gel transition temperature (T_c), the increased fluorescence response following heat treatment from all vesicle candidates was to be expected.

The extent of passive leakage of internal agent from the vesicle compositions indicates that thermal sterilisation of vesicles through moist heat methods would not be compatible for stability of vesicles. It is also possible to conclude from this that sterilisation through dry heat would not be compatible for maintaining the stability of the vesicles.

6.5 Filter sterilisation

The development of commercial filtration membranes for the removal of bacterial contamination from liquids began in 1922, leading to the introduction and manufacture of membranes in two pore sizes: 0.45 µm and 0.80 µm. Prior to this, fibrous asbestos filter pads (Seitz filters), where separation was achieved based on absorption of bacteria to inner porous structure and random entrapment, were utilised. The efficiency of these commercial filtration membranes was questioned in the late 1960's following the discovery of a *pseudomonas* species in a post-sterilised solution, leading to the introduction of 0.22 µm and eventually 0.1 µm filters.

Sterile filtration methods are employed extensively in the production of particle and bacteria free medical solutions. Although, this has proved problematic as the physiochemical and biological complexity of medical solutions has increased. There has hence been an elevated requirement for validation of filter efficiency against bacterial species, high standards of operation and activity-testing of the obtained sterilised ample.

6.5.1 Filtration process

The filter sterilisation process involves passing a mixture of fluids and particles through a porous medium capable of trapping the solids. This is achieved either mechanically or randomly, using a surface, depth or screen filter. The cost efficiency of filters used

individually to obtain a high volume of size-exclusion-solution is not favourable, hence a combination of filters is often utilised. Depth filters have a high dirt-handling capacity; large quantities of contaminants can be trapped in a torturous maze of flow channels. Surface filters trap large particles at the surface of the polymeric microfiber matrix; with some trapping of smaller particles occurring within the membrane matrix. Screen filters allow controlled and predictable particle removal.[2]

6.5.2 Filter contamination

There are three possible sources of contamination to a filter membrane from a solution: dissolved impurities, suspended particles and microorganisms. Dissolved impurities can be inorganic (ionic) or organic particles and solid particles can be all manner of things, including colloidal solids, metals, cotton, dust and lint. However, it is the microorganisms that can prove most problematic; dead they can be responsible for premature filter blockages, and alive they can multiply at logarithmic rates, causing blockage and overburden of the filters. The extent of these contamination difficulties can be managed through manufacture area and equipment cleanliness, use of ultrapure water, careful storage and the minimisation of human impact.[2]

6.5.3 Filter sterilisation of vesicles

Filter sterilisation involved pressurising the vesicles through 0.1, 0.22 and 0.45 µm filter membranes. The 0.22 and 0.45 µm filter membranes, manufactured by Merck Millipore, were composed of mixed cellulose esters, and the 0.1 µm filter (also Merck Millipore) was composed of polyvinylidene fluoride (PVDF). Each of the filters had a process volume capability of 100 ml.

The stability of vesicles to filter sterilisation treatment was carried out on three vesicle candidates containing 5(6)-CF, formulated in chapter 3 - Vesicle development - stability, namely DSPG-DP, DOPC-DS and TCDA-DS. Each of these vesicles was extruded through a 100 nm porous membrane during formulation, giving vesicles of between 80 – 120 nm. The fluorescence intensity response of filtered vesicles following addition of the lytic surfactant triton (discussed in 3.3.5 Vesicle membrane solubilisation – a positive lytic control) and the

control HEPES buffer was compared to the same response of non-filtered vesicles, Figure 6-7.

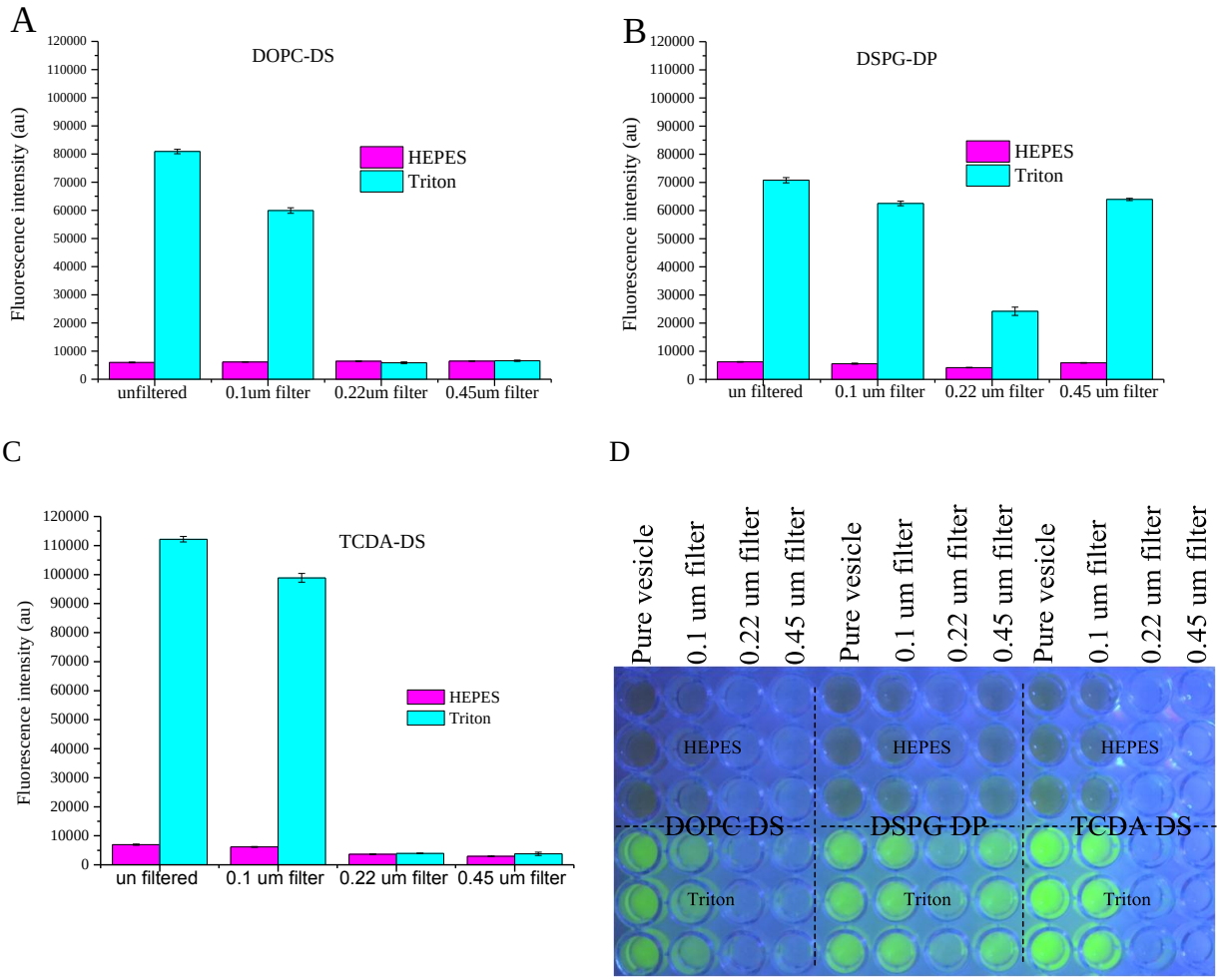

Figure 6-7. Filtration of three vesicle types was carried out with 0.1, 0.22 and 0.45 µm filters, and vesicles obtained were compared to control vesicles; all with HEPES and Triton; where A), B) and C) are fluorescence intensity measurement graphs of DOPC-DS, DSPG-DP and TCDA-DS vesicles respectively; and D) is an actual photograph of the vesicles before and after filtration.

Each of the vesicles were successfully pressurised through the filter membranes, i.e. a sample solution was obtained after filtration. Although each of the vesicle types indicated stability to sterilisation through a 0.1 µm filter, there was some loss of max-fluorescence on addition of triton. This potentially indicates that some of the vesicles are trapped on the filter. Despite this, the PVDF provided a favourable membrane material for passage of vesicles through the filter when compared to the mixed-cellulose filters. The fluorescence response of TCDA-DS and DOPC-DS vesicles following sterilisation with 0.22 and 0.45 µm filters was significantly small both with HEPES buffer and triton, indicating that nearly all of the vesicles were

trapped within the membrane pores, however this could have been proved definitively using DLS measurements. The anionically charged nature of the DSPG lipid (present at 10 mol %) can be assumed to be playing a role in ensuring elution of the vesicles through these cellulose filters.

6.5.4 Vesicle stability – filter sterilisation

Phospholipid vesicles are known to be stable to extrusion through nanoporous membranes; a process which is carried out during manufacture to ensure unilamellar monodisperse vesicles within this investigation. It is possible to conclude from this that vesicles should be stable to filtration through pores of 0.1, 0.22 and 0.45 µm. However, the trapping and sticking of some vesicle compositions onto certain filter sterilising membrane materials would be costly and problematic. This could potentially be overcome by using filter membranes composed of materials that would allow the free-flow of vesicles; such as PVDF which showed promising delivery of sterilised vesicles at a pore size of 0.1 µm.

6.6 Vesicle sterilisation - conclusions

Within this investigation, the emphasis was placed upon vesicle stability to sterilisation techniques, as opposed to actual sterilising efficiency of the technique employed.

It is possible to conclude that radiative treatment of vesicles using a ^{137}Cs gamma source showed excellent potential for ensuring structure of vesicle is maintained without passive diffusion of internal agents. The expected response to bacterial supernatant, following addition to both gamma-treated and control vesicles, was obtained. However the actual fluorescent intensity response of gamma treated vesicles following addition of *P.aeruginosa* supernatant and the surfactant triton was decreased compared to control vesicles i.e. it had a lower F_{max}. This may be due to the gamma radiation interacting, sequestering and degrading the carboxyfluorescein, reducing its maximum fluorescence following unquenching. Interestingly, the fluorescent response of gamma treated vesicles following the addition of *S.aureus* MSSA 476 was greater than that measured for the control vesicles, although the maximum fluorescence level is still lower than that obtained following addition of the aforementioned lytic agents.

The thermal treatment of vesicles was unsurprisingly deemed to not be an appropriate technique for achieving sterilisation. This was a result of the low crystalline to gel transition temperatures of the phospholipids used. Above these temperatures, at the sterilising temperatures investigated within this study, passive leakage of the internal agent was increased.

The use of filter sterilisation indicated a promising method towards obtaining bioburden-free stable vesicles when utilising membranes composed of PVDF (0.1 µm). The potential trapping of vesicles on the mixed cellulose membranes (0.22 and 0.45 µm) was indicated from a low fluorescence intensity following pressurisation through the filter. The composition of the obtained solution could be further investigated utilising DLS, which would enable measurements of the solute/vesicle sizes. Further work could be carried out investigating the use of PVDF or other membrane compositions as non-vesicle-trapping matrices at different pore sizes.

Ultimately, the sterilisation of vesicles may be achieved prior to inclusion within, or more likely, following incorporation into the dressing. Two alternative sterilisation techniques are introduced, and the development of methods towards achieving sterile vesicles during formulation are discussed in the following sections.

6.6.1 Alternative sterilisation technologies

There has been increased interest into the development of low temperature sterilisation systems that can yield sterilised materials. An ideal technology would provide reduced process times, improved materials compatibility, decreased environmental impact, increased capacity and decreased costs. An example of a potential low temperature technique for sterilisation is vaporised hydrogen peroxide (vH_2O_2). This can be applied on its own, or alongside gas plasma or ozone and has shown good potential sterilisation of surfaces including re-usable metal and non-metal medical devices.[10] This technique may not be appropriate for treatment of vesicles-in-a-dressing due to the high oxidising potential of vH_2O_2. The use of low temperature plasma for inactivation of microorganisms was commercialised in the 1990s due to its low toxicological profile, rapid processing time and low environmental impact.[2] This is discussed in more detail in chapter 8 although its sterilising effect is not the focus.

6.6.2 Alternative solution - solvent free vesicles

An alternative pathway towards achieving self-sterilised vesicles is through solvent-free vesicle methodologies. This process could potentially be considered as self-sterilising, due to the high temperatures attained during synthesis.[11]

The majority of vesicle preparatory methods require volatile organic solvents, such as chloroform and methanol, or detergents to solubilise the lipids. Although these residues can be minimised, traces of these solvents and detergents may remain in the final vesicle solution and potentially contribute to vesicle instability and final product toxicity.[12] Development of methods in which the utilisation of solvents is avoided may prove beneficial, with regard to final product cost, toxicity and life cycle. The introduction of a novel method in 2005 by Mozafari *et al.*, known as the heating method, fulfils these specifications.[11] Mozafari *et al.* have since gone on to modify and improve this method, making it scalable and simple, for the delivery of plasmid DNA, reported in 2007.[13] This proposed method was further modified for vesicle preparation in a preliminary study for the synthesis of solvent-free vesicles suitable for applications within this project.

The response of solvent-free vesicles to the standard bacteria (*S.aureus* MSSA 476, *P.aeruginosa* PAO1 and *E.coli* DH5α bacteria - discussed in 4.2 Bacteria), and the growth of each of these bacteria within the solvent-free vesicles is given in Figure 6-8:

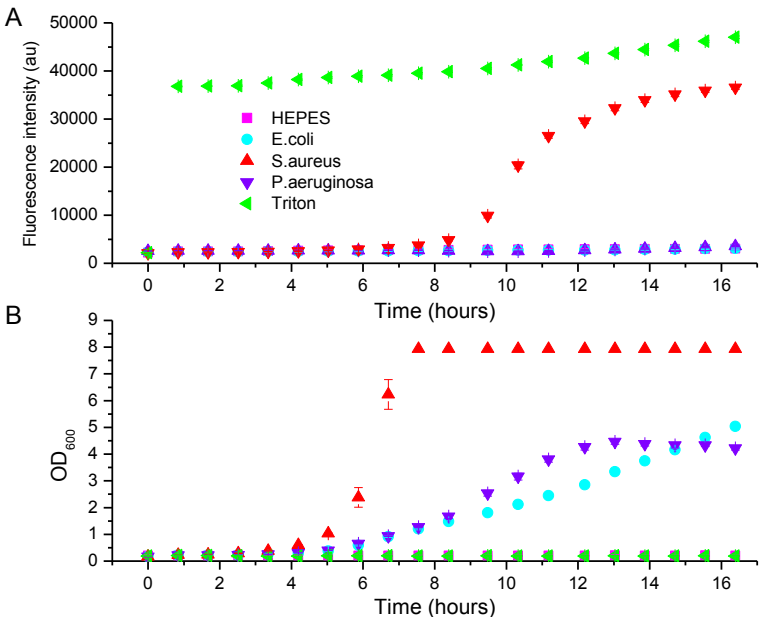

Figure 6-8. The response of solvent-free vesicles to *S.aureus* MSSA 476, *P.aeruginosa* PAO1 and *E.coli* DH5α bacteria, and the growth of each of these bacteria within the solvent-free vesicles.

A major difference between the solvent-free and standard-synthesis (normal) vesicle is the measured and observable fluorescence response. Although the measured fluorescence response given in Figure 6-8 (A) indicates a favourable sensitivity to *S.aureus* MSSA 476, there is no increased response to *P.aeruginosa* PAO1 and the intensity is not as great as that measured for normal vesicles, indicating that further development is required. However, the bacteria growth in solvent-free vesicles compared to normal vesicles could be considered slightly amplified. This could be due to trace amounts of glycerol, commonly found in growth media solutions where it can be utilised by bacteria as a carbon source. Although this may not be advantageous within a wound environment, within lab based experiments, this could be beneficial. The presence of EDTA within the normal-vesicle buffer solution used during manufacture could be problematic in bacteria growth, as it is known to increase bacterial membrane permeability and decrease cell viability.[14]

Further development of this solvent-free methodology could prove advantageous for the synthesis of vesicles required on a large scale, or for medical and cosmetic application, with the potential self-sterilising aspect proving beneficial.

6.7 References

1. Nicholson, W. L.; Munakata, N.; Horneck, G.; Melosh, H. J.; Setlow, P. Resistance of Bacillus Endospores to Extreme Terrestrial and Extraterrestrial Environments. *Microbiology and Molecular Biology Reviews* **2000,** 64, 3, 548-572.
2. Block, S. S. *Disinfection, sterilization and preservation*. 5th ed.; Lippincott Williams and Wilkins: **2001**.
3. Ginoza, W. The Effects of Ionizing Radiation on Nucleic Acids of Bacteriophages and Bacterial Cells. *Annual Review of Microbiology* **1967,** 21, 1, 325-368.
4. Sparrow, A. H.; Underbrink, A. G.; Sparrow, R. C. Chromosomes and Cellular Radiosensitivity: I. The Relationship of D0 to Chromosome Volume and Complexity in Seventy-Nine Different Organisms. *Radiation Research* **1967,** 32, 4, 915-945.
5. Davies, R.; Sinskey, A. J. Radiation-Resistant Mutants of Salmonella typhimurium LT2: Development and Characterization. *Journal of Bacteriology* **1973,** 113, 1, 133-144; Town, C. D.; Smith, K. C.; Kaplan, H. S. Production and repair of radiochemical damage in Escherichia coli deoxyribonucleic acid; its modification by culture conditions and relation to survival. *J Bacteriol* **1971,** 105, 1, 127-35.
6. Daly, M. J. A new perspective on radiation resistance based on Deinococcus radiodurans. *Nat Rev Microbiol* **2009,** 7, 3, 237-45.
7. Zuidam, N. J.; Versluis, C.; Vernooy, E. A. A. M.; Crommelin, D. J. A. Gamma-irradiation of liposomes composed of saturated phospholipids. Effect of bilayer composition, size, concentration and absorbed dose on chemical degradation and physical destabilization of liposomes. *Biochimica et Biophysica Acta (BBA) - Biomembranes* **1996,** 1280, 1, 135-148.

8. Hwang, K. J.; Mauk, M. R. Fate of lipid vesicles *in vivo* – Gamma ray perturbed angular-correlation study. *Proceedings of the National Academy of Sciences of the United States of America* **1977,** 74, 11, 4991-4995.
9. Papahadjopoulos, D.; Nir, S.; Ohki, S. Permeability properties of phospholipid membranes: Effect of cholesterol and temperature. *Biochimica et Biophysica Acta (BBA) - Biomembranes* **1972,** 266, 3, 561-583.
10. Schneider, P. M. New technologies and trends in sterilization and disinfection. *American Journal of Infection Control* **2013,** 41, 5, S81-S86.
11. Mozafari, M. R. Nanoliposomes: From Fundamentals to Recent Developments. Mortazavi, S. M., Ed. Trafford Publishing: **2005**.
12. Lord, R. C. C. Osmosis, osmometry, and osmoregulation. *Postgraduate Medical Journal* **1999,** 75, 880, 67-73.
13. Mortazavi, S. M.; Mohammadabadi, M. R.; Khosravi-Darani, K.; Mozafari, M. R. Preparation of liposomal gene therapy vectors by a scalable method without using volatile solvents or detergents. *Journal of Biotechnology* **2007,** 129, 4, 604-613.
14. Riondet, C.; Cachon, R.; Waché, Y.; Alcaraz, G.; Diviès, C. Measurement of the intracellular pH in Escherichia coli with the internally conjugated fluorescent probe 5- (and 6-)carboxyfluorescein succinimidyl ester. *Biotechnology Techniques* **1997,** 11, 10, 735-738.

Chapter 7 Vesicle modification

The importance of modification of vesicle structures to improve both the specificity and stability of vesicles has shown massive potential for increasing the applicability of vesicles. The development of so called *intelligent* vesicles, responsive to pH and temperature fluctuations, is discussed in detail in chapter 3 (3.1.2 Intelligent vesicles), and investigations within this work have yielded vesicles that have proven to be both stable and selectively sensitive. The potential scope of vesicles in medical products can be further expanded on through development of modifications to these capsules.

7.1 Vesicle modifications

Desired reactivities and stabilities of vesicles can be achieved through modifications of vesicle structure, (see Chapter 3) or through placement within a hydrogel (see Chapter 5); both investigated and discussed previously. An alternative approach towards achieving stability or altered sensitivity could be through conjugation of the vesicle to removable protective agents. The conjugated binding of vesicle bilayers to different capsule forming agents could be considered to provide a pseudo-secondary membrane. These coatings could be ionically or covalently bound to the vesicle, providing a stabilising environment, until the active agent within the vesicle is required.

An example of such a vesicle modification system that has been widely investigated and reported upon is the development of PEGylated vesicles. The PEG is attached to the phospholipid head group and forms a stabilising protective coating around the vesicle, which aids its permeability, ensures a long-circulating profile *in-vivo*, and promotes host retention.[1] Importantly, under localised pathological conditions within a host, such as acidic pH conditions in tumours, the PEG-coating can be readily detached, ensuring delivery of active agents from the unprotected vesicle.[2]

Within this investigation, hyaluronic acid (HA) is utilised to provide a biodegradable capsule around the vesicles. The HA can be degraded in the presence of hyaluronidase (HLase) enzymes, produced from pathogenic bacteria, depicted in Figure 7-1. Following degradation of the capsule, toxins released concurrently from the bacteria can lyse the selectively sensitive vesicle and an active agent can be released.

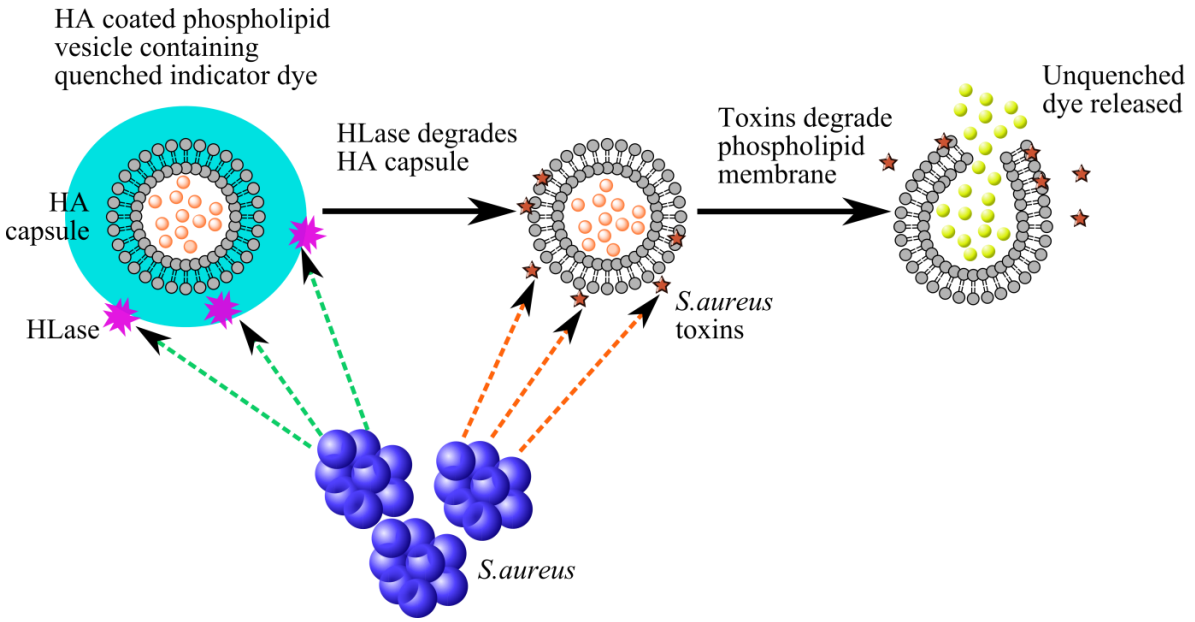

Figure 7-1. A schematic demonstrating the desired effect of vesicles coated with hyaluronic acid (HA) in the presence of hyaluronidase (HLase) producing bacteria (e.g. *S.aureus*). Encapsulation of an active agent within the vesicles can be used to indicate the presence of, or treat the cause of, infection.

7.1.1 Hyaluronic acid

Hyaluronic acid (HA), commonly referred to as hyaluronate, is a linear, very high molecular weight (average molecular mass from 10000, up to 1.2 million Da) glycosaminoglycan copolymer comprised of alternating D-glucuronic acid and N-acetyl-D-glucosamine units, shown in Figure 7-2. HA can be found in all connective tissue,[3] it is naturally occurring; with up to 50 % of it being localised in the skin,[4] and is both hydrophilic and nonimmunogenic. These properties make it an ideal scaffold in both its modified and cross-linked hydrogel state.[5]

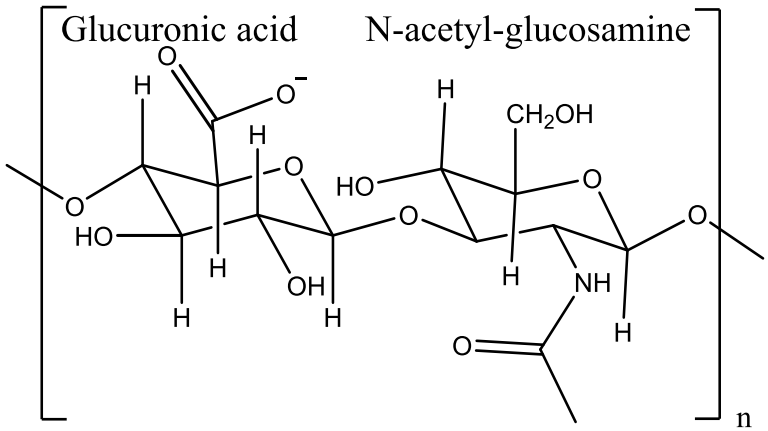

Figure 7-2. The copolymers of hyaluronic acid in their β-bond cross-linked form: [α-1,4-D-glucuronic acid-β-1,3-N-acetyl-D-glucosamine]$_n$

The application of HA as a scaffold has developed as a result of its unique chemical properties. HA is available at a range of molecular weights, achieved by controlled degradation with HLase, it has the ability to be remodelled enzymatically *in vivo* and in the presence of specific cell types (e.g. mature cells unique to cartilage - chondrocytes), and it has the potential to be functionalised with reactive groups or undergo cross-linking reactions to form hydrogels.[6] In addition to these attributes, HA is innately non-adhesive to cells,[7] yet retains the ability to be functionalised or blended with cell-adhesion additives to tailor this property.[8]

A primary advantage of using HA to coat the vesicles is its known role in angiogenesis, increasing cell motility and proliferation, proven by Trochon *et al.* using the cell receptor CD44, and a monoclonal antibody against CD44, and measuring the stimulating effect of hyaluronan polysaccharide on endothelial cell proliferation and migration.[9]

7.1.2 Hyaluronidase

Hyaluronidase (HLase) is the general term used to describe enzymes that are able to break down HA, and these can generally be divided into three types; hyaluronate-4-glycanohydrolases, testicularly derived, hyaluronate-3-glycanohydrolases, produced primarily by leeches, and bacterial HLases. The first two types degrade HA to form tetrasaccharides, whereas bacterial HLases act as endo-*N*-acetylhexosaminidases; eliminating across the β-1,4 linkage,[4] shown in Figure 7-3.

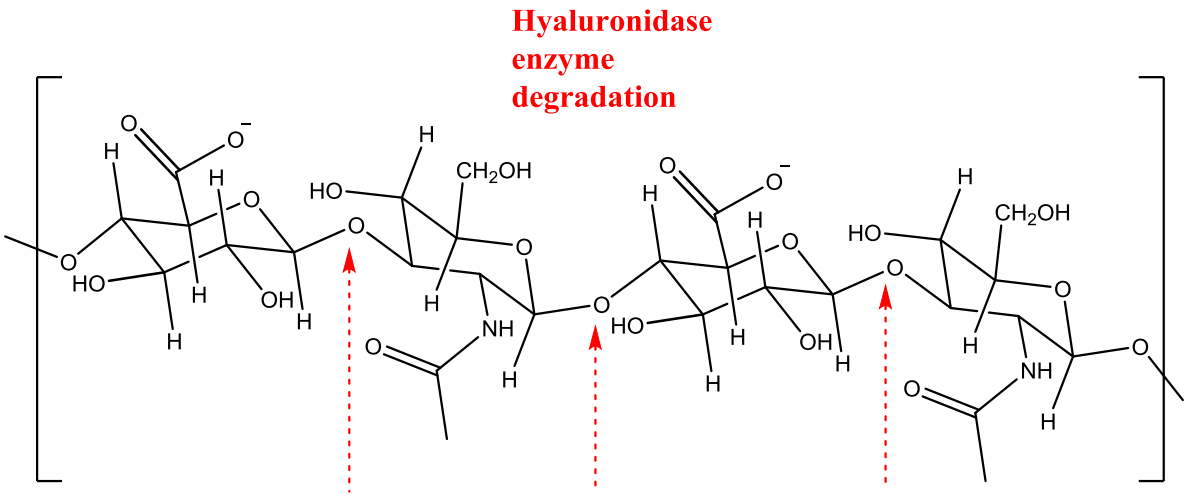

Figure 7-3. Potential sites of action of hyaluronidase on hyaluronic acid.

HLase is produced by a wide variety of microorganisms; however gram negative organisms only produce the enzyme periplasmically, reducing its likelihood of playing a role in pathogenesis. As a result of this, it is the HLases produced by gram positive organisms that are excreted into the extracellular matrix that are of interest to this investigation. Gram-positive organisms that are capable of producing HLases include *Streptococcus*, *Peptostertococcus*, *Propionibacterium*, *Stretomyces*, *Clostridium* and *Staphylococcus*. Many of these HLase excreting strains of bacteria are able to cause infection at a mucosal or skin surface of a host.[4]

7.1.3 Hyaluronic acid coated vesicles

The hyaluronic acid was prepared by dissolving 10 mg ml^{-1} in HEPES buffer, followed by stirring for 4 hours; resulting in a clear gel with a favourable rheology, which following activation was added to relevant vesicles in a 2:1 ratio. The stabilised vesicles TCDA-DS developed and discussed in Chapter 3 - Vesicle development - stability, containing the self-quenched dye 5(6)-CF, were utilised for this investigation; only differing in their size, following extrusion through 200 nm membranes. Specific attachment of the HA to the vesicles was achieved by the incorporation of stearylamine (SA).

7.1.4 Incorporation of stearylamine into vesicles

For *specific* HA attachment the TCDA-DS vesicles were modified by the incorporation of 6 mol % SA; added from a 100 mM stock solution (in $CHCl_3$), at the same point of formulation as the other membrane components, followed by the formation of the dehydrated thin film. The alignment of the SA is proposed to occur alongside the lipids in the membrane, with protrusion of the amine externally from the bilayer to allow attachment to occur, depicted in Figure 7-4.

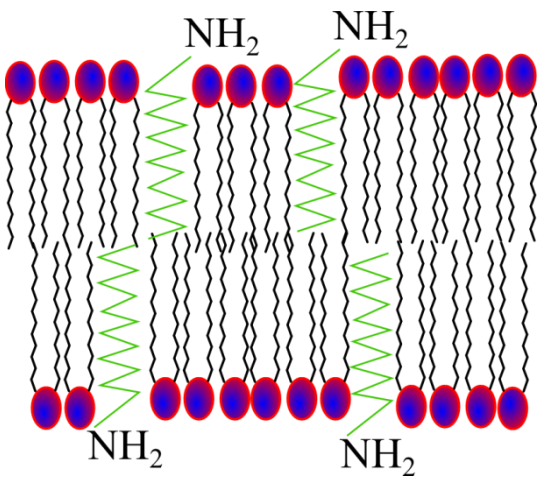

Figure 7-4**.** The proposed alignment of SA alongside phospholipids in a membrane. The amine protrudes outside of the membrane allowing conjugation to the hyaluronic acid in the presence of EDC and NHS.

7.1.5 Hyaluronic acid – vesicle coupling

Coupling of the SA-TCDA-DS vesicles to the HA was achieved using the coupling agents ethyl(dimethylaminopropyl) carbodiimide (EDC) and *N*-hydroxysuccinimide (NHS). The HA was first activated by the EDC, followed by addition of the NHS, and finally this was added to the vesicles, depicted in Figure 7-5.

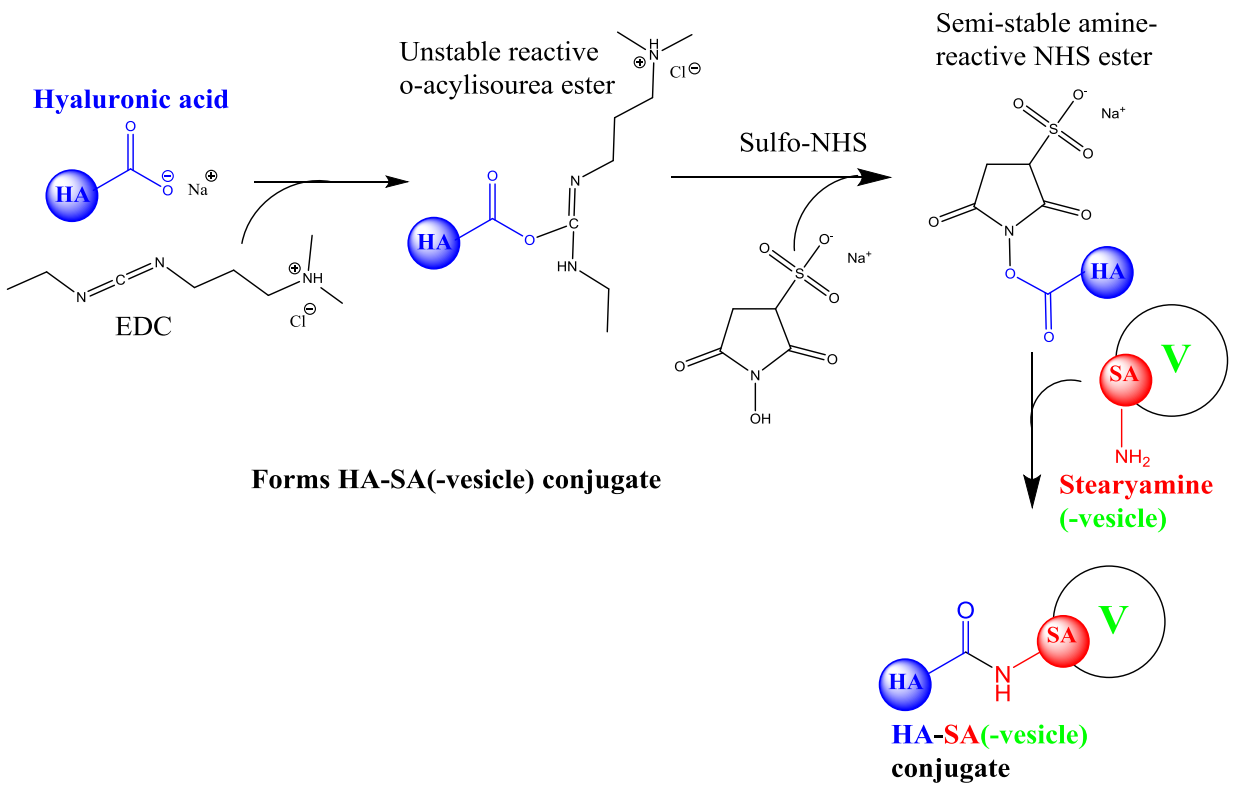

Figure 7-5. Formation of the HA-SA(-vesicle) conjugate, achieved through activation of the carboxylic acid moiety of D-glucuronic acid from HA with EDC to form an unstable reactive o-acylisourea ester, followed by addition of NHS to form an amine reactive ester that readily reacts with SA(-vesicle) to form a HA-SA(-vesicle) conjugate.

Proof of the formation of specific conjugation of the HA to SA-TCDA-DS vesicles was obtained through the use of dynamic light scattering (DLS) size measurements. Standard TCDA-DS vesicles were coated with activated HA and the size measurements were compared to uncoated vesicles of both types, results shown in Figure 7-6.

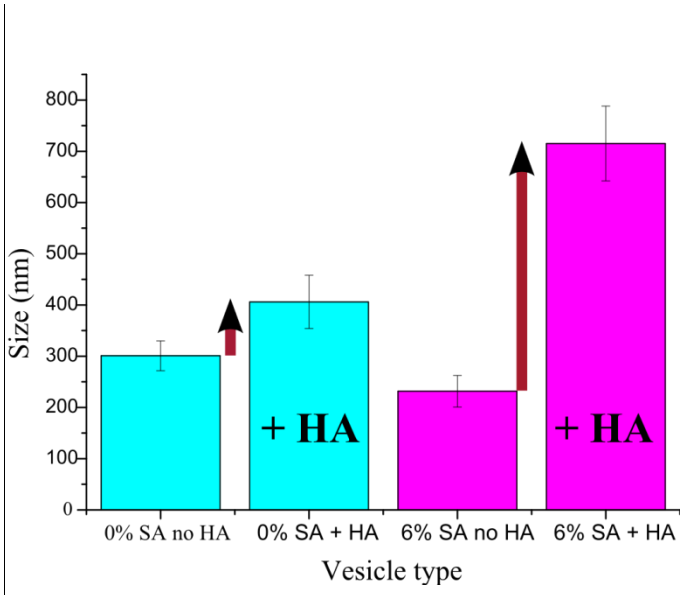

Figure 7-6. DLS of HA coated vesicles compared to uncoated vesicles. The HA coated vesicles are larger in size than their corresponding un-coated vesicles.

The *specific* conjugation of HA to SA-TCDA-DS vesicles was evidently achieved, however *non-specific* binding of the HA to the TCDA-DS vesicles appears to be taking place too. This effect is probably due to the quaternary amine on the DSPE lipids reacting with the activated semi-stable amine reactive NHS ester.

7.1.6 Proof of principle

The specifically and non-specifically HA conjugated vesicles were compared according to their fluorescence response on addition of isolated delta (δ) toxin. δ-toxin is an amphipathic α-helical toxin, commonly secreted by *S.aureus*, which can insert into phospholipid bilayers and induce a detergent-like solubilisation of the membrane.[10] The effect of δ-toxin on the coated vesicles was compared to the effect of coated vesicles that have been incubated with hyaluronidase (from bovine testes) prior to addition of the δ-toxin, shown in Figure 7-7.

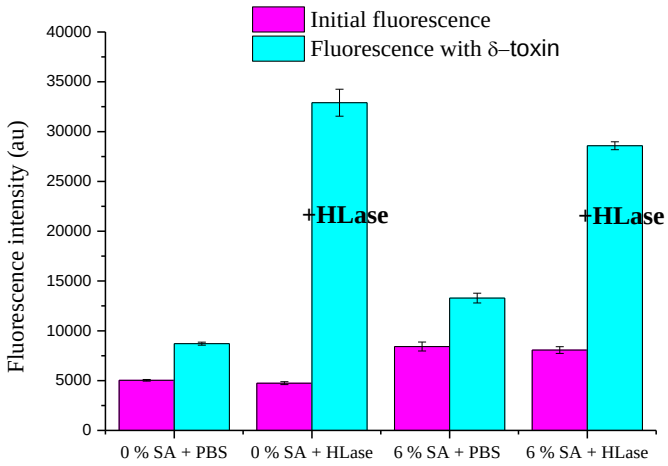

Figure 7-7. The effect of δ-toxin with or without HLase on HA coated vesicles (0 % SA – non-specifically, 6 % SA – specifically conjugated). Fluorescence intensity is shown prior to addition of any agents, and following incubation with δ-toxin for 5 min.

From Figure 7-7, it can be seen that the presence of HLase increases the susceptibility of the HA-coated vesicles to the δ-toxin, resulting in an amplified fluorescence value compared to the respective non-HLase treated vesicles of each type. Unsurprisingly, the specific binding from the vesicles containing 6 % SA provides a network that is more difficult to penetrate and degrade then the non-specifically bound (0 % SA) HA coated vesicles. The diminished diffusion of the δ-toxin to the vesicle surface was indicated by a decreased level of maximum fluorescence. Following on from the success of this preliminary proof-of-principal investigation, the reactivity of the HA-coated vesicles with bacteria strains was investigated.

7.1.7 HA-coated vesicles with bacterial supernatant

The specifically and non-specifically HA-coated TCDA-DS vesicles were treated with two *S.aureus* strains, a known HLase positive strain MSSA H560, which was first acquired from a hospital in Oxford, UK, and a HLase negative strain MRSA ST239µ2. The ST239µ2 is an attenuated strain of *S.aureus* with the same DNA sequence as MRSA TW20 (a highly resistant and transmissible strain), although it does not share its level of pathogenicity.[11] Hyaluronidase assays, carried out by J. Bean within the group, have indicated the HLase negative nature of ST239µ2, of which the data can be found in the SI (SI-Figure 6). Interestingly, TW20 is HLase positive.

The two vesicle types were treated in a similar way to the δ-toxin experiment in the preliminary investigation. Supernatant (SN) from the two bacterial strains was incubated with

the vesicles, either immediately, or following addition of HLase, and the fluorescence response was measured, shown in Figure 7-8.

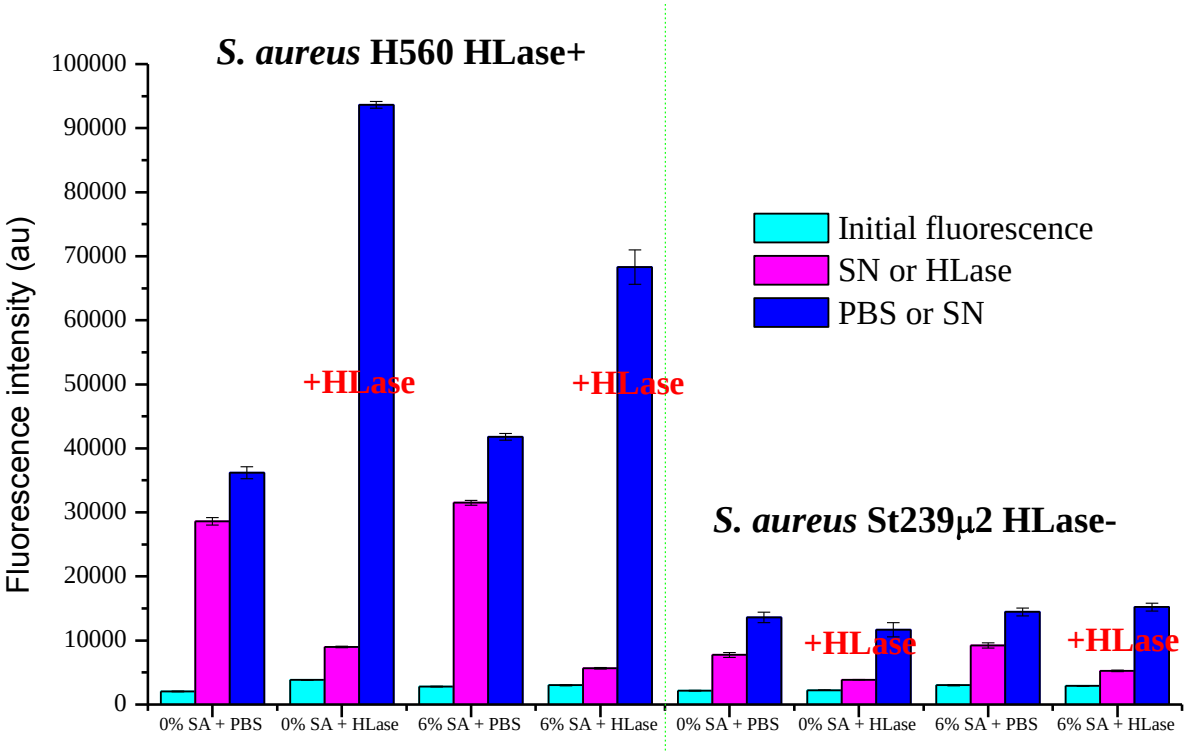

Figure 7-8. The addition of HLase positive (H560) and HLase negative (ST239µ2) bacterial SN to HA-coated vesicles, with additional HLase added to each vesicle type.

Results from Figure 7-8 illustrate that the HLase positive strain MSSA H560 is able to diffuse its lytic peptides successfully through the degraded HA capsule, indicated by increased fluorescence intensity, without the addition of added HLase. However, following addition of extra HLase the fluorescence intensity is amplified, indicating an increasing ease of diffusion of the *S.aureus* lytic peptides through the degraded capsule.

There is a reported, suspected link between HLase production and amplified toxicity of the bacterial strain,[4] and this is of particular relevance here, where the pathogenic nature of ST239µ2 was shown to be not as effective as H560. It would be desirable to have a HLase negative strain of bacteria with an increased pathogenicity; however assays within the group have not yet elucidated any.

7.2 Vesicle modifications – conclusions

The creation of HA-coated vesicles which are responsive to both HLase producing bacteria and HLase with δ-toxin was achieved. The incorporation of the 5(6)-CF dye into the vesicles ensured that response measurements, based on capsule and vesicle susceptibility to HLase and bacterial toxins, could be made.

The use of specific binding through the incorporation of SA into the vesicle bilayer may help to improve the quantity of HA coupled to the vesicle, as suggested by DLS measurements, which could be beneficial at a skin interface. However, the non-specifically bound HA, presumably conjugated to the quaternary amine of DSPE, provided an alternative coated vesicle system. This system had an increased capacity for susceptibility to HA capsule degradation with smaller quantities of HLase and therefore lysis from related bacterial lytic peptides was more easily achieved.

Further work into the relevance and applicability of this system could be achieved following incorporation of different concentrations of SA into the bilayer; affecting the extent of bonding that can occur between the vesicles and the HA. This could affect the degradation ability of bacterial HLase and toxins through the coating and the bilayer, effectively increasing or decreasing the measured response. In addition to this, other hyaluronidase positive and negative bacterial strains could be investigated to increase the scope of this system. The stability profile of the vesicles, with different concentrations of SA incorporated, both free of- and attached to- HA could be measured using the protocol developed for the stability response parameter, introduced in chapter 3. The results from this would give a good indication of the possible protective role of a HA coating on vesicles.

The development of vesicles conjugated to intelligent coatings capable of providing both protective and functional properties, achieved through HA-coupling within this investigation, could provide an ideal pathway to vesicle systems which are selectively active and responsive.

7.3 References

1. Maeda, H.; Sawa, T.; Konno, T. Mechanism of tumor-targeted delivery of macromolecular drugs, including the EPR effect in solid tumor and clinical overview of the prototype polymeric drug SMANCS. *J Control Release* **2001,** 74, 1-3, 47-61.

2. Karanth, H.; Murthy, R. S. pH-sensitive liposomes--principle and application in cancer therapy. *J Pharm Pharmacol* **2007,** 59, 4, 469-83.
3. Laurent, T. C. L., Ulla BG Fraser, J Robert E. The structure and function of hyaluronan: An overview. *Immunol. Cell Biol.* **1996,** 74, 2, A1-A7.
4. Hynes, W. L.; Walton, S. L. Hyaluronidases of Gram-positive bacteria. *FEMS Microbiology Letters* **2000,** 183, 2, 201-207.
5. Patterson, J.; Siew, R.; Herring, S. W.; Lin, A. S. P.; Guldberg, R.; Stayton, P. S. Hyaluronic acid hydrogels with controlled degradation properties for oriented bone regeneration. *Biomaterials* **2010,** 31, 26, 6772-6781.
6. Park, Y. D.; Tirelli, N.; Hubbell, J. A. Photopolymerized hyaluronic acid-based hydrogels and interpenetrating networks. *Biomaterials* **2003,** 24, 6, 893-900.
7. Pavesio, A.; Renier, D.; Cassinelli, C.; Morra, M. Anti-adhesive surfaces through hyaluronan coatings. *Medical device technology* **1997,** 8, 7, 20-27.
8. Liu, L. S.; Thompson, A. Y.; Heidaran, M. A.; Poser, J. W.; Spiro, R. C. An osteoconductive collagen/hyaluronate matrix for bone regeneration. *Biomaterials* **1999,** 20, 12, 1097-108.
9. de Keyzer, Y. L. F.; Vaudry, C. J. S. R. P.; JM, H. K.; JP, L.; Bastard, C.; Dacher, J.; Eurin, D. L. P.; JL, F. M. D.-R.; Tonon, M. A. L. C.; Flaman, J. Evidence of involvement of CD44 in endothelial cell proliferation, migration and angiogenesis in vitro. *International journal of cancer* **1996,** 66, 5, 664-8.
10. Verdon, J.; Girardin, N.; Lacombe, C.; Berjeaud, J. M.; Hechard, Y. delta-hemolysin, an update on a membrane-interacting peptide. *Peptides* **2009,** 30, 4, 817-23.
11. Holden, M. T.; Lindsay, J. A.; Corton, C.; Quail, M. A.; Cockfield, J. D.; Pathak, S.; Batra, R.; Parkhill, J.; Bentley, S. D.; Edgeworth, J. D. Genome sequence of a recently emerged, highly transmissible, multi-antibiotic- and antiseptic-resistant variant of methicillin-resistant Staphylococcus aureus, sequence type 239 (TW). *J Bacteriol* **2010,** 192, 3, 888-92.

Chapter 8 Microplasma jet treatment of vesicles

8.1 Plasma healthcare applications

Plasma has been used as a germicide for sterilisation of medical equipment,[1] industrial food packaging,[2] and biomaterial devices such as implants.[3] Advantages of plasma processing over alternative treatments include speed and cleanliness of treatment, depending on the gas chosen, environmental safety and relatively uniform process results.[4, 5] Different plasma techniques include sputtering and etching, implantation, deposition and spraying.[6]

Plasma surface modification (PSM) is often utilised for the etching, cross-linking and activation of surfaces, especially polymers. The gas composition and plasma conditions, ions, electrons, fast neutrals and radicals must be altered according to surface type to minimise degradation and aging effects.[7] Importantly with PSM treatment, the bulk properties of the material remain unaltered, while surface properties such as wettability, adhesion,[8] biocompatibility[9] and topography[10] may be manipulated to suit the application.

Early medical related reports indicate that the use of plasma at wound interfaces can have positive medical applications. This is a result of the bactericidal and fungicidal effects resulting from the reactive species, charging reactions, ultraviolet radiation (UVR), optical and infrared emissions, and heat.[11] The use of high temperature plasma to sterilise medical equipment in the removal and destruction, cutting and cauterizing of tissue and for cosmetic tissue restructuring is fairly well established.[12]

Atmospheric plasma in treatment at wound interfaces has the potential to have an *in vitro* bactericidal effect on pathogenic bacteria.[13] The sterilisation technique allows rapid non-contact decontamination, with the potential for targeted application possible within small pores and microscopic openings.[14]

8.1.1 Plasma – a brief history

Naturally occurring plasma state material predates the beginning of research into this field. The majority of the universe is in the plasma state - solids, liquids and gases are restricted to isolated regions. Plasma is now recognised as the key element to understanding the formation of magnetic fields in planets, stars and galaxies as well as other cosmic phenomena.[15] Commonly recognised and observable examples include stellar galaxies, nebulae, cosmic

rays, the sun, the ionosphere and aurora in the upper atmosphere, and lightning and corona discharges in the lower atmosphere.[16]

The beginning of the field of *plasma* science is often attributed to the Nobel laureate Irving Langmuir who, in 1929,[17] coined the term 'plasma' to denote the ionised gas containing equal densities of electrons and protons, known as quasineutrality, in the comparatively field-free region between the sheaths in an arc discharge tube. Active research into electrical discharges had been carried out by prominent physicists including J. J. Thomson, J. S. Townsend and W. Crookes in the preceding fifty years.

Recent advances since the 1960's and commercialisation of research relating to plasma physics have resulted in modifications of surfaces in biological, automotive, aerospace, packaging and electronics industries. Cost effective modifications of surfaces, including cleaning, ablation, cross-linking and chemical modification,[5] can be achieved at exposure times of less than one second.[18]

8.1.2 The 4th state of matter

Plasma is known as the fourth state of matter, (depicted in Figure 8-1) and is generally defined as being a partially or fully ionised gaseous species of high energy that makes up over 99 % of the universe. A distinction can be made between the strength of bonds that hold their constituent particles together. The state of the substance depends on an equilibrium between the random kinetic energy (thermal energy) of the substances' atoms or molecules, and the interparticle binding forces. Increasing the energy within a solid or liquid substance leads to a phase transition, when the binding potential within a substance is overcome. The transition from a gas to a plasma is not a thermodynamic phase transition, as it occurs from interactions with an external magnetic or electric field of external or self-induced origin.[16] It can also occur following a gradual increase of the substances' temperature; an atomic gas is formed as a result of particle collisions, with an increasing fraction of the atoms possessing sufficient kinetic energy to overcome the binding energy of the outermost orbital electrons, resulting in an ionised gas or plasma.[19]

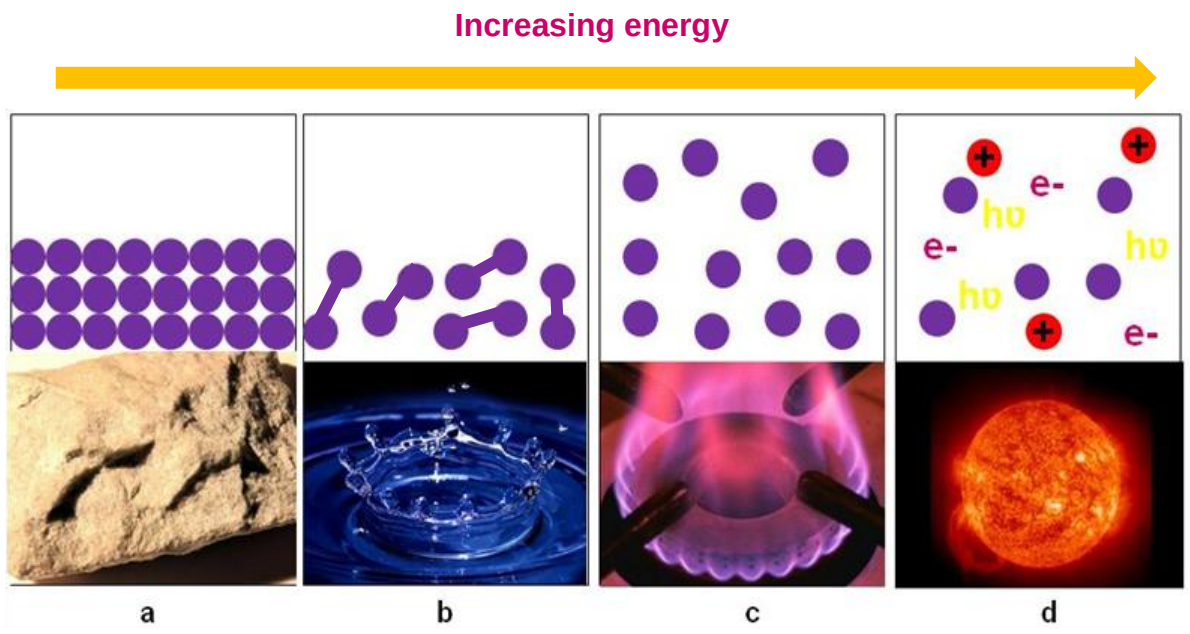

Figure 8-1. The fourth state of matter: Plasma. The addition of energy ensures progression from a) the solid state, where molecules are tightly bonded together, to b) the liquid state, where molecules have restricted movement, to c) the gas state, where molecules are unbounded and free to move, and finally to d) the plasma state, where some ionisation occurs and quasineutrality is achieved.

Plasma is comprised of photons, positive and negative ions, atoms, free radicals and excited and non-excited molecules. These can all potentially exert an influence on their surroundings. The extent of this influence, in addition to the mode of action of the plasma, can depend upon the plasma gas and on the doses and fluxes of plasma-activated species, as well as the configuration of the plasma device and the microstructure of the plasma. Secondary effects, such as etching/ablation, dehydration, temperature increases, pH changes, electrical currents and generation of activated species downstream of the plasma in the surrounding air and biological environment, are also likely to be important.

8.1.3 Plasma medicine

The non-thermal nature, selective targeting properties of plasma jets, coupled with non-destructive characteristic claims on biological material,[20, 21] has led to a potential paradigm shift in treatment therapies. Extensive research into the use of plasma jets for treatment of chronic skin wounds,[13, 22] dentistry applications,[23] and for antibacterial activity[24, 25] has been

carried out. In addition to this, blood coagulation is routinely carried out using thermal plasma and high temperatures.[26]

Mapping of the cellular response to plasma jets has limited reporting in the literature. Until recently, more effort has been dedicated to studying the effect of non-equilibrium plasma on prokaryotic cells; however structural differences between complex eukaryotes and prokaryotes indicate that the response would differ substantially.[27] Preliminary mammalian cell work has been carried out investigating conditions of jet use that result in necrosis (cell death due to catastrophic injury), or apoptosis (an internal process of cell self-destruction). A power of 50 mW for one second was found to be favourable for avoiding apoptosis, with cell detachment still observable.[20, 28] Cell detachment, reattachment and surface functionalization of human hepatocytes (HEPG2) has also been shown with a miniature atmospheric-pressure glow discharge plasma torch.[29]

Work completed by Ermolaeva *et al.* discusses the use of a rat model with a superficial slash wound infected with *P.aeruginosa* and *S.aureus*. Initial results suggested increased wound closure, and the elimination of *P.aeruginosa*, however *S.aureus* was still present in the plasma treated model, and wound healing eventually slowed to less than the control (18 days compared to 15 days).[25] These results suggest selective antimicrobial properties of plasma treatment, but indicate a potential negative effect on the surrounding wound environment.

The risks associated with the use of plasma in medicine for direct treatment often relate to the plasma temperature, power transfer from the plasma, UVR, radicals, generation of toxic gases[30] and electromagnetic fields which could induce electrolysis in the tissue or stimulation of nerve or muscle cells.[31]

8.1.4 Atmospheric plasma

Atmospheric gaseous plasma has shown potential as a promising emerging technology in healthcare applications.[32, 33] Cold atmospheric plasmas have temperatures of approximately 300K (room temperature), and are classified as either direct, indirect or hybrid (barrier corona discharge) systems. Direct plasma systems utilise the material that is being treated (sample surface or tissue) as one of the plasma electrodes, ensuring the flow of UVR, charged and uncharged particles, and the current, through the desired treatment medium.[32] Indirect plasma systems use two separate electrodes and a carrier gas to ensure effective delivery of active agents to the material that is being treated.[11, 34] Hybrid plasmas use a grounded wire mesh

electrode with a lower electrical resistance than the material that is being treated, allowing the current to pass through the mesh.[13]

The link between prevalence of bacteria colonisation in a wound and subsequent rate of that wound healing[35] has indicated the necessity for a treatment that can kill bacteria non-specifically without damaging surrounding eukaryotic tissue. In 2005, the Max Plank Institute for Extra-terrestrial Physics, Germany, introduced the MicroPlaSter (ADTEC Plasma Technology Co. Ltd.); a plasma source capable of providing contact-free and painless sterilisation of wounds. This source reportedly ensures homogenous delivery of the active particles using argon gas, from a distance of about 20 mm, with a treatment area of approximately 5 cm in diameter. In 2010, Isbary *et al.* reported a prospective phase II *in vivo* clinical trial investigating the effect of regular MicroPlaSter cold plasma treatment on bacterial load in 36 patients with chronic skin ulcers, with a decrease in bacterial count being measured.[13]

Additionally, there is evidence from cell culture studies that treatment with plasma could encourage rate of cell growth.[36] In one such study, an application of 30 s or 4 J cm^{-2} of plasma treatment increased the rate of proliferation of endothelial cells by double in comparison to un-treated cultures (five days post treatment). This proliferation is accredited to the plasma-initiated release of reactive oxygen species mediated fibroblast growth factor-2 (FGF2), which, along with other signals, activate invasion of local cells into surrounding tissue to form new blood vessels (angiogenesis).[37] Although longer exposure times (>60 s or 8 J cm^{-2}) were found to provide a lethal dose resulting in cell death.[38]

8.1.5 Microplasma jet

The term microplasma describes a special class of electrical geometries where at least one dimension is in the sub-millimetre length scale.[39] Microplasma jets are uniquely characterised by atmospheric / high pressure stability,[40] non equilibrium thermodynamics,[41, 42] non-Maxwellian electron energy distribution functions (EEDFs)[43], high electron densities[42] and versatility of use. Microplasma jets have the potential to provide a safe plasma source, being non-thermal, ignitable at atmospheric pressure, and without any electrical and chemical risks, for biomedical applications.[44]

8.2 Proposal: a synthetic biological sensor

A synthetic biological sensor, containing vesicles, can be developed to monitor the interaction of plasma with soft, hydrated biological material. Incorporation of vesicles, containing the self-quenched dye 5(6)-carboxyfluorescein, (as discussed in Chapter 3 - Vesicle development - stability), into a hydrated proteinaceous environment comprising 5 % (w/v) gelatin, can be used to map any plasma induced damaging effects through vesicle destruction. Gelatin was introduced in Chapter 5 (for favourable properties see Table 5-1), and showed favourable vesicle stabilising potential for delivery of the vesicles in topical form to a wound.

The depth of plasma penetration into the sensor matrix can be measured, and the angle of treatment investigated, to monitor if these factors significantly influence the nature and level of damage. This can be achieved through observation of the release of the quenched fluorescent dye from within the vesicles and subsequent un-quenching.

This sensor model can potentially be used to unravel the roles of different plasma species and the direct effect of whole plasma contact, from those of primary and secondary species. Primary effects involve those emanating directly from the plasma and secondary effects involve those species created in the 'target' tissue. This type of insight could be useful in the future development of safe and effective plasma medical technologies.

8.3 Plasma jet treatment of the synthetic sensor

8.3.1 Plasma jet parameters

An initial range finding experiment was carried out to ensure that the plasma jet made visible contact with a synthetic sensor sample mounted on a silica sheet. A range of helium gas flow rates (0.05-1 $Lmin^{-1}$), voltages (3.5-6 kV) and distances from the sample (1-7 mm) were investigated. The minimum distance and helium flow rate required for contact at each voltage is shown in Figure 8-2.

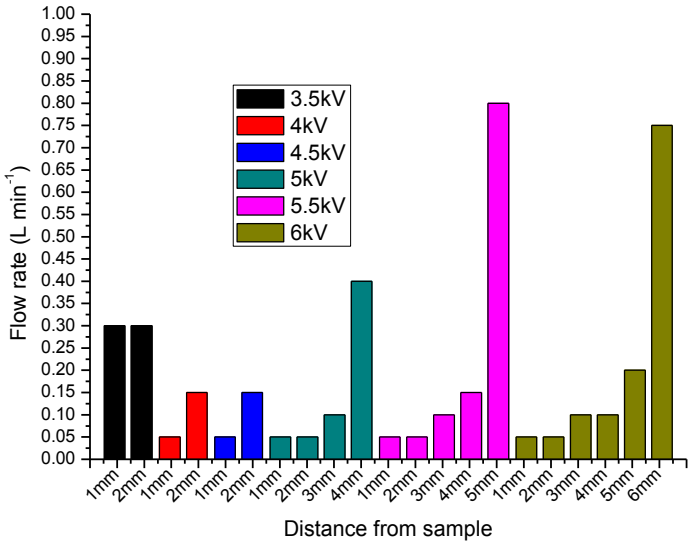

Figure 8-2. Plasma jet contact with vesicles on a silica backed sample with a range of helium gas flow rates, voltages and distances from the sample. The minimum distance and flow rate required for visible contact to be observed at different voltages is shown; distances where no contact is made have been omitted. A frequency of 10 KHz was maintained for each condition.

From the initial results, a voltage of 5.5 kV and a relatively low flow rate of 0.1 $Lmin^{-1}$ were selected for continued experiments. A low flow rate was desirable to prevent dehydration of the vesicles (which resulted in osmotic induced lysis). Further operational parameters were investigated for the interaction of the micro plasma jet with the synthetic biological sensor, namely treatment time, distance (*d*) and treatment angle.

8.3.2 Sensitivity of the biological synthetic sensor

Vesicle lysis can be artificially induced through physical (e.g. dehydration), thermal or chemical agents (e.g. surfactants), or through biological agents (e.g. pathogens, bacterial toxins or enzyme digestion).[45] This known sensitivity of vesicles was investigated using the synthetic biological sensor. This allowed a comparison to be made between the lytic effects of the surfactant triton (a chemical agent introduced in 3.3.5 Vesicle membrane solubilisation – a positive lytic control), the supernatant of *S.aureus* RN4282 and phospholipase A2 (biological agents introduced in 4.2.1.2 The relevance of MSSA RN4282 and 4.3 Bacterial toxin interactions with membranes, respectively) and following treatment with the plasma jet at a *d* of 3 mm for 300 s (physical). As discussed previously MSSA RN4282 is a naturally

occurring strain of *S.aureus* that produces and secretes small amounts of exoproteins but elevated quantities of toxic shock syndrome toxin (TSST).[46] Phospholipase A2 is an enzyme that catalyses the hydrolysis at the *sn*-2 position of membrane phospholipids, resulting in the liberation of arachidonic acid (AA)[47] and the consequential destabilisation of cells / vesicles (see Figure 4-1).

The synthetic biological sensor was added (100 µl) to a 96 well plate followed by either treatment with the plasma jet at a *d* of 3 mm for 300 s or incubated with 50 µl of the lytic reagents at 37 °C for 2 h. Fluorescence intensity measurements were obtained using a Fluostar Omega microplate reader (λ_{ext} = 485 ± 12 nm and λ_{em} = 520 nm).

A similar level of damage was measured following plasma jet treatment when compared to the natural (biological) and synthetic (chemical) cytolytic agents, Figure 8-3, indicating a similar level of rupture of vesicles.

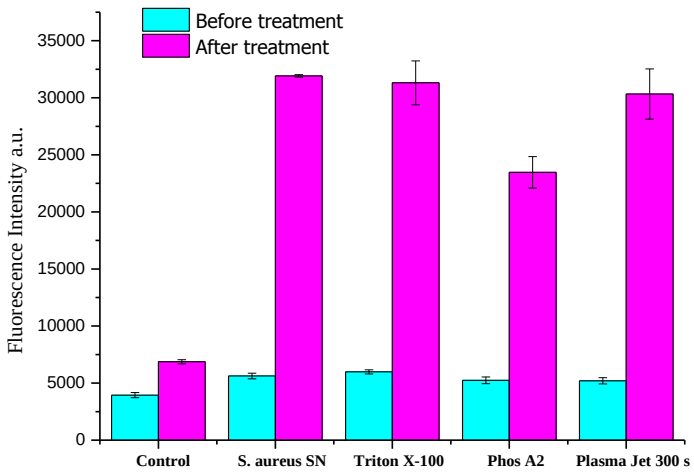

Figure 8-3. The comparative fluorescence of the sensor after 2 h of incubation with a control (HEPES buffer), *S.aureus* RN4282 supernatant (SN), Triton X-100, Phospholipase A2 (Phos A2) and after treatment with the plasma jet (perpendicular to the sample surface) at a *d* of 3 mm for 300 s was measured.

The data from Figure 8-3 indicates that the plasma jet can potentially induce a similar level of damage in vesicles compared to natural and synthetic cytolytic reagents.

8.3.3 Treatment and analysis of the synthetic biological sensor

The synthetic biological sensor was treated for three different amounts of time (15, 60 and 300 s) and at two separation distances between the end of the glass capillary tube and the surface of the sensor (2 and 3 mm). Treatment times of 15, 60 and 300 s were used as a proof of principle study range representative of an 'appropriate' range of times to potentially guarantee observation of the regimes of interest. Comparative treatments were carried out using neutral helium gas (i.e. no plasma was generated) directed onto the sensor using the same parameters. Further controlled comparative treatments were also carried out using plasma directed onto a gelatin matrix containing non-encapsulated (5(6)-CF.

8.3.3.1 Brightfield and fluorescence Microscopy

Brightfield and fluorescence microscopy was utilised to visualise and analyse the effects following treatment of the synthetic sensor with plasma and neutral helium, and compare the results were compared to a plasma treated control. The resultant images following perpendicular treatment of the synthetic biological sensor at a *d* of 3 mm for 15, 60 and 300 s with plasma is given in Figure 8-4.

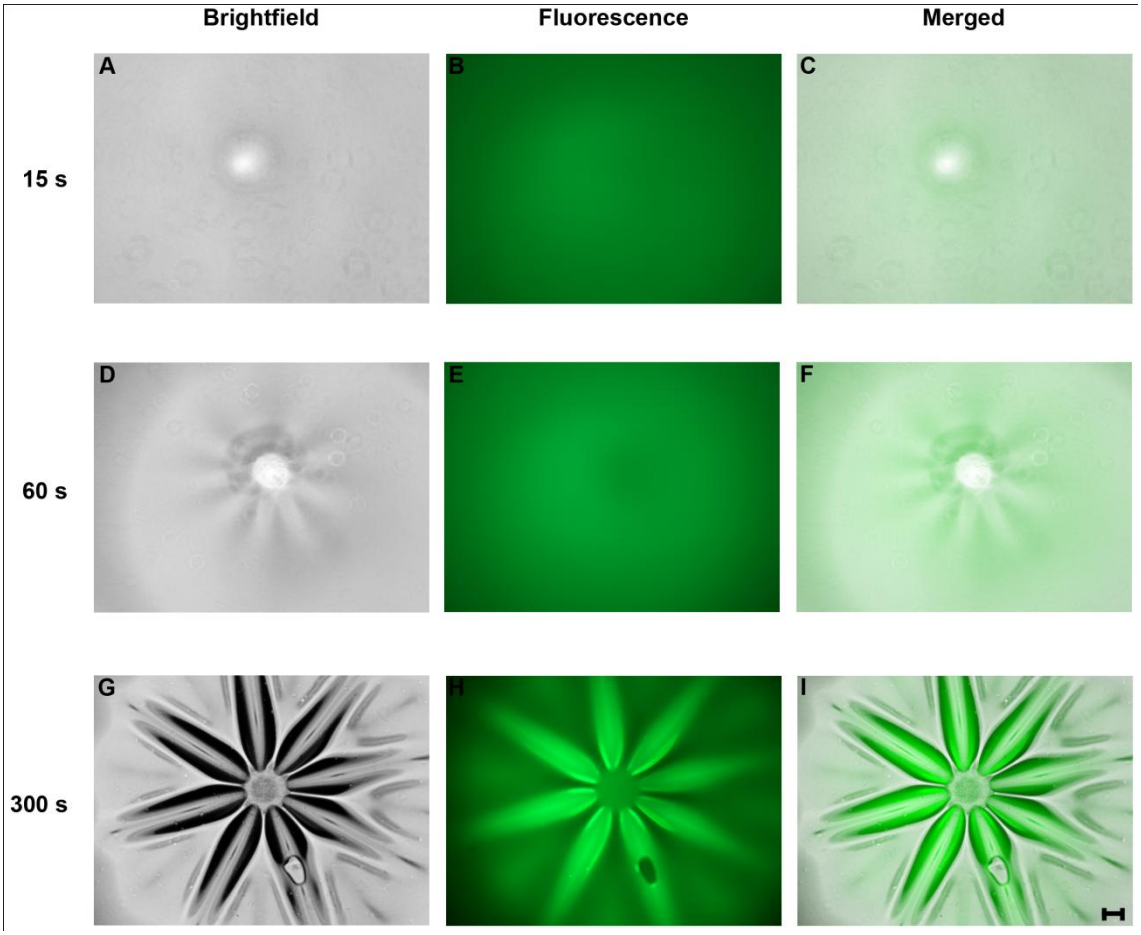

Figure 8-4. Perpendicular treatment of synthetic sensor with the plasma jet for 15 (A-C), 60 (D-F) and 300 (G-I) s at a *d* of 3 mm. The figure shows brightfield (A, D and G), fluorescence (B, E and H) and combined (merged) brightfield and fluorescence (C, F and I) images. Scale bar = 200 µm.

The plasma jet can be observed to be puncturing a hole through the gelatin after 15 s of treatment and longer treatment times. A star-shaped pattern of microchannels formed within the gelatin matrix after a plasma jet treatment time of 300 s (brightfield images) and a higher level of fluorescence indicated an increased level of vesicle damage within these microchannels.

The resultant images following perpendicular treatment of the synthetic biological sensor at a *d* of 3 mm for 15, 60 and 300 s with neutral helium is given in Figure 8-5.

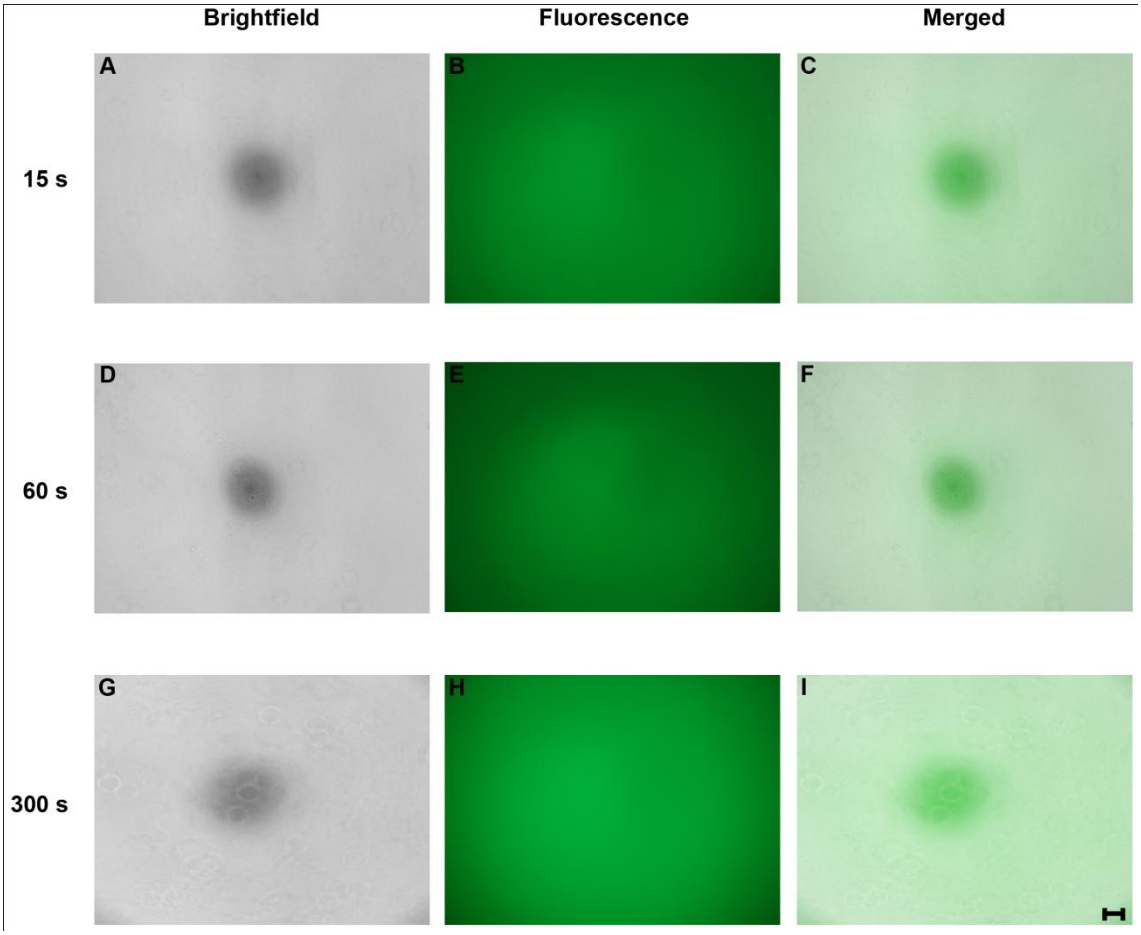

Figure 8-5**.** Perpendicular treatment of synthetic sensor with the neutral gas flow only (i.e. no plasma) for 15 (A-C), 60 (D-F) and 300 (G-I) s at a *d* of 3 mm. The figure shows brightfield (A, D and G), fluorescence (B, E and H) and combined (merged) brightfield and fluorescence (C, F and I) images. Scale bar = 200 µm.

Images A, D and G in Figure 8-5 display a central dark circular region for each of the treatment times, indicating damage to the synthetic tissue directly in the line of sight of the helium gas flow from the capillary tube. However, no significant increase in the fluorescence of the 5(6)-CF at the damaged area of the gelatin was measured (B, E and H).

The plasma jet had a very different effect on the synthetic biological sensor when compared to the effect of the neutral gas treatment. A hole in the gelatin matrix region (upon the area directly exposed to the plasma jet), was observed after 15 s of plasma treatment (see Figure 8-4, A), indicating a greater depth of damage in comparison to the neutral gas. After treatment for 60 s, a star shaped pattern of microchannels was observed, developing within the sensor matrix and radiating from the centre of the treatment area (D, F). This pattern becomes larger and more distinct after 300 s of treatment (G, H, I). A marked increase or pattern of fluorescence, matching the star-shape obtained for 60 s, was not observed for

treatment times of 15 and 60 s (B, C, E and F), however an increased fluorescence following the same star pattern etching into the damaged gelatin was detected (H, I).

To confirm that the increased fluorescence signal observed in the synthetic biological sensor was the result of plasma jet damage to the vesicles, the effect of plasma treatment on the gelatin matrix prepared with the 5(6)-CF dye suspended freely within it (i.e. no vesicles) was measured, given in Figure 8-6.

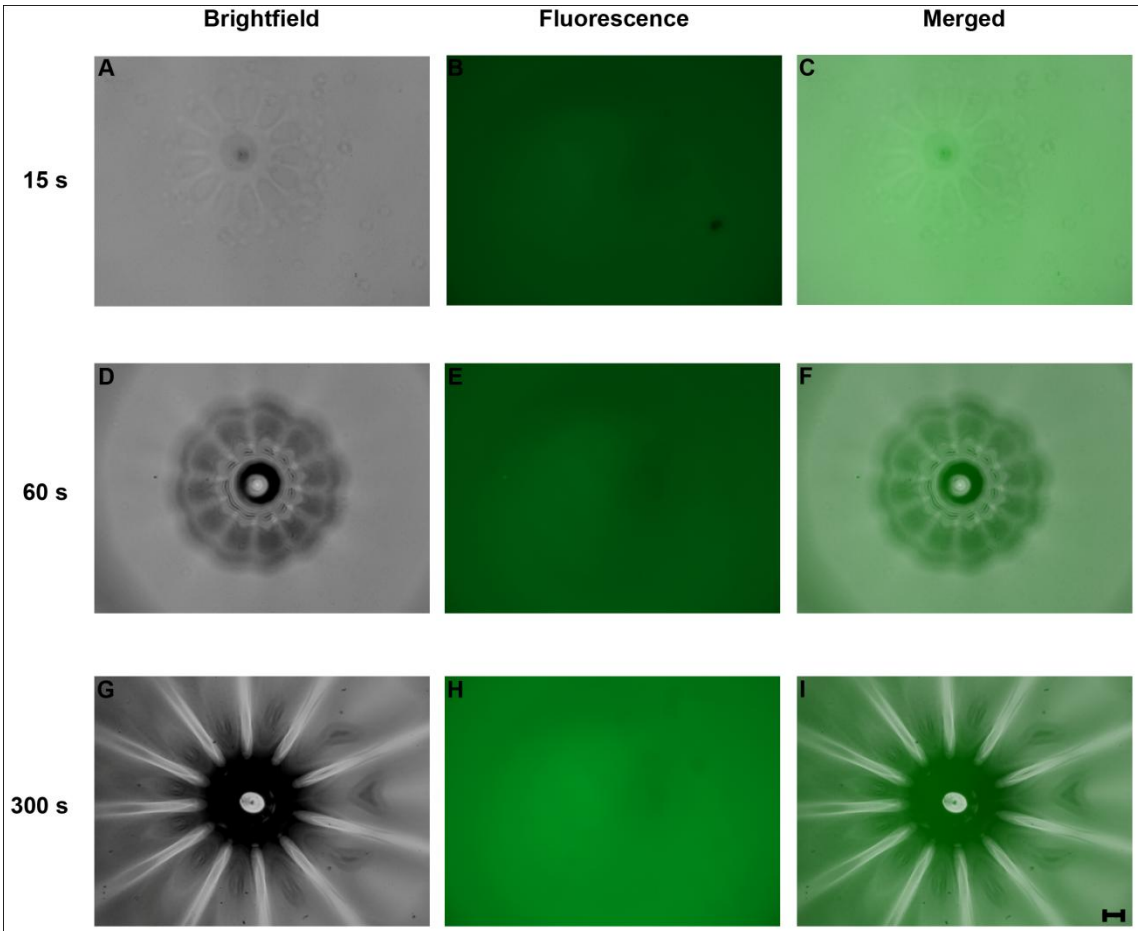

Figure 8-6. Perpendicular plasma jet treatment of the gelatin matrix prepared with 5(6)-CF freely suspended within the matrix, without the presence of vesicles. Treatment was carried out for 15 (A-C), 60 (D-F) and 300 (G-I) s at a d of 3 mm. The figure shows brightfield (A, D and G), fluorescence (B, E and H) and combined (merged) brightfield and fluorescence (C, F and I) images. Scale bar = 200 µm

The same pattern of microchannels formed (A, D, F, G, I - Figure 8-6), however the fluorescent signal from the gelatin-5(6)-CF matrix did not appear to change. This confirms that the change in the fluorescence signal within the biological sensor was caused by vesicle rupture, resulting from direct or indirect plasma damage.

8.3.3.2 Fluorescent intensity profiles

The fluorescence intensity profile of the treatment area of the synthetic sensor was measured and used to quantify the level of vesicle damage caused by the neutral gas and the plasma jet. This was achieved using fluorescence intensity values from 60 data points by measuring 20 different positions at a distance of 45 µm across the center of each treatment area, results shown in Figure 8-7. To enable a direct comparison between each image, all of the images were taken using the same camera exposure times (48 ms) and gain settings.

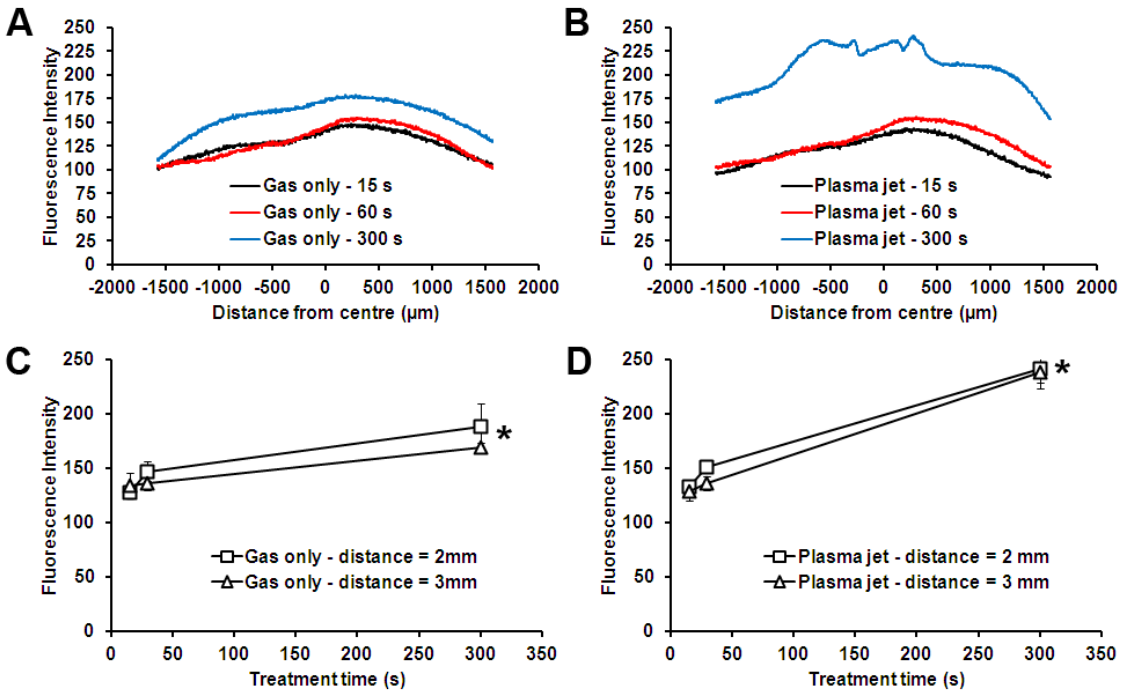

Figure 8-7. Analysis of 5(6)-CF fluorescence intensity profiles of the synthetic tissue after perpendicular treatment with the neutral gas (A and C) and plasma jet (B and D). Graphs A and B show representative fluorescence profiles of the treatment area after treatment for different times at a fixed *d* of 3 mm. Graphs C and D show the fluorescence intensity values measured at the centre of the treatment area after different treatment times at a *d* of 2 and 3 mm. *Plasma jet treatments carried out for 300 s were statistically significantly different to the 300 s gas only treatments ($p < 0.0001$ for both treatment distances).

Results from Figure 8-7 indicate that a treatment time of 300 s with the neutral gas or plasma jet resulted in an enhancement of fluorescence from the synthetic tissue. This indicates that both processes damage the vesicles, although plasma jet treatment for 300 s resulted in a

significantly higher level of damage to the vesicles compared to the other treatment conditions.

The 5(6)-CF fluorescence intensity profiles of the synthetic tissue after neutral gas and plasma jet treatment show a higher fluorescence signal level in the centre of the treatment area (Figure 8-7, A and B). An increase in treatment time increased the fluorescence response signal for both the neutral gas and plasma jet treatment (C and D). This indicates a higher level of vesicle damage at the centre of the treatment area directly exposed to the gas flow and plasma jet, and that the level of sensor damage is directly related to treatment time. A higher level of 5(6)-CF fluorescence within the gelatin matrix was detected after plasma jet treatment for 300 s, which was statistically higher than the neutral gas treatment at the same time point. Based on this specific configuration a conclusion can be drawn that a plasma jet exposure time of 300 s was required to induce a significant level of sensor damage. This conclusion was consistent for treatment distances of both 2 and 3 mm.

8.3.3.3 Confocal microscopy

Confocal microscopy was used to analyse the depth of damage to the vesicles within the synthetic biological sensor following plasma jet treatment, shown in Figure 8-8. In corroboration with the fluorescence images and data obtained, the level and depth of damage to the vesicles, and hence the fluorescence intensity, appeared to increase with longer plasma jet exposure times (A-C).

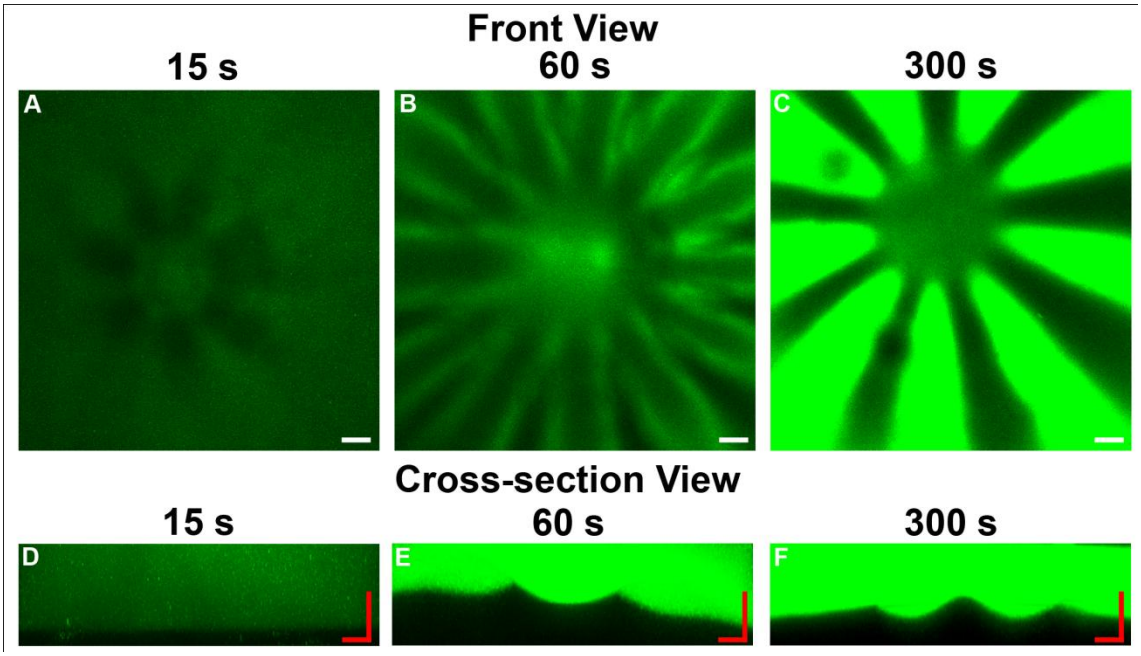

Figure 8-8. Confocal microscopy images of the synthetic tissue after perpendicular plasma jet treatment for 15 (A and D), 60 (B and E) and 300 (C and F) s at a *d* of 3 mm. The vesicles were damaged at a depth greater than 150 µm below the surface of the gelatin matrix. Horizontal and vertical scale bars = 100 µm.

At each treatment time, the distribution of the damaged vesicles could be monitored due to the high sensitivity of the confocal microscope. Analysis utilising Z-stacking measurements to form vertically stacked cross-sectional images for each treatment time allowed the depth of plasma treatment damage to be determined. For each of the treatment times the vesicles within the gelatin matrix were damaged by the plasma jet at a depth of over 150 µm (D – F).

8.3.4 Parallel plasma jet treatment

Comparative treatment of the synthetic biological sensor with the plasma jet was carried out in parallel to the surface (i.e. 180°), at a separation distance of 3 mm. This treatment enabled the plasma plume to flow across the surface of the sensor rather than direct, head on contact. This angle appeared to significantly reduce the level of damage to both the vesicles and gelatin. Damage caused by the plasma jet was only detected after 300 s of treatment, shown in Figure 8-9. The neutral gas did not damage the synthetic sensor at all following this treatment time.

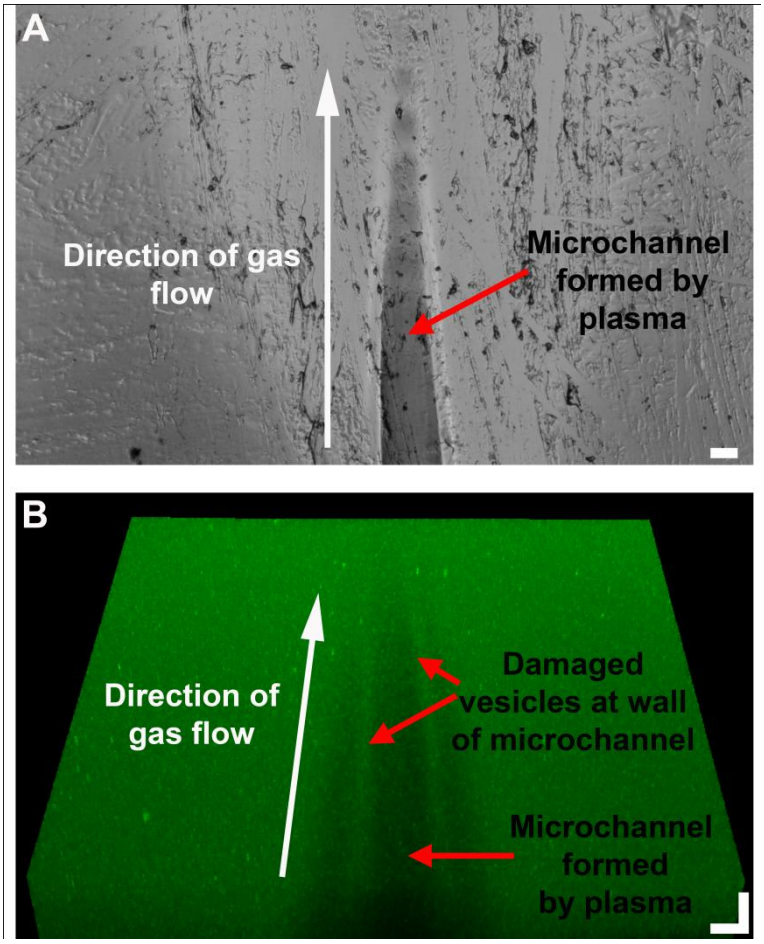

Figure 8-9. Parallel treatment of the synthetic sensor with the plasma jet where A) shows a brightfield micrograph of the plasma jet treated synthetic tissue and B) shows the corresponding confocal microscope image. Treatment was carried out at a *d* of 3 mm for 300 s. Horizontal and vertical scale bars = 100 µm.

At an angle of 180° to the sensor, the plasma jet etched a single microchannel into the gelatin matrix and damaged the vesicles only at the walls of the channel. This microchannel can be seen to taper to a fine point following the path of the gas flow and the corresponding confocal microscope image indicates only minimal damage to the vesicles at the walls of the microchannel.

8.3.5 Plasma jet treatment through a vesicle suspension

In addition to the synthetic biological sensor, comparative treatment of vesicles in a suspension with a plasma jet bubbled through was investigated. The vesicle suspension solution, HEPES buffer, was significantly less viscous than gelatin, allowing an easy flow of plasma through the sample. The sensitivity of this system to external agents ensured that any

fluorescence resulting from vesicle rupture and release of the fluorophore into the suspension was detectable. No significant damage was caused to the vesicles by either the gas flow or plasma jet, shown in Figure 8-10.

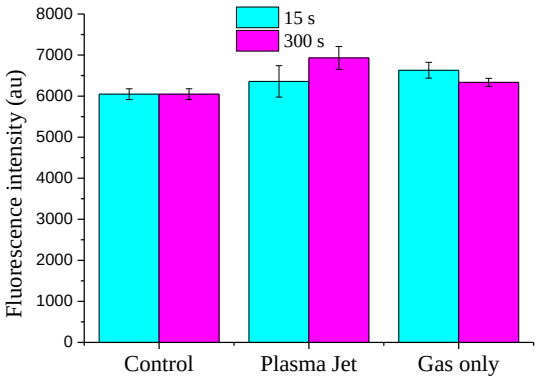

Figure 8-10**.** Plasma jet treatment of a suspension of vesicles.

This application of plasma through the vesicle suspension and lack of significant damage indicates that the HEPES buffer may shield the vesicles from the plasma jet and any primary or generated reactive species or collisional movement of free moving particles may diffuse the potential damaging agents, at the doses investigated in this study. Work carried out with help from N. T. Thet.

8.4 Microplasma jet treatment of vesicles - conclusions

The effect of plasma jet on the synthetic biological sensor synthesised has enabled controlled analysis of the degree of rupture of vesicles under different conditions (time, distance and angle), allowing conclusions with regard to the plasma jet mode of action to be drawn. The damage caused by the comparative neutral gas treatment colliding with the sample resulted in a movement of the gelatin matrix creating a hole of ~0.2 mm^2 (smaller than the capillary tube internal diameter of 0.8 mm^2). The damage caused by the plasma jet was significantly greater, with movement of the gelatin matrix up to an area of 7.5 mm^2.

The differences between the damage measured allow conclusions to be drawn about the interactions occurring at the sensor. Upon head-on contact of the neutral gas with the gelatin matrix, the sample, at point of contact and in surrounding areas for longer treatment times, is most likely partially dehydrated as the helium gas flow penetrates the sample. Additionally, some physical movement of the soft gelatin tissue away from the path of the gas flow is observed. The plasma jet induced damage is more complex, with the creation of star shaped

microchannels radiating out from the centre of the treatment area. Speculation with regard to what is occurring can be made based on pertaining literature relating to plasma jets. The plasma jet contains charged (active) species within a succession of hypersonic propagating bullets, with velocities of 7-100 km s^{-1},[48] much faster than the neutral gas velocities (~10 ms^{-1}). The helium gas can penetrate through the surface of the sensor and ensure conduction of the active plasma bullets into the matrix.[49] The presence of mutually repulsive ion charges carried within the helium stream causes the cylindrically symmetric plasma streams to split into an integer number of channels. The plasma bullets continue to carry the gas through the sample as a result of ion momentum transfer to the neutral gas, forming equally spaced radial spokes.[50, 51] The reactive species propagated into the sample with the neutral gas are then able to damage the vesicles within the formed micro channels. The number of microchannels formed can vary, and this can be accredited to subtle differences within the matrix environment (e.g. gelatin composition).

The formation of microchannels allows for the penetration of the reactive oxygen and nitrogen (RONS) into the sample, achieving a depth of damage / treatment of > 150 μm. Importantly the rigidity of the treated material is known to have a strong effect on the depth of penetration. This microchannel formation effect was not observed after similar plasma jet treatments of a rigid organic polymer (treated areas are circular),[52] indicating that different plasma jet components are involved.

A lower level of vesicle damage was induced by the neutral gas compared to the plasma jet, and this decreased amount of vesicle damage is expected as rupture was only achieved through dehydration or pressure.[53] Damage caused to the sample as a direct result of plasma treatment can include etching,[54] chemical attack (such as lipid peroxidation from plasma-produced hydroxyl radicals),[29, 33] electrostatic charging,[55] or cleavage of the chemical bonds by activated plasma species.[56]

The directional nature of plasma jets has proven to play an important role in the depth and quantity of vesicle damage within the sample, as proven by the microstructures formed within the gelatin when applied head-on or in parallel to the sample. The reactive species (RONS) can be considered to react laterally across surfaces, in particular rigid surfaces, resulting in larger treatment areas than the capillary jet delivery tube.[52] In corroboration with these findings, Leduc *et al.* demonstrate that the plasma treatment of biological cells is highly directional; with their data showing that the plasma components responsible for cell permeabilisation are limited to points where the plasma comes into contact with the cells.[57]

Within the scope of this investigation, it was considered that the directional nature of the plasma jet was responsible for the micro structural changes within the sample. This was particularly relevant with regard to formation of RONS, due to the short effective activity distances. RONS can be considered secondary plasma species, i.e. not directly created within the plasma, and based on existing literature, their mode of action on bilayer vesicle rupture could be from the initiation of lipid peroxidation leading to chemically induced vesicle rupture and the consequent release of the fluorescent dye.[14, 29, 57]

A study by Lademann *et al.* showed that the stratum corneum can be permeabilised by plasma treatment to increase the depth of penetration of a topically applied model drug, in the form of a fluorescent dye, through the skin barrier.[58] This effect was speculated to be due to plasma damage of the lipid bilayers, and correlates with the results obtained within this investigation; providing further proof that the microstructural changes observed could prove an ideal pathway for the penetration of topical agents.

The directional nature of the plasma can be further highlighted following treatment in parallel with the surface of a sample. Damage from the plasma can only occur from propagated bullets directly along the surface, creating a single micro channel with reduced vesicle damage. This observation can be explained by a lower concentration of excited species impacting on the sensor.

The complexity of natural tissue raises questions about the validity of the relatively simple synthetic sensor utilised in this study. However, at a basic level the membrane of the vesicles emulates the membrane surrounding eukaryotic cells with the collagen derived gelatin acting as the extracellular matrix.

8.4.1 Soft tissue plasma treatment

The results obtained within this investigation, whilst only preliminary, could provide important information on ideal operating parameters of plasma sources on soft tissue treatment applications. For example, a homogenous plasma treatment area could be achieved using an array of plasma jets[51] or by raster scanning the plasma source across the tissue.[59] In addition to this, further attention may be given to the effects of potentially damaging plasma components, e.g. radicals and RONS,[60] and the negative health effects on the patient following their diffusion and migration into the body.

A major advantage of the synthetic biological sensor is the lack of variation between samples commonly seen in cell and tissue-based assays. The low level of protein content (5 % (w/v)) and a potentially increased fragility and sensitivity of the 'cells' may allow detection of effects more readily. However, the proof-of-principle sensor established for this investigation could potentially have a level of sophistication and increased biological relevance built in; for example by increasing the protein concentration to allow a closer resemblance to a tissue-system. Comparable studies reporting treatment of proteins and organic polymers suggest the primary response would be ablation, surface oxidation and cross-linking,[61] hence an increased protein sensor system would be predicted to be less sensitive - making subsurface effects more difficult to measure.

Additional sophistication to the synthetic sensor could be made by the introduction of RNA and DNA, proteins, enzymes or cells, alteration to the gelatin matrix rigidity and engineering of the vesicle through modification of their sensitivity to external agents or addition of fluorescently tagged lipids or nanocrystal markers (quantum dots).[62]

8.5 References

1. Awakowicz, H. H. a. N. B. a. J. W. a. P. A double inductively coupled plasma for sterilization of medical devices. *Journal of Physics D: Applied Physics* **2007,** 40, 14, 4145; Laroussi, M. Sterilization of contaminated matter with an atmospheric pressure plasma. *Plasma Science, IEEE Transactions on* **1996,** 24, 3, 1188-1191.
2. Schneider, J.; Baumgärtner, K. M.; Feichtinger, J.; Krüger, J.; Muranyi, P.; Schulz, A.; Walker, M.; Wunderlich, J.; Schumacher, U. Investigation of the practicability of low-pressure microwave plasmas in the sterilisation of food packaging materials at industrial level. *Surface and Coatings Technology* **2005,** 200, 1–4, 962-966.
3. Awakowicz, T. G. a. M. O. a. D. O. C. a. V. A. K. a. U. C. a. T. S.-S. a. H. H. a. P. Characterization of stationary and pulsed inductively coupled RF discharges for plasma sterilization. *Plasma Physics and Controlled Fusion* **2005,** 47, 5A, A353.
4. Barton, D.; Bradley, J. W.; Steele, D. A.; Short, R. D. Investigating Radio Frequency Plasmas Used for the Modification of Polymer Surfaces. *The Journal of Physical Chemistry B* **1999,** 103, 21, 4423-4430.
5. Liston, E. M.; Martinu, L.; Wertheimer, M. R. Plasma surface modification of polymers for improved adhesion: a critical review. *Journal of Adhesion Science and Technology* **1993,** 7, 10, 1091-1127.
6. Chu, P. K.; Chen, J. Y.; Wang, L. P.; Huang, N. Plasma-surface modification of biomaterials. *Materials Science and Engineering: R: Reports* **2002,** 36, 5–6, 143-206.
7. Hegemann, D.; Brunner, H.; Oehr, C. Plasma treatment of polymers for surface and adhesion improvement. *Nuclear Instruments and Methods in Physics Research Section B: Beam Interactions with Materials and Atoms* **2003,** 208, 281-286.
8. Westerdahl, C. A. L.; Hall, J. R.; Schramm, E. C.; Levi, D. W. Gas plasma effects on polymer surfaces. *Journal of Colloid and Interface Science* **1974,** 47, 3, 610-620; Gerenser,

L. J. An x-ray photoemission spectroscopy study of chemical interactions at silver/plasma modified polyethylene interfaces: Correlations with adhesion. *Journal of Vacuum Science & Technology A: Vacuum, Surfaces, and Films* **1988,** 6, 5, 2897-2903; Sapieha, S.; Cerny, J.; Klemberg-sapieha, J. E.; Martinu, L. Corona Versus Low Pressure Plasma Treatment: Effect on Surface Properties and Adhesion of Polymers. *The Journal of Adhesion* **1993,** 42, 1-2, 91-102.

9. Lee, H. B.; Kim, S. S.; Khang, G. *The Biomedical Engineering Handbook*. Second Edition ed.; CRC Press and IEEE Press: Taylor and Francis Group, **1995**; p 1656.

10. Ryan, M. E.; Badyal, J. P. S. Surface Texturing of PTFE Film Using Nonequilibrium Plasmas. *Macromolecules* **1995,** 28, 5, 1377-1382; D. Beake, B.; S. G. Ling, J.; J. Leggett, G. Correlation of friction, adhesion, wettability and surface chemistry after argon plasma treatment of poly(ethylene terephthalate). *Journal of Materials Chemistry* **1998,** 8, 12, 2845-2854.

11. Shimizu, T.; Steffes, B.; Pompl, R.; Jamitzky, F.; Bunk, W.; Ramrath, K.; Georgi, M.; Stolz, W.; Schmidt, H.-U.; Urayama, T.; Fujii, S.; Morfill, G. E. Characterization of Microwave Plasma Torch for Decontamination. *Plasma Processes and Polymers* **2008,** 5, 6, 577-582.

12. Bogle Ma, A. K. A. D. J. S. EValuation of plasma skin regeneration technology in low-energy full-facial rejuvenation. *Archives of Dermatology* **2007,** 143, 2, 168-174; Elsaie, M. L.; Kammer, J. N. Evaluation of plasma skin regeneration technology for cutaneous remodeling. *Journal of Cosmetic Dermatology* **2008,** 7, 4, 309-311; Kilmer, S.; Semchyshyn, N.; Shah, G.; Fitzpatrick, R. A pilot study on the use of a plasma skin regeneration device (Portrait PSR3) in. *Lasers Med Sci* **2007,** 22, 2, 101-9.

13. Isbary, G.; Morfill, G.; Schmidt, H. U.; Georgi, M.; Ramrath, K.; Heinlin, J.; Karrer, S.; Landthaler, M.; Shimizu, T.; Steffes, B.; Bunk, W.; Monetti, R.; Zimmermann, J. L.; Pompl, R.; Stolz, W. A first prospective randomized controlled trial to decrease bacterial load using cold atmospheric argon plasma on chronic wounds in patients. *British Journal of Dermatology* **2010,** 163, 1, 78-82.

14. Zimmermann, M. G. K. a. G. K. a. G. M. a. T. N. a. T. S. a. J. v. D. a. J. L. Plasma medicine: an introductory review. *New Journal of Physics* **2009,** 11, 11, 115012.

15. Peratt, A. L. *Physics of the Plasma Universe*. Springer-Verlag Berlin Heidelberg New York: **1992**; p 372.

16. Watson, C. J. H. Introduction to Plasma Physics. In *Plasma Physics*, Keen, B. E., Ed. The Institute of Physics, 47 Belgrave Square, LondonTechno House, Redcliffe Way, Bristol **1974**; p 1-21.

17. Langmuir, I. The Interaction of Electron and Positive Ion Space Charges in Cathode Sheaths. *Physical Review* **1929,** 33, 6, 954-989.

18. Strobel, M.; Lyons, C. S.; Mittal, K. L. *Plasma Surface Modification of Polymers: Relevance to Adhesion*. VSP BV: The Netherlands, **1994**.

19. Bittencourt, J. A. *Fundamentals of Plasma Physics*. 3rd ed.; Springer Verlag New York, Inc: **2004**.

20. Kroesen, E. S. a. A. J. F. a. W. W. S. a. G. M. W. Plasma needle: a non-destructive atmospheric plasma source for fine surface treatment of (bio)materials. *Plasma Sources Science and Technology* **2002,** 11, 4, 383.

21. Sladek, E. S. a. I. E. K. a. R. E. J. Superficial treatment of mammalian cells using plasma needle. *Journal of Physics D: Applied Physics* **2003,** 36, 23, 2908; Shashurin, A.; Keidar, M.; Bronnikov, S.; Jurjus, R. A.; Stepp, M. A. Living tissue under treatment of cold plasma atmospheric jet. *Applied Physics Letters* **2008,** 93, 18, 181501-3.

22. Lademann, J.; Richter, H.; Alborova, A.; Humme, D.; Patzelt, A.; Kramer, A.; Weltmann, K.-D.; Hartmann, B.; Ottomann, C.; Fluhr, J. W.; Hinz, P.; Hubner, G.;

Lademann, O. Risk assessment of the application of a plasma jet in dermatology. *Journal of Biomedical Optics* **2009,** 14, 5, 054025-6.
23. Rupf, S.; Lehmann, A.; Hannig, M.; Schäfer, B.; Schubert, A.; Feldmann, U.; Schindler, A. Killing of adherent oral microbes by a non-thermal atmospheric plasma jet. *Journal of Medical Microbiology* **2010,** 59, 2, 206-212; Lee, H. W.; Kim, G. J.; Kim, J. M.; Park, J. K.; Lee, J. K.; Kim, G. C. Tooth Bleaching with Nonthermal Atmospheric Pressure Plasma. *Journal of Endodontics* **2009,** 35, 4, 587-591.
24. Daeschlein, G.; von Woedtke, T.; Kindel, E.; Brandenburg, R.; Weltmann, K.-D.; Jünger, M. Antibacterial Activity of an Atmospheric Pressure Plasma Jet Against Relevant Wound Pathogens in vitro on a Simulated Wound Environment. *Plasma Processes and Polymers* **2010,** 7, 3-4, 224-230.
25. Ermolaeva, S. A.; Varfolomeev, A. F.; Chernukha, M. Y.; Yurov, D. S.; Vasiliev, M. M.; Kaminskaya, A. A.; Moisenovich, M. M.; Romanova, J. M.; Murashev, A. N.; Selezneva, I. I.; Shimizu, T.; Sysolyatina, E. V.; Shaginyan, I. A.; Petrov, O. F.; Mayevsky, E. I.; Fortov, V. E.; Morfill, G. E.; Naroditsky, B. S.; Gintsburg, A. L. Bactericidal effects of non-thermal argon plasma in vitro, in biofilms and in the animal model of infected wounds. *Journal of Medical Microbiology* **2011,** 60, 1, 75-83.
26. Kalghatgi, S. U.; Fridman, G.; Cooper, M.; Nagaraj, G.; Peddinghaus, M.; Balasubramanian, M.; Vasilets, V. N.; Gutsol, A. F.; Fridman, A.; Friedman, G. Mechanism of Blood Coagulation by Nonthermal Atmospheric Pressure Dielectric Barrier Discharge Plasma. *Plasma Science, IEEE Transactions on* **2007,** 35, 5, 1559-1566.
27. Laroussi, M. Low-Temperature Plasmas for Medicine? *Plasma Science, IEEE Transactions on* **2009,** 37, 6, 714-725.
28. Kieft, I. E.; Darios, D.; Roks, A. J. M.; Stoffels, E. Plasma treatment of mammalian vascular cells: a quantitative description. *Plasma Science, IEEE Transactions on* **2005,** 33, 2, 771-775.
29. Yonson, S.; Coulombe, S.; Leveille, V.; Leask, R. L. Cell treatment and surface functionalization using a miniature atmospheric pressure glow discharge plasma torch. *Journal of Physics D-Applied Physics* **2006,** 39, 16, 3508-3513.
30. Weltmann, K. D.; Kindel, E.; Brandenburg, R.; Meyer, C.; Bussiahn, R.; Wilke, C.; von Woedtke, T. Atmospheric Pressure Plasma Jet for Medical Therapy: Plasma Parameters and Risk Estimation. *Contributions to Plasma Physics* **2009,** 49, 9, 631-640.
31. Zenker, M. Argon Plasma Coagulation. **2008**; Vol. 3.
32. Fridman, G.; Friedman, G.; Gutsol, A.; Shekhter, A. B.; Vasilets, V. N.; Fridman, A. Applied Plasma Medicine. *Plasma Processes and Polymers* **2008,** 5, 6, 503-533.
33. Zimmermann, G. E. M. a. M. G. K. a. J. L. Focus on Plasma Medicine. *New Journal of Physics* **2009,** 11, 11, 115011.
34. Stoffels, R. E. J. S. a. E. Deactivation of Escherichia coli by the plasma needle. *Journal of Physics D: Applied Physics* **2005,** 38, 11, 1716.
35. Robson, M. C.; Heggers, J. P. Delayed wound closures based on bacterial counts. *Journal of Surgical Oncology* **1970,** 2, 4, 379-383.
36. Tipa, R. S.; Stoffels, E. Effects of Plasma Treatment on Wounds. In *13th International Conference on Biomedical Engineering*, Lim, C.; Goh, J. H., Eds. Springer Berlin Heidelberg: **2009**; 23, 1385-1388.
37. Nugent, M. A.; Iozzo, R. V. Fibroblast growth factor-2. *The International Journal of Biochemistry & Cell Biology* **2000,** 32, 2, 115-120.
38. Kalghatgi, S.; Friedman, G.; Fridman, A.; Clyne, A. Endothelial Cell Proliferation is Enhanced by Low Dose Non-Thermal Plasma Through Fibroblast Growth Factor-2 Release. *Annals of Biomedical Engineering* **2010,** 38, 3, 748-757.

39. Sankaran, D. M. a. R. M. Microplasmas for nanomaterials synthesis. *Journal of Physics D: Applied Physics* **2010,** 43, 32, 323001.
40. Chen, J. G. E. a. S.-J. P. a. N. P. O. a. K.-F. Recent advances in microcavity plasma devices and arrays: a versatile photonic platform. *Journal of Physics D: Applied Physics* **2005,** 38, 11, 1644.
41. Kurunczi, P.; Abramzon, N.; Figus, M.; Becke, K. Measurement of rotational temperatures in high pressure microhollow cathode (MHC) and capillary plasma electrode (CPE) discharges. *acta physica slovacca* **2004,** 54, 2, 115-124.
42. Schmidt-Böcking, C. P. a. M. M. a. A. B.-D. a. O. H. a. S. S. a. T. J. a. K. N. a. H. Characterization of a high-pressure microdischarge using diode laser atomic absorption spectroscopy. *Plasma Sources Science and Technology* **2002,** 11, 4, 476.
43. Iza, F.; Lee, J. K.; Kong, M. G. Electron Kinetics in Radio-Frequency Atmospheric-Pressure Microplasmas. *Physical Review Letters* **2007,** 99, 7, 075004.
44. Hong, Y. C.; Uhm, H. S. Microplasma jet at atmospheric pressure. *Applied Physics Letters* **2006,** 89, 22, 221504-3.
45. Thet, N. T.; Hong, S. H.; Marshall, S.; Laabei, M.; Toby, A.; Jenkins, A. Visible, colorimetric dissemination between pathogenic strains of Staphylococcus aureus and Pseudomonas aeruginosa using fluorescent dye containing lipid vesicles. *Biosens Bioelectron* **2013,** 41, 538-43; Zhou, J.; Loftus, A. L.; Mulley, G.; Jenkins, A. T. A. A Thin Film Detection/Response System for Pathogenic Bacteria. *Journal of the American Chemical Society* **2010,** 132, 18, 6566-6570; Bhakdi, S.; Weller, U.; Walev, I.; Martin, E.; Jonas, D.; Palmer, M. A guide to the use of pore-forming toxins for controlled permeabilization of cell membranes. *Med Microbiol Immunol* **1993,** 182, 4, 167-75; Williams, T. L.; Johnson, B. R.; Urbanc, B.; Jenkins, A. T.; Connell, S. D.; Serpell, L. C. Abeta42 oligomers, but not fibrils, simultaneously bind to and cause damage to ganglioside-containing lipid membranes. *Biochem J* **2011,** 439, 1, 67-77.
46. Vojtov, N.; Ross, H. F.; Novick, R. P. Global repression of exotoxin synthesis by staphylococcal superantigens. *Proceedings of the National Academy of Sciences* **2002,** *99* (15), 10102-10107; Subedi, A.; Ubeda, C.; Adhikari, R. P.; Penadés, J. R.; Novick, R. P. Sequence analysis reveals genetic exchanges and intraspecific spread of SaPI2, a pathogenicity island involved in menstrual toxic shock. *Microbiology* **2007,** 153, 10, 3235-3245.
47. Kudo, I.; Murakami, M. Phospholipase A2 enzymes. *Prostaglandins & Other Lipid Mediators* **2002,** 68–69, 3-58.
48. Laroussi, M.; Hynes, W.; Akan, T.; Xinpei, L.; Tendero, C. The Plasma Pencil: A Source of Hypersonic Cold Plasma Bullets for Biomedical Applications. *Plasma Science, IEEE Transactions on* **2008,** 36, 4, 1298-1299; Shi, J.; Zhong, F.; Zhang, J.; Liu, D. W.; Kong, M. G. A hypersonic plasma bullet train traveling in an atmospheric dielectric-barrier discharge jet. *Physics of Plasmas* **2008,** 15, 1, 013504-5.
49. Bradley, J.-S. O. a. Y. A.-G. a. J. W. Time-resolved mass spectroscopic studies of an atmospheric-pressure helium microplasma jet. *Journal of Physics D: Applied Physics* **2011,** 44, 36, 365202.
50. Bradley, J.-S. O. a. O. T. O. a. C. H. a. R. M. a. K. K. a. J. W. Imaging gas and plasma interactions in the surface-chemical modification of polymers using micro-plasma jets. *Journal of Physics D: Applied Physics* **2011,** 44, 15, 155206.
51. Kong, Z. C. a. Q. N. a. D. L. B. a. J. L. W. a. C. S. R. a. D. Z. W. a. M. G. Spatially extended atmospheric plasma arrays. *Plasma Sources Science and Technology* **2010,** 19, 2, 025003.

52. Szili, E. J.; Al-Bataineh, S. A.; Bryant, P. M.; Short, R. D.; Bradley, J. W.; Steele, D. A. Controlling the Spatial Distribution of Polymer Surface Treatment Using Atmospheric-Pressure Microplasma Jets. *Plasma Processes and Polymers* **2011,** 8, 1, 38-50.
53. Mardones, G.; González, A. Selective plasma membrane permeabilization by freeze-thawing and immunofluorescence epitope access to determine the topology of intracellular membrane proteins. *Journal of Immunological Methods* **2003,** 275, 1–2, 169-177; Chouinard-Pelletier, G.; Leduc, M.; Guay, D.; Coulombe, S.; Leask, R.; Jones, E. A. Use of inert gas jets to measure the forces required for mechanical gene transfection. *BioMedical Engineering OnLine* **2012,** 11, 1, 67.
54. Wells, R. K.; Badyal, J. P. S.; Drummond, I. W.; Robinson, K. S.; Street, F. J. A comparison of plasma-oxidized and photo-oxidized polystyrene surfaces. *Polymer* **1993,** 34, 17, 3611-3613.
55. Laroussi, M. Low Temperature Plasma-Based Sterilization: Overview and State-of-the-Art. *Plasma Processes and Polymers* **2005,** 2, 5, 391-400.
56. Bryant, P. M.; Szili, E. J.; Whittle, T.; Park, S.-J.; Eden, J. G.; Al-Bataineh, S.; Steele, D. A.; Short, R. D.; Bradley, J. W. The use of a micro-cavity discharge array at atmospheric pressure to investigate the spatial modification of polymer surfaces. *Surface and Coatings Technology* **2010,** 204, 14, 2279-2288.
57. Coulombe, M. L. a. D. G. a. R. L. L. a. S. Cell permeabilization using a non-thermal plasma. *New Journal of Physics* **2009,** 11, 11, 115021.
58. Lademann, O.; Richter, H.; Meinke, M. C.; Patzelt, A.; Kramer, A.; Hinz, P.; Weltmann, K.-D.; Hartmann, B.; Koch, S. Drug delivery through the skin barrier enhanced by treatment with tissue-tolerable plasma. *Experimental Dermatology* **2011,** 20, 6, 488-490.
59. Tan, H. M. L.; Fukuda, H.; Akagi, T.; Ichiki, T. Surface modification of poly(dimethylsiloxane) for controlling biological cells' adhesion using a scanning radical microjet. *Thin Solid Films* **2007,** 515, 12, 5172-5178.
60. Graves, D. B. The emerging role of reactive oxygen and nitrogen species in redox biology and some implications for plasma applications to medicine and biology. *Journal of Physics D: Applied Physics* **2012,** 45, 26, 263001.
61. Szili, E. J.; Al-Bataineh, S. A.; Ruschitzka, P.; Desmet, G.; Priest, C.; Griesser, H. J.; Voelcker, N. H.; Harding, F. J.; Steele, D. A.; Short, R. D. Microplasma arrays: a new approach for maskless and localized patterning of materials surfaces. *RSC Advances* **2012,** 2, 31, 12007-12010.
62. Sukhanova, A.; Devy, J.; Venteo, L.; Kaplan, H.; Artemyev, M.; Oleinikov, V.; Klinov, D.; Pluot, M.; Cohen, J. H. M.; Nabiev, I. Biocompatible fluorescent nanocrystals for immunolabeling of membrane proteins and cells. *Analytical Biochemistry* **2004,** 324, 1, 60-67.

Chapter 9 Conclusions

This work investigated the stabilisation, modification, delivery and treatment of phospholipid based vesicles for applications in advanced wound management. A primary focus of this was towards engineering a dressing suitable for use on paediatric burn wounds, and development of this product was discussed in chapters three, four, five and six. Chapters seven and eight offer a variation on the advanced wound management theme. Chapter seven introduces a new protective and selectively responsive coating based on coupled hyaluronic acid to the vesicles, suitable for placement in a wound dressing. Finally, chapter eight discussed the utilisation of vesicles as a synthetic sensor / tissue mimic to model any damaging effects of micro plasma jet treatment. Overall conclusions can be drawn based on each chapter of work; and good progression was made towards achieving a dressing suitable for wound management.

Chapter three has presented the development of a range of different stabilised vesicles, with the creation of a library of over 70 different compositions. The encapsulation of a fluorescent self-quenched dye (5(6)-CF) ensured that lysis of bilayer membranes and passive leakage of internal components could be tracked and measured following release and un-quenching. Five potential candidates displayed the desired stability at 37 °C for 14 days, and comparisons between these were made using the stability response parameter. These vesicle formulations were then subjected to further investigations with regard to varying pH values (5, 6, 7 and 8 - representative of a wound environment) and temperature ranges (5 °C, -20 °C, -80 °C and flash freezing – representative of potential storage conditions) for 14 days. Three successful vesicle compositions were then utilised collectively or individually in the work that followed, namely TCDA-DS, DOPC-DS and DSPG-DP.

Chapter four has presented an investigation into the selective sensitivity of the three aforementioned successfully stabilised vesicles to two strains of pathogenic bacteria, *P.aeruginosa* PAO1 and *S.aureus* MSSA476, in comparison to the non-pathogenic strain *E.coli* DH5α. Vesicle lysis and release of the encapsulated dye was desired in the presence of the pathogenic bacterial toxins only, and the extent of this effect varied depending on the vesicle bilayer composition. This was postulated to be due to the interaction and repulsion between localised charge distributions on the vesicle membrane or the availability of phase boundaries within the membrane at 37 °C. In addition to this the effect of burn wound exudate on vesicle stability and sensitivity was measured. Stability results following

incubation are promising against passive diffusion of the encapsulated agents. However, it can be postulated that sequestering of added lytic agents by the wound exudate may be occurring, potentially preventing vesicle lysis from occurring. The three vesicle candidates successfully demonstrated selective sensitivity to the pathogenic bacteria, and good stability in wound exudate, and so were utilised for incorporation into a wound dressing prototype system.

Chapter 5 has presented work on the development of a prototype dressing, based on a topical open hydrogel formulation. This formulation was required to be able to incorporate stable vesicles without increasing passive diffusion of internal agents at 37 °C for 14 days, whilst maintaining the pathogenic bacteria sensitivity profile that is essential for this project. Of the four hydrogels investigated, three have indicated some promising stabilising compatibility with the vesicle candidates and, importantly, have ensured that the required selective sensitivity profile following addition of bacterial toxins is still achieved (gelatin, hypromellose and agarose). The fourth hydrogel (Carbopol 981P NF), proved insufficient at stabilising the vesicle candidates over the desired time period. Further investigations are required to determine whether any of the compatible hydrogels display any probiotic properties. In addition to this development of occlusive systems based on these hydrogel formulations may prove beneficial within a wound environment.[1]

Chapter 6 has presented an introductory investigation into vesicle stability to sterilisation techniques. The emphasis of this investigation was not on the actual sterilising efficiency of the technique employed. Instead the ability of the vesicles to maintain their structure, including continual encapsulation of their internal agents following treatment was of primary concern. Although, each of the sterilisation techniques investigated were carried out to an extent that would have ensured that complete sterilisation of the vesicle solution was achieved (gamma radiation, autoclaving and filter treatment with pores smaller than 0.22 µm). Results indicated that radiation treatment of vesicles using the isotope ^{137}Cs as a gamma source showed excellent potential for ensuring structure of vesicle is maintained without passive diffusion of internal agents. The thermal treatment of vesicles was (unsurprisingly) found to significantly increase the extent of passive leakage of internal agent. This was due to the known increased sensitivity of the vesicle compositions at temperatures above their T_c. The use of filters to achieve sterile vesicles was encouraging; membrane material was found to play a role in the ability of the vesicles to diffuse through the pores.

Chapter 7 has investigated the modification of vesicle structure through conjugation to a HA protective and responsive coating. The HA-coupled vesicles were found to be able to respond to a prototype system using purified δ-toxin and HLase, and the more bio-relevant response was observed following incubation with bacteria supernatant of a HLase producing strain (*S.aureus* MSSA H560) compared to a negative strain (*S.aureus* MRSA ST239µ2). The protective and responsive nature of the HA-coupled vesicles to HLase producing bacteria could provide an innovative method towards achieving protected, stabilised and selectively sensitive vesicles.

Chapter 8 has presented an investigation into the interaction of an atmospheric micro plasma jet with a synthetic biological sensor, composed of phospholipid vesicles in a gelatin matrix. Atmospheric plasma has been extensively researched for treatment of chronic skin wounds,[2] however the mapping and reporting of cellular response to treatment is limited. This study has enabled analysis into the degree of damage caused by the plasma treatment based on a variation of experimental parameters, such as treatment time (15, 60 and 300 s), distance from the jet (2 and 3 mm) and direction of jet (parallel or perpendicular). Following perpendicular treatment, the plasma jet was found to create star shaped microchannels radiating out from the centre of the treatment area, presumably from active species within the plasma, allowing penetration of RONS into the sensor; and this resulted in measurable vesicle damage. The complexity of natural tissue compared to the relatively simple synthetic sensor utilised in this study is important to note. However, at a basic level the membrane of the vesicles emulates the membrane surrounding eukaryotic cells with the collagen derived gelatin acting as the extracellular matrix.

This project has successfully investigated the development of advanced wound management techniques, with the outcomes including a prototype selectively sensitive topical wound dressing, a selectively responsive, protected vesicle coated system, and a synthetic biological sensor suitable for mapping atmospheric plasma damage. Wound management improvements, innovation and new technologies are highly desirable, and the importance of this work ensures that there is scope for continual development in the wound management sector.

9.1 References

1. Petrulyte, S. Advanced textile materials and biopolymers in wound management. *Dan Med Bull*, **2008,** 55, 1, 72-7.
2. Isbary, G.; Morfill, G.; Schmidt, H. U.; Georgi, M.; Ramrath, K.; Heinlin, J.; Karrer, S.; Landthaler, M.; Shimizu, T.; Steffes, B.; Bunk, W.; Monetti, R.; Zimmermann, J. L.; Pompl, R.; Stolz, W. A first prospective randomized controlled trial to decrease bacterial load using cold atmospheric argon plasma on chronic wounds in patients. *British Journal of Dermatology*, **2010,** 163, 1, 78-82.

Appendix 1 – Supporting information

SI-Figure 1. The fluorescence kinetic profiles over 25 hours for the three primary vesicle candidates following incubation with the three standard bacterial species 205
SI-Figure 2. The growth and fluorescence kinetic profiles over 18 hours for three vesicle types with AGR+ and AGR-..... 206
SI-Figure 3. The kinetic growth of AGR+ and AGR- bacteria species 207
SI-Figure 4. The effect of gamma radiation on DPPG-DP vesicles 208
SI-Figure 5. Heat treatment of three vesicle types..... 209
SI-Figure 6. The HLase assay results of the HLase negative strain ST239µ2 210

SI-Table 1. Vesicle compositions synthesised and an indication of their thermal stability .. 204

Vesicle Name	Main lipid constituent	Secondary component	Stabilising agent	Long term stability 14 days / 37 °C
DMPC/DPPE	DMPC 78%	Cholesterol 20% DMPE 2%	None	Poor
TCDA-DM1	DMPC 68%	Cholesterol 20% DMPE 2%	TCDA 10%	Poor
TCDA-DM2	DMPC 63%	Cholesterol 20% DMPE 2%	TCDA 15%	Poor
TCDA-DM3	DMPC 63%	Cholesterol 15% DMPE 2%	TCDA 20%	Poor
TCDA DM4	DMPC 40%	Cholesterol 20% DMPE 2%	TCDA 38%	Poor
TCDA-DM5	DMPC 53%	Cholesterol 20% DMPE 2%	TCDA 25%	Poor
PEG-DM1	DMPC 53%	Cholesterol 20% DMPE 2%	TCDA 15% PEG 1000 10%	Poor
PEG-DM2	DMPC 53%	Cholesterol 20% DMPE 2%	TCDA 25% PEG 1000 5%	Poor
PEG_n-DM3	DMPC 73%	Cholesterol 20% DMPE 2%	PEG_n ($_n$=550,1000, 2000) 5%	Poor
PEG_n-DM4	DMPC 68%	Cholesterol 20% DMPE 2%	PEG_n ($_n$=550,1000, 2000) 10%	Poor
TCDA-DP1	DPPC 63%	Cholesterol 20% DPPE 2%	TCDA 15%	Excellent
TCDA-DP2	DPPC 53%	Cholesterol 20% DPPE 2%	TCDA 25%	Excellent
TCDA-DS1	DSPC 73%	Cholesterol 20% DSPE 2%	TCDA 5%	Good
TCDA-DS2	DSPC 63%	Cholesterol 20% DSPE 2%	TCDA 15%	Good
TCDA-DS3	DSPC 53%	Cholesterol 20% DSPE 2%	TCDA 25%	Excellent
TCDA-DS4	DSPC 58%	Cholesterol 20% DSPE 2%	TCDA 15%	Excellent
TCDA-DS5	DSPC 63%	Cholesterol 25% DSPE 2%	TCDA 10%	Good
TCDA-DH1	DHPC 58%	Cholesterol 25% DHPE 2%	TCDA 15%	Good
TCDA-DH2	DHPC 53%	Cholesterol 20% DHPE 2%	TCDA 25%	Good
DPPC-DS	DSPC 63%	Cholesterol 25% DSPE 2%	DPPC 10%	Good
DOPC-DS1	DSPC 76%	Cholesterol 20% DSPE 2%	DOPC 2%	Excellent
DOPC-DS2	DSPC 74%	Cholesterol 20% DSPE 2%	DOPC 4%	Poor
DOPC-DS3	DSPC 70%	Cholesterol 20% DSPE 2%	DOPC 8%	Poor
DPPG-DP1	DPPC 80%	Cholesterol	DPPG	Good

		10%	10%	
DPPG-DP2	DPPC 55%	Cholesterol 20% DSPC 15%	DPPG 10%	Good
DPPG-DP3	DPPC 68%	Cholesterol 20% DPPE 2%	DPPG 10%	Good
DPPG-DP4	DPPC 53%	Cholesterol 20% DSPC 15%	DPPG 10% DPPE 2%	Excellent
DSPG-DP1	DPPC 53%	Cholesterol 20% DSPC 15%	DSPG 10% DPPE 2%	Excellent
DSPG-DP2	DPPC 55%	Cholesterol 20% DSPC 15%	DSPG 10%	Good
DPPC/DPPE	DPPC 78%	Cholesterol 20% DPPE 2%	None	Good
DSPC-DP1	DPPC 73%	Cholesterol 20% DPPE 2%	DSPC 5%	Good
DSPC-DP2	DPPC 63%	Cholesterol 20% DPPE 2%	DSPC 15%	Good
DSPC-DP3	DPPC 53%	Cholesterol 20% DPPE 2%	DSPC 25%	Good
DHPC/DHPE	DHPC 78%	Cholesterol 20% DHPE 2%	None	Good
DSPC-DH1	DHPC 73%	Cholesterol 20% DHPE 2%	DSPC 5%	Good
DSPC-DH2	DHPC 63%	Cholesterol 20% DHPE 2%	DSPC 15%	Good
DSPC-DH3	DHPC 53%	Cholesterol 20% DHPE 2%	DSPC 25%	Good
DHPC-DS1	DSPC 73%	Cholesterol 20% DSPE 2%	DHPC 5%	Good
DHPC-DS2	DSPC 63%	Cholesterol 25% DSPE 2%	DHPC 10%	Good
DHPC-DS3	DSPC 68%	Cholesterol 20% DSPE 2%	DHPC 10%	Good
DHPC-DS4	DSPC 63%	Cholesterol 20% DSPE 2%	DHPC 15%	Good
DHPC-DS5	DSPC 53%	Cholesterol 20% DSPE 2%	DHPC 25%	Good
DHPC-DS6	DSPC 58%	Cholesterol 25% DSPE 2%	DHPC 15%	Good
DHPC-DS7	DSPC 53%	Cholesterol 25% DSPE 2%	DHPC 20%	Good
DHPC-DS8	DSPC 48%	Cholesterol 25% DSPE 2%	DHPC 25%	Good
DHPC-DS9	DSPC 43%	Cholesterol 25% DSPE 2%	DHPC 30%	Good
DHPC-DS10	DSPC 58%	Cholesterol 30% DSPE 2%	DHPC 10%	Good
DHPC-DS11	DSPC 53%	Cholesterol 35% DSPE 2%	DHPC 10%	Poor
DHPC-DS12	DSPC 48%	Cholesterol 40% DSPE 2%	DHPC 10%	Poor
DHPC-DP1	DPPC 73%	Cholesterol 20% DPPE 2%	DHPC 5%	Good
DHPC-DP2	DPPC 63%	Cholesterol 20%	DHPC 15%	Good

		DPPE 2%		
DHPC-DP3	DPPC 53%	Cholesterol 20% DPPE 2%	DHPC 25%	Good
Chol-DS1	DSPC 63%	DHPC 10% DSPE 2%	Chol 25%	Good
Chol-DS2	DSPC 58%	DHPC 10% DSPE 2%	Chol 30%	Good
Chol-DS3	DSPC 53%	DHPC 10% DSPE 2%	Chol 35%	Good
Chol-DS4	DSPC 48%	DHPC 10% DSPE 2%	Chol 40%	Good
DMDAP-DM1	DMPC 48%	Cholesterol 20% DMPE 2%	TCDA 25% DMDAP 5%	Poor
DMDAP-DM2	DMPC 53%	Cholesterol 20% DMPE 2%	TCDA 20% DMDAP 5%	Poor
DMDAP-DM3	DMPC 43%	Cholesterol 20% DMPE 2%	TCDA 25% DMDAP 10%	Poor
Bio-DM1	DMPC 68%	Cholesterol 30%	DPPE-biotin 2%	Poor
Bio-DM2	DMPC 53%	Cholesterol 20%	TCDA 25% DPPE-biotin 2%	Good
Bio-DP1	DPPC (76%)	Cholesterol 20% DPPE 2%	DPPE-biotin 2%	Good
Bio-DP2	DPPC 79%	Cholesterol 20%	DPPE-biotin 1%	Good
Bio-DP3	DPPC 78%	Cholesterol 20% DPPE 1%	DPPE-biotin 1%	Good
Bio-DP4	DPPC 76%	Cholesterol 20% DPPE 1%	DPPE-biotin 3%	Good
Bio-DP5	DPPC 53%	Cholesterol 20% DPPE 1%	DPPE-biotin 1% DHPC 25%	Good
Bio-DP6	DPPC 51%	Cholesterol 20% DPPE 1%	DPPE-biotin 3% DHPC 25%	Good
Bio-DP7	DPPC 53%	Cholesterol 20% DPPE 1%	DPPE-biotin 1% DSPC 25%	Good
Bio-DP8	DPPC 51%	Cholesterol 20% DPPE 1%	DPPE-biotin 3% DSPC 25%	Good
Bio-DP9	DPPC 54%	Cholesterol 20%	TCDA 25% DPPE-biotin 1%	Good
Bio-DP10	DPPC 53%	Cholesterol 20% DPPE 1%	DPPE-biotin 1% DSPC 25%	Good
Bio-DP11	DPPC 51%	Cholesterol 20% DPPE 2% DSPC 15%	DPPE-biotin 2% DPPG 10%	Good
Bio-DP12	DPPC 76%	Cholesterol 20% DPPE 2%	DPPE-biotin 2%	Good
Bio-DP13	DPPC 61%	Cholesterol 20% DPPE 2%	DPPE-biotin 2% TCDA 15%	Good
Bio-DS1	DSPC 79%	Cholesterol 20%	DPPE-biotin 1%	Good
Bio-DS2	DSPC 71%	Cholesterol 20% DPPE 2%	DPPE-biotin 5% DOPC 2%	Good
DSPC/DSPE	DSPC 78%	Cholesterol 20% DSPE 2%	None	Excellent
DDAB-DP1	DPPC	Cholesterol 20%	DDAB 0.1%	Excellent

	52.9%	DPPE 2%	DPPG 10% DSPC 15%	
DDAB-DP2	DPPC 52.8%	Cholesterol 20% DPPE 2%	DDAB 0.2% DPPG 10% DSPC 15%	Excellent
DDAB-DP3	DPPC 52.7%	Cholesterol 20% DPPE 2%	DDAB 0.3% DPPG 10% DSPC 15%	Excellent
DDAB-DP4	DPPC 52.5%	Cholesterol 20% DPPE 2%	DDAB 0.5% DPPG 10% DSPC 15%	Excellent
SA-DS1	DSPC 62.5%	Cholesterol 20% DSPE 2%	SA 0.5% TCDA 15%	Excellent
SA-DS2	DSPC 62%	Cholesterol 20% DSPE 2%	SA 1% TCDA 15%	Excellent
SA-DS3	DSPC 61%	Cholesterol 20% DSPE 2%	SA 2% TCDA 15%	Excellent
SA-DS4	DSPC 59%	Cholesterol 20% DSPE 2%	SA 4% TCDA 15%	Excellent
SA-DS5	DSPC 57%	Cholesterol 20% DSPE 2%	SA 6% TCDA 15%	Excellent
DDAB/SA-DS1	DSPC 61.9%	Cholesterol 20% DSPE 2%	SA 1% DDAB 0.1% TCDA 15%	Excellent
DDAB/SA-DS2	DSPC 60.9%	Cholesterol 20% DSPE 2%	SA 2% DDAB 0.1% TCDA 15%	Excellent
CoenzymeA-DP1	DPPC 76%	Cholesterol 20% DPPE 2%	Coenzyme A 2%	Good
CoenzymeA-DP2	DPPC 73%	Cholesterol 20% DPPE 2%	Coenzyme A 5%	Good

SI-Table 1. Vesicle compositions synthesised and an indication of their thermal stability at 14 days / 37 °C. The following terms indicate stability according to Equation 3-29 (referenced from thesis): Poor = vesicles form but are very leaky (S = 1) over a period of 14 days, Good = vesicles from and are stable at 4 °C and 37 °C for greater than 1 day (S = 1.50 - 2.50), Excellent = vesicles form and are stable at 4 °C and 37 °C for a period of 14 days (S = 2.51+). Vesicles are named according to their stabilising agent, followed by their primary lipid component.

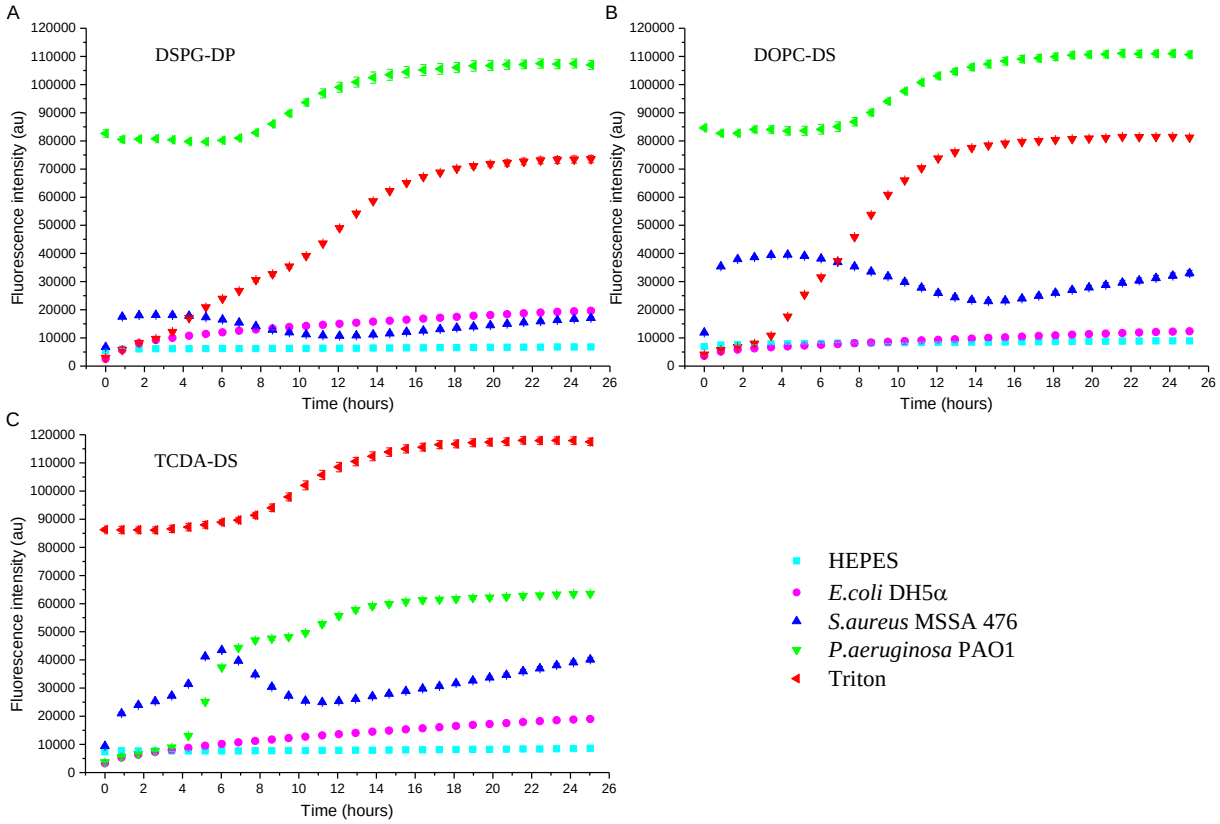

SI-Figure 1. The fluorescence kinetic profiles over 25 hours for the three primary vesicle candidates following incubation with the three standard bacterial species; *E.coli* DH5α (non-pathogenic), *S.aureus* MSSA 476 and *P.aeruginosa* PAO1 (pathogenic), relating to the end point data given in Figure 4-5.

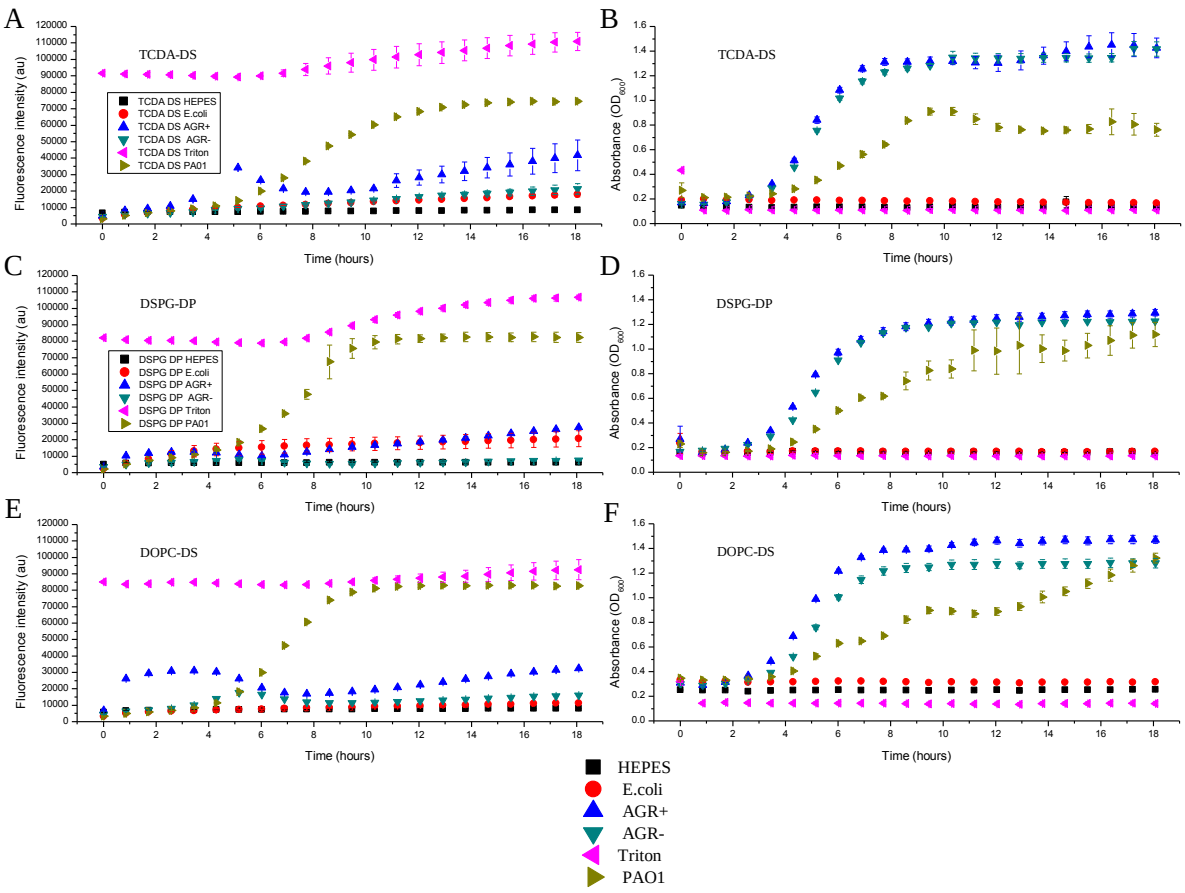

SI-Figure 2. The growth and fluorescence kinetic profiles over 18 hours for three vesicle types with AGR+ and AGR- bacterial species, compared to the standard pathogenic strain *P.aeruginosa* PAO1 and non-pathogenic strain *E.coli* DH5α, relating to the end point data given in Figure 4-7.

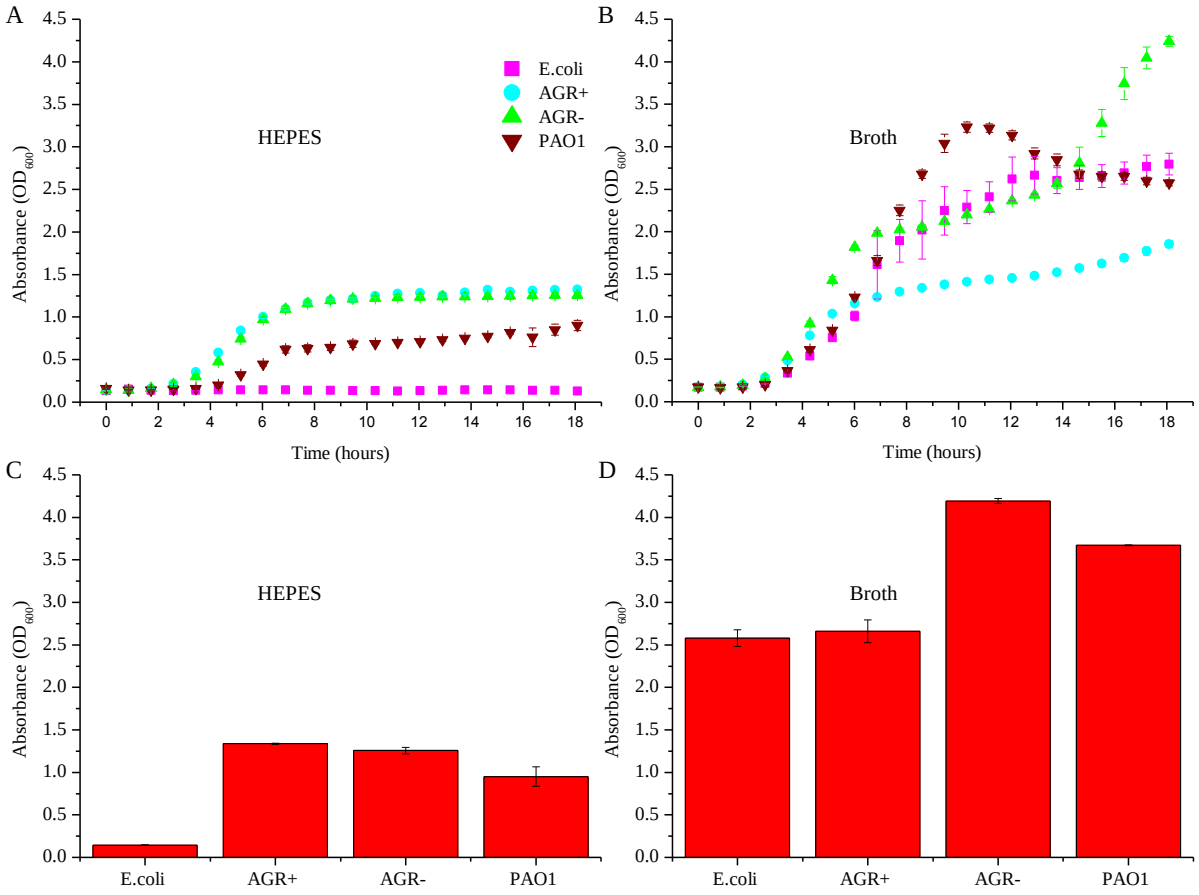

SI-Figure 3. The kinetic growth of AGR+ and AGR- bacteria species in a comparative, non-vesicle containing solution (HEPES) and in ideal nutrient rich conditions (broth), and end growth after 24 hours, compared to the standard pathogenic strain *P.aeruginosa* PAO1 and non-pathogenic strain *E.coli* DH5α, relating to the end point data given in Figure 4-7.

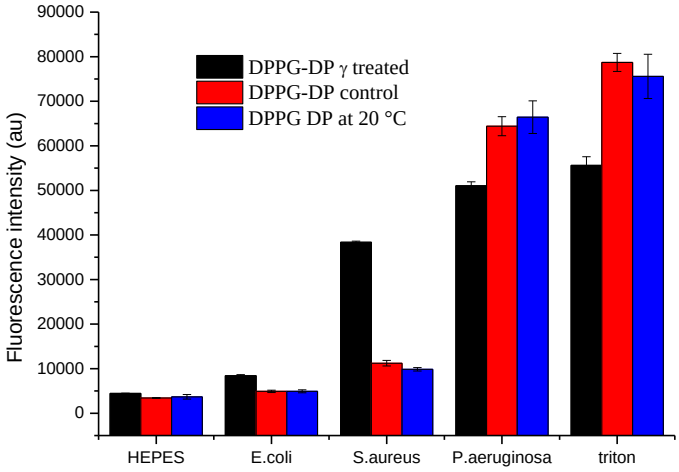

SI-Figure 4. The effect of gamma radiation on DPPG-DP vesicles. The fluorescence intensity graph indicates good measurable fluorescence of all vesicles treated with lytic agents (M = MSSA 476, P = PAO1, T = triton), compared to the low fluorescence of all vesicles with non-lytic agents (H = HEPES, E = DH5α).

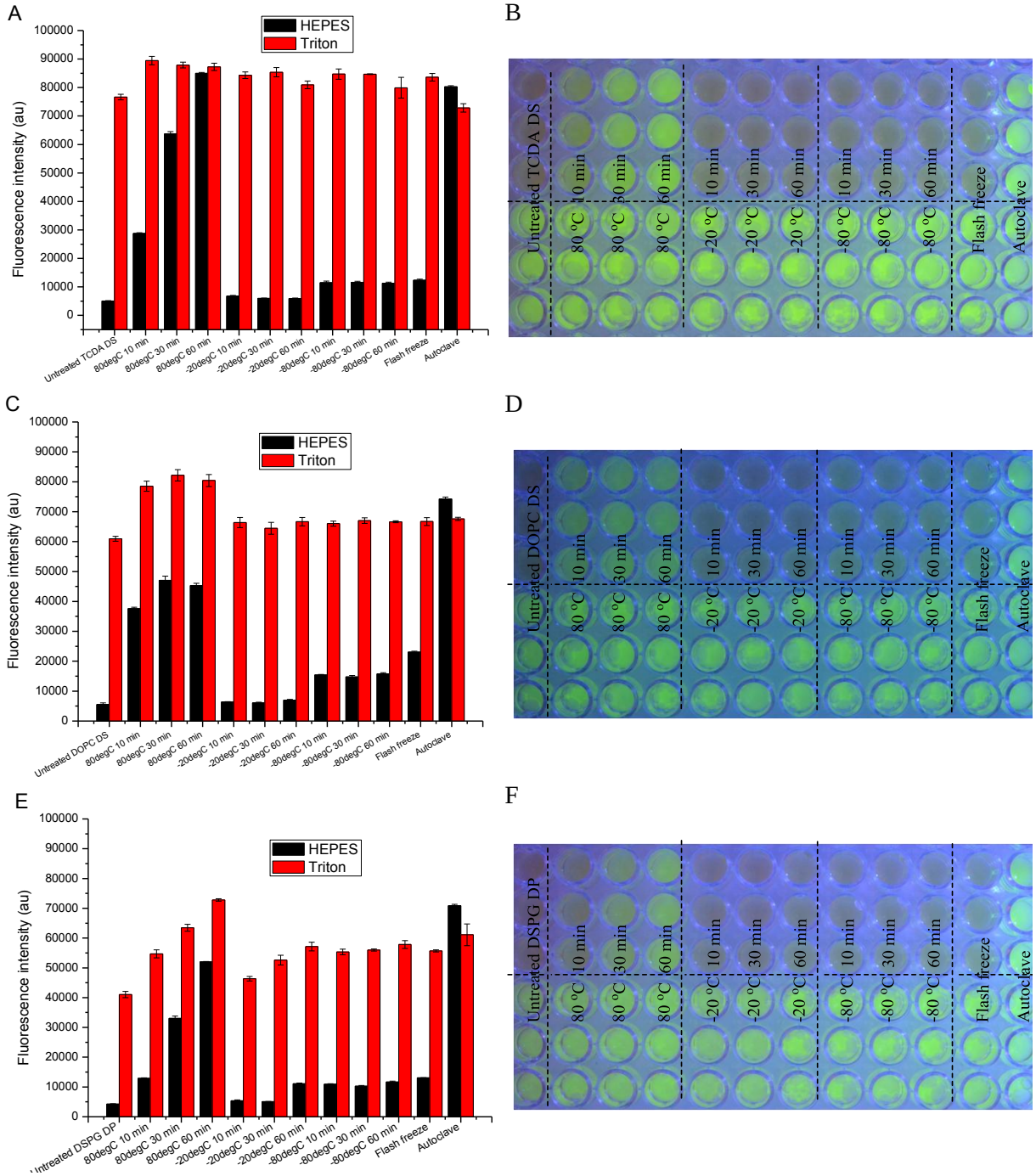

SI-Figure 5. Heat treatment of three vesicle types carried out at 80 °C, -20 °C and -80 °C for 10, 30 and 60 minutes, and compared to control vesicles, flash freezing with liquid nitrogen (5 minutes) and autoclaving (120 °C, 60 minutes), all with HEPES and Triton. A), C) and E) are fluorescence intensity measurement graphs of TCDA DS, DOPC DS and DSPG DP vesicles respectively; and B), D) and F) are photographs of the vesicles before and following treatment.

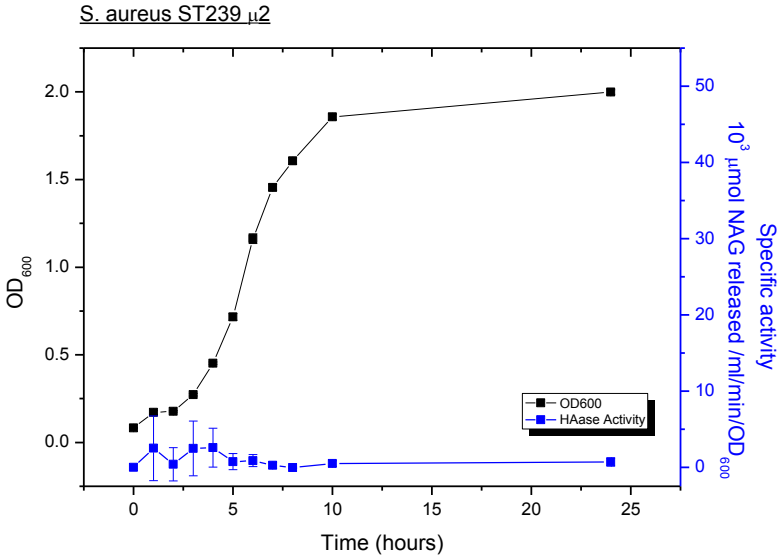

SI-Figure 6. The HLase assay results of the HLase negative strain ST239µ2, which shows the growth of bacteria over 25 hours, and the corresponding lack of production of the hyaluronic acid breakdown-component N-acetylglucosamine, measured per ml / per min / per OD_{600} from a known stock of HA (0.6 mg/ml) throughout this time. Results from J. Bean.

Appendix 2 – Original publications

1. S. Marshall, J. Bean, A. T. A. Jenkins, A two component nanocapsule for detection of lytic toxins secreted by *Staphylococcus aureus*, *Chemical Communications*, **2013**, Manuscript in preparation.

2. S. Marshall, S. H. Hong, N. T. Thet, A. T. A. Jenkins, The effect of lipid and fatty acid composition of phospholipid vesicles on long term stability and their response to *Staphylococcus aureus* and *Pseudomonas aeruginosa* supernatants, *Langmuir*, **2013**, 29, 23.

3. S. Marshall, A. T. A. Jenkins, S. A. Al-Bataineh, R. D. Short, S. H. Hong, N. T. Thet, J. S. Oh, J. W. Bradley, E. J. Szili. Studying the Cytolytic Activity of Gas Plasma with Self-Signalling Phospholipid Vesicles Dispersed within a Gelatin Matrix, *J. Phys. D.* **2013**, 46, 18.

4. N. T. Thet, S. H. Hong, S. Marshall, M. Laabei, A. T. A. Jenkins, Visible, colourimetric dissemination between pathogenic strains of *Staphylococcus aureus* and *Pseudomonas aeruginosa* using fluorescent dye containing lipid vesicles, *Biosensors and Bioelectronics* **2012**, 41, 1.

5. A. T. A. Jenkins, N. T. Thet, J. Zhou, S. H. Hong, S. Marshall, A microbiologically sensitive “intelligent” burns dressing concept, *Burns*, **2011**, 37, S5.